

AN EVALUATION OF SITE FACTORS IN BUILDING CODES

by

Jonathan Taylor

B.Sc. in Civil Engineering, University of Glasgow (1983)

SUBMITTED TO THE DEPARTMENT OF CIVIL ENGINEERING
IN PARTIAL FULFILLMENT OF THE REQUIREMENTS
FOR THE DEGREE OF

MASTER OF SCIENCE IN CIVIL ENGINEERING

at the

MASSACHUSETTS INSTITUTE OF TECHNOLOGY

June 1992

Copyright © 1992 Massachusetts Institute of Technology

Signature of Author _____
Department of Civil Engineering
January 17, 1992

Certified by _____
Professor Robert V. Whitman
Thesis Supervisor

Accepted by _____
Professor Eduardo Kausel
Chairman, Department Committee on Graduate Students

ARCHIVES
MASSACHUSETTS INSTITUTE
OF TECHNOLOGY

MAR 01 1992

LIBRARIES

AN EVALUATION OF SITE FACTORS IN BUILDING CODES

by

Jonathan Taylor

Submitted to the Department of Civil Engineering on January 17, 1992
in partial fulfillment of the requirements for the Degree of
Master of Science in Civil Engineering

ABSTRACT

Current building code criteria accounting for local site response are compared with recently proposed alternatives, and with the results of SHAKE analyses of typical profiles from a number of U.S. metropolitan areas. It was found that, in general, sites in the western United States are adequately covered, while sites in the east are not. This is considered to be due to a combination of lower levels of shaking and higher impedance ratios in the east. By examining the results of additional SHAKE analyses for profiles with varying impedance ratios, it was shown that site factors can be considered the product of an impedance and a soil factor; impedance factors computed from the SHAKE analyses are discussed. Based on these studies, and the results of a survey of earthquake engineering professionals also undertaken as part of this research, suggested alterations to current code criteria are made.

Thesis Supervisor:
Title:

Professor Robert V. Whitman
Professor of Civil Engineering

ACKNOWLEDGEMENTS

I gratefully acknowledge the advice and assistance from my advisor, Professor Robert V. Whitman, whose clear explanations and analysis guided me through the complexities of local site response, and enabled the research to be undertaken.

This study was funded by a grant from the National Center for Earthquake Engineering Research, State University of New York at Buffalo.

I am also grateful to the following people:

- Dr. Alfredo Urzua, who provided the SHAKE program and also helped familiarize me with it.
- Paul Friberg, who assisted with downloading of input earthquakes from the Lamont Doherty database.
- the participants in the Site Effects Workshop in Buffalo in October 1991, who provided useful suggestions and helped clarify several topics. In particular, Dave Perkins first suggested a study similar to that presented in Chapter 5. J.P. Singh provided guidance on the selection and scaling of earthquakes, and although there was not enough time to really incorporate his suggestions, a more critical and thorough analysis of the results of the SHAKE studies was achieved through his input.
- my wife Margaret, for things too numerous to mention, but which included helping to proof and type the thesis.
- and, finally, my family who have helped support me over the years and who have always been there when I needed them.

TABLE OF CONTENTS

Abstract	2
Acknowledgements	3
Table of Contents	4
List of Figures	5
List of Tables	11
1. INTRODUCTION	
1.1 Objective	12
1.2 Structure of the Thesis	12
2. BACKGROUND	
2.1 Factors Influencing Seismic Hazard Potential	14
2.2 Characterization of Earthquake Ground Motions	16
2.3 Local Site Response	19
2.4 Building Code Provisions	23
2.5 Alternative Provisions for Local Site Response	25
2.6 Conclusions	26
3. SITE CATEGORIES QUESTIONNAIRE	
3.1 Discussion of Results	54
4. SHAKE ANALYSES OF TYPICAL SOIL PROFILES	
4.1 Description of SHAKE	63
4.2 Description of Soil Profiles and Local Seismicity	65
4.3 Dynamic Soil Properties	67
4.4 Selection and Scaling of Input Earthquakes	68
4.5 Design Response Spectra	71
4.6 Site Specific Response Analyses	71
4.7 Discussion of Results	72
5. INVESTIGATION OF THE EFFECTS OF IMPEDANCE RATIO ON LOCAL SITE RESPONSE	
5.1 Description of SHAKE analyses	118
5.2 Presentation of Results	119
5.3 Discussion of Results	120
5.4 Application to Analysis of City Profiles	124
5.5 Conclusions	124
6. DISCUSSION	
6.1 Site Category Definitions	150
6.2 Site Factors	151
6.3 Design Response Spectra	153
7. CONCLUSIONS AND RECOMMENDATIONS	
7.1 Conclusions	155
7.2 Recommendations	156
References	158
Appendix A	
Input Earthquake Response Spectra and Time Histories	164

LIST OF FIGURES

- Figure 2-1 Comparison of Magnitude Scales. (After Campbell, 1985)
- Figure 2-2 Location of Major Earthquakes in the United States through 1970. (After Coffman, 1982)
- Figure 2-3 Comparison of Attenuation Equation Relationships. DB corresponds to Donovan and Bornstein (1978); I to Idriss (1987); JB to Joyner and Boore (1982); and C from Campbell (1985). (After Joyner and Boore, 1988)
- Figure 2-4 Typical Accelerograph Record. (After Seed and Idriss, 1982)
- Figure 2-5 Typical Accelerogram and Integrated Velocity and Displacement Time Histories. (After Seed and Idriss, 1982)
- Figure 2-6 Illustration of Importance of Structural Period on Response. (After Seed and Idriss, 1982)
- Figure 2-7 Typical Example of Fourier Spectrum. (After Roesset and Whitman, 1969)
- Figure 2-8 Displacement, Velocity, and Acceleration Response Spectra for El Centro earthquake (1940) S00E Component; damping ratio = 0.02. (After Gupta, 1990)
- Figure 2-9 Tripartite Response Spectrum for El Centro earthquake (1940) S00E Component; damping ratio = 0.02. (After Gupta, 1990)
- Figure 2-10 Amplification Curve for Shallow Uniform Soil Profile, Rigid Base Rock, and Constant Damping Ratio. (After Roesset and Whitman, 1969)
- Figure 2-11 Amplification Curve for Shallow Uniform Soil Profile, Elastic Base Rock, and Constant Damping Ratio. (After Roesset and Whitman, 1969)
- Figure 2-12 Variation of Normalized Shear Modulus and Damping Ratio with Level of Shear Strain for Sand. (After Seed and Idriss, 1970)
- Figure 2-13 Comparison of Normalized Modulus Reduction Relationships for Sand (After Iwasaki et al, 1978)
- Figure 2-14 Variation of Normalized Shear Modulus and Damping Ratio with Level of Shear Strain and Plasticity Index. (After Dobry and Vucetic, 1991)

- Figure 2-15 Empirical Normalized Response Spectra for Different Site Geological Conditions. (After Seed and Idriss, 1976)
- Figure 2-16 Average Empirical Spectra for Different Geological Conditions. (After Mohraz, 1976)
- Figure 2-17 Comparison of UBC and NEHRP Design Response Spectra
- Figure 2-18 Contour Map of Effective Peak Acceleration in the continental United States for a nominal recurrence interval of 500 years. (After BSSC, 1988)
- Figure 2-19 Contour Map of Spectral Acceleration for 0.3 second period covering the eastern United States. (After Algermissen and Whitman, 1991)
- Figure 2-20 Contour Map of Spectral Acceleration for 1.0 second period covering the eastern United States. (After Algermissen and Whitman, 1991)
- Figure 2-21 Approximate Method of Computing a Design Response Spectrum from only Two Spectral Ordinates. (After Donovan, 1991)
- Figure 2-22 Proposed Alternative Site Factor Provisions Utilizing a Matrix of Factors. (After Woodward Clyde et al, 1991)
-
- Figure 3-1 Site Categories Questionnaire
- Figure 3-2 Geographical Distribution of Questionnaire Sendees.
- Figure 3-3 Geographical Distribution of Questionnaire Respondents.
- Figure 3-4 Summary of Results of Site Categories Questionnaire: Frequency of Occurrence of Different Site Categories.
- Figure 3-5 Summary of Results of Site Categories Questionnaire: Sites which Cause Difficulty
- Figure 3-6 Summary of Results of Site Categories Questionnaire: General Information on Site Specific Response Studies.
- Figure 3-7 Summary of Results of Site Categories Questionnaire: Suggested Alterations to Current Code Provisions.

- Figure 4-1 Outline of Soil Parameters Required by SHAKE. (After Schnabel et al, 1972)
- Figure 4-2 Comparison of results from SHAKIE with results from more rigorous analyses. (After Martin and Seed, 1982)
- Figure 4-3 Description of Boston Profiles Analyzed
- Figure 4-4 Map Outlining the Seismicity of the Boston Area. (After WGC, 1989)
- Figure 4-5 Description of St. Louis Profile Analyzed
- Figure 4-6 Map Describing the New Madrid Seismic Zone. (After Ng et al, 1989)
- Figure 4-7 Description of Memphis Profiles Analyzed
- Figure 4-8 Description of San Francisco Profiles Analyzed
- Figure 4-9 Map Providing Details of Californian Seismicity. (After Algermissen et al, 1991)
- Figure 4-10 Description of Seattle Profile Analyzed
- Figure 4-11 Map Outlining the Seismicity of the Seattle Area. (After Ho et al, 1991)
- Figure 4-12 Contour Map of Effective Peak Acceleration in the continental United States for a nominal recurrence interval of 500 years. (After BSSC, 1988)
- Figure 4-13 Schematic Representation of the Calculation of EPA from Response Spectrum. (After BSSC, 1988)
- Figure 4-14 Comparison of Response Spectra and Ratio of Response Spectra for Boston Profile #1.
- Figure 4-15 Computed Surface Response Spectra for Boston Profile #1.
- Figure 4-16 Comparison of Response Spectra and Ratio of Response Spectra for Boston Profile #2.
- Figure 4-17 Computed Surface Response Spectra for Boston Profile #2.
- Figure 4-18 Input Earthquake Base Response Spectra for Boston.
- Figure 4-19 Comparison of Response Spectra and Ratio of Response Spectra for St. Louis Profile #1.

- Figure 4-20 Computed Surface Response Spectra for St. Louis Profile #1.
- Figure 4-21 Input Earthquake Base Response Spectra for St. Louis.
- Figure 4-22 Comparison of Response Spectra and Ratio of Response Spectra for Memphis Profile #1.
- Figure 4-23 Computed Surface Response Spectra for Memphis Profile #1.
- Figure 4-24 Comparison of Response Spectra and Ratio of Response Spectra for Memphis Profile #2.
- Figure 4-25 Computed Surface Response Spectra for Memphis Profile #2.
- Figure 4-26 Input Earthquake Base Response Spectra for Memphis.
- Figure 4-27 Comparison of Response Spectra and Ratio of Response Spectra for San Francisco Profile #1.
- Figure 4-28 Computed Surface Response Spectra for San Francisco Profile #1.
- Figure 4-29 Comparison of Response Spectra and Ratio of Response Spectra for San Francisco Profile #2.
- Figure 4-30 Computed Surface Response Spectra for San Francisco Profile #2.
- Figure 4-31 Comparison of Response Spectra and Ratio of Response Spectra for San Francisco Profile #3.
- Figure 4-32 Computed Surface Response Spectra for San Francisco Profile #3.
- Figure 4-33 Input Earthquake Base Response Spectra for San Francisco.
- Figure 4-34 Comparison of Response Spectra and Ratio of Response Spectra for Seattle Profile #1.
- Figure 4-35 Computed Surface Response Spectra for Seattle Profile #1.
- Figure 4-36 Input Earthquake Base Response Spectra for Seattle.
- Figure 4-37 Map of Boston showing Spectral Ratios Computed for $T = 0.5$ seconds. (After Wysocky, 1990)
- Figure 4-38 Estimated Spectra for the Seattle Area Computed Using Attenuation Relationships. (After Crouse, 1991)
- Figure 4-39 Variation of Peak Ratio of Response with Thickness-weighted Impedance Ratio for City Profiles Analyzed.

- Figure 5-1 Description of Profiles Analyzed with Varying Impedance Ratio.
- Figure 5-2 Acceleration Time Histories of Input Earthquakes for Analysis of Impedance Effects.
- Figure 5-3 Input Earthquake Base Response Spectra for Analysis of 150 ft Thick Soil Column with a Varying Thickness of Soft Clay Between Medium Sand.
- Figure 5-4 Response Spectra for a 150 ft Thick Soil Column with a Soft Clay Layer Between Medium Dense Sand from the Kern County (1952) Pasadena Record with a Peak Input Acceleration of 0.1g.
- Figure 5-5 Ratio of Response Spectra for a 150 ft Thick Soil Column with a Soft Clay Layer Between Medium Dense Sand from the Kern County (1952) Pasadena Record with a Peak Input Acceleration of 0.1g.
- Figure 5-6 Response Spectra for a 150 ft Thick Soil Column with a Soft Clay Layer Between Medium Dense Sand from the Kern County (1952) Pasadena Record with a Peak Input Acceleration of 0.3g.
- Figure 5-7 Ratio of Response Spectra for a 150 ft Thick Soil Column with a Soft Clay Layer Between Medium Dense Sand from the Kern County (1952) Pasadena Record with a Peak Input Acceleration of 0.3g.
- Figure 5-8 Response Spectra for a 150 ft Thick Soil Column with a Soft Clay Layer Between Medium Dense Sand from the Kern County (1952) Pasadena Record with a Peak Input Acceleration of 0.5g.
- Figure 5-9 Ratio of Response Spectra for a 150 ft Thick Soil Column with a Soft Clay Layer Between Medium Dense Sand from the Kern County (1952) Pasadena Record with a Peak Input Acceleration of 0.5g.
- Figure 5-10 Response Spectra for a 150 ft Thick Soil Column with a Soft Clay Layer Between Medium Dense Sand from the Imperial Valley (1979) Superstition Mountain N135 Record with a Peak Input Acceleration of 0.1g.
- Figure 5-11 Ratio of Response Spectra for a 150 ft Thick Soil Column with a Soft Clay Layer Between Medium Dense Sand from the Imperial Valley (1979) Superstition Mountain N135 Record with a Peak Input Acceleration of 0.1g.
- Figure 5-12 Response Spectra for a 150 ft Thick Soil Column with a Soft Clay Layer Between Medium Dense Sand from the Imperial Valley (1979) Superstition Mountain N135 Record with a Peak Input Acceleration of 0.3g.

- Figure 5-13 Ratio of Response Spectra for a 150 ft Thick Soil Column with a Soft Clay Layer Between Medium Dense Sand from the Imperial Valley (1979) Superstition Mountain N135 Record with a Peak Input Acceleration of 0.3g.
- Figure 5-14 Response Spectra for a 150 ft Thick Soil Column with a Soft Clay Layer Between Medium Dense Sand from the Imperial Valley (1979) Superstition Mountain N135 Record with a Peak Input Acceleration of 0.5g.
- Figure 5-15 Ratio of Response Spectra for a 150 ft Thick Soil Column with a Soft Clay Layer Between Medium Dense Sand from the Imperial Valley (1979) Superstition Mountain N135 Record with a Peak Input Acceleration of 0.5g.
- Figure 5-16 Peak Ratio of Response Spectra for a 150 ft Thick Soil Column with a Soft Clay Layer Between Medium Dense Sand.
- Figure 5-17 Amplification of Spectral Acceleration in a 150 ft Thick Soil Column with a Soft Clay Layer Between Medium Dense Sand.
- Figure 5-18 Soil Factors Computed Using Response Spectra for the S1 Medium Dense Sand Profiles (H=0) as Baseline, for Imperial Valley (1979) and Kern County (1952).
- Figure 5-19 Impedance Factors Computed Using Response Spectra for the Soil Profiles on Bedrock with a Shear Wave Velocity of 2500 fps as Baseline, for Kern County (1952).
- Figure 5-20 Impedance Factors Computed Using Response Spectra for the Soil Profiles on Bedrock with a Shear Wave Velocity of 2500 fps as Baseline, for Imperial Valley (1979).
- Figure 5-21 Impedance Factors for City Profiles Analyzed Computed By Factoring out the Effects of the Soil Column and the Level of Shaking from the Peak Ratio of Response Spectra.
- Figure 5-22 Variation of Computed Impedance Factor with Bedrock Shear Wave Velocity for City Profiles Analyzed.

LIST OF TABLES

- Table 2-1 Comparison of Lateral Force Provisions in Building Codes. (After Luft, 1989)
- Table 2-2 UBC Site Categories and Soil Factors. (After UBC, 1988)
- Table 2-3 NEHRP Site Categories and Soil Factors. (After BSSC, 1988)
- Table 2-4 Comparison of Soil Factors and Spectral Ratios in UBC and NEHRP.
- Table 2-5 Detailed Geotechnical Information for Assigning Sites to Categories. Numbers such as 3-65 etc. refer to New York Classification System. (After Jacob, 1990)
-
- Table 4-1 Values of K_2 Factor for Use in Equation 4.3 to Calculate the Small Strain Shear Modulus of a Cohesionless Soil.
- Table 4-2 Input Earthquakes for SHAKE Analyses.
- Table 4-3 Summary of Input Earthquake Time History Characteristics and Modifications for input into SHAKE.
- Table 4-4 Spectral Acceleration Values for Seattle and San Francisco. (After Perkins, personal communication)
-
- Table 5-1 Results of Analyses with Varying Impedance Ratio.
- Table 5-2 Factors Used to Compute Impedance Factors from Peak Ratio of Response Spectra for City Profiles.

CHAPTER 1

INTRODUCTION

1.1 Objective

Since the late 1960's, the modification of earthquake motions by local geological conditions has been recognized as an important factor in the seismic hazard potential at a site. Building codes account for variations in local site response by including a site factor or an elastic response spectrum which is dependent on local soil conditions. The site factor is one parameter used in the calculation of the lateral force which would be exerted on a structure during an earthquake.

Current national building code provisions concerning local site effects date from studies carried out in the early 1970's. In recent years, however, particularly since the Michoacan earthquake in Mexico in 1985 and the Loma Prieta earthquake in San Francisco in 1989, local site effects have become better documented and understood. There is now concern in the professional and academic communities that national building codes have not been modified to incorporate more recent advances in the understanding of local site effects

This thesis evaluates current code provisions by comparing the results of site specific response analyses with the existing code provisions and with other more recently proposed methods for accounting for local site effects. Factors affecting local site response which are not explicitly included in the current code provisions, such as impedance ratio, are investigated and discussed.

1.2 Structure of the Thesis

In Chapter 2, a brief review of the factors influencing seismic hazard is provided. The influence of local site effects on seismic response is discussed, and ways in which this has been incorporated into US building codes since the mid 1970's is

described. A survey of researchers and practitioners in the seismic field was undertaken in order to gather information and views on perceived problems with present code requirements. The results of this survey are presented in Chapter 3.

Site specific response analyses of nine typical soil profiles from five major metropolitan areas in the United States were carried out using the SHAKE program. The results were compared to building code provisions and to other suggested methods of accounting for site response. These findings are presented in Chapter 4. Additional SHAKE analyses were performed in order to investigate the effects of the impedance ratio between the base rock and the soil column. Different soil profiles at three levels of shaking were analyzed. The results are described in Chapter 5 and compared with site specific response analyses presented in Chapter 4.

In Chapter 6, the implications of the results of the research undertaken are discussed, and possible changes to the current code provisions presented. Conclusions and recommendations from the research are summarized in Chapter 7.

CHAPTER 2

BACKGROUND

In this chapter, a review of the present code provisions concerning local site effects is provided. The factors influencing the damage potential of earthquakes is first of all described. A description of site response effects and how these have been accounted for in building codes is then provided. Finally, some recent proposals for alternative methods of generating elastic response spectra are reviewed.

2.1 Factors Influencing Seismic Hazard Potential

The factors influencing the degree of potential destructiveness of a given earthquake have been described in numerous professional papers (e.g. Seed and Idriss 1982, Aki 1988, Joyner and Boore 1988). Potential seismic hazard depends principally on the following factors:

- magnitude of the earthquake;
- earthquake source;
- mechanism of energy release;
- epicentral distance of the site;
- attenuation characteristics of the base rock;
- local site conditions;
- structural period.

The magnitude of an earthquake is a measure of the amount of energy released and is closely related to the duration of shaking. Several different scales are used to measure earthquake magnitude, including local Magnitude M_l , moment Magnitude M , and body wave Magnitude M_b , and there is considerable confusion regarding their use. Figure 2-1 shows the relationship between the Moment Magnitude and the other scales. These scales are described and compared by Herrmann and Nuttli (1984), and Joyner & Boore (1988).

The source of earthquakes in the U.S. can be generally divided into four categories:

- (i) Western US (WUS) -- this category includes the type of earthquakes typical of those experienced in California; they are result of near surface continental crustal movements such as occur along the San Andreas Fault;
- (ii) Eastern US (EUS)-- the source is less well defined but is considered but is considered to be faults in crystalline rocks at depths of 10 to 20 kilometers;
- (iii) Subduction Zone events typical of the Pacific Northwest and Alaska; these occur at the margins of tectonic plates at depths of up to 100 kilometers.
- (iv) Earthquakes in Hawaii associated with volcanic activity.

A map indicating the major earthquakes in the United States through 1970 is shown in Figure 2-2.

The characteristics of earthquakes in the above four categories are quite distinct, most notably in the frequency content of the motions. Subduction Zone and EUS earthquakes generally have more high frequency components than those in the WUS category, and EUS earthquakes are typically of smaller magnitude and occur less frequently.

Variations in the mechanism of energy release, such as the type of fault, depth of rupture, and stress drop at the rupture, are thought to affect the type of motion experienced (McGarr, 1984, Crouse et al, 1988).

Earthquake motions experience anelastic and geometric attenuation with distance from the source, which reduces ground motion amplitudes and tends to filter out some of the higher frequency components. The degree of attenuation is a function of the properties of the rock through which the waves travel, with softer rock generally causing more attenuation. This contributes to the generally higher frequency content of EUS earthquakes, since the geology of the EUS comprises older crystalline rocks, while the WUS has younger sedimentary deposits.

Since earthquake motions attenuate with distance from the source, the epicentral distance of a site is a controlling factor in the intensity of ground motion. Joyner

and Boore (1988) point out however, that accurately describing epicentral distance can be difficult since source movements may have occurred over many miles; hypocentral distance is often a more meaningful quantity for analysis purposes. Numerous empirical attenuation relationships correlating the level of shaking at a site to earthquake magnitude and distance have been proposed (summarized by Joyner & Boore, 1988), and some of them are compared in Figure 2-3. The equations are generally of the form:

$$\log(y) = A_i + d \log(r) + kr + s \quad (\text{Eq. 2.1})$$

where y is a ground motion parameter, A_i and r are a measure of the earthquake magnitude and epicentral distance respectively, and the other factors are constants from the regression analysis of the data set of earthquakes analyzed.

The above factors all contribute to the characteristics of the ground motion in the base rock beneath a site. Modification of these movements by local site effects will depend on the site geology and on the surrounding topography. Since topographic effects, including such features as ridges and valleys are not yet fully understood, and are unlikely to be included in building codes in the near future, this research will be concerned only with effects of site geology.

The period of a structure at a site influences seismic hazard potential since the structural response depends on the relationship between the structural period and frequency components of the earthquake. This is discussed in more detail in subsequent sections.

2.2 Characterization of Earthquake Ground Motions

From the previous brief discussion, it is apparent that the seismic hazard potential is dependent on numerous complex factors. Earthquake ground motions are most often described by an accelerogram, such as that shown in Figure 2-4. The accelerogram is a record of the time history of acceleration of one component of motion at the site and is measured by an accelerograph. Three components of the motion are usually

recorded; two mutually perpendicular horizontal components and one vertical component. Seismic studies are usually concerned mainly with the horizontal components.

The acceleration time history can be integrated to give velocity and displacement time histories, an example of which is shown in Figure 2-5. The generation of these time histories is subject to difficulties inherent with integration, which have been discussed by Joyner and Boore (1988).

The accelerogram therefore provides motion time histories from which can be inferred the following parameters:

- peak acceleration
- peak velocity
- peak displacement
- duration of shaking

The latter is often taken as the time between first and last occurrences of 0.05g or 0.1g.

Although peak ground acceleration is commonly used to characterize the potential damage at a site, other factors including peak ground velocity and displacement, and frequency content, are often more important. For example, the Michoacan earthquake in 1985 that devastated parts of Mexico City had relatively low peak accelerations of 0.12g.

The use of time histories to characterize earthquakes is deficient because information about the frequency content of the motions cannot easily be visualized. This is important, because as will be discussed in the following sections, the response of a site, and any structures at the site, depends on these frequencies. An example from Seed and Idriss (1982) illustrates this point and is shown in Figure 2-6. A stiff structure subjected to a low frequency motion will have very little response, while motions at or near the natural period of the structure will be amplified.

In order to describe the frequency content of earthquakes, Fourier spectra or response spectra are most commonly used. Fourier analysis reduces the time history into a series of regular sinusoidal functions which can be added to recreate the original time history. A Fourier spectrum is a plot of Fourier amplitude versus frequency, and an example is shown in Figure 2-7.

The use of response spectra to characterize ground motions was first developed by Biot (1941) and Housner (1941). Response spectra are considered to be the most comprehensive measure of an earthquake since different factors such as frequency content, maximum ground acceleration, and to some extent intensity (Seed and Idriss, 1982) can be observed. In addition, response spectra are easily applied in the calculation of the response of a structure (Roesset and Whitman, 1969). Response spectra are derived from the solution of the partial differential equation describing vibration of a one degree of freedom (1DOF) system:

$$\frac{\partial^2 u}{\partial t^2} + 2\omega\beta\frac{\partial u}{\partial t} + \omega^2 u = a(t) , \quad (\text{Eq. 2.2})$$

where u = relative displacement, ω = natural frequency of 1DOF oscillator, β = damping ratio, and $a(t)$ is the acceleration time history causing vibration. For a given input time history, Equation 2.2 can be solved for many 1DOF systems with different natural frequencies at a constant damping ratio. In earthquake engineering a damping ratio of 5 percent is most commonly used. The earthquake response spectrum is a plot of the computed maximum response versus the natural frequency of the 1DOF systems, where the spectral ordinates can be acceleration (S_a), velocity (S_v), or displacement (S_d). Examples of these spectra for the El Centro 1940 earthquake are shown in Figure 2-8. The spectra are related by the following equations:

$$S_a = \omega S_v = \omega^2 S_d \quad (\text{Eq. 2.3})$$

Because of this relationship, the three quantities can be plotted on tripartite logarithmic paper, as shown for the El Centro 1940 earthquake in Figure 2-9.

Although the response spectrum is derived for 1DOF systems, it can be applied directly to multiple degree of freedom systems (e.g. Seed and Idriss, 1982).

One of the main advantages of the response spectrum is that it can be easily applied in the calculation of the design earthquake forces for a structure. For example, for relatively stiff structures, the maximum base shear force can be estimated from:

$$V_{\max} \sim WS_a/g \quad (\text{Eq 2.4})$$

where V_{\max} = maximum base shear, W = weight of the structure, S_a = spectral acceleration corresponding to the natural frequency of the structure, and g = acceleration due to gravity.

2.3 Local Site Response

Observations of local concentration of earthquake damage date from the 1800's (Wysockey, 1990), but it was not until the late 1960's that researchers successfully formulated a theory relating site conditions to the modification of seismic motions (Idriss and Seed, 1969). The development of this theory occurred largely as a result of an investigation into the 1967 Caracas earthquake, in which considerable damage was focussed in an area where there was a local depression in bedrock (Seed et al, 1972).

Since then, considerable progress in the understanding of local site response has been made, although considerable uncertainties still exist. In recent years, the 1985 Michoacan and the 1989 Loma Prieta earthquakes demonstrated the effects of local site conditions and helped to focus additional research.

This section will describe the theories developed to characterize site modification of earthquake motions, and will discuss the factors controlling these effects.

There are two main causes of modification of earthquake motions in the bedrock beneath a site by the overlying soil column:

- (i) resonance effects from earthquake frequency components close to the natural frequency of the profile;
- (ii) impedance effects due to the contrast between softer soil deposits and underlying stiffer earth.

The first effect is a more widely recognized phenomenon, although the effects of the second are probably more common (Joyner and Boore, 1988).

The theory for response of a soil deposit has been described by for example, Kanai (1952), and Idriss and Seed (1968). The outline presented below more closely follows that provided by Roesset and Whitman (1969) and Whitman (unpublished), since they more clearly describe the two sources of amplification effects.

The theory is developed by first considering the equation of motion for a uniform, continuous layer of soil resting on a *rigid* base and subjected to a forced harmonic vibration:

$$\rho \frac{\partial^2 y}{\partial t^2} = G \frac{\partial^2 y}{\partial x^2} + \eta \frac{\partial y}{\partial x} \frac{\partial}{\partial t} - \rho C \sin \Omega t \quad (\text{Eq. 2.5})$$

where ρ = soil density, y = relative displacement of a point in the soil to the base, η = damping constant, G = soil shear modulus, and $C \sin \Omega t$ = forcing function.

It can be shown that the amplification, defined as the ratio of the absolute acceleration at the top of the layer to that at the base, is a function of the excitation frequency:

$$A(\Omega) = 1/(\cos \phi), \quad \text{where } p^2 = \rho \Omega^2 / (G + i\eta \Omega) \quad (\text{Eq. 2.6})$$

and that if there is no damping:

$$A(\Omega) = 1/(\cos \beta), \quad \text{where } \beta = H \Omega \sqrt{(G/\rho)}. \quad (\text{Eq. 2.7})$$

Eq 2.7 implies that the amplification will become infinity if $\cos \beta=0$, i.e.

$$\beta = (2n-1)\pi/2 \quad (\text{Eq. 2.8})$$

corresponding to

$$\Omega = \frac{(2n-1)\pi}{2H} \sqrt{(G/\rho)} = \omega_n \quad (\text{Eq.2.9})$$

where ω_n is the nth natural frequency of the layer. If $n=1$, the frequency is described as the fundamental frequency and corresponds to:

$$f_1 = C_s/4H \quad (\text{Eq. 2.10})$$

where C_s is the shear wave velocity $= \sqrt{(G/\rho)}$.

Figure 2-10 illustrates the variation of response with frequency.

Now, considering a uniform layer on an *elastic* base, it can be shown that the amplification, defined as the ratio of displacement at the free surface of the soil to the displacement at the free surface of the base if the soil was not present, is given by:

$$A(\omega) = 1/(\cos p_s H + \mu \sin p_s H) , \quad \text{where } \mu = C_r \rho_r / C_s \rho_s \quad (\text{Eq. 2.11})$$

Defining the amplification for the elastic rock as $A_2(\omega)$, and for rigid rock as $A_1(\omega)$, and assuming small damping, the following approximate expression can be derived:

$$1/A_2(\omega) = 1/IR + 1/A_1(\omega) , \quad (\text{Eq. 2.12})$$

where $IR=1/\mu =$ impedance ratio. Figure 2-11 shows the amplification function with the effects of the elastic half-space included. It can be seen that the response does not tend to infinity as was the case for a rigid base shown in Figure 2-10.

The effect of the impedance ratio can be considered as a radiation damping term describing the loss of energy by the system into the base rock; the softer the underlying bedrock, the more damping there will be and the smaller the resulting amplification.

The above discussion greatly simplifies the theory in order to present only the main controlling factors. Clearly, adaptation of the theory to real sites with multiple layers, and transient rather than harmonic motions, involves considerable complexities.

From the foregoing discussion several conclusions can be drawn. Firstly, the different components of earthquake motions will be modified in different ways; those components with a frequency higher than the natural frequency of the profile will be de-amplified, while those close to the natural period will be amplified. In addition, the fundamental frequency is dependent on a combination of the stiffness and depth of the profile. Furthermore, damage to a structure at a site will depend on its natural frequency. It should be noted that the theory presented only models one dimensional elastic response of the profile. During high levels of shaking the soil will behave inelastically which will reduce the response.

Two and three dimensional effects are not yet fully understood, but include such features as ridges and valleys which are suspected of respectively focussing and dispersing earthquake waves. Other effects include sediment filled basins, which are thought to alter ground motion by generating surface waves (Aki, 1988).

It should be noted from Equations 2.5 and 2.6 that the response is dependent on the soil damping and shear modulus, which are non-linear functions of shear strain. Empirical relationships for shear modulus and damping versus strain for sand and clay were proposed by Seed and Idriss (1970), and are shown in Figure 2-12. Hardin and Drnevich (1972), Makdisi and Seed (1978), and others have proposed similar curves for sand, and a comparison of some of the curves for shear modulus is shown in Figure 2-13.

For clays it has been shown that the modulus and damping versus strain relationships are dependent on plasticity index, with high plasticity clays retaining their small strain properties at higher strain levels (Dobry and Vucetic, 1987, Sun et al 1987). Dobry and Vucetic (1991) have recently proposed relationships for shear modulus and damping versus strain as a function of plasticity index, which are shown in Figure 2-14.

Consequently the response at high levels of shaking must include the effects of deformations in the non-linear range. An equivalent linear analysis achieving this was first proposed by Seed and Idriss (1968), and is still the most commonly used solution. True non-linear analyses, such as described by Martin and Seed (1978), provide a more rigorous solution, but require more detailed soil parameters to be defined. It should be noted that uncertainties in these parameters may be as important as the limitations of the equivalent linear method.

2.4 Building Code Provisions

In the early to mid 1970's, a few detailed studies of the effects of geological conditions on site response were undertaken (e.g. Mohraz et al, 1972, Seed et al, 1976, Mohraz, 1976). The study by Seed et al (1976) included 104 earthquake records, primarily from California, but also some from Japan, and only limited information about the soils conditions was available. The response spectra for the different geological categories for the 50th and 84th percentile are shown in Figure 2-15 together with a suggested average design spectrum. The median of a similar study by Mohraz (1976) is shown in Figure 2-16.

Thus, with the development of the theories presented in the previous section, and empirical analyses of the database of earthquake records, it was clear that site response could be related to the geological conditions. However, the adoption of criteria into building codes to include these effects was a long process.

A soil factor was first introduced into the Structural Engineer's Association of California (SEAOC) Lateral Force Recommendations in 1974, and varied between

1.0 and 1.5, depending on how close the fundamental period of the structure was to that of the profile. Relating the soil factor to the fundamental period of the profile was later discontinued because of difficulties and uncertainties in calculating the period, particularly at sites where there is no definitive rock to great depths.

The current code provisions essentially date from the 1974 SEAOC edition and from the Applied Technology Council (1978) report commonly known as ATC3-06. The ATC3-06 report introduced the use of three site categories defined for different geological conditions, and the soil factor for the categories varied from 1 to 1.5. These recommendations were made on the basis of engineering judgement and on the empirical studies discussed above. During preparation of ATC3-06 four different categories were defined, but this was deemed too complicated by code officials, and in the final report, sites on rock were combined into one category with shallow, stiff soil.

The ATC3-06 report was prepared as a guideline for drafters of building codes. There are a number of different national or model codes in the United States which can be adopted by local state or city building code officials. The main codes are the Unified Building Code (UBC), National Earthquake Hazard Reduction Program (NEHRP) Recommended Provisions, American National Standards Institute (ANSI), and SEAOC. A detailed comparison of these codes was provided by Luft (1989), and a summary describing the main provisions of the codes is shown in Table 2-1.

In this study, the UBC and NEHRP provisions will be compared with other proposed provisions and with site specific response analyses. The 1985 edition of both UBC and NEHRP were based on ATC3-06. In their 1988 revisions, design elastic response spectra were included for use in more detailed analyses of structures. After the Michoacan earthquake of 1985, an additional site category, S4, for soft clay was included in both UBC and NEHRP, although a response spectrum for S4 was not included in UBC. The code site categories and soil factors are shown in Tables 2-2 and 2-3, and the design spectra are compared in Figure 2-17. A point to note is that in UBC the spectral ratios from the design spectra are not equal to the soil factors; the spectral ratios for UBC are shown in Table 2-4.

The normalized spectra in both UBC and NEHRP are scaled by a peak acceleration obtained from an appropriate contour map such as that shown in Figure 2-18. One problem with this approach is that different spectral ordinates are amplified at different periods; acceleration, velocity, and displacement are amplified more in the short, intermediate and long periods respectively.

2.5 Alternative Provisions for Local Site Response

When the NEHRP 1991 provisions are published, the Appendix will include an alternative approach for generating elastic response spectra. This method utilizes probabilistic ground motion hazard maps and has been described by Algermissen et al (1991). Maps of spectral acceleration have been prepared for S2 sites using appropriate attenuation relationships and seismo-tectonic models. Figures 2-19 and 2-20 show the spectral acceleration maps for 0.3 second and 1.0 second periods for EUS for a nominal 500 year recurrence interval. It has been shown that a method of generating the entire spectrum using only the 0.3 and 1.0 second ordinates approximates the complete spectrum sufficiently accurately (Algermissen, 1991), and the method is illustrated in Figure 2-21. The response spectrum is constructed by plotting the 0.3 second value as the limiting spectral acceleration at small periods, and at higher periods the curve is drawn proportional to frequency through the value from the 1.0 second contour map.

Donovan (1991) proposed a similar method for profiles with a fundamental period greater than one second which incorporates the site period into construction of the response spectrum; instead of plotting the spectral acceleration from the 1.0 second contour map at 1.0 second, it is plotted at the fundamental soil period, and the response spectrum curve is drawn through this point proportional to frequency. This alternative approach has no theoretical basis, but it does have some intuitive appeal, since the design spectrum will be increased at the site period. This method suffers from problems mentioned previously regarding calculation of the site period.

Jacob (1990) proposed a design code for New York City with some important differences from UBC and NEHRP. An additional category for rock was included

with a soil factor of 0.67, and the S4 soil factor was increased to 2.5. This provides an amplification of nearly four between sites on rock and sites on soft clay. The above changes were made to try and account for the increased amplification thought to occur in EUS through the effects of higher impedance ratios. In addition, much more detailed information on how to assign sites to the appropriate site category was provided, details of which are shown in Table 2-5.

At a recent workshop (Whitman, 1992), the use of a large matrix of factors including the effects of source characteristics, impedance ratio, level of shaking, and soil column properties was proposed. Depending on the number of categories in each variable, as many as 90 factors may have to be evaluated. The relative influences of the different factors will be examined in this thesis. A similar approach using a simpler matrix proposed for use in Illinois is shown in Figure 2-22.

2.6 Conclusions

The current code provisions are based on empirical studies from the 1970's which included primarily Californian data. Since then, considerable information on local site response has been collected and shortcomings in the code provisions recognized. In addition, earthquake codes in general have changed from an empirical approach to a more probabilistic basis. The current code provisions are therefore in need of review.

	ANSE	NIDHRP	SEAOC and UBC-1988	UBC-1985
(1) Base shear formula	$V = ZIKCSW$	$V = C_p W$	$V = \frac{ZICW}{R}$	$V = ZIKCSW$
(2) Numerical coefficient C_p or C_s	$C = \frac{1}{15T^{0.5}}$	$C_p = \frac{1.2AV_s}{RT^{0.5}}$	$C = \frac{1.25S}{T^{0.5}}$	$C = \frac{1}{15T^{0.5}}$
(3) Upper limits	$C < \text{or} = 0.12$ $CS < \text{or} = 0.14$ $CS < \text{or} = 0.11$ for S_3 in Zones 3 and 4	$C_p < \text{or} = \frac{2.5A_s}{R}$ $C_p < \text{or} = \frac{2.0A_s}{R}$ for S_3 or S_4 when $A_s > \text{or} = 0.30$	$C < \text{or} = 2.75$	$C < \text{or} = 0.12$ $CS < \text{or} = 0.14$
(4) Lower limits	None	$C_p > \text{or} = C_s (C_s, T_s)$	$\frac{C_p}{R} > \text{or} = 0.075$ $\frac{C_p}{R} > \text{or} = 0.8C(T_s)$ ($T_s = T$ from Method A)	None
(5) Zone factor	Z	A_s and A_p	Z	Z
(6) Importance factor	I	Seismic Hazard Exposure Group	I	I
(7) Structural system factor	K	R	R_p	K
(8) Soil factor	$S_1 = 1.0$ $S_2 = 1.2$ $S_3 = 1.5$	$S_1 = 1.0$ $S_2 = 1.2$ $S_3 = 1.5$ $S_4 = 2.0$	$S_1 = 1.0$ $S_2 = 1.2$ $S_3 = 1.5$ $S_4 = 2.0$	$S = 1 + \frac{T}{T_s} - 0.5 \left(\frac{T}{T_s} \right)^2$ $S = 1.2 + 0.6 \frac{T}{T_s} - 0.3 \left(\frac{T}{T_s} \right)^2$ for $\frac{T}{T_s} < \text{or} > 1.0$ resp. or $S_1 = 1.0$ $S_2 = 1.2$ $S_3 = 1.5$

Table 2-1 Comparison of Lateral Force Provisions in Building Codes. (After Luft, 1989)

Type	Description	S Factor
S_1	<p>A soil profile with either:</p> <p>(a) A rock-like material characterized by a shear-wave velocity greater than 2,500 feet per second or by other suitable means of classification, or</p> <p>(b) stiff or dense soil condition where the soil depth is less than 200 feet.</p>	1.0
S_2	A soil profile with dense or stiff soil conditions, where the soil thickness exceeds 200 feet, or a profile consisting of a thin layer of soft clay up to 20 feet thick overlying rocklike material.	1.2
S_3	A soil profile 40 feet or more in depth containing more than 20 feet of soft to medium stiff clay but not more than 40 feet of soft clay.	1.5
S_4	A soil profile containing more than 40 feet of soft clay. Alternatively soils falling into this category may have a design spectrum determined by special geotechnical study reflecting the site specific conditions.	2.0

Table 2-2

UBC Site Categories and Soil Factors. (After UBC, 1988)

Type	Description	S Factor
S ₁	Rock of any characteristic, either shale-like or crystalline in nature (characterized by a shear wave velocity greater than 2500 fps), or stiff soil conditions where the soil depth is less than 200 ft and the soil types overlying rock are stable deposits of sands, gravels or stiff clays.	1.0
S ₂	Deep cohesionless or stiff clay soil conditions, including sites where the soil depth exceeds 200 ft and the soil types overlying rock are stable deposits of sands, gravels, or stiff clays.	1.2
S ₃	Soft-to-medium stiff clays and sands characterized by 30 ft or more of soft- to medium-stiff clay with or without intervening layers of sand or other cohesionless soils	1.5
S ₄	Soft clays or silts greater than 70 ft in depth and characterized by a shear wave velocity of less than 400 fps.	2.0

Table 2-3 NEHRP Site Categories and Soil Factors. (After BSSC, 1988)

UBC		NEHRP	
Soil Factor	Spectral Ratio	Soil Factor	Spectral Ratio
1.0	1.0	1.0	1.0
1.2	1.5	1.2	1.2
1.5	2.3	1.5	1.5
2.0	n/a	2.0	2.3

Table 2–4 Comparison of Soil Factors and Spectral Ratios in UBC and NEHRP

<u>Type</u>	<u>Thickness</u> (feet)	<u>Description</u> (for Definition of Material Class see appended Note 1, and for Velocity V* and Blow Count N* see Note 5)	<u>S-Factor</u>
S0:		A base of hard rock materials of class 1-65 to 2-65 with shear wave (interval) velocities greater than 7,000 feet per second (fps) overlain by a profile which contains	2/3
	<60	3-65 to 5-65 materials with shear veloc. V*>2000 fps (blow count N*>50); or	
	<30	3-65 to 7-65 materials with V*>1000 fps (N*>20); or	
	<15	3-65 to 11-65 materials with V*>500 fps (N*>10).	
S1:		A base of intermediate to soft rock or hardpan materials of class 3-65 to 5-65 with shear wave velocities greater than 2500 fps or blow counts greater than 80 overlain by a profile which contains	1.0
	<200	3-65 to 7-65 materials with V* > 2000 fps (N*>50); or	
	<100	3-65 to 8-65 materials with V*> 1000 fps (N*>20); or	
	<40	3-65 to 11-65 materials with V*> 500 fps (N*>10); or	
	<100	3-65 to 7-65 materials with V* > 2000 fps (N*>50) and/or less than 25 ft of 6-65 to 11-65 materials with V*> 500 fps (N*>10).	
S2:		A base of hardpan, gravel or sand materials of class 5-65 to 7-65 with shear wave velocities greater than 2,000 fps or blow counts greater than 50 overlain by a profile which contains	1.2
	>200	5-65 to 8-65 materials with V* > 2000 fps (N*>50), or	
	100-200	5-65 to 11-65 materials with V* between 1000 & 2000 fps (N*=20 to 50); or	
	40 - 100	5-65 to 11-65 materials with V* between 500 & 1000 fps (N*= 10 to 20); or	
	<40	7-65 to 11-65 materials with V* between 300 & 500 hps (N*=7 to 10).	
S3		Any profile which contains	1.5
	>200	5-65 to 11-65 with V* between 1000 & 2000 fps (N*=20 to 50); or	
	100-200	5-65 to 11-65 with V* between 500 & 1000 fps (N*=10 to 20); or	
	40 - 100	7-65 to 11-65 with V* between 300 & 500 fps (N*=7 to 10); or	
	<40	7-65 to 11-65 with V*<300 fps (N*<7).	
S4:		Any profile which contains	2.5
	>200	5-65 to 11-65 with V* between 500 & 1000 fps (N*=10 to 20); or	
	>100	7-65 to 11-65 with V* between 300 & 500 fps (N*=7 to 10); or	
	>40	7-65 to 11-65 with V*<300 fps (N*<7).	

Table 2-5

Detailed Geotechnical Information for Assigning Sites to Site Categories. Numbers such as 3-65 etc. refer to New York City Classification System. (After Jacob, 1990)

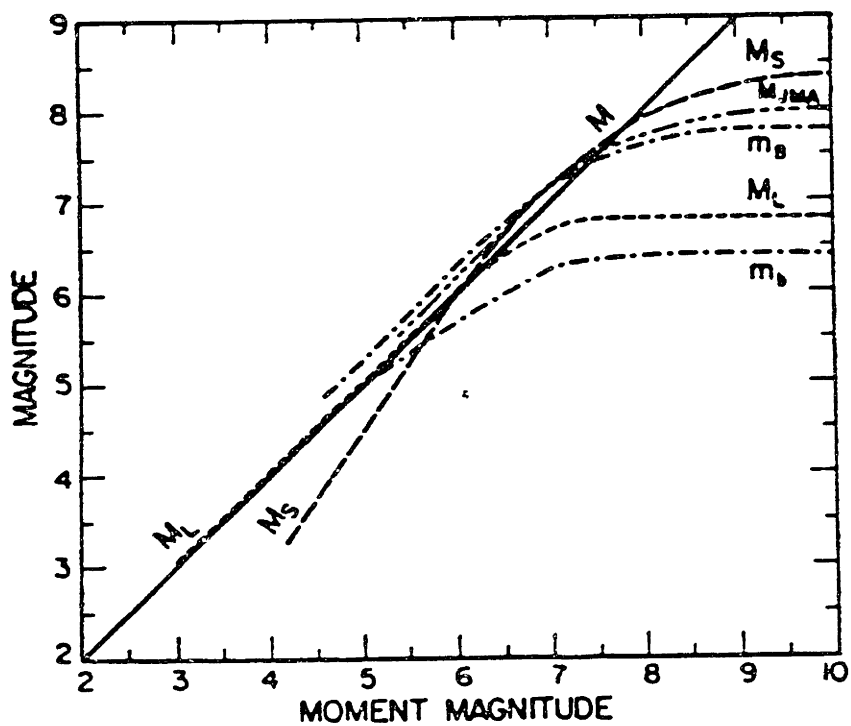


Figure 2-1 Comparison of Magnitude Scales (after Campbell, 1985).

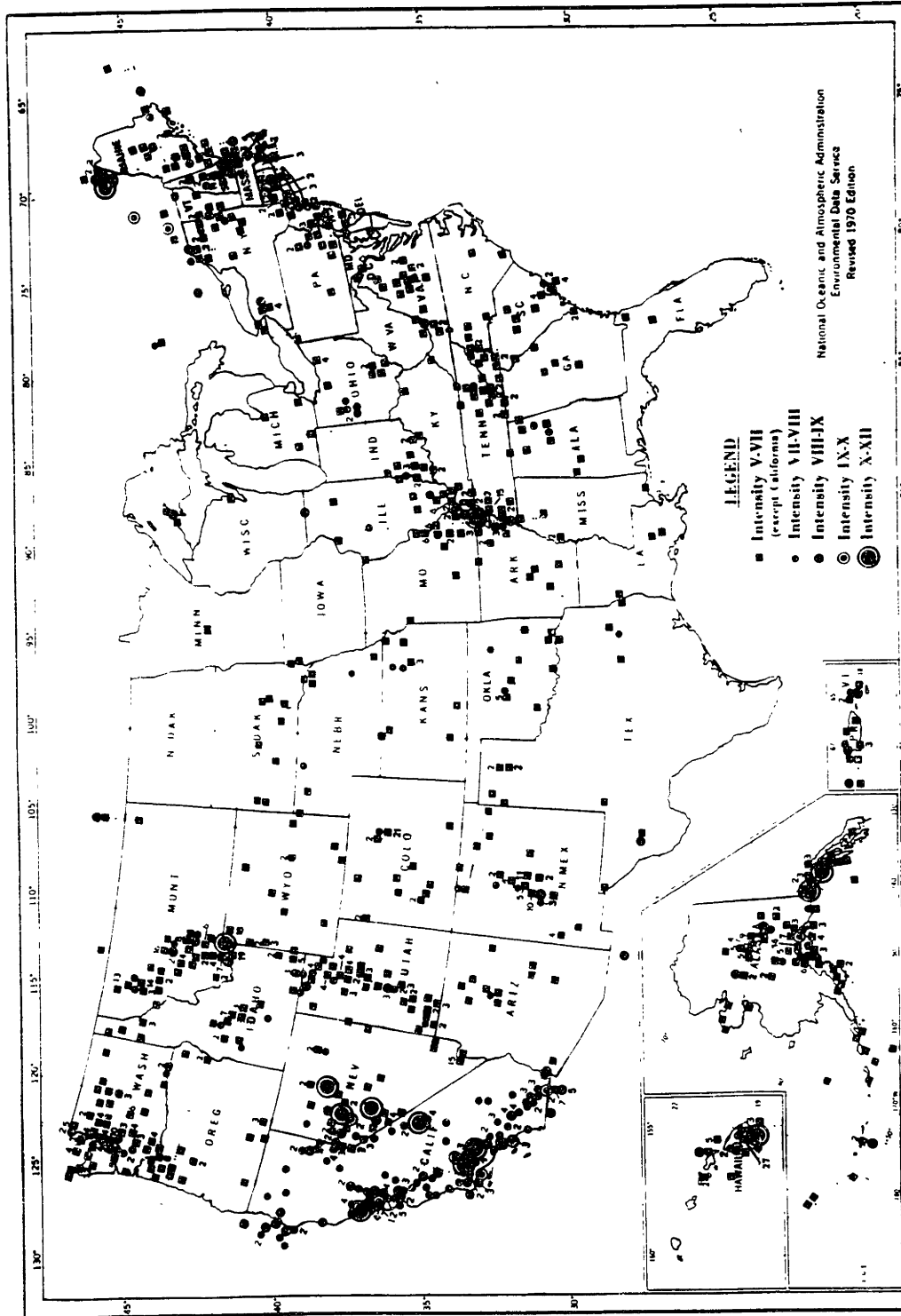


Figure 2-2 Location of Major Earthquakes in the United States through 1970 (After Coffman, 1982)

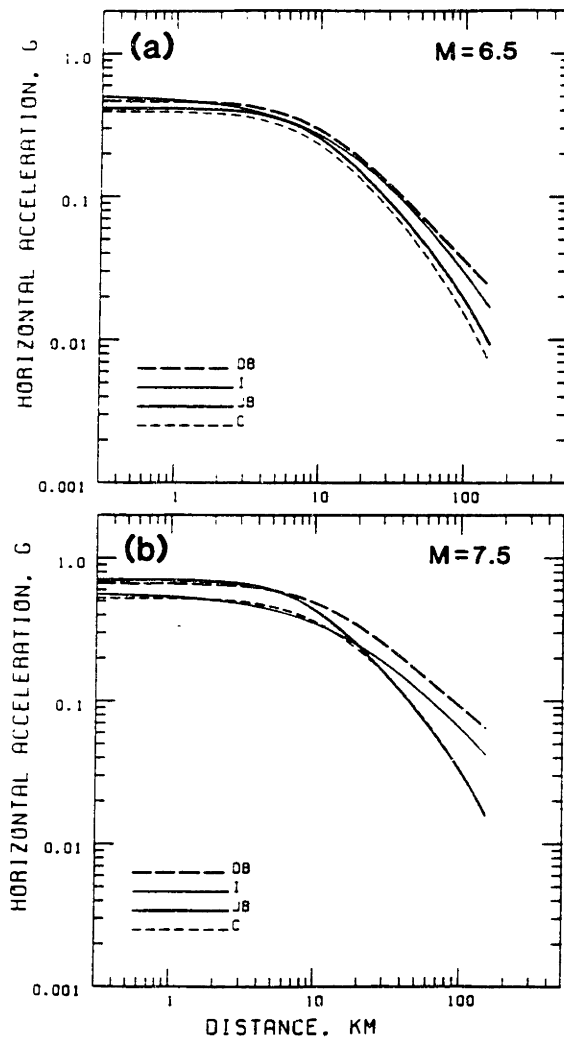


Figure 2-3

Comparison of Attenuation Equation Relationships. DB corresponds to Donovan and Bornstein (1978); I to Idriss (1987); JB to Joyner and Boore (1982); and C to Campbell (1985). (After Joyner and Boore, 1988)

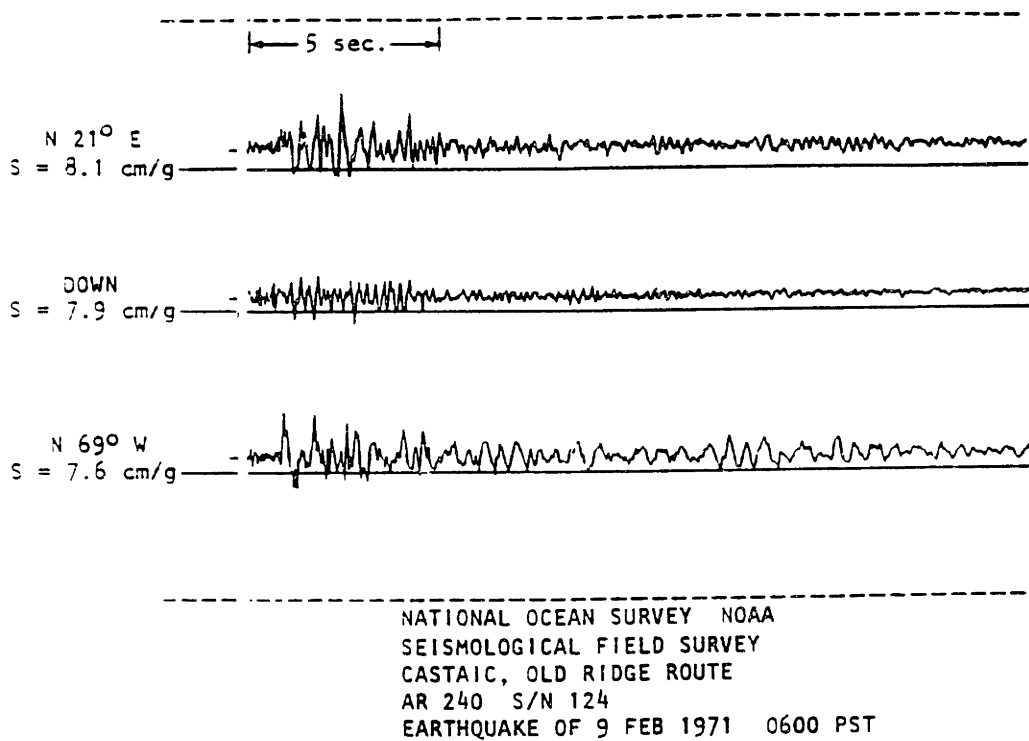


Figure 2-4 Typical Accelerograph Record (after Seed and Idriss, 1982)

SAN FERNANDO EARTHQUAKE FEB 9, 1971 - 0600 PST
 11-1 137 71.135.0 15910 VENTURA BLVD., BASEMENT, LOS ANGELES, CAL. COMP S81E
 ● PEAK VALUES: ACCEL = 140.2 CM/SEC/SEC VELOCITY = -16.1 CM/SEC DISPL = -7.1 CM

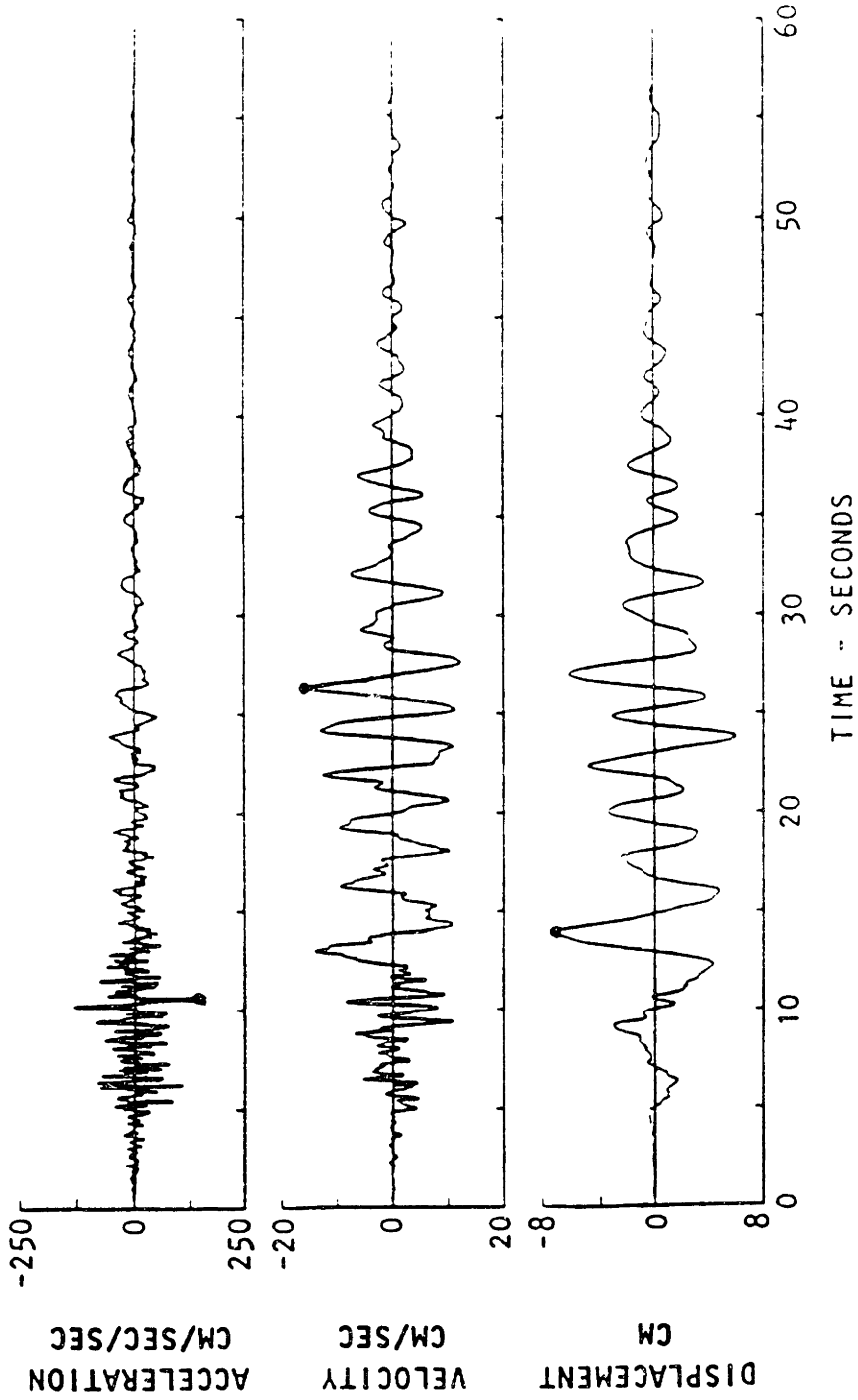
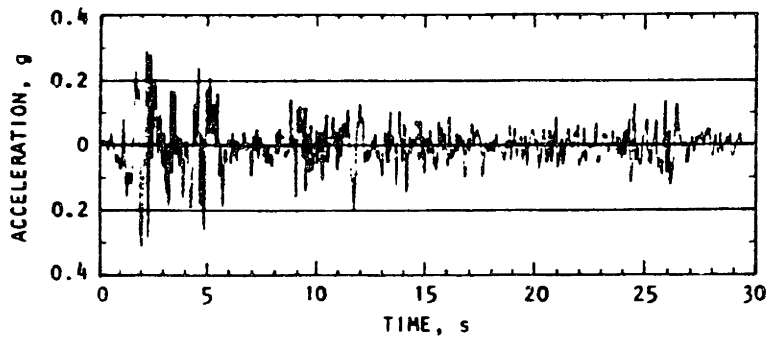
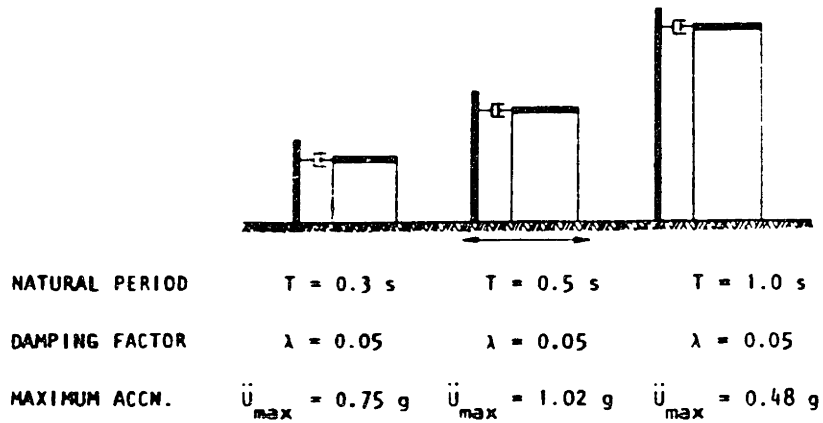
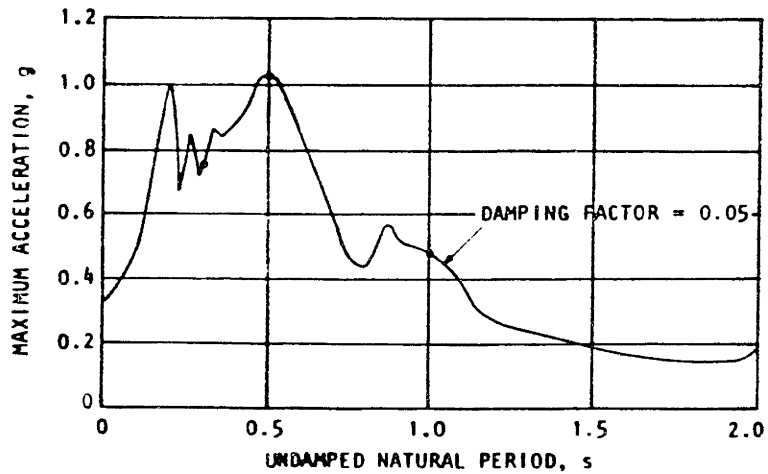


Figure 2-5 Typical Accelerogram and Integrated Velocity and Displacement Time Histories. (After Seed and Idriss, 1982)



ACCELEROGRAM, EL CENTRO, CALIFORNIA EARTHQUAKE, MAY 18, 1940
(N-S COMPONENT)



ACCELERATION RESPONSE SPECTRUM, EL CENTRO GROUND MOTIONS

Figure 2-6 Illustration of Importance of Structural Period on Response.
(After Seed and Idriss, 1982)

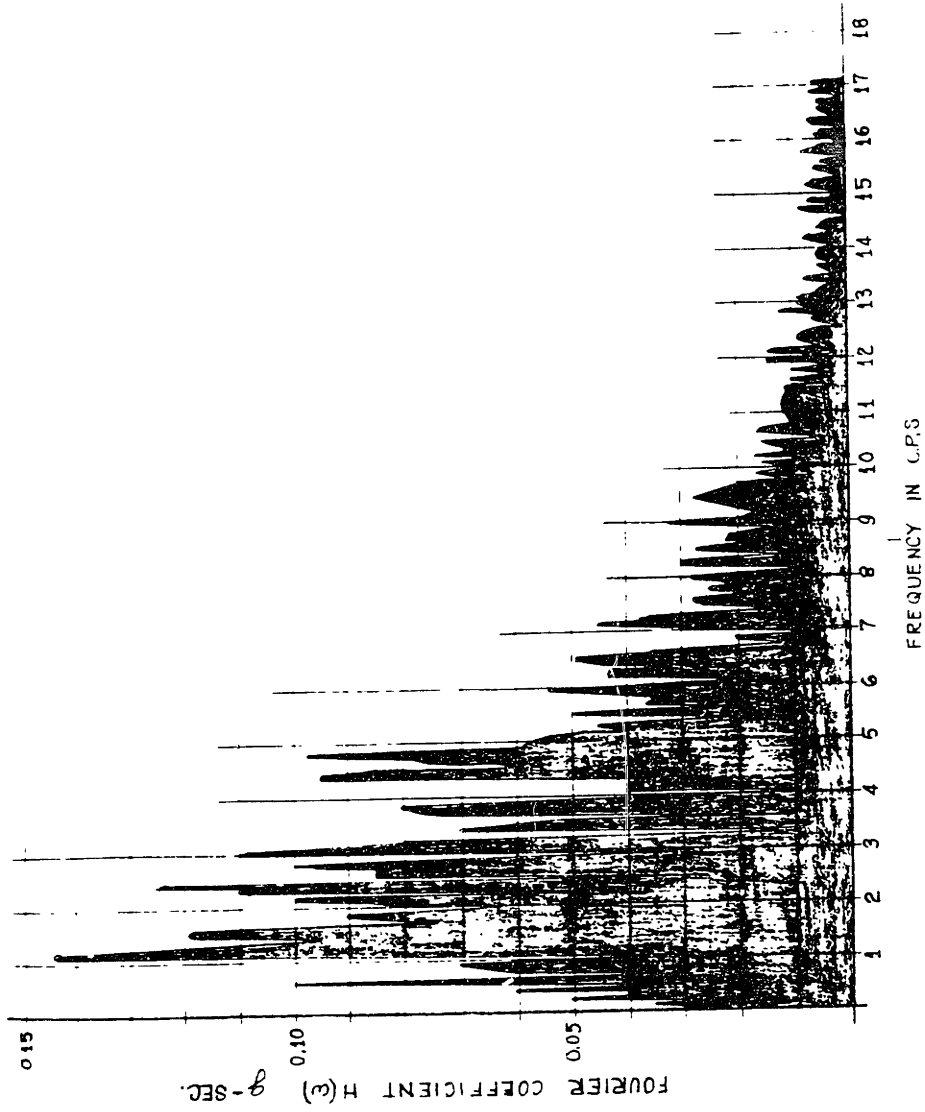


Figure 2-7 Typical Example of Fourier Spectrum. (After Roesset and Whitman, 1969)

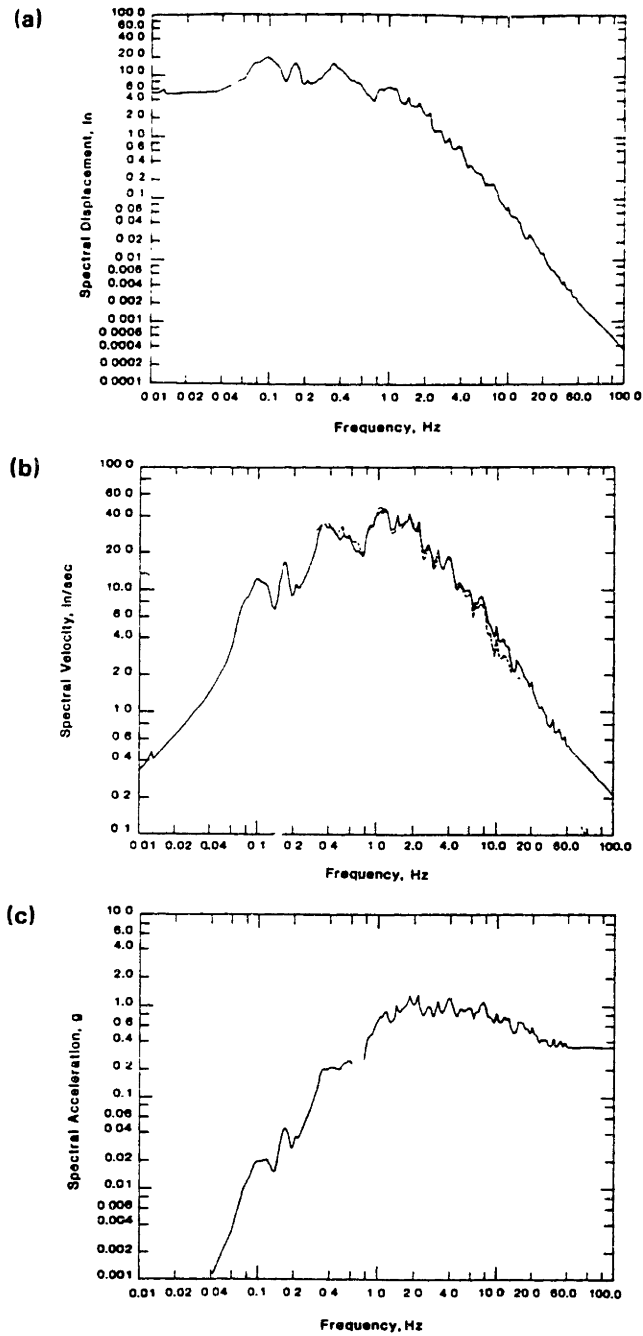


Figure 2-8 Displacement, Velocity, and Acceleration Response Spectra for El Centro earthquake (1940) S00E Component; damping ratio = 0.02. (After Gupta, 1990)

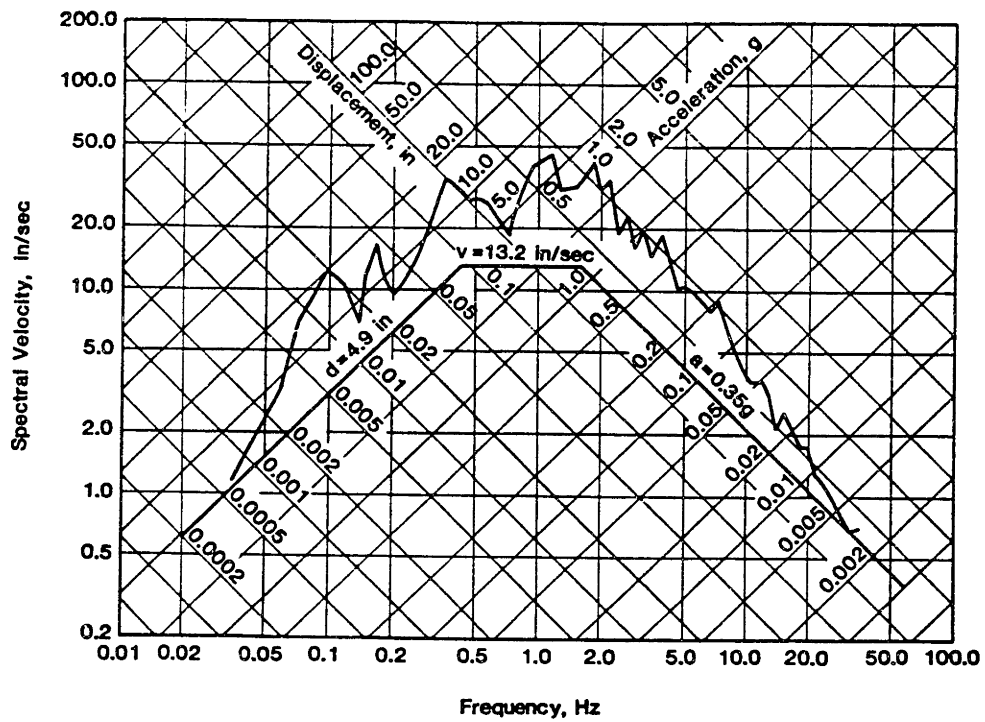


Figure 2-9 Tripartite Response Spectrum for El Centro earthquake (1940) S00E Component; damping ratio = 0.02. (After Gupta, 1990)

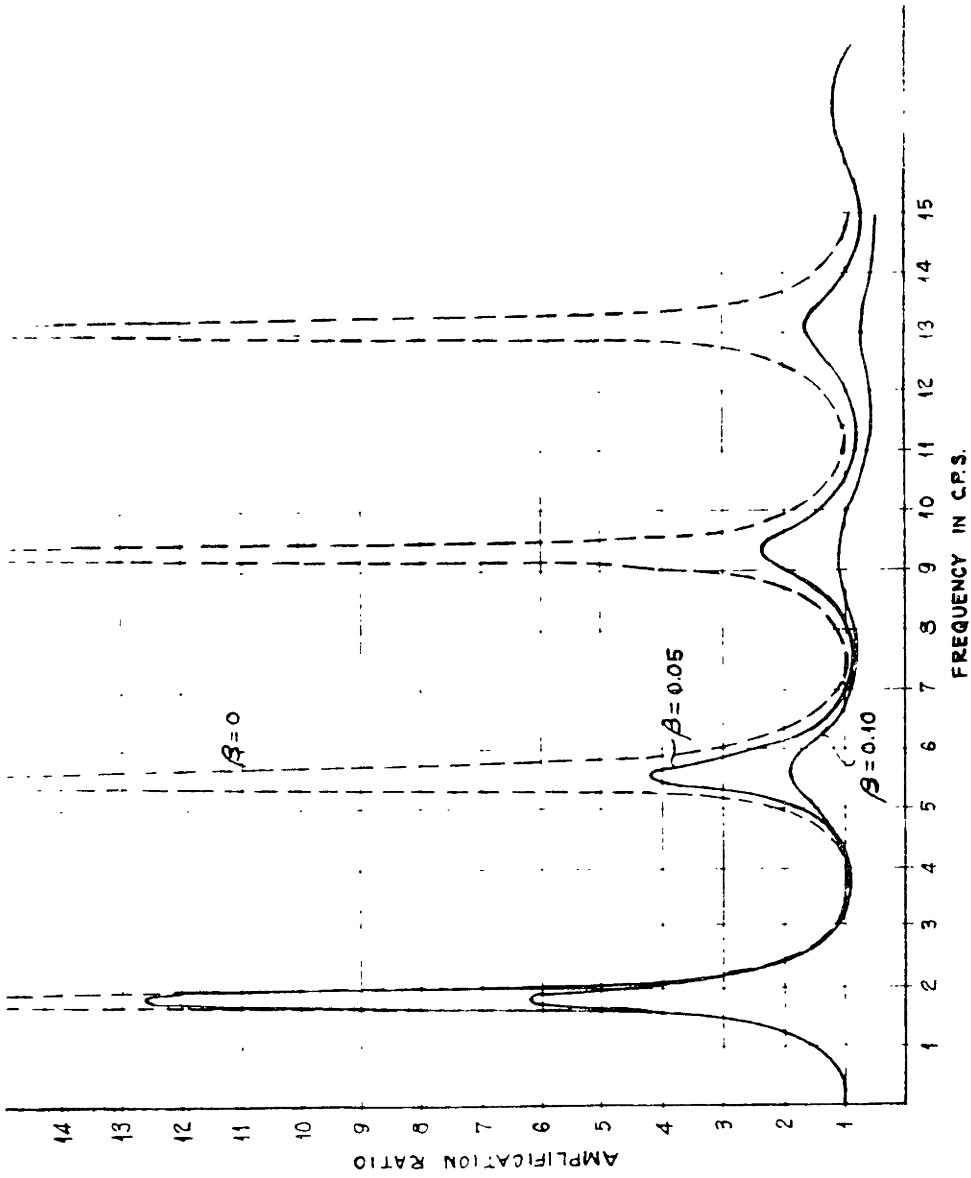


Figure 2-10 Amplification Curve for Shallow Uniform Soil Profile, Rigid Base Rock, and Constant Damping Ratio. (After Roesset and Whitman, 1969)

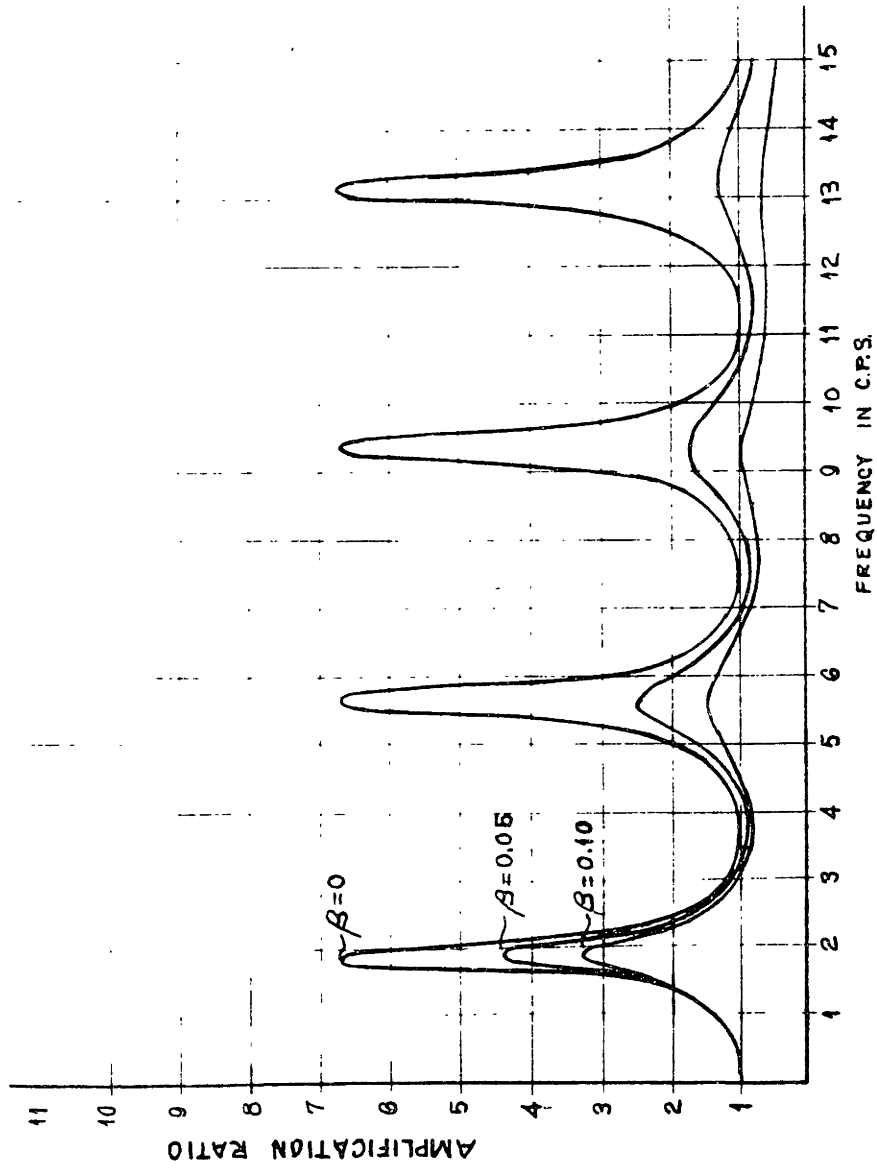


Figure 2-11 Amplification Curve for Shallow Uniform Soil Profile, Elastic Base Rock, and Constant Damping Ratio. (After Roesset and Whitman, 1969)

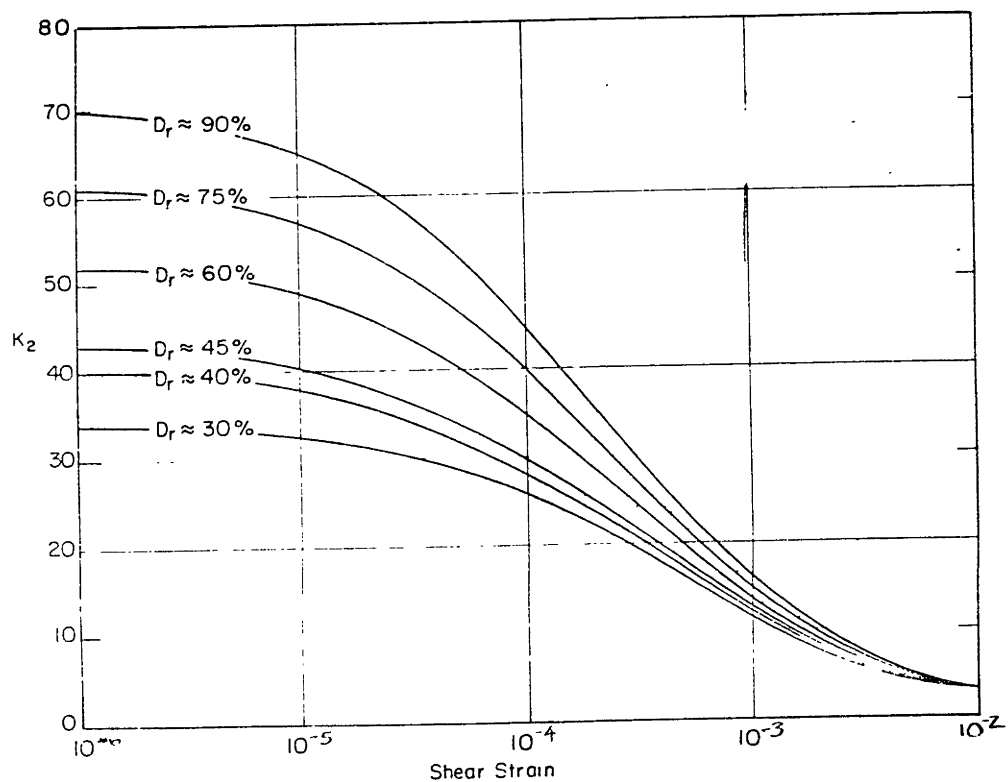


Figure 2-12 Variation of Normalized Shear Modulus and Damping Ratio with Level of Shear Strain. (After Seed and Idriss, 1970)

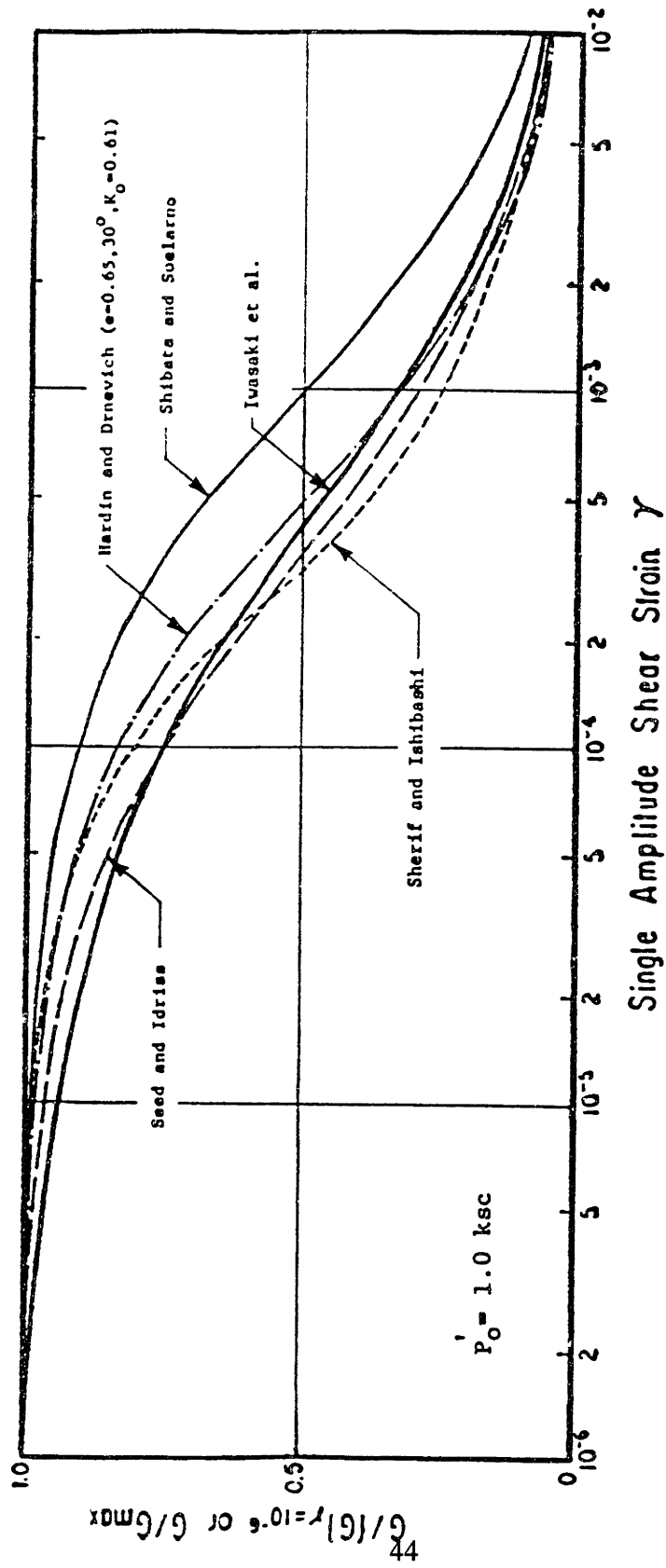


Figure 2-13 Comparison of Normalized Modulus Reduction Relationships for Sand (After Iwasaki et al, 1978)

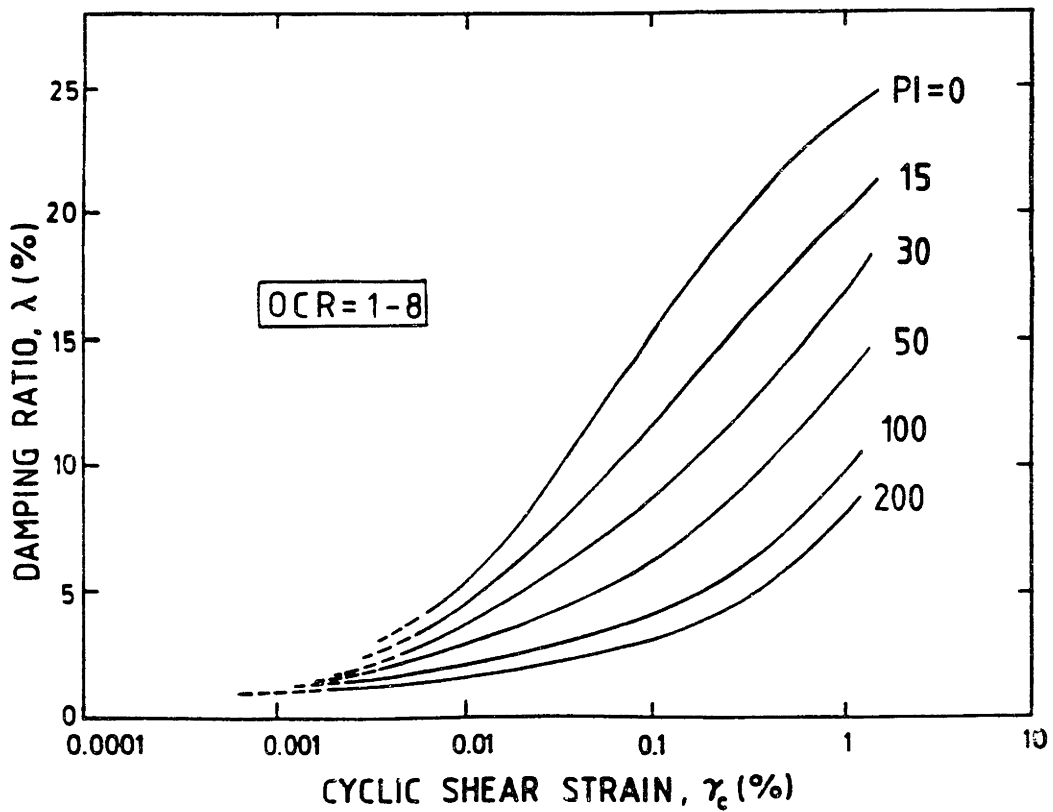
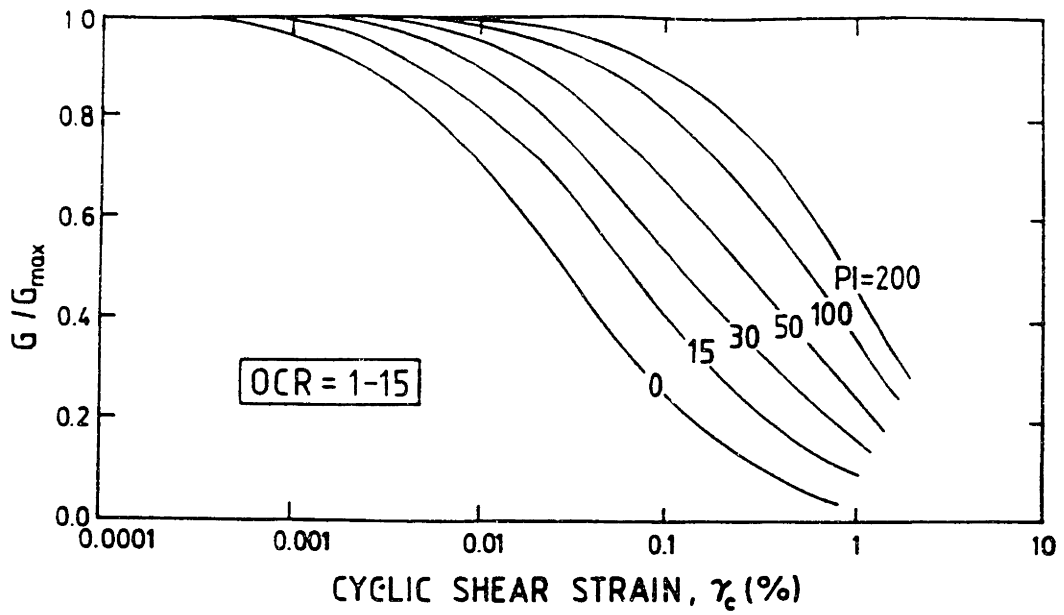
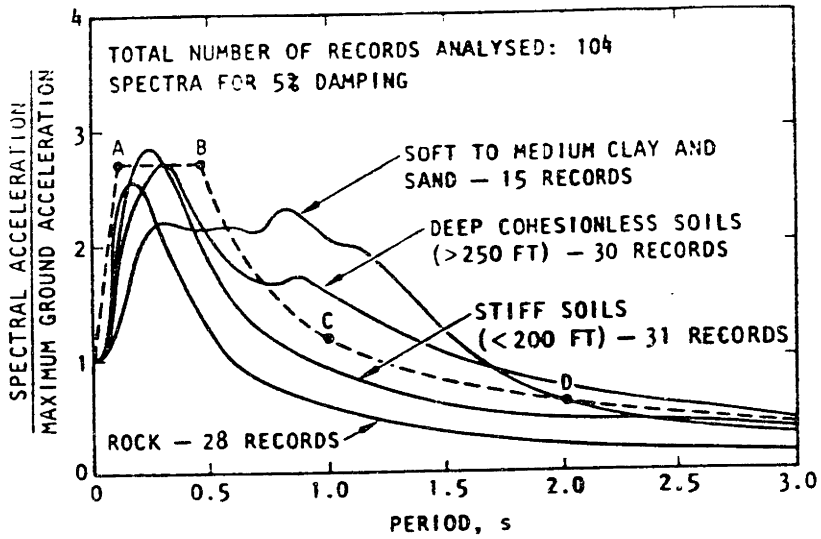
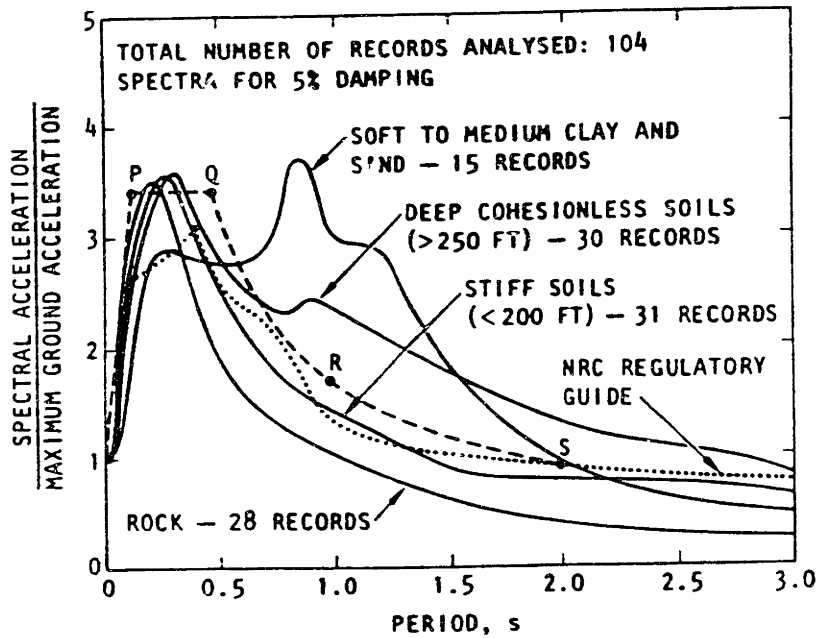


Figure 2-14 Variation of Normalized Shear Modulus and Damping Ratio with Level of Shear Strain and Plasticity Index. (After Dobry and Vucetic, 1991)



Average acceleration spectra for different site conditions.



84th percentile spectra for different site conditions.

Figure 2-15 Empirical Normalized Response Spectra for Different Site Geological Conditions. (After Seed and Idriss, 1982)

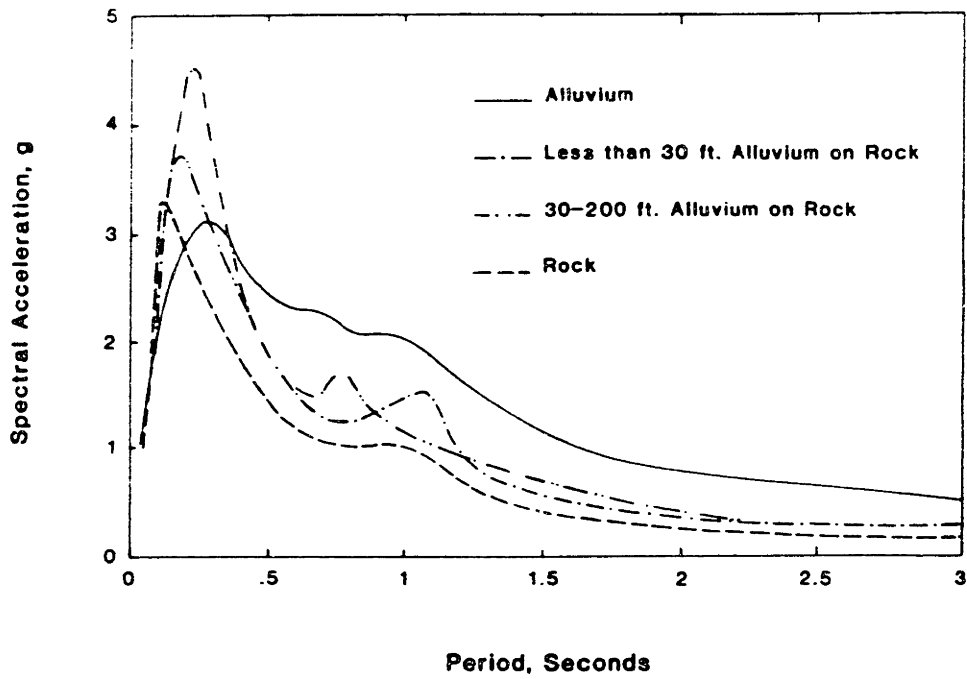


Figure 2-16 Average Empirical Spectra for Different Geological Conditions (After Mohraz, 1976)

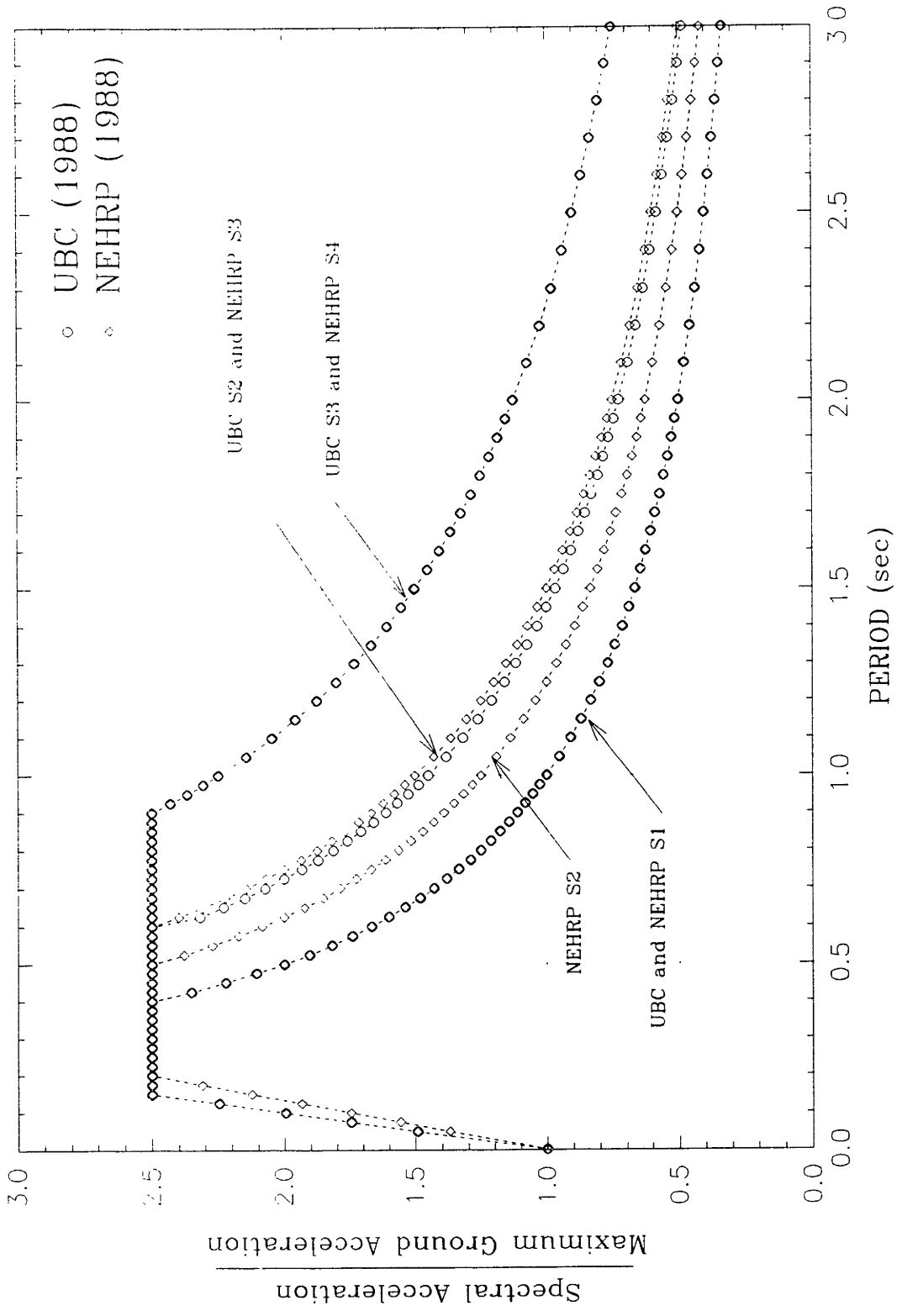


Figure 2-17 Comparison of UBC and NEHRP Design Response Spectra.

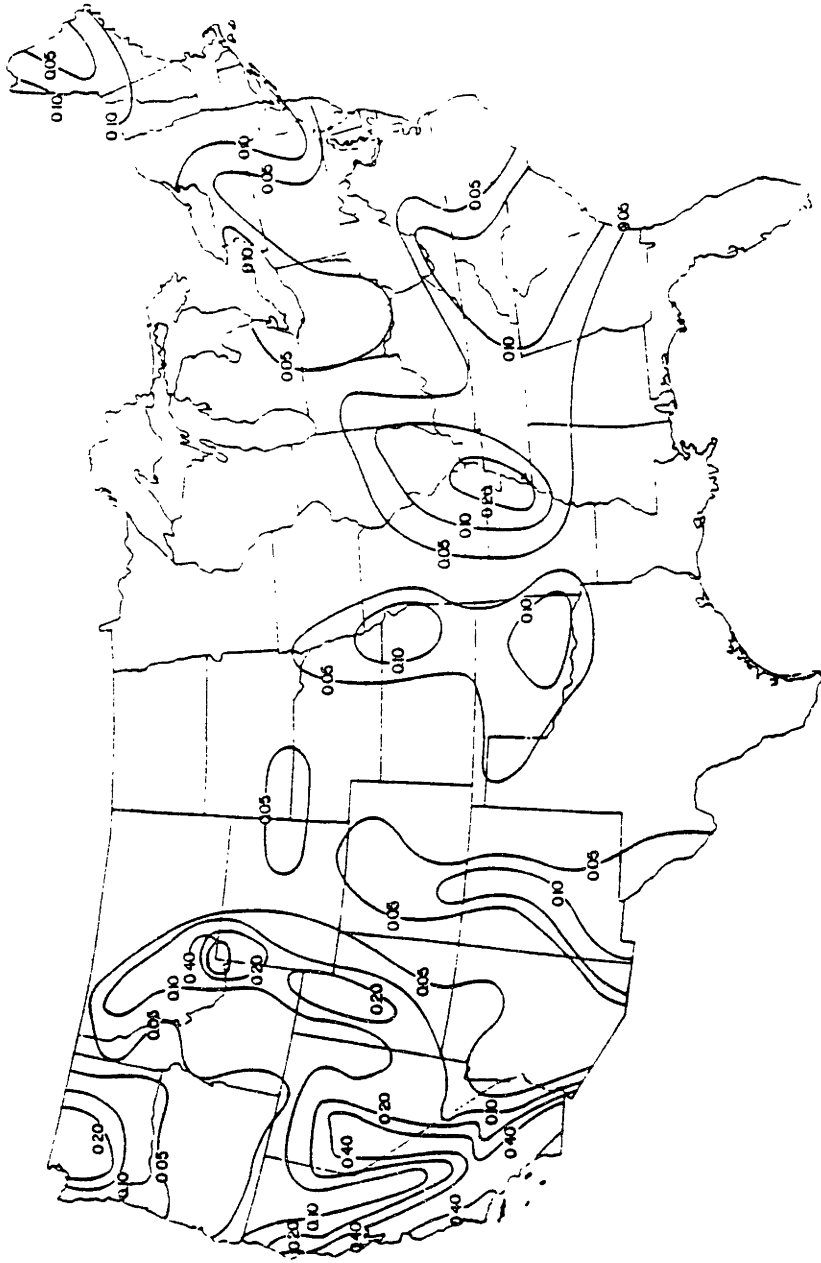


Figure 2-18 Contour Map of Effective Peak Acceleration in the continental United States for a nominal recurrence interval of 500 years. (After BSSC, 1988)

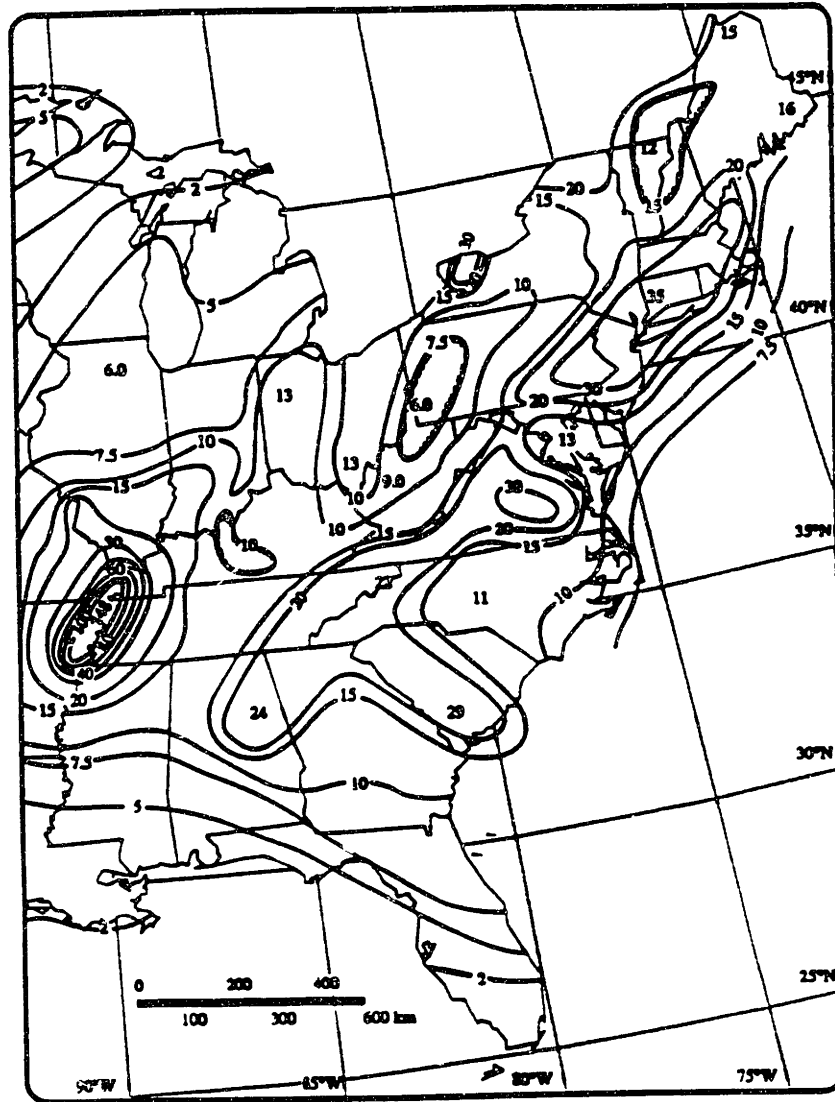


Figure 2-19 Contour Map of Spectral Acceleration for 0.3 second period, covering the eastern United States. (After Algermissen and Whitman, 1991) 50

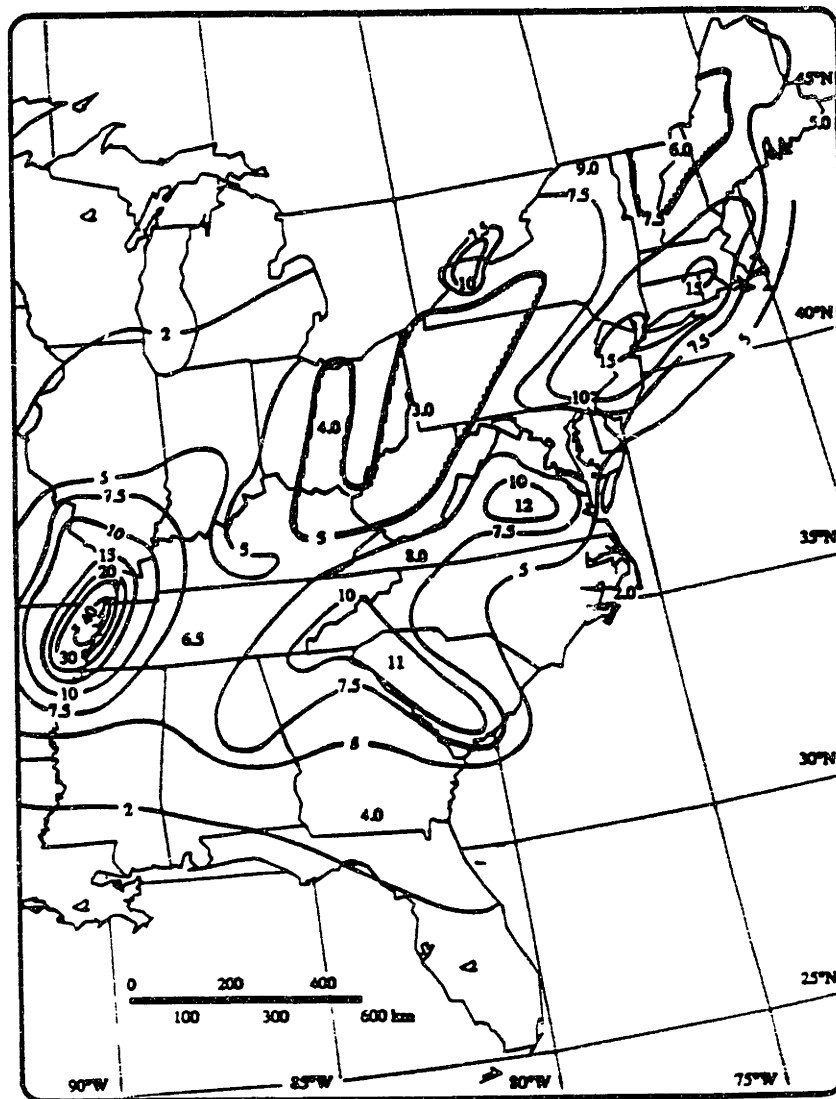


Figure 2-20 Contour Map of Spectral Acceleration for 1.0 second period, covering the eastern United States. (After Algermissen and Whitman, 1991)

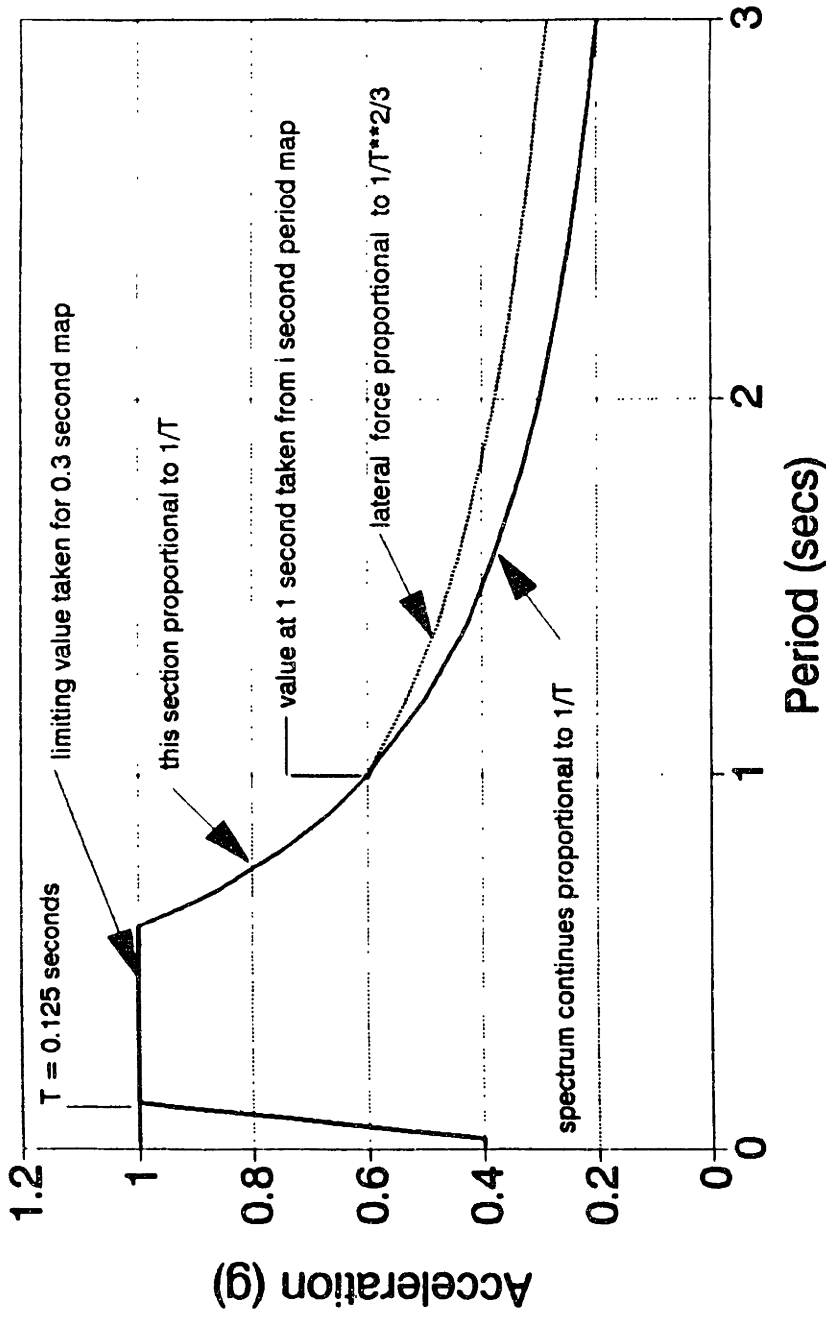


Figure 2-21 Approximate Method of Computing a Design Response Spectrum from only Two Spectral Ordinates. (After Donovan, 1991)

Table B-1

Soil Categories	
Type	Description
0	Bedrock < 20 ft deep
1	Shallow stream valley deposits (less than 20 ft deep), loess, residual soil, or till, where the depth to bedrock is less than 200 ft. (Firm to very hard or medium dense to very dense soil.)
2	Same as above, except depth to bedrock > 200 ft.
3	Stream valley deposits: 20 ft < depth < 50 ft. (potentially with > 20 ft of soft clay and with loose sand and silt)
4	Potentially soft glacial lake deposits: 20 ft < depth < 50 ft. (potentially with > 20 ft of soft clay or clayey silt)
5	Stream valley deposits, depth > 50 ft. (potentially with > 20 ft of soft clay, and with loose sand and silt)
6	Potentially soft glacial lake deposits, depth > 50 ft. (potentially with > 20 ft of soft clay or clayey silt)

Table B-2

Estimated Soil Amplification Factors, Based on Soil Categories				
Peak Bedrock Acceleration	Type 0	Types 1 & 2	Types 3 & 4	Types 5 & 6
0.1 g	1.0	1.2	1.8	2.4
0.3 g	1.0	1.1	1.2	1.3
0.5 g	1.0	1.0	0.9	0.9

Figure 2-22 Proposed Alternative Site Factor Provisions Utilizing a Matrix of Factors. (After Woodward Clyde et al, 1991)

CHAPTER 3

SITE CATEGORIES QUESTIONNAIRE

A questionnaire was sent to 35 experienced researchers and professionals in the seismic engineering field during July and August, 1991. The purpose of the questionnaire was to collect information on the use of current site categories, to investigate the kinds of problems experienced, and to obtain suggestions for improvement. A copy of the questionnaire is shown in Figure 3-1. and a summary of the geographical distribution of the sendees is shown in Figure 3-2.

3.1 Discussion of Results

Responses were received for nine different metropolitan areas or regions: Anchorage AK; Vancouver BC; San Francisco CA; New England; St Louis MO; Portland OR; Memphis TN; Salt Lake City UT; and Seattle WA. Fourteen people replied and one person provided details of three different Metropolitan areas, thus making a total of 16 responses. The geographical distribution of responses is shown in Figure 3-3, and the results are summarized in Figures 3-4 through 3-7.

It can be seen from Figure 3-4 that S2 and S3 soil profiles are more commonly encountered than S1. This supports the conclusion of a workshop (Whitman, in preparation) that S2 instead of S1 should be the reference category with a soil factor of 1.0.

The results in Figure 3-5 indicate that in general, there is seldom difficulty in assigning sites to categories. It was anticipated that more problems would be described by the respondents, although the lack of difficulty may be due to the fact that geotechnical engineers are used to making judgements with limited information.

Figure 3-6 describes the wide variation in peak ground acceleration used around the US, which generally corresponded to UBC provisions. Figure 3-6 also indicates that site specific response studies are rarely carried out, although their use is becoming

more common.

Figure 3-7 summarizes suggestions for alteration of the current categories and definitions. It can be seen that many of the suggestions related to the S4 site category, about which there seems to be considerable uncertainty. It should be noted that although many alterations to code criteria were suggested, several respondents considered the current code provisions satisfactory.

SITE CATEGORIES QUESTIONNAIRE

4 Can you suggest better definitions for standard site categories?

SITE CATEGORIES QUESTIONNAIRE From _____ Organization _____ Metropolitan Area _____

If you have experience in more than one metropolitan area, please xerox this sheet and complete these tables for each area

1 TYPICAL SITE CONDITIONS -1

Within the metropolitan area where you have the most experience, how often are sites encountered that fall into?

	Never	Very seldom	Fairly often	Often	Always
S1	___	___	___	___	___
S2	___	___	___	___	___
S3	___	___	___	___	___
S4	___	___	___	___	___

Please check the appropriate box on each line.

How often do you encounter serious difficulties in deciding which site category to assign to a site?

	Never	Very seldom	Fairly often	Often	Always
	___	___	___	___	___

Please describe the types of sites that give difficulties.

2 What peak ground acceleration is now typically assumed for design of projects in your area? Does this acceleration apply atop rock (how hard?) or atop soil (what category of soil?)

3 How common is it to perform site-specific response analyses in your area?

	Never	Very seldom	Fairly often	Often	Always
	___	___	___	___	___

5. Do you feel that the relative soil factors assigned to the current categories are reasonable? If not, what would you suggest?

Figure 3 -- 1 Site Categories Questionnaire

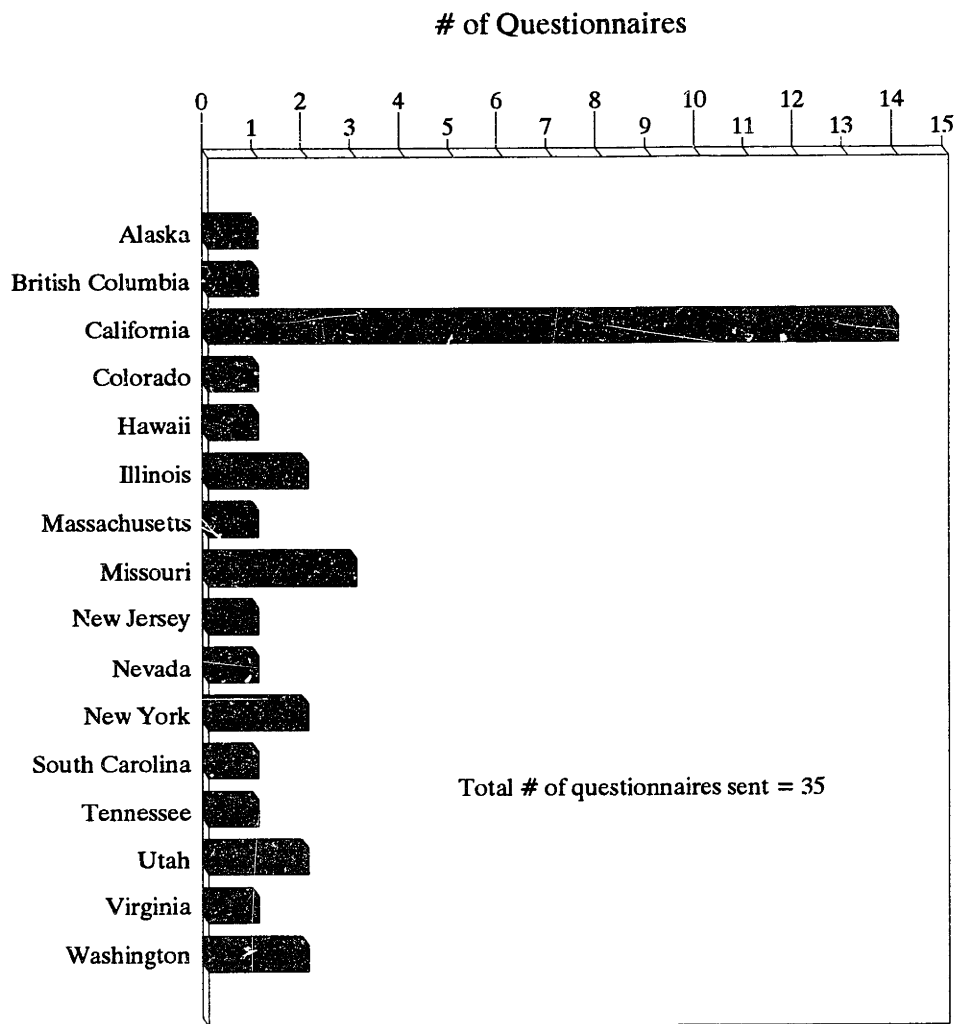


Figure 3-2 **Geographical Distribution of Questionnaire Sendees**

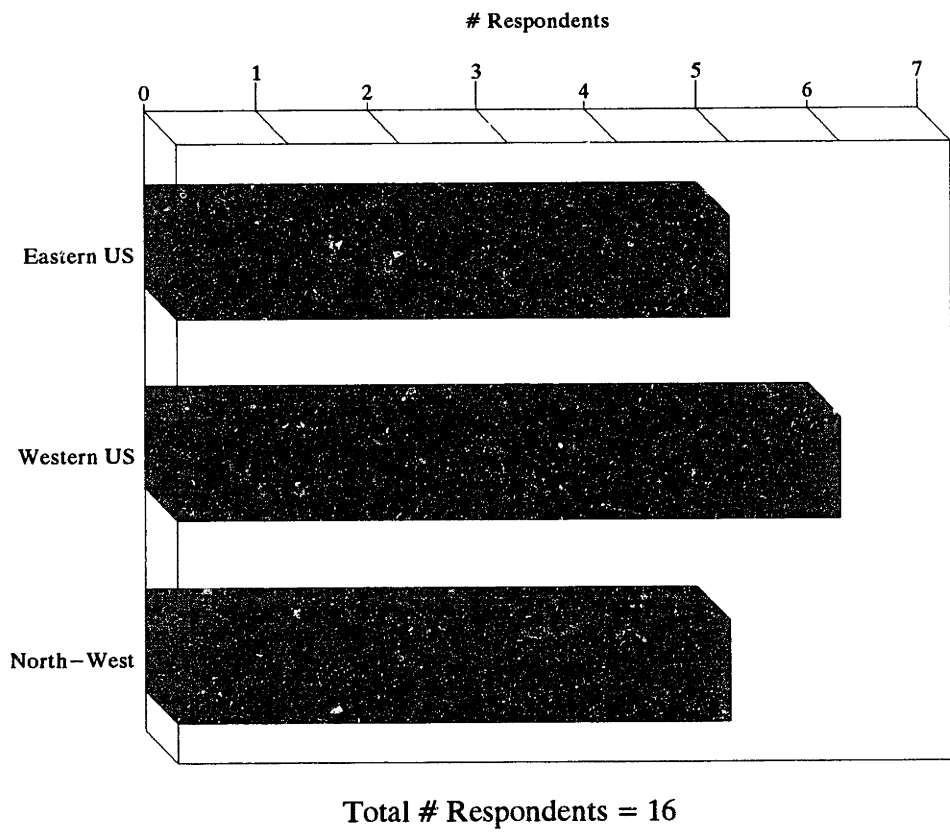


Figure 3-3 Geographical Distribution of Questionnaire Respondents

Q. How Often Do Sites Fall into the Current Code Categories ?

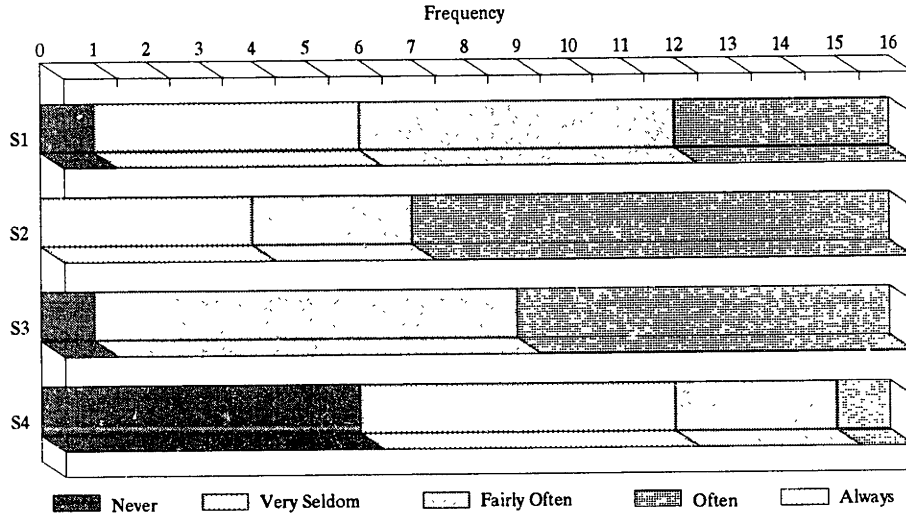
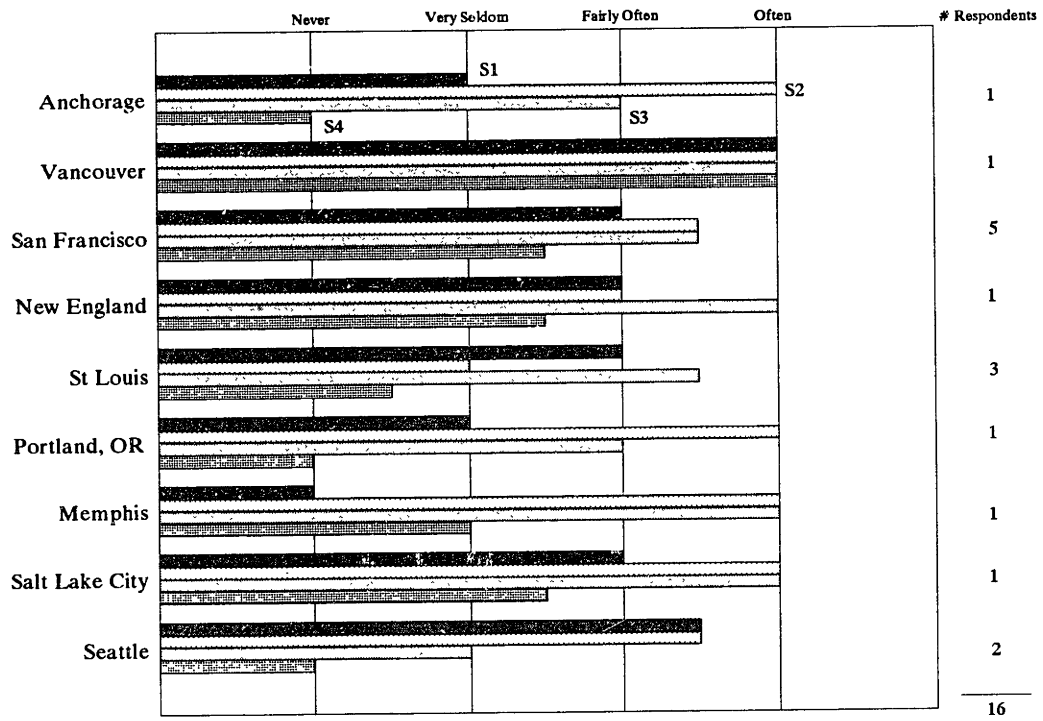
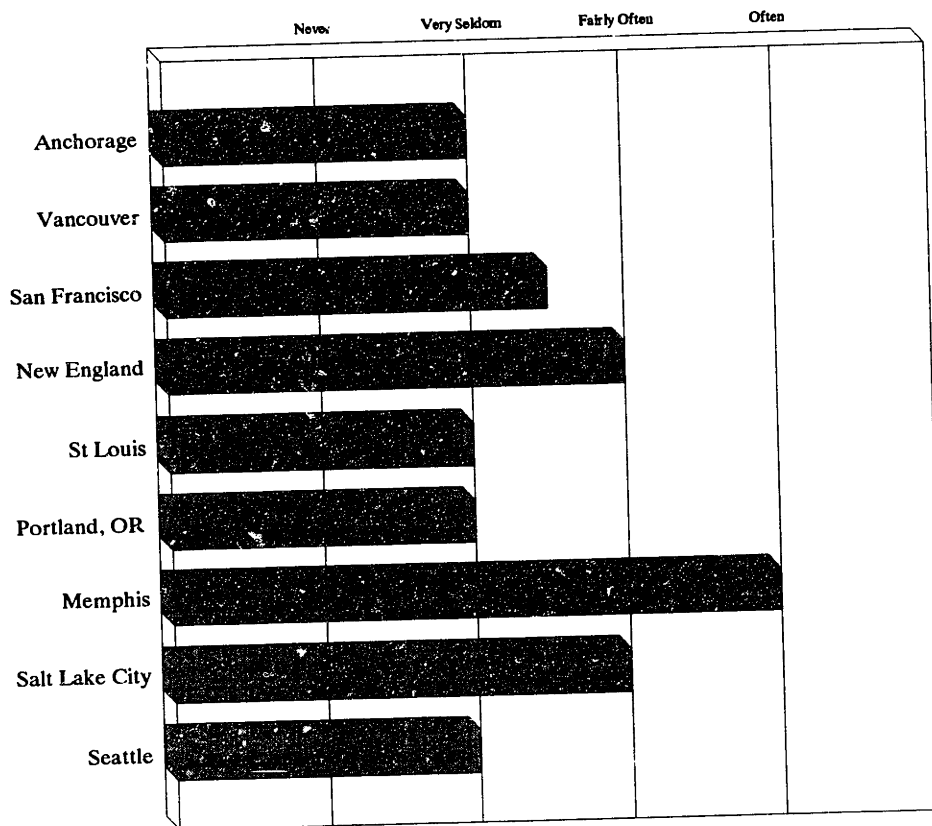


Figure 3-4 Summary of Results of Site Categories Questionnaire: Frequency of Occurrence of Different Categories

Q. How Often Are Problems Encountered in Assigning Sites to Site Categories ?

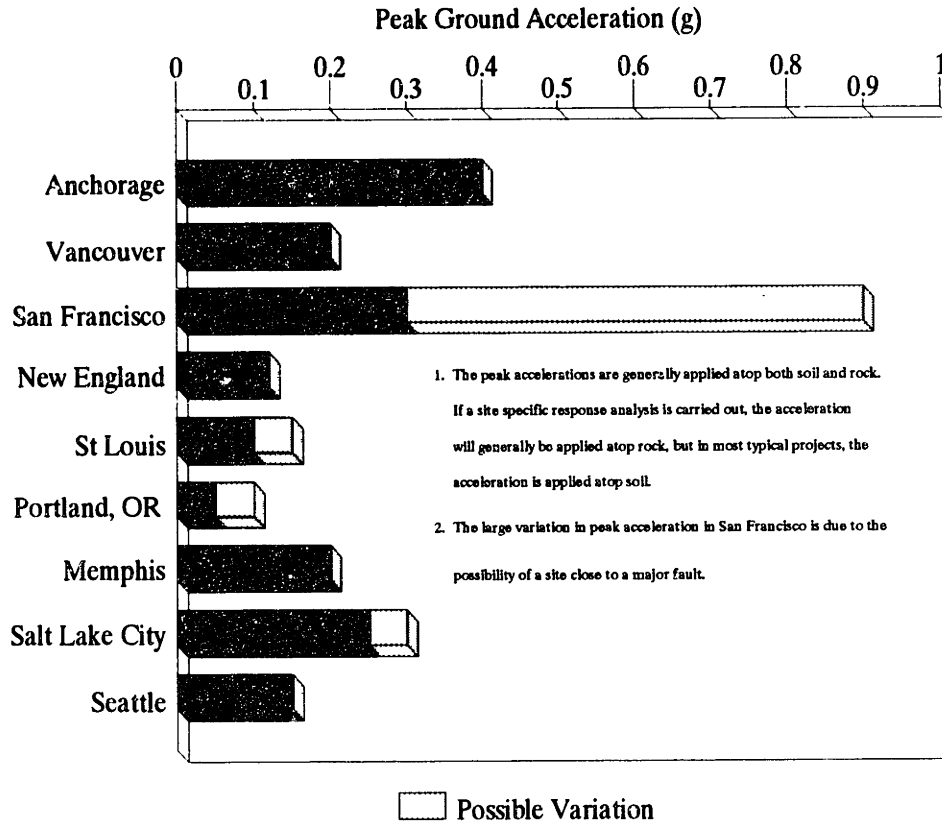


Q. What Types of Sites Cause Difficulties ?

- Very deep but stable deposits, such as stiff alluvium, which can be classified as S2 or S3, or hard glacial till or residual soils which can be S1 or S2
- Some sand deposits which may be prone to liquefaction and are strictly not classified as S3 or S4
- Sites with variable layering, particularly unstable soft deposits interbedded with stiffer layers
- Soft relatively unstable deposits underlain by very deep stiffer material

Figure 3-5 Summary of Results of Site Categories Questionnaire:
Sites which Cause Difficulty

Q. What Peak Acceleration is Typically Used in Design Projects ?



Q. How Common Is It to Perform Site Specific Response Analyses in Your Area?

- In general, site specific responses are very rarely carried out.
- In the Western US and Northwest, particularly since the Loma Prieta Earthquake, it is becoming fairly common to carry out site specific response analyses for high rise buildings, highway bridges and other major public works projects
- Liquefaction studies are carried out fairly often, particularly in San Francisco

Figure 3-6 Results of Site Categories Questionnaire: General Information on Site Specific Response Studies.

Q. Can You Suggest Better Definitions for Standard Site Categories?

- The soil period could be incorporated into the construction of response spectra
- Profiles could be a function of shear wave velocity, depth and velocity contrast
- Clearer definitions of loose, stiff etc. are required, possibly by using SPT N60
- There could be a separate category for rock instead of including it with shallow stiff soils
- The S2 site category should have an upper limit of the soil profile depth
- The definition for clay in S4 should include a plasticity index or factor
- S4 should be changed to include thickness of clay > 10 feet
- S5 could be added to include Clay thickness > 40 feet
- Soft clay in S4 should have shear wave velocity defined between 200 and 250 fps, instead of 500 fps as currently
- The confusion arising from different definitions in different codes needs to be cleared up
- The site category could be tied to peak bedrock acceleration as well as to soil type and thickness
- Since amplification is non-linear in zones of high seismicity (high pga), and soft sites attenuate or "limit" accelerations, simple rules for limiting pga as a function of soil strength could be introduced

Q. Are the Relative Soil Factors for Current Categories Reasonable ?

- The current ratios are satisfactory
- The response spectrum shape should be included instead of just a factor
- For the eastern US, the peak ground acceleration is evaluated for hard rock condition while site categories use soft rock as reference site.
- The factor for rock is probably too high in the longer period range, because it is lumped in with shallow stiff soils
- There is a lot of uncertainty about the factors for soft soil sites, S3 and S4, and these should be revised as more information becomes available
- The current ratios for S4, particularly in the 0.5 to 2.0 second period range, underestimate spectral accelerations, which may provide a dis-incentive to carry out site specific response analyses.
- The factor for S4 should be increased to 2.5

Figure 3-7

**Summary of Results of Site Categories Questionnaire:
Suggested Alterations to Current Code Criteria**

CHAPTER 4

SHAKE ANALYSES OF TYPICAL SOIL PROFILES

A site specific response analysis was undertaken for nine typical soil profiles in five major metropolitan areas: Boston; Memphis; St Louis; San Francisco; and Seattle. The response spectra computed were then compared with several other methods for generating surface response spectra: UBC 1988; NEHRP 1988; NEHRP 1991; and a similar method to NEHRP 1991 incorporating soil period (Donovan 1991). The site specific response analyses were undertaken using the SHAKE program.

4.1 Description of SHAKE

The SHAKE program (Schnabel and Lysmer, 1972) provides one of the simplest methods to calculate site response, and has been used extensively since it was first developed. The program computes the response in a soil profile from the continuous solution to the wave equation, considering vertically propagating shear waves through horizontal soil layers resting on an elastic half space. Earthquake motions are considered by use of the Fast Fourier Transform algorithm and can be specified at any layer, but are normally input at the top of the underlying elastic half-space.

The properties of the soil layers are characterized by the thickness, h , density ρ , shear modulus G , and damping ratio β . Figure 4-1 describes the input required by SHAKE. For clays, the small strain shear modulus is taken as constant over the depth of the layer and is specified by the user for each layer. From the following relationship,

$$C_s = \sqrt{(G/\rho)} \quad (\text{Eq. 4.1})$$

either the shear wave velocity (C_s) or the shear modulus can be specified. In this study, if field measurements of the shear wave velocity were available, these data were used; if only shear strength data were available, the following relationship was

used to prepare the input modulus:

$$G = 1600 S_u \quad , \quad (\text{Eq. 4.2})$$

where S_u is the undrained shear strength.

For sands, the shear modulus has been shown to vary with confining stress, and SHAKE uses the following relationship to calculate G:

$$G = 1000 K_2 \sqrt{\sigma_0} \quad , \quad (\text{Eq. 4.3})$$

where σ_0 is the effective confining stress and K_2 is a factor depending on relative density which is specified by the user. Table 4-1 provides details of K_2 for different relative densities.

The shear modulus and damping ratio are non-linear functions of the level of shear strain, and an equivalent linear analysis (Idriss and Seed, 1968) is used to compute the appropriate values. This is an iterative process in which initial estimates of soil properties are input into a linear analysis to calculate shear strains, which are then used to obtain a better estimate of the soil properties, and the process is repeated until the initial and computed values converge. Effective strains are used in this analysis since for earthquake motions an average level of strain rather than simply the peak value will determine the soil properties. For this study, an effective strain of 0.65 times the peak strain was used.

The main advantage of the SHAKE program is its simplicity. The wide extent of its use has resulted in the availability of detailed documentation of its accuracy and its limitations (Constantopoulos et al 1973, Finn et al 1982, Shannon and Wilson et al, 1980, Martin and Seed 1982). Numerous other programs, such as MASH (Martin & Seed, 1978), permit non-linear analysis by direct integration in the time domain, but more detailed soil properties are required, and the studies cited above have proven the accuracy of the equivalent linear method. One well-documented fault with the equivalent linear method is the attenuation of motions in the high frequency range above 5 to 10 cps, which is caused by overestimating the soil damping

(Constanopoulos et al, 1973, Martin and Seed, 1982). Figure 4-2 provides details of one comparison of SHAKE with more rigorous solutions.

The SHAKE program employs a total stress analysis and does not take into account build-up of pore pressure in saturated cohesionless soils. Other programs, such as DESRA incorporate this effect, although SHAKE produces comparable results as long as pore pressure build-up is not large (Finn et al, 1982).

Since SHAKE is a one-dimensional analysis, the effects of sloping layers or variable half-space cannot be included.

4.2 Description of Soil Profiles and Local Seismicity

The soil profiles and properties were developed from information provided by respondents to the Site Categories Questionnaire and from appropriate professional papers. Details of the soil properties and the local seismicity for each profile investigated are as follows:

Boston: Two profiles were selected in downtown Boston from an earlier study by Wysocky (1990), and are shown in Figure 4-3. Both would be strictly classified as S1 under usual site category definitions, because the shear wave velocity of Boston Blue Clay is around 575 fps and the S4 category is typically limited to clays with shear wave velocities less than 500 fps. Clearly, however, the soft Boston Blue Clay will cause some amplification of earthquake motions in the same manner as other soft clay deposits. The bedrock is argillite which is relatively hard when unweathered and provides a high impedance ratio. The seismicity of the north-eastern United States (NEUS) is often characterized by assuming a random, homogeneous distribution in space, because no conclusive relation between earthquakes and mapped faults has been established (Jacob, 1990). Earthquake return periods are estimated to be in the hundreds of years (Wysocky, 1990). In New England, the largest earthquake experienced since settlement in the 1600's was the Cape Ann Earthquake of 1755 which is estimated to have been around magnitude 6, with Modified Mercalli Intensities of VII in Boston (Wysocky, 1990). More recently, the Saguenay

earthquake in Quebec in 1988 had a magnitude of 6.0 and Modified Mercalli Intensity of VII (Wysockey, 1990). Figure 4-4 describes the seismicity of the Boston area.

St. Louis: One profile representative of downtown St. Louis was analyzed and is shown in Figure 4-5. It comprises stable deposits of sand, silt, and clay and would be classified as S1 according to UBC 1988. The bedrock below downtown St. Louis is hard crystalline limestone which creates a high impedance ratio. It should be noted that the bedrock surface is highly irregular, and a detailed site response analysis would have to include two or three dimensional effects.

The main source of seismic hazard to the St. Louis area is the New Madrid fault region in south-eastern Missouri, the site of the famous 1811 and 1812 earthquakes. They are still the most severe earthquake known to have been experienced in North America, and have been estimated at Modified Mercalli Intensity of IX in St. Louis (Nuttli, 1973). The New Madrid fault zone is around 200 km south of St. Louis, and a summary of the seismic activity from 1974 to 1988 is shown in Figure 4-6.

Memphis: Two profiles from Memphis were analyzed and are shown in Figure 4-7. The Memphis area is in the central part of the Mississippi Embayment and has no well-consolidated rock deposits down to depths of around 3000 feet. Because of the large depth to hard rock, the profiles are classified as S2. They present a problem in carrying out a site response analysis, since the modification of the input motions will depend on the elevation at which they are applied. The input elevation was selected at the base of the Jackson formation at around 200 foot depth (Ng et al, 1989).

Memphis is around 100 to 150 km from the New Madrid fault zone which is shown in Figure 4-6, and was discussed in the previous section.

San Francisco: Three profiles from San Francisco were analyzed and are shown in Figures 4-8. They comprise a broad range of sites, from the S2 profile which is typical of many Californian sites to the S4 site representative of many waterfront areas. Profile #3 is interesting in that with a depth of soft clay of 50 feet, it would be classified as S3 according to the NEHRP definitions and S4 according to UBC.

San Francisco is, of course, located in the most seismically active region in the United States, with numerous near surface faults documented and monitored. The San Francisco earthquake of 1906 with a Richter Magnitude greater than 8 (Singh 1991), and the recent Loma Prieta earthquake in 1989 with a shear wave magnitude of 7.1, are two of the main seismic events to have occurred in recent times. The location of the Loma Prieta earthquake and the major faults contributing to the seismicity of the San Francisco area is shown in Figure 4-9.

Seattle: One typical profile from Seattle was analyzed and is shown in Figure 4-10. This is from downtown Seattle with deep overconsolidated glacial deposits to depths of around 300 feet and relatively soft sandstone bedrock below this. The profile is classified as S2.

The Seattle area is one of the most seismically active regions in the United States, due to the relative proximity of the Cascadia Subduction Zone. Subduction zone earthquakes of magnitude 6 are estimated to have a return period of between 5 and 10 years, and there have been two earthquakes in the last fifty years with magnitudes greater than or equal to 6.5 (Ho et al, 1991). Large subduction zone earthquakes with long recurrence intervals are also considered likely. The geological factors contributing to the seismicity of the area are illustrated in Figure 4-11.

4.3 Dynamic Soil Properties

The version of SHAKE used in this study allowed one modulus and damping versus shear strain relationship each to be input for clay and for sand.

The relationships used for sand were those proposed by Seed and Idriss (1970), and shown in Figure 2-12. The relationships used for clay were those proposed by Dobry and Vucetic (1991) and are shown in Figure 2-14.

4.4 Selection and Scaling of Input Earthquakes

The selection and scaling of input earthquakes is a particularly difficult task. Ideally, a seismic hazard analysis at each location, such as described by Jacob (1990) for New York City, would be carried out. This would yield estimates of earthquake magnitude and epicentral distance for a given return period, and would be used with attenuation relationships to derive a response spectrum and values of peak acceleration and velocity for rock. Earthquake records which conformed to these computed criteria would then be selected from a database, and input into the SHAKE program.

Unfortunately, the above procedure is not really practical for this study, particularly with respect to selection of earthquakes to the estimated criteria, since an extensive database, especially for EUS earthquakes, does not exist. In addition, a detailed seismic hazard study for each city analyzed is beyond the scope of this study. Consequently, a simplified procedure for selection and scaling of input earthquakes was employed, and the limitations of this method will be discussed.

Input earthquakes were obtained from the National Center for Earthquake Engineering (NCEER) database at Lamont Doherty Geological Observatory (Friberg et al, 1990), and details of the earthquakes are summarized in Table 4-2. Appendix A contains acceleration time histories and computed response spectra as well as other pertinent information about the records. It was decided to use only recorded earthquakes because of well-documented problems with some synthetic records (e.g. Christian 1988, Singh, 1986). The records were selected primarily on the basis of site geology, earthquake magnitude, and peak ground acceleration. Only records described as being recorded on sites immediately overlying bedrock were selected in order to eliminate any soil modification prior to input into SHAKE. The records were obtained primarily from sites described as free-field or single story structures to minimize any effect of structures on the recorded motion. In order to obtain records with energy levels and durations representative of a major earthquake, only records from earthquakes with a magnitude greater than around 6.0 were selected.

For the Boston, St Louis and Memphis profiles, only earthquakes recorded on "hard" rock sites were selected, in order to account for eastern attenuation characteristics. Because of the above selection criteria, there were only a limited number of eastern US records available (in fact, only those from Saguenay 1988), and earthquakes recorded on hard rock sites in California, as well as subduction zone events in Alaska and Chile were used.

For San Francisco profiles there were generally sufficient earthquake records on "soft" rock sites satisfying the above criteria, although there were few with sufficiently high peak accelerations.

For the Seattle profile, only subduction zone events were employed, but no records were available from the Puget Sound area, so records were obtained from Alaskan, and Central and South American events.

Since earthquakes around magnitude 6.0 were selected at various epicentral distances and with different peak ground motion parameters, depending on the seismicity of the site location, different return periods or hazard levels would be implied by the analyses. It was attempted to obtain records from an epicentral distance similar to the main anticipated seismic source for each site, but this was not possible due to the scarcity of available records. It was therefore necessary to scale the records by an appropriate factor so that uniform hazard spectra could be obtained.

A technically sound and rigorous way to modify the input earthquakes would be to scale by peak velocity, and, after examining the resulting time histories and response spectra, to manually edit the acceleration time histories to remove undesirable peaks or frequency components (Singh, personal communication). This procedure clearly requires considerable judgement and experience, and would be very time-consuming.

Another alternative procedure would be to scale by trying to match the earthquake response spectra to a design rock spectrum, such as UBC S1. However, clearly the spectra would match over only part of the design spectrum, and interpretation of the results would be difficult. In addition, the UBC S1 design spectrum is representative of shallow stiff soil and may not be reasonable for "hard" rock sites.

For this study it was decided to simply scale the records by peak acceleration. The main problem with this procedure is that the earthquake response spectrum is amplified in a different manner at different periods; at low periods acceleration is amplified predominantly, while at intermediate and long periods, velocity and displacement respectively are amplified. Consequently, by scaling the peak acceleration, a distortion of the longer period response will occur.

In addition, recent recordings at the SMART-1 array in Taiwan indicate that measurements of peak acceleration are spatially highly variable, even over distances around 10 to 20 metres, while peak velocity and displacement appear to be more stable (Singh, personal communication).

Scaling by peak acceleration does have the advantages of providing a consistent procedure among the different profiles, and it is also simple, practical and commonly used. In addition, the problems are understood, and a qualitative assessment of the deficiencies in the results can be made. Furthermore, ratios of response spectra will be computed which will to some extent reduce the distortions introduced by this scaling procedure.

The peak acceleration for normalization of the input record was obtained from the effective peak acceleration contour map published in the NEHRP Recommended Provisions (BSSC, 1988) and is included as Figure 4-12. This hazard map is based on a nominal return period of 500 years, the same as the code design elastic response spectra. Effective peak acceleration is defined in Figure 4-13, and although it is not necessarily the same as peak rock acceleration, the difference is sufficiently minor to allow its use in this study.

Table 4-3 provides details of the input earthquakes and the scaling factor used to modify the peak acceleration for each profile.

4.5 Design Response Spectra

In order to evaluate the code response spectra, the results of the site specific response analyses were compared with the UBC and NEHRP 1988 provisions, and also with two methods based on probabilistic hazard maps: a method prepared for the NEHRP 1991 Recommended Provisions, and a similar method proposed by Donovan (1991).

The UBC and NEHRP response spectra were obtained by multiplying the normalized spectra in these publications by the appropriate effective peak acceleration taken from Figure 4-12, (i.e. the same acceleration which was used as input in the SHAKE analysis).

The design response spectra for NEHRP 1991 were computed using a method described in Algermissen and Whitman (1991) and were described in Chapter 2. The 0.3 and 1.0 second spectral acceleration maps used in the analyses were included previously as Figures 2-19 and 2-20. The spectral ordinates for Seattle and San Francisco are shown in Table 4-4.

The contour maps were developed for an S2 site, and so for other site categories, the final spectra were obtained by factoring the 1.0 second ordinate by the ratio of the site soil factor to 1.2 (the code S2 soil factor).

4.6 Site Specific Response Analyses

For each soil profile, ten different earthquakes were input at the surface of bedrock, and the base and ground surface response spectra were computed by SHAKE. The mean and the mean plus one standard deviation of the computed surface response spectra were then plotted against the code elastic design spectra and those generated by other methods.

The mean and the mean plus one standard deviation of the ratio of the surface to base response spectra (RRS) were then plotted to provide a measure of the amplification of the input ground motion by the soil profile.

The computed surface response spectra for the ten input earthquakes were also plotted and the UBC 1988 code spectrum for the soil profile shown for comparison.

The base response spectra for the input earthquakes were also plotted, with the UBC 1988 S1 profile shown for comparison.

4.7 Discussion of Results

The results of the site specific response analyses are shown on Figures 4-14 through 4-36.

In Figures 4-14, 4-16 and 4-19 for the Boston and the St Louis profiles, it can be seen that at periods less than 1.0 second the code design spectra are considerably less than the computed mean plus one standard deviation surface response spectrum. At periods between 0.5 and 1.0 second this is due to amplification at the site period which ranged from 0.6 to 0.9 seconds. At periods less than around 0.5 seconds this is due to the input earthquakes having spectral accelerations at low periods greater than 2.5 times the peak rock acceleration, and is demonstrated in Figures 4-18, 4-21.

A particular point to note from Figures 4-18 and 4-21, is the extent to which the Saguenay earthquakes, which are the largest recorded earthquakes in the EUS, are smaller than many of the other input earthquakes. It could be argued that the Saguenay records would have been more representative if higher input accelerations had been applied to them, but it is clear that distortions introduced by scaling by peak acceleration and by the choice of input earthquake have influenced the computed spectra markedly.

Of more interest therefore, are the plots of RRS, shown on Figures 4-14, 4-16 and 4-19. It can be seen that between periods of 0.5 and 1.0 seconds spectral ratios can be in excess of 4. This is in agreement with a previous detailed study of the Boston area (Wysockey, 1990), a summary of which is included as Figure 4-37. Spectral amplifications of four are important observations, since the code spectra assume that

for S1 sites, the surface and input response will be similar at low periods. (They are in fact assumed equal since S1 combines rock and stiff shallow profiles, but although the spectrum is representative of the stiff soil profile, spectral amplifications from rock to S1 sites of around 4 are not considered, with 1.5 a more reasonable estimate of the code provisions.)

The results for the Memphis profiles shown in Figures 4-22 through 4-26 indicate that the UBC and NEHRP code spectra by and large satisfactorily envelope the mean plus one standard deviation of the computed surface response spectrum, with spectral amplification reaching a maximum between 1.5 and 2 at longer periods.

The results for the three San Francisco profiles shown in Figures 4-27 through 4-33 also imply that the code spectra are satisfactory. At short periods the input motions are de-amplified, particularly for the softer sites, and the codes provide an overly conservative design.

The results for the Seattle profile shown in Figures 4-34 through 4-36 indicate that at low periods the code spectra are considerably less than those computed. This is probably due partly to source effects, with spectral accelerations at low periods from the subduction zone events being larger than 2.5 times the peak ground acceleration, as can be seen in Figure 4-36. However, there is also an influence from the selection and scaling procedures for the input earthquakes, because the computed mean response spectrum in Figure 4-38 is larger than that computed from recently derived attenuation equations for a magnitude 8.5 earthquake at 50 km epicentral distance (Crouse 1991), which is shown in Figure 4-38.

Comparing the Boston and St Louis results with those of the other profiles, the difference in the shape of the RRS is quite noticeable; for Boston and St Louis there is a fairly sharp peak around the natural period of the soil profile with spectral ratios in excess of 4, and decreasing to around 2 at other periods. For the other cities there is a general trend of increasing spectral ratio with period to maxima between 1.5 and 3. This difference in shape and magnitude is considered a result of the combination between the lower levels of shaking and the higher impedance ratios for the Boston and St Louis profiles. This will be discussed in more detail in Chapters 5

and 6.

It can also be seen from Figures 4-14 through 4-36 that, in general, the EUS cities with high impedance ratios and low levels of shaking are less well covered by existing codes. Clearly distortions arising from the selection and scaling of input records contribute to this, but these findings are in agreement with other research for New York (Jacob, 1990).

The probabilistic hazard maps of spectral acceleration from NEHRP 1991 in general seem to provide satisfactory design spectra, and although somewhat more conservative than current codes, typically provide similar spectra. The most notable difference between the current code and the NEHRP 1991 design spectra can be seen in the results for the San Francisco profiles; the NEHRP 1991 spectra provide a very conservative design, although this is probably due to the wide variation in anticipated ground motion in San Francisco. On the other hand, although more conservative than the code spectra for the Seattle site investigated, the NEHRP 1991 spectra showed good agreement with computed surface response using SHAKE.

The effects of the modification of the NEHRP 1991 spectra suggested by Donovan (1991) can only be seen in the San Francisco profiles analyzed, since the modification is only applicable to sites with a fundamental period greater than one second. It can be seen that the proposed modification produced very conservative results, especially for the S2 profile which had a site period around 2 seconds.

Several researchers have pointed to the impedance ratio as an important factor in site response in the EUS (e.g. Roesset and Whitman 1969), and called for its more explicit inclusion in building codes (Jacob 1990). The relevant theory was described in Chapter 2, and in order to investigate if any trend could be ascertained, for each earthquake analyzed, the peak RRS was plotted against the thickness weighted impedance ratio, and is shown in Figure 4-39. A trend can be observed, but this plot includes the effects of amplification from the soil column and from the level of shaking. The following chapter investigates the relative influences of these factors and analyzes the results from this chapter further.

Type of Soil	K2
Loose Sand	35
Medium Dense Sand	50
Dense Sand	70
Very Dense Sand	90
Very Dense Sand and Gravel	130–190

Values of Shear Modulus and Effective Confining Stress in Eq. 4.3 must be in psf to use the above factors

Table 4–1 Values of K2 factor for Use in Equation 4.3 to Calculate the Small Strain Shear Modulus of a Cohesionless Soil

Symbol	Event Parameters										Site Parameters			Trace Parameters			
	Name	Location	Mag	Mag	Mag	Mag	Mag	Mag	Location	Bedrock Type	Structure	Epicentral Distance (km)	Peak Acc'n (cm/sec ²)	Peak Acc'n (g)	Component		
			L	B	W	S	S										
AK1	Alaskan Subduction Zone	AK	N/A	7.6	6.5	N/A	N/A	N/A	Sitka Observatory, AK	Greywacke	Free-field	48.4	93.8	0.10	N90		
AK2	Sitka	AK	N/A	7.6	6.5	N/A	N/A	N/A	Sitka Observatory, AK	Greywacke	Free-field	34.6	91.3	0.09	N90		
AK3	Alaskan Subduction Zone	AK	N/A	7.6	6.5	N/A	N/A	N/A	Sanak, AK	N/A	N/A	46.9	110	0.11	N188		
AK4	Alaskan Subduction Zone	AK	N/A	7.6	6.5	N/A	N/A	N/A	Chernabura, AK	N/A	N/A	12.1	95	0.10	N343		
AND1	Andreanof Islands, Alaska	AK	N/A	N/A	N/A	7.1	7.1	7.1	Adak, AK	Basalt	N/A	68.6	162.6	0.19	N270		
ELS1	San Salvador	CA	N/A	5.0	N/A	6.9	6.9	6.9	Nat'l Geog Inst	Pumice	1-Story Bldg	13.6	391.6	0.40	N180		
IMP1	Imperial Valley 1979	CA	7.0	5.7	N/A	N/A	6.0	6.0	Superstition Mountain	Granite	1-Story Bldg	57.6	189.2	0.19	N135		
IMP2	Imperial Valley 1981	CA	N/A	5.5	N/A	N/A	6.0	6.0	Superstition Mountain	Granite	1-Story Bldg	25.5	102.5	0.10	N135		
LOM1	Santa Cruz Mtns (Loma Prieta)	CA	7.0	N/A	N/A	7.1	7.1	7.1	UCSC/LICK Lab	Limestone	1-Story Bldg	23.2	433.1	0.44	N0		
LOM2	Santa Cruz Mtns (Loma Prieta)	CA	7.0	N/A	N/A	7.1	7.1	7.1	Presidio	Serpentine	Free-Field	101.9	194.9	0.20	N90		
LOM3	Santa Cruz Mtns (Loma Prieta)	CA	7.0	N/A	N/A	7.1	7.1	7.1	Yerba Buena Island	Franciscan Melange	1-Story Bldg	98.9	65.8	0.07	N90		
LOM4	Santa Cruz Mtns (Loma Prieta)	CA	7.0	N/A	N/A	7.1	7.1	7.1	Rincon Hill, SF	Franciscan Melange	Free-Field	98.4	88.5	0.09	N90		
LOM5	Santa Cruz Mtns (Loma Prieta)	CA	7.0	N/A	N/A	7.1	7.1	7.1	Gavilan College	Sandstone, Shale, Chert	Instrument Shelter	21.8	433.6	0.44	N90		
MEX1	Michoacan, Mexico City	Mexico	N/A	6.3	N/A	7.6	7.6	7.6	La Villita	Tonalite	Free-field	40.2	280.4	0.29	N90		
MH1	Morgan Hill	CA	6.2	N/A	N/A	N/A	6.0	6.0	Gilroy #6, CA	N/A	1-Story Bldg	36.7	280.4	0.29	N90		
SAG1	Saguena	Quebec	N/A	N/A	N/A	N/A	6.0	6.0	Station 16	N/A	2-Story Bldg	43.1	128.7	0.13	N124		
SAG2	Saguena	Quebec	N/A	N/A	N/A	N/A	6.0	6.0	Station 20	N/A	Seismic Vault	90.4	123.1	0.13	N0		
SFER1	San Fernando	CA	N/A	6.2	N/A	N/A	N/A	N/A	Catic OR Route, CA	Sandstone	Instrument Shelter	27	265.4	0.27	N291		
VALP1	Valparaiso Central Chile	Chile	N/A	6.7	N/A	7.8	7.8	7.8	Valparaiso University	Volcanic	1-Story Bldg	26.2	162	0.17	N160		
VALP2	Valparaiso Central Chile	Chile	N/A	6.7	N/A	7.8	7.8	7.8	Papudo	Granite	1-Story Bldg	79.7	226.4	0.23	N140		
VALP3	Valparaiso Central Chile	Chile	N/A	6.3	N/A	N/A	7.2	7.2	Lillole Basement	Sandstone and Volcanic	1-Story Bldg	166.5	200	0.20	N10		
WHIT1	Whittier	CA	6.1	N/A	N/A	N/A	N/A	N/A	Garvey Reservoir	N/A	N/A	N/A	460	0.47	N330		
WHIT2	Whittier	CA	6.1	N/A	N/A	N/A	N/A	N/A	Pacifica	Tertiary Sandstone	1-Story Bldg	37.1	154.9	0.16	N90		

Table 4-2 Input Earthquakes for Shake Analyses

Earthquake			Trace Parameters					Amplification of Recorded Motion				
Symbol	Name	Site Location	Epicentral Distance (km)	Peak Acc'n (cm/sec ²)	Peak Acc'n (g)	Peak Velocity (cm/sec)	Peak Disp't (cm)	Boston 0.1g	St Louis 0.12g	Memphis 0.20g	San Francisco 0.4g	Seattle 0.2g
AK1	Alaskan Subduction Zone	Sitka Observatory	48.4	93.8	0.10	6.1	1.9	1.0	1.3	2.1		2.1
AK2	Sitka	Sitka Observatory	34.6	91.3	0.09	9.2	6.2	1.1	1.3	2.1		2.1
AK3	Alaskan Subduction Zone	Sanak	46.9	110.0	0.11	4.0	0.3					1.8
AK4	Alaskan Subduction Zone	Chernabura	12.1	95.0	0.10	7.0	2.0					2.1
AND1	Andreasof Islands, Alaska	Adak	68.6	182.8	0.19	7.9	4.1					1.1
ELS1	San Salvador	Nat'l Geog. Inst.	13.6	391.6	0.40	N/A	N/A					0.5
IMP1	Imperial Valley 1979	Superstition Mountain	57.6	189.2	0.19	9.0	1.8	0.5	0.6	1.0	2.1	
IMP2	Imperial Valley 1991	Superstition Mountain	25.5	102.5	0.10	7.6	1.9	1.0	1.1	1.9	3.8	
LOM1	Santa Cruz Mtns (Loma Prieta)	UCSC/LICK Lab	23.2	433.1	0.44	21.2	6.6	0.2	0.3	0.5		
LOM2	Santa Cruz Mtns (Loma Prieta)	Presidio	101.9	194.9	0.20	N/A	N/A					6.0
LOM3	Santa Cruz Mtns (Loma Prieta)	Yerba Buena Island	98.9	65.8	0.07	14.7	3.2					4.4
LOM4	Santa Cruz Mtns (Loma Prieta)	Rincon Hill, SF	98.4	88.5	0.09	11.6	3.2					4.4
LOM5	Santa Cruz Mtns (Loma Prieta)	Gavilan College	21.8	433.6	0.44	20.9	6.3					0.9
MEX1	Michoacan, Mexico City	La Villita	40.2	120.9	0.12	10.1	3.0					1.6
MH1	Morgan Hill	Gilroy #6	36.7	280.4	0.29	23.2	5.2					1.4
SAG1	Saguenay	Station 16	43.1	128.7	0.13	2.4	0.2	0.8	0.9	1.5		
SAG2	Saguenay	Station 20	90.4	123.1	0.13	4.2	0.3	0.8	1.0	1.6		
SFER1	San Fernando	Castic OR Route	27.0	265.4	0.27	27.5	9.0	0.4	0.4	0.7	1.5	
VALP1	Valparaiso Central Chile	Valparaiso University	26.2	162.0	0.17	14.8	3.2					1.2
VALP2	Valparaiso Central Chile	Papudo	79.7	226.4	0.23	N/A	N/A	0.4	0.5			0.9
VALP3	Valparaiso Central Chile	Loliso Basement	166.5	200.0	0.20	N/A	N/A	0.5	0.6	1.0		1.0
WHIT1	Whittier	Garvey Reservoir	3.0	460.0	0.47	N/A	N/A					0.9
WHIT2	Whittier	Pacolina	37.1	154.9	0.16	7.6	1.1					2.5
							#	10	10	9	9	10
							Max	1.1	1.3	2.1	6.0	2.1
							Min	0.2	0.9	0.5	0.9	0.5
							Avg	0.7	0.8	1.4	2.8	1.4
							Std	0.3	0.8	1.4	1.4	0.6

Note
Blank entries indicate soil profile was not analyzed for the earthquake

Table 4-3 Summary of Input Earthquake Time History Characteristics and Modifications for Input into SHAKE

90% Non-Exceedance (years)	Period (sec)	Spectral Acceleration (g)	
		Seattle	San Francisco
50	0.3	0.8	1.8-2.0
	1	0.35	1

**Table 4-4 Spectral Acceleration Values for Seattle and San Francisco
(After Perkins, D., personal communication)**

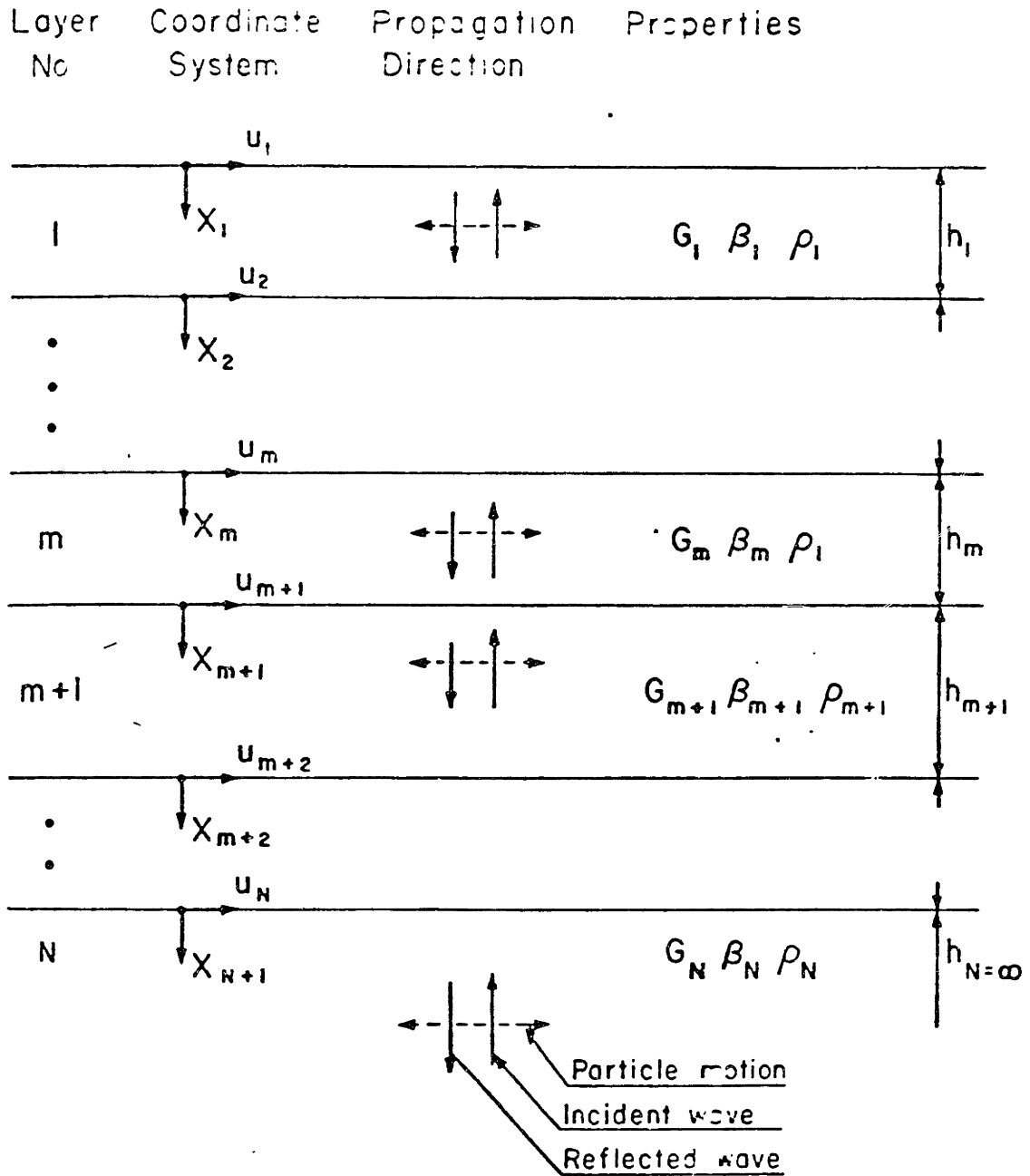
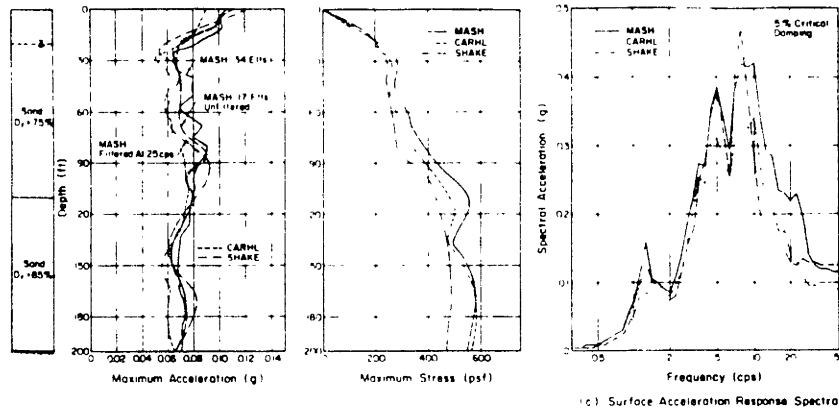


Figure 4-1 Outline of Soil Parameters Required by SHAKE. (After Schnabel et al, 1972)

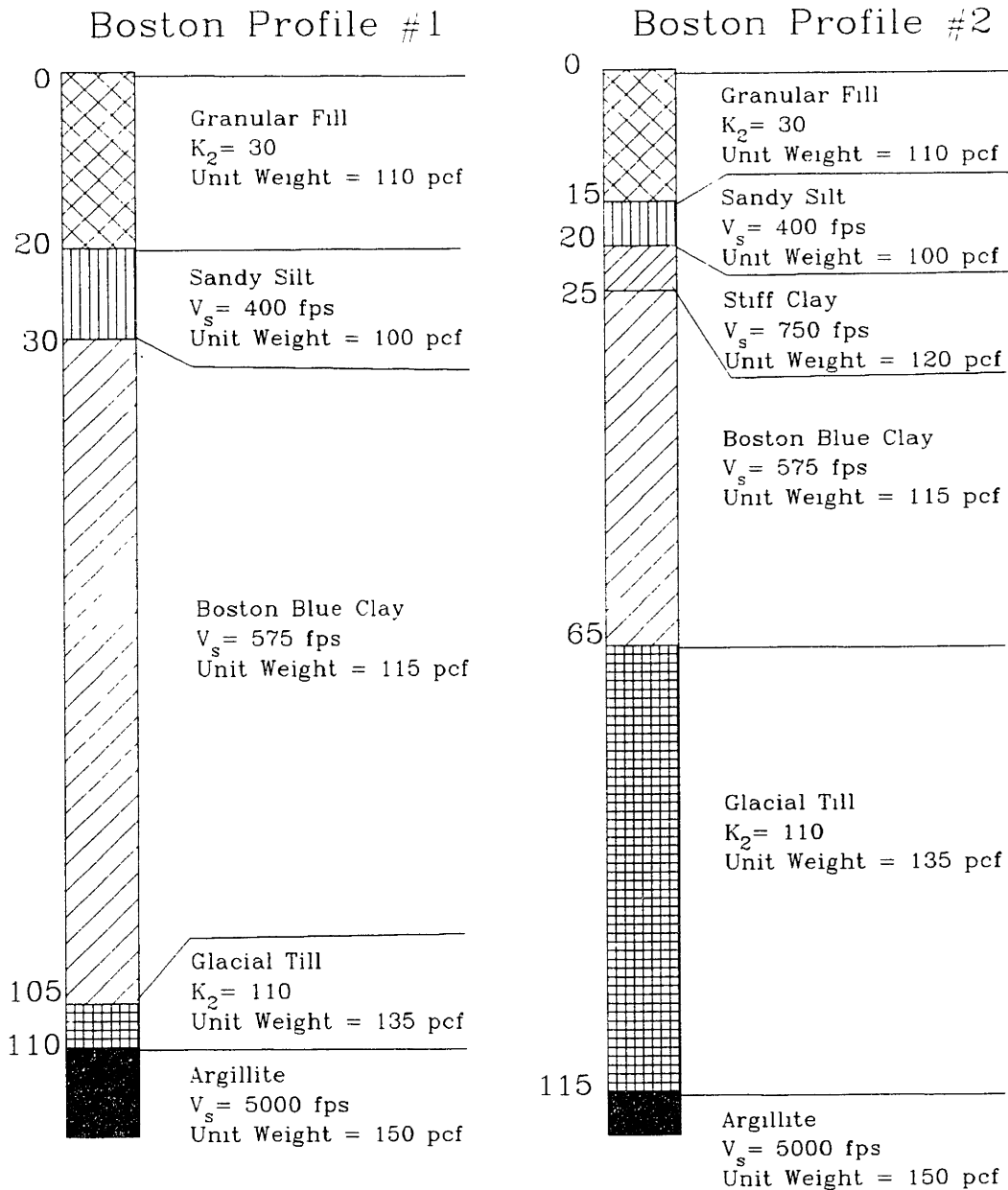


—Site Study No. 3—State Building, San Francisco

—Subjective Comparison between Methods of Analysis

Site (1)	Profile of maximum accelerations (2)	Profile of maximum shear stresses (3)	Shape of ground response spectra (4)
No 1—Melendy Ranch 100 ft dry sand 0.57 g at base	FAIR below 15 ft High rate of change of accelerations above 15 ft with depth from SHAKE not found in other methods	GOOD below 15 ft. Stresses 75% higher by SHAKE above 15 ft	GOOD for frequencies below 4 cps High attenuation by SHAKE of frequencies above 8 cps
No 2—Nigata 250 ft sand 0.15 g at base	GOOD between SHAKE and MASH. Lower accelerations by CARHL above 100 ft	GOOD	EXCELLENT below 5 cps Removal of higher frequencies by SHAKE
No 3—State Building, San Francisco 200 ft sand 0.07 g at base	EXCELLENT	EXCELLENT	EXCELLENT
No 4—Oron Boulevard 800 ft sand and gravel 0.26 g at base	GOOD to EXCELLENT	EXCELLENT	POOR between SHAKE and other methods—Removal of frequencies higher than 5 cps by SHAKE
No 5—Caraballeda, Venezuela 290 ft sand, sand and gravel clay 0.055 g at base	GOOD to EXCELLENT	GOOD to EXCELLENT	EXCELLENT
No 6—Palos Grandes, Venezuela 645 ft sand and gravel 0.050 g at base	EXCELLENT	GOOD to EXCELLENT	EXCELLENT below 5 cps. Removal of higher frequencies by SHAKE.

Figure 4-2 Comparison of results from SHAKE with results from more rigorous analyses. (After Martin and Seed, 1982)



Notes:

1. For granular soils the shear modulus is calculated from the equation $G = 1000K_2 \sqrt{\sigma_0}$, where G = shear modulus, σ_0 = effective confining stress, and K_2 is shown above
2. V_s = shear wave velocity.
3. All depths are in feet
4. Both profiles would be strictly classified as UBC S1, although the soft Boston Blue Clay will amplify seismic motions in a manner similar to an S3 or S4 site
5. The thickness-weighted fundamental period before shaking of profiles #1 and #2 are 0.7 and 0.6 seconds respectively
6. The water table is at a depth of 10 feet

Figure 4-3 Description of Boston Profiles Analyzed

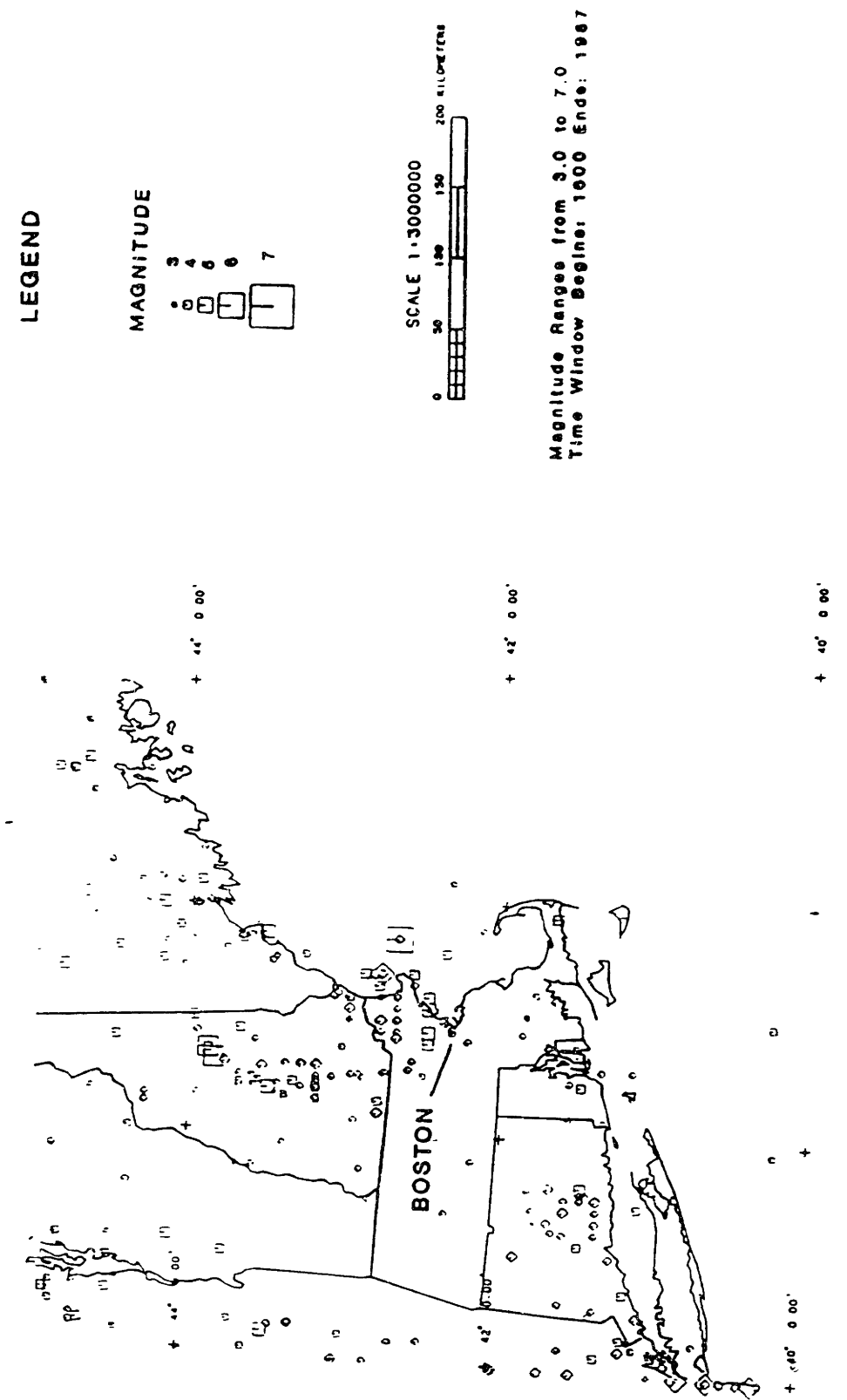
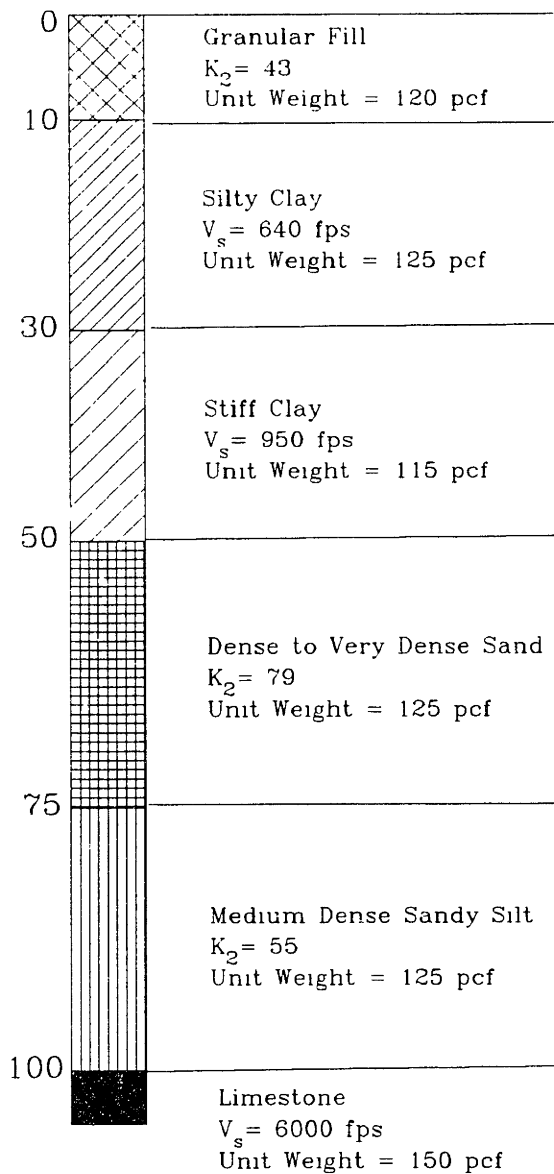


Figure 4-4 Map Outlining the Seismicity of the Boston Area. (After WGC 1989)

St. Louis Profile #1



Notes:

- 1 For granular soils the shear modulus is calculated from the equation $G=1000K_2 \sqrt{\sigma_0}$, where G = shear modulus, σ_0 = effective confining stress, and K_2 is shown above
- 2 V_s = shear wave velocity.
- 3 All depths are in feet
- 4 The profile would be classified as UBC S1
- 5 The thickness-weighted fundamental period before shaking of the profile is 0.4 seconds
- 6 The water table is at a depth of 20 feet

Figure 4-5 Description of St. Louis Profile Analyzed

New Madrid Seismic Zone : 1974 - 1988

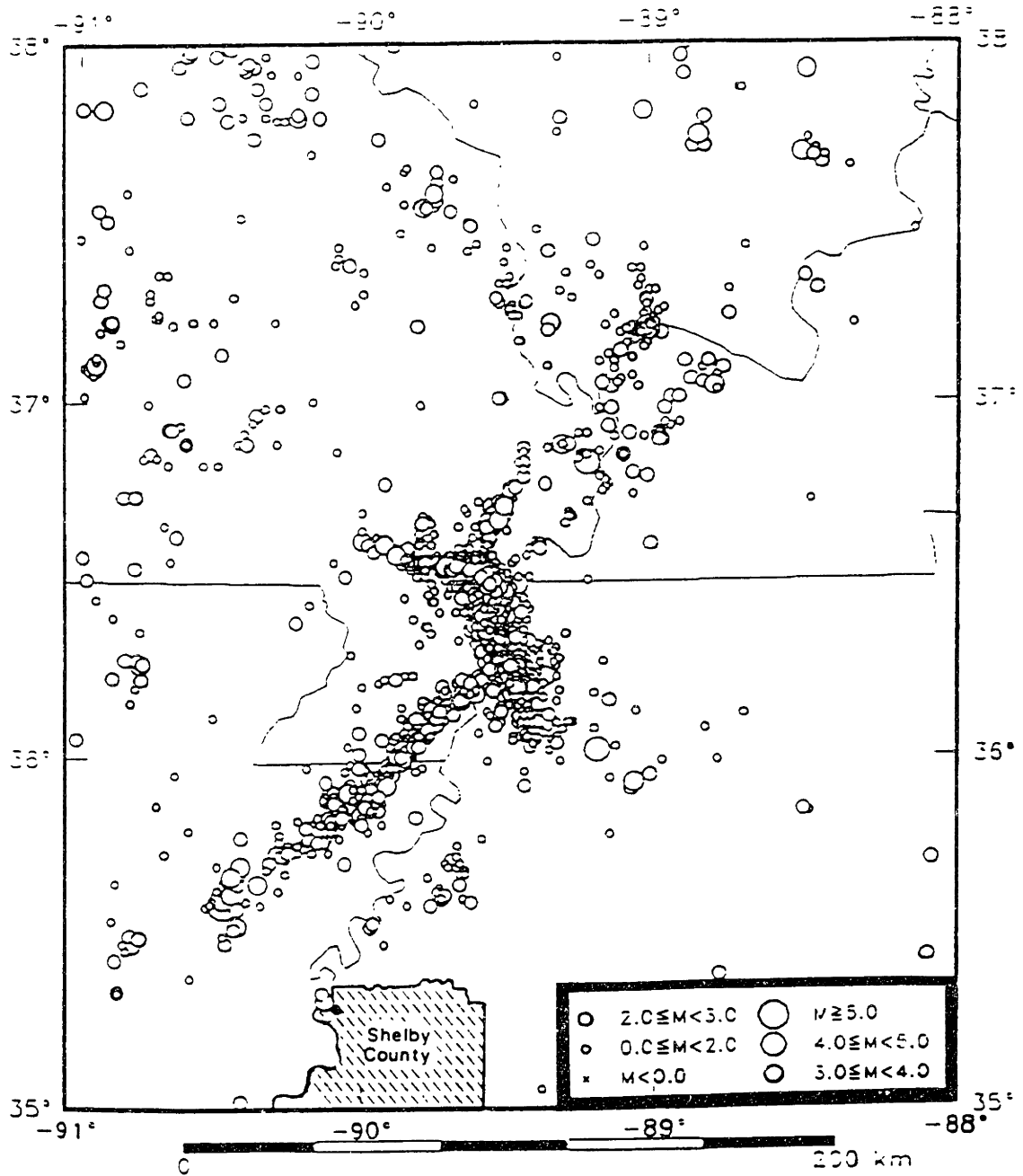
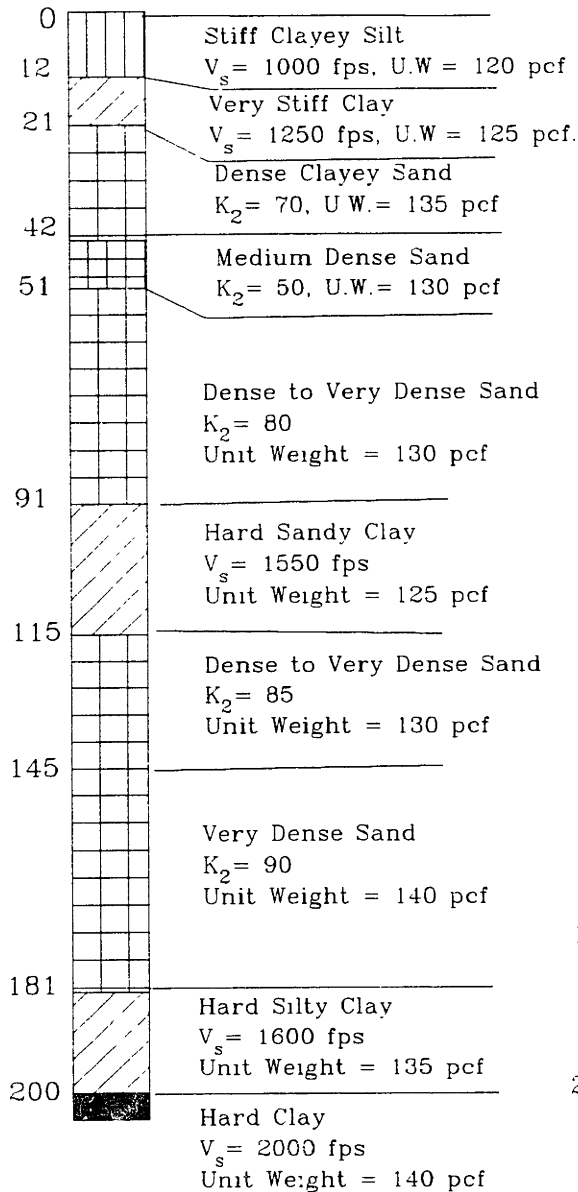
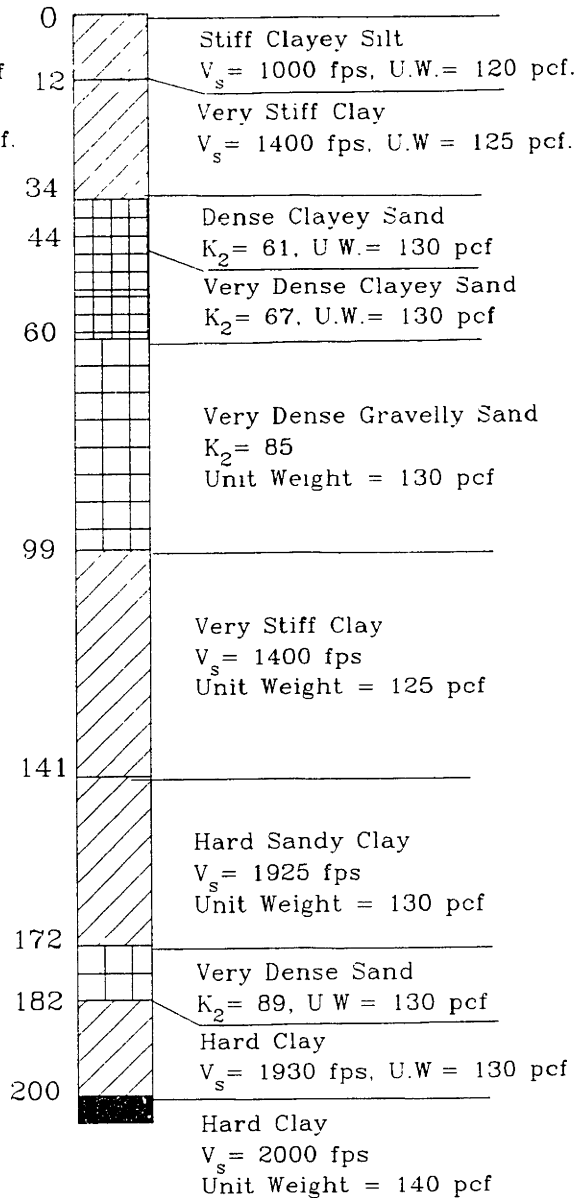


Figure 4-6 Map Describing the New Madrid Seismic Zone. (After Ng et al, 1989)

Memphis Profile #1



Memphis Profile #2

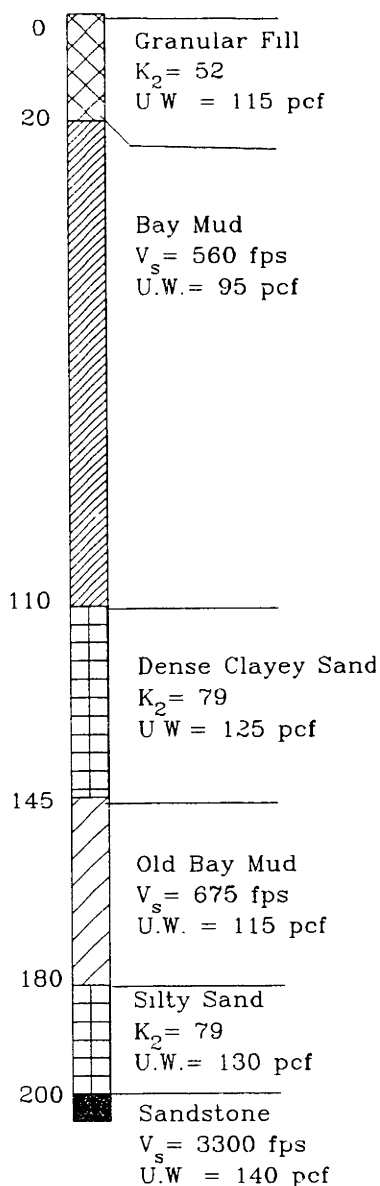


Notes:

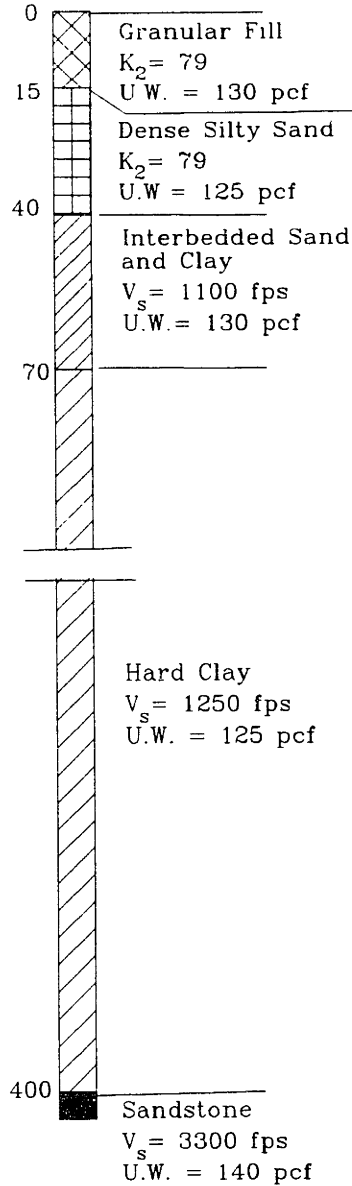
- 1 For granular soils the shear modulus is calculated from the equation $G = 1000K_2 \sqrt{\sigma_0}$, where G = shear modulus, σ_0 = effective confining stress, and K_2 is shown above
- 2 V_s = shear wave velocity
- 3 All depths are in feet
- 4 Both profiles are classified as UBC S2
- 5 The thickness-weighted fundamental period before shaking of both profiles is 0.6 seconds
- 6 The water table in Profiles #1 and #2 is at a depth of 30ft and 18ft respectively

Figure 4--7 Description of Memphis Profiles Analyzed

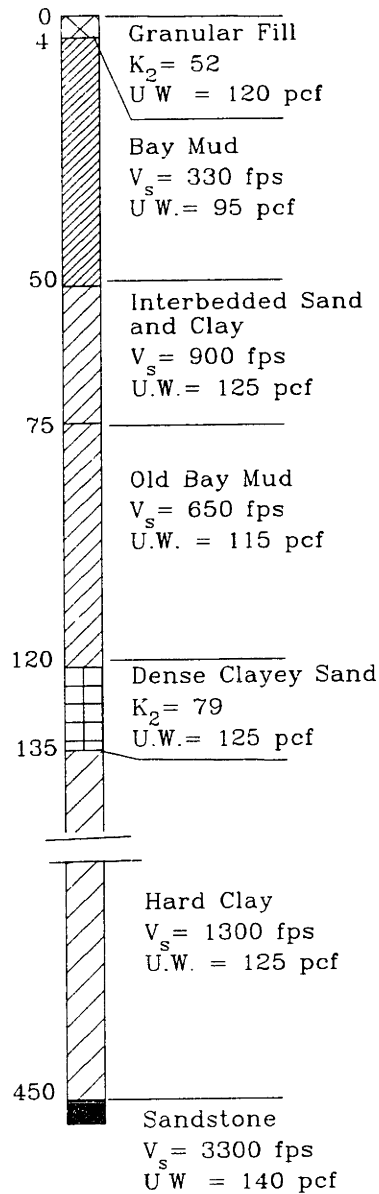
San Francisco Profile #1



San Francisco Profile #2



San Francisco Profile #3

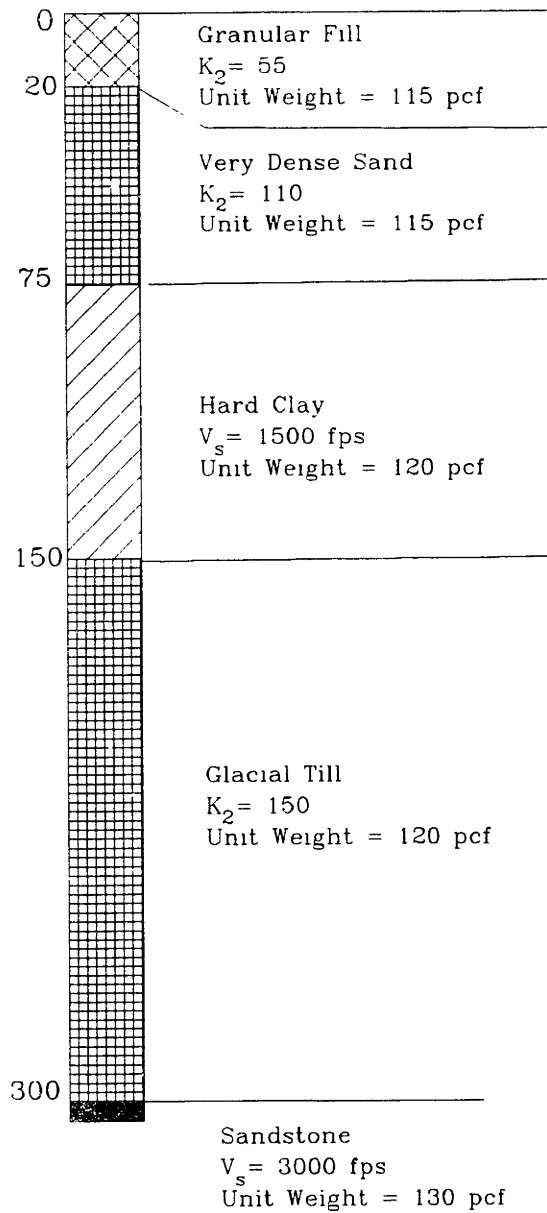


Notes:

1. For granular soils the shear modulus is calculated from the equation $G=1000K_2 \sqrt{\sigma_0}$, where G = shear modulus, σ_0 = effective confining stress, and K_2 is shown above
2. V_s = shear wave velocity, U.W. = Unit Weight
3. All depths are in feet
4. Profile #1 is classified as S4, and Profile #2 as S2. Profile #3 would be classified as UBC S4, and as NEHRP S3.
5. The thickness-weighted fundamental period before shaking of profiles #1, #2 and #3, are 1.1, 1.3, and 2.0 seconds respectively
6. The water table is at a depth of 20 feet in each profile

Figure 4-8 Description of San Francisco Profiles Analyzed

Seattle Profile #1



Notes:

1. For granular soils the shear modulus is calculated from the equation $G=1000K_2 \sqrt{\sigma_0}$, where G = shear modulus, σ_0 = effective confining stress, and K_2 is shown above
2. V_s = shear wave velocity
3. All depths are in feet.
4. The profile would be classified as UBC S2.
5. The thickness-weighted fundamental period before shaking of the profile is 0.7 seconds
6. The water table is at a depth of 20 feet

Figure 4-10 Description of Seattle Profile Analyzed

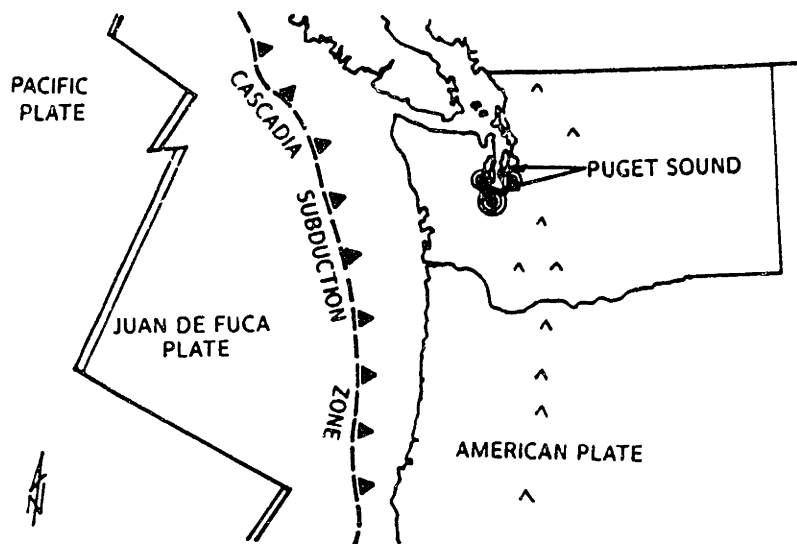


Figure 4-11 Map Outlining the Seismicity of the Seattle Area. (After Ho et al, 1991)

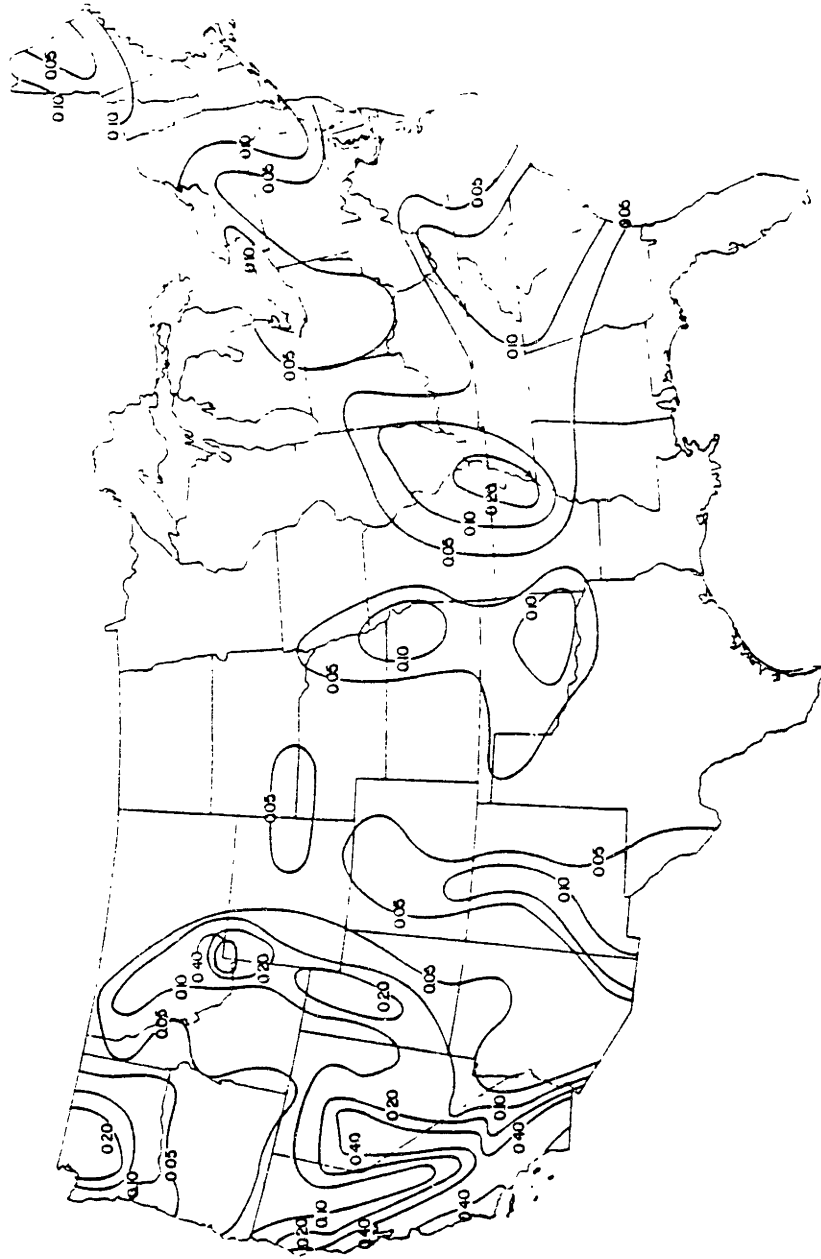


Figure 4-12 Contour Map of Effective Peak Acceleration in the continental United States for a nominal recurrence interval of 500 years. (After BSSC, 1988)

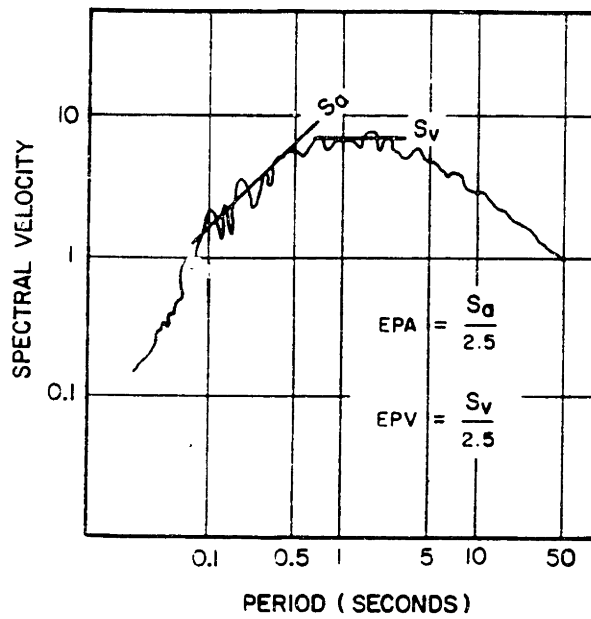


Figure 4-13 Schematic Representation of the Calculation of EPA from a Response Spectrum. (After BSSC, 1988)

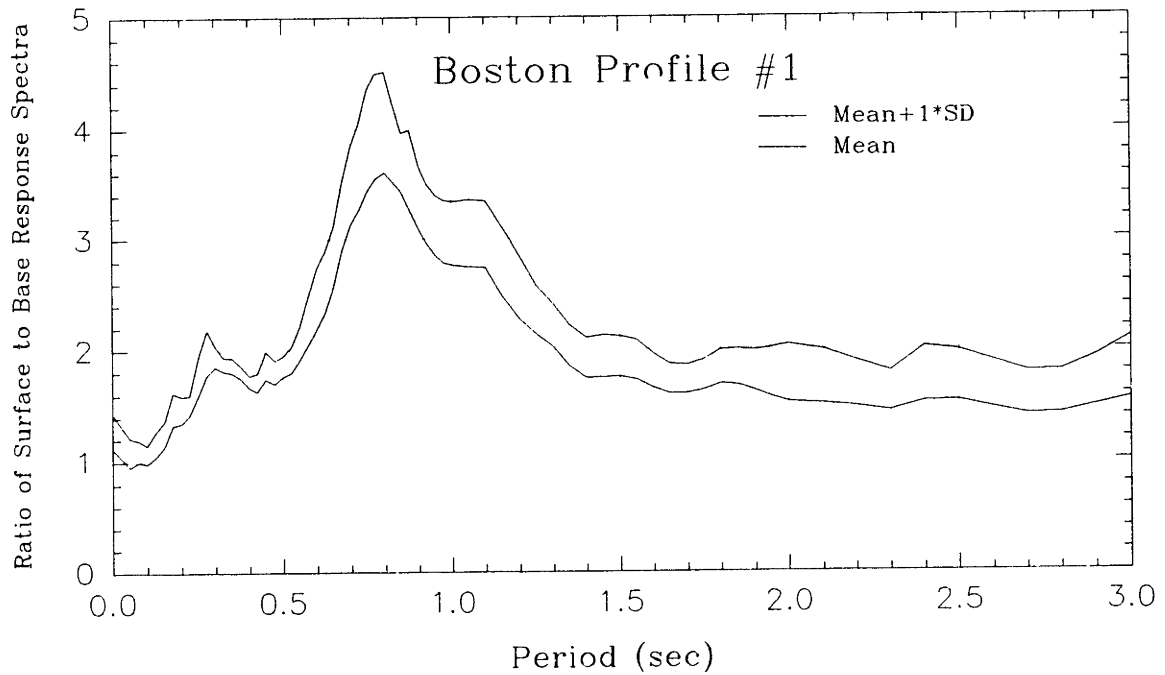
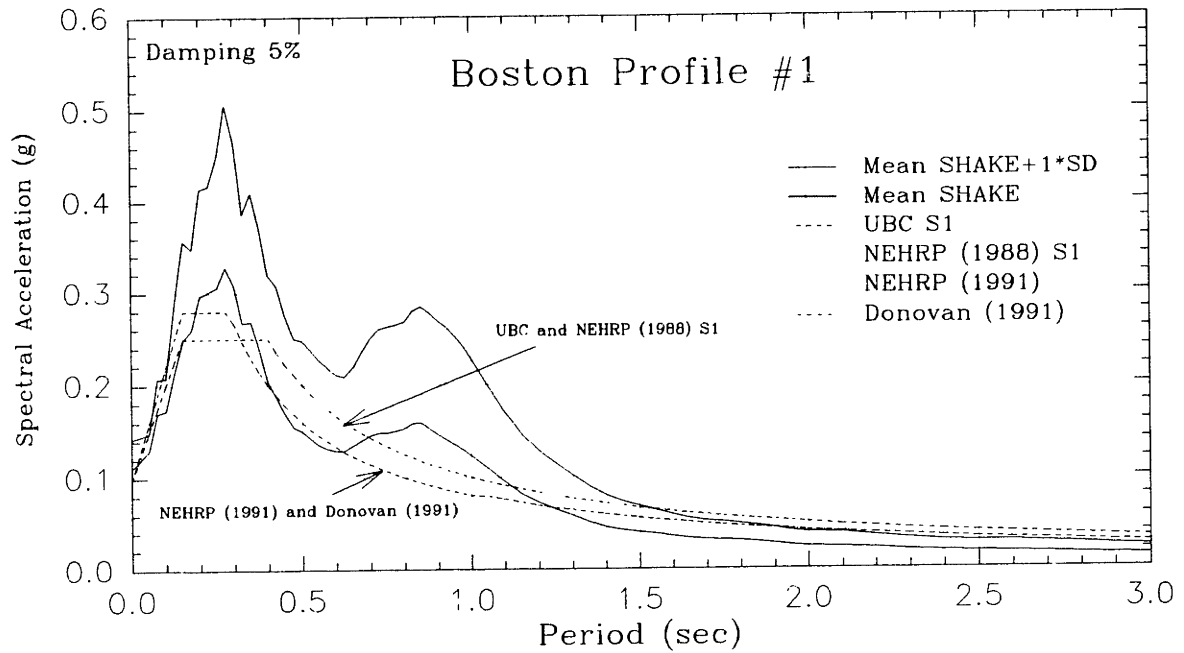


Figure 4-14 Comparison of Response Spectra and Ratio of Response Spectra for Boston Profile #1.

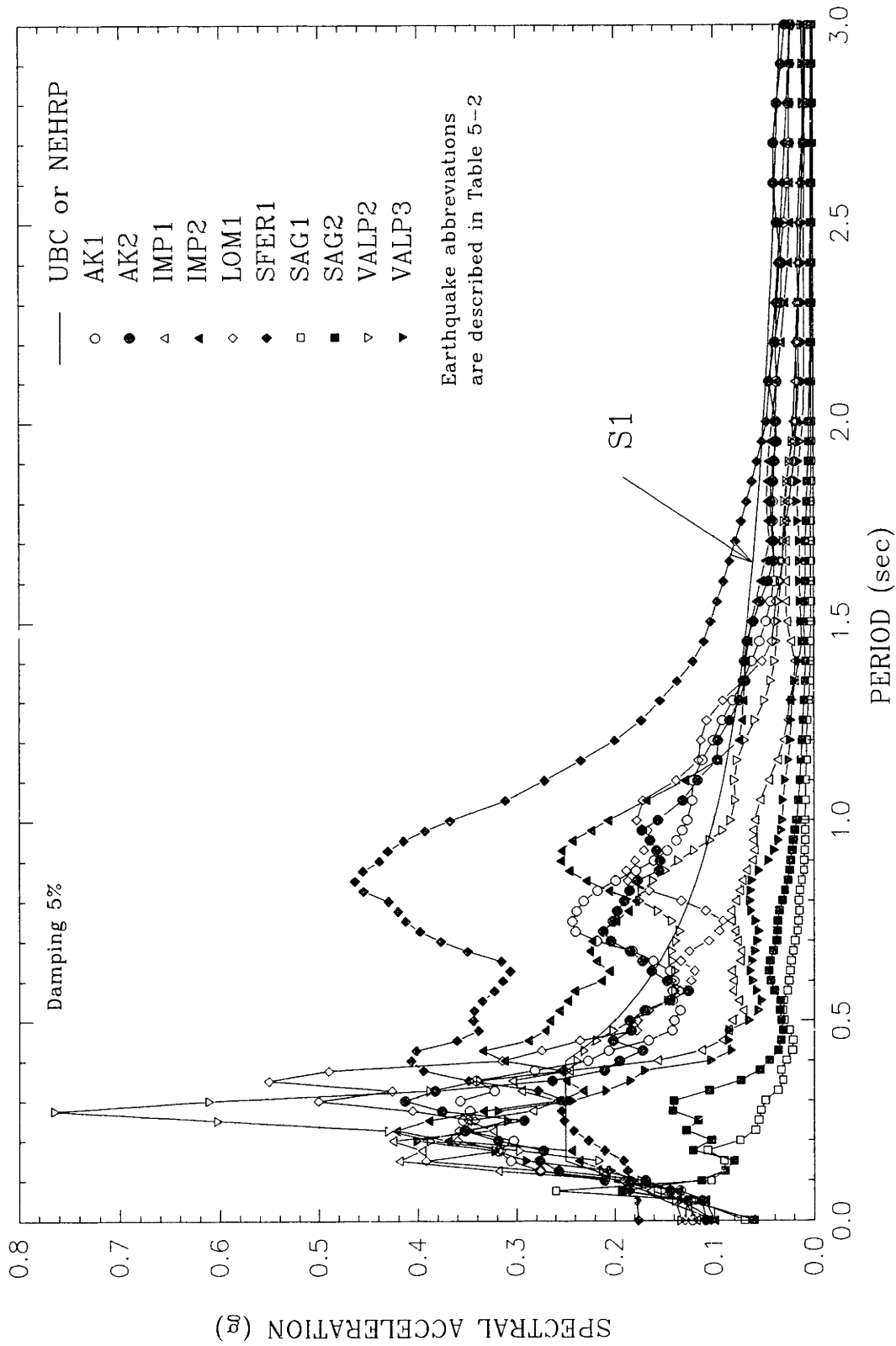


Figure 4-15 Computed Surface Response Spectra for Boston Profile #1.

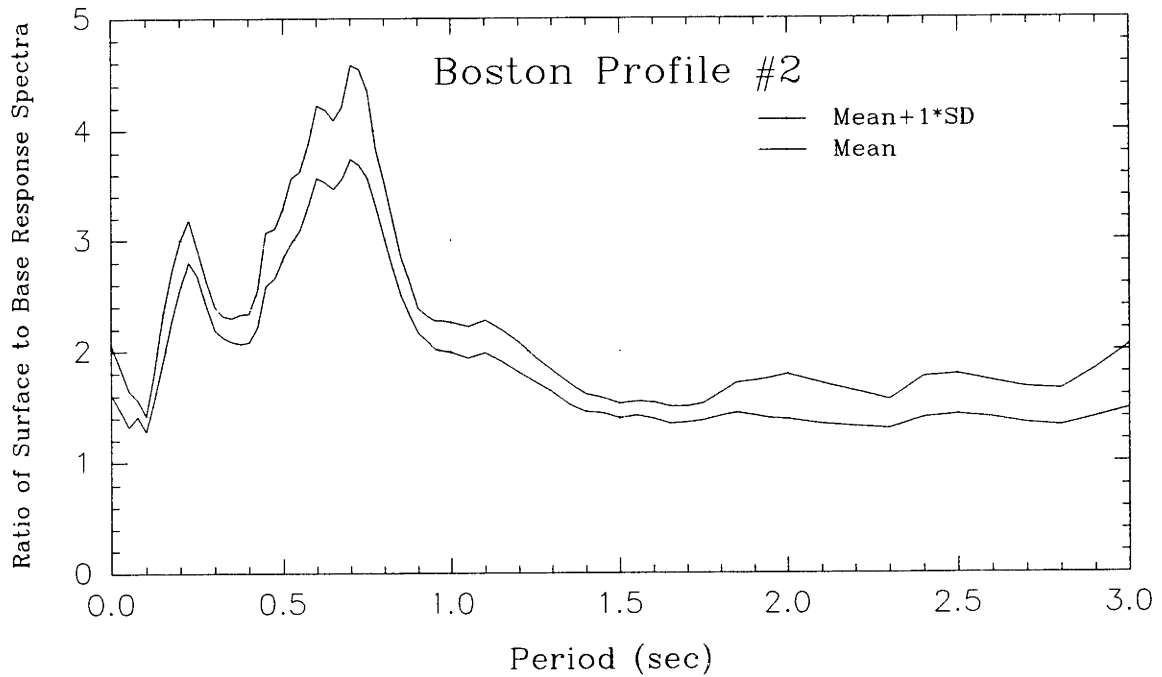
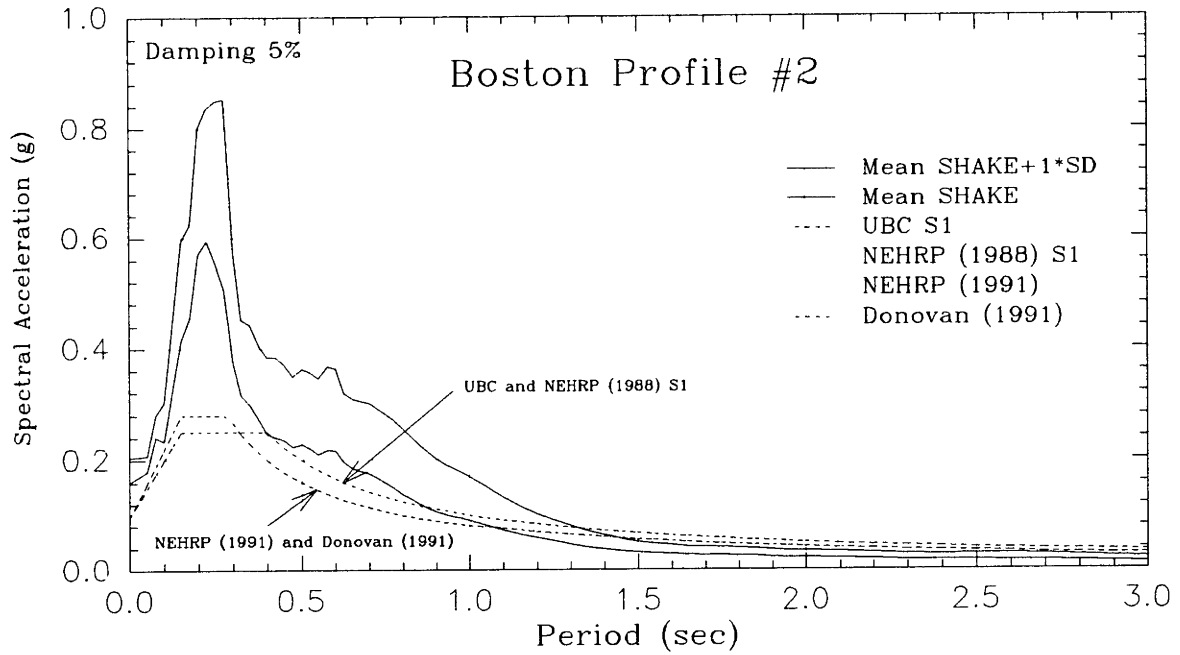


Figure 4-16 Comparison of Response Spectra and Ratio of Response Spectra for Boston Profile #2.

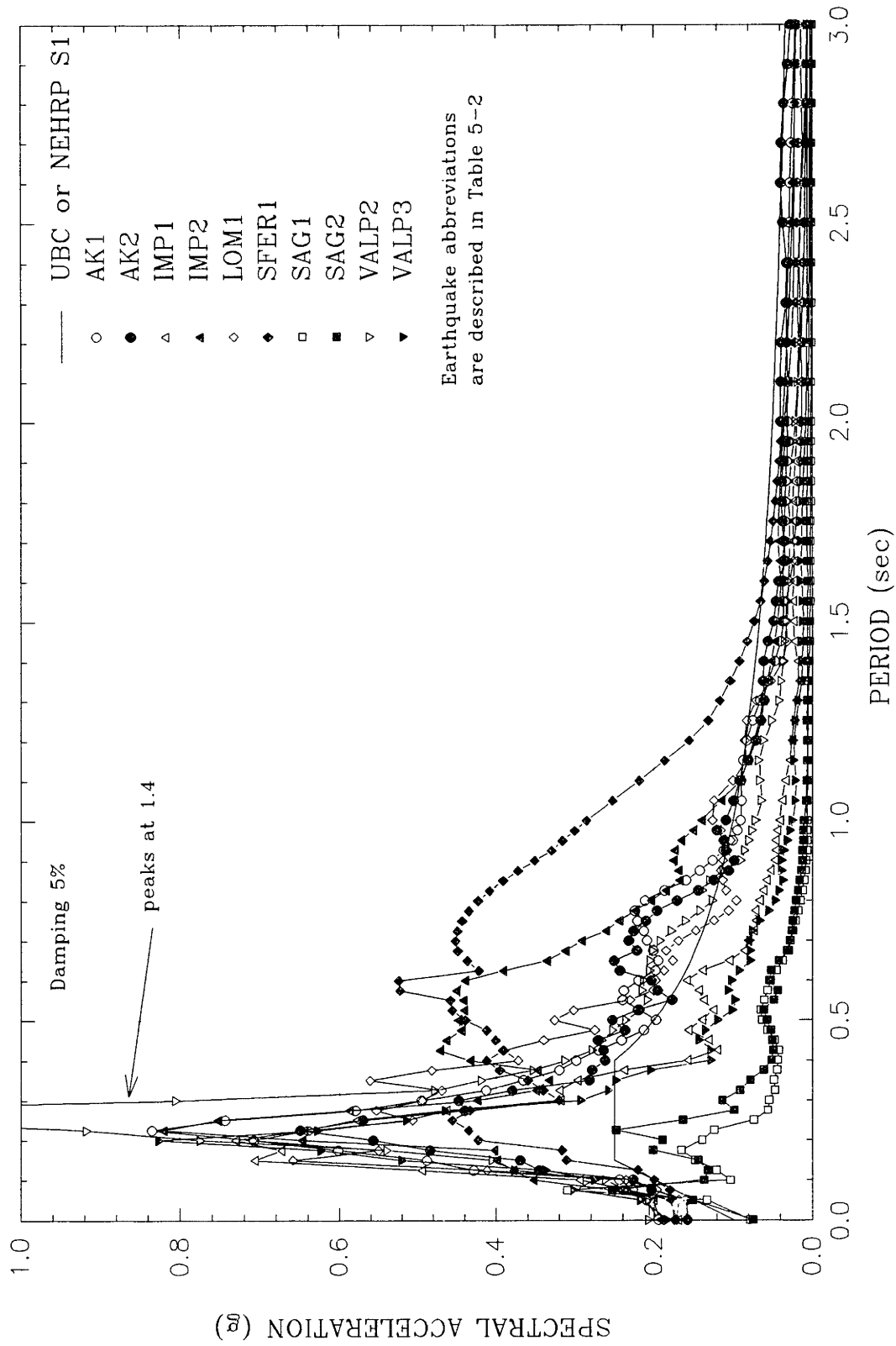


Figure 4-17 Computed Surface Response Spectra for Boston Profile #2

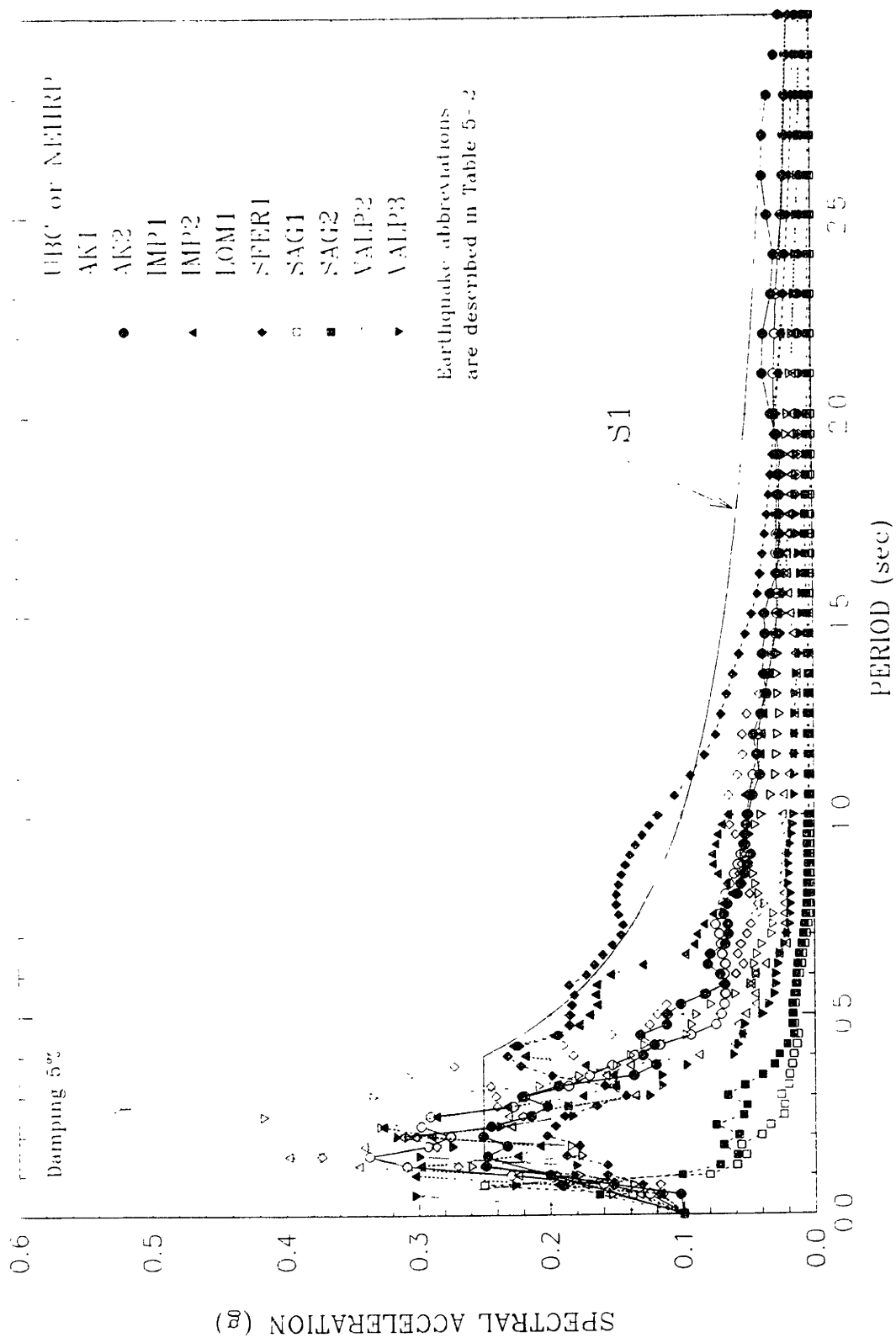


Figure 4-18 Input Earthquake Base Response Spectra for Boston

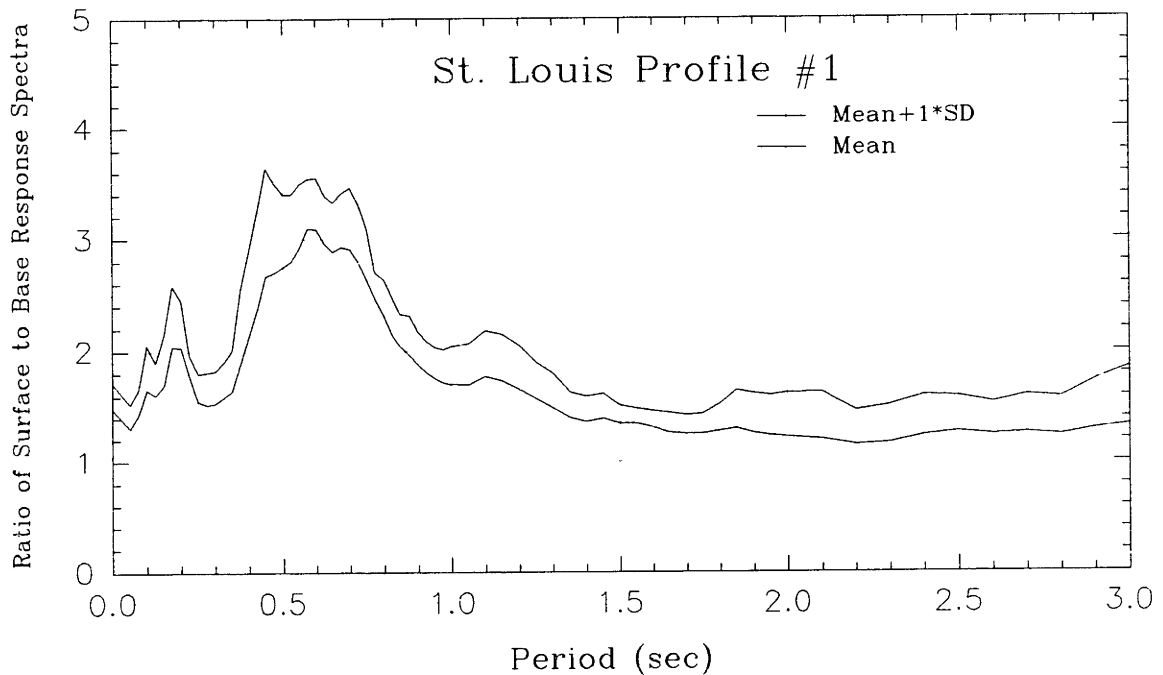
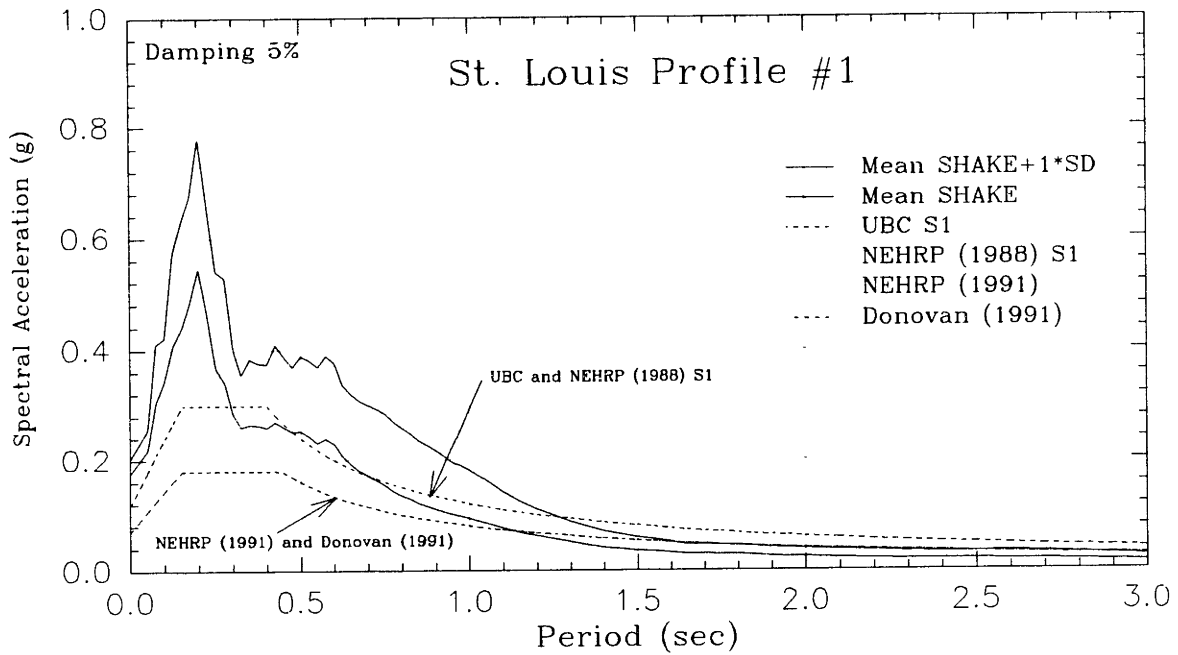


Figure 4-19 Comparison of Response Spectra and Ratio of Response Spectra for St. Louis Profile #1.

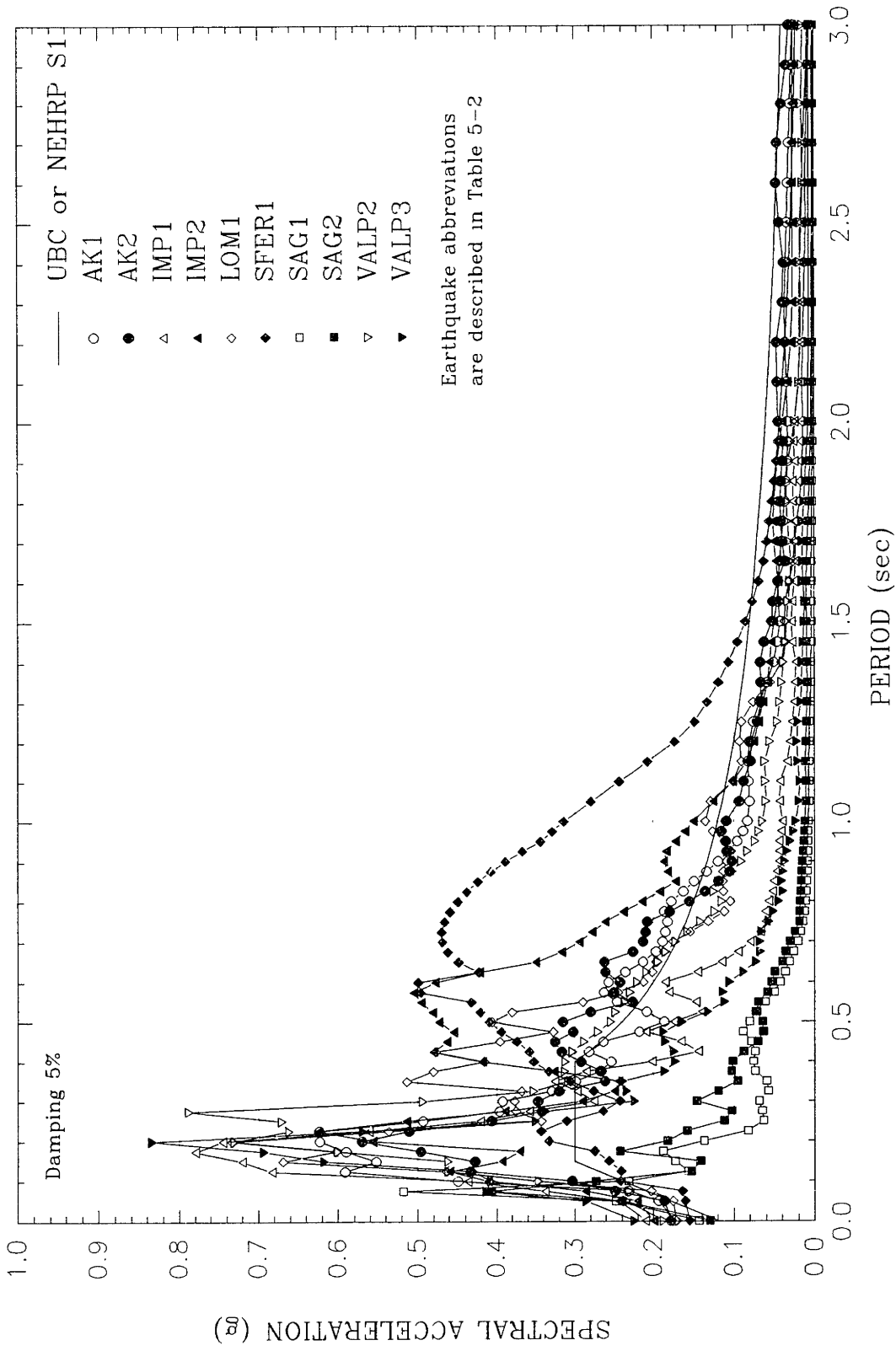


Figure 4-20 Computed Surface Response Spectra for St. Louis Profile #1.

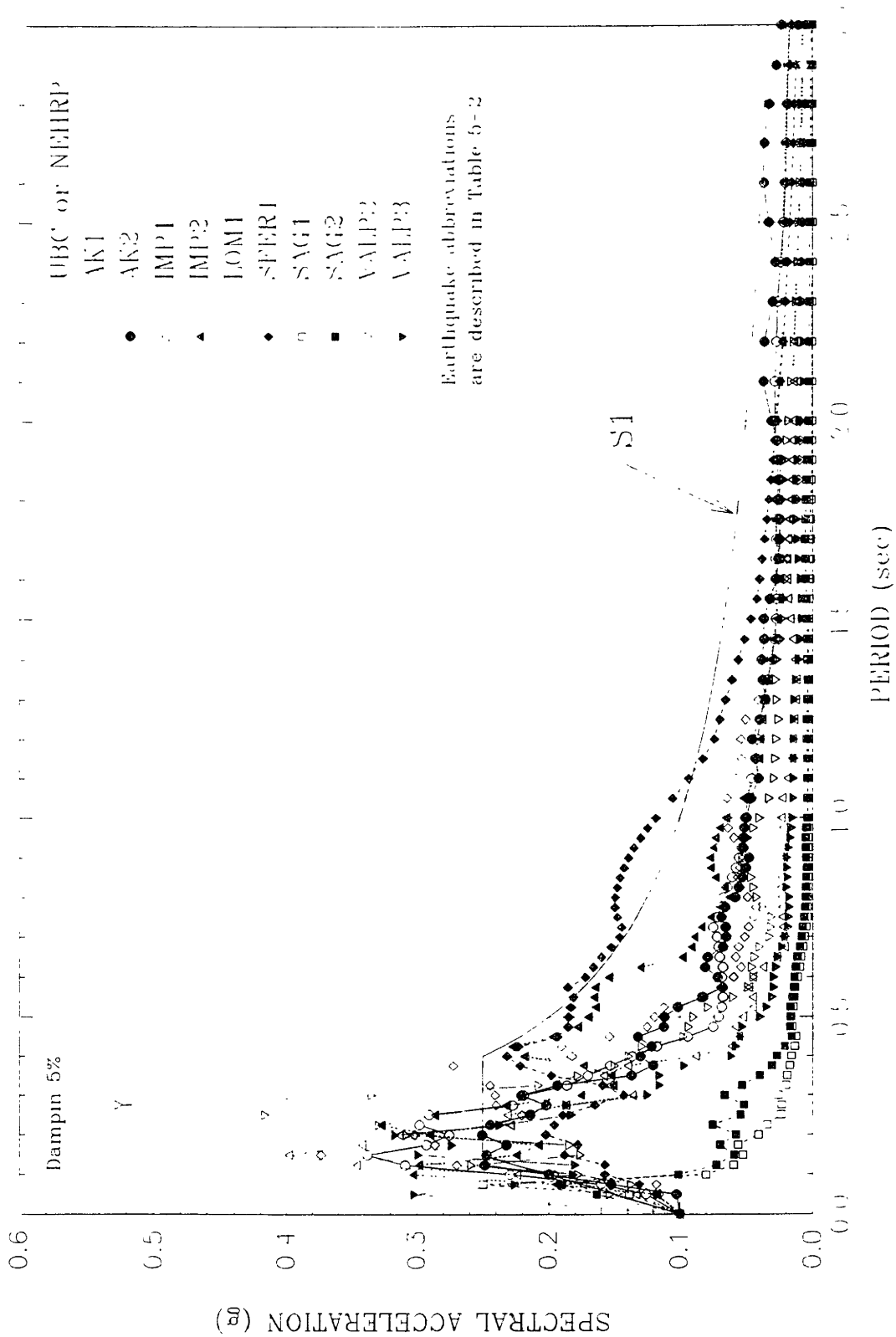


Figure 4-21 Input Earthquake Base Response Spectra for St. Louis

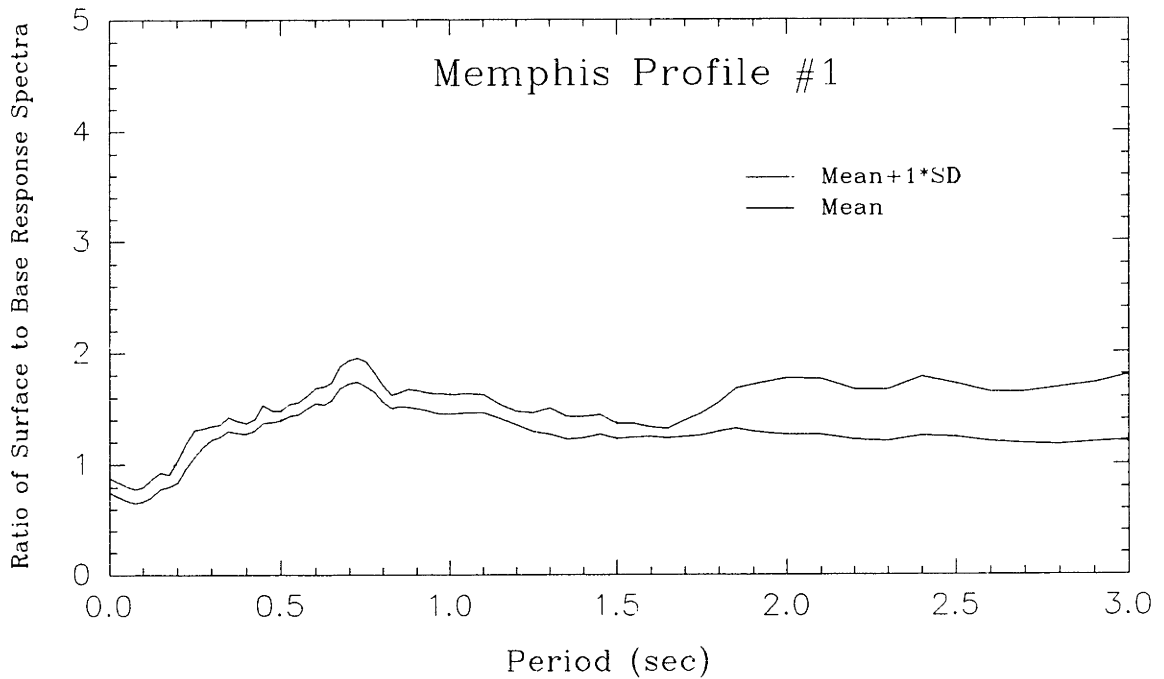
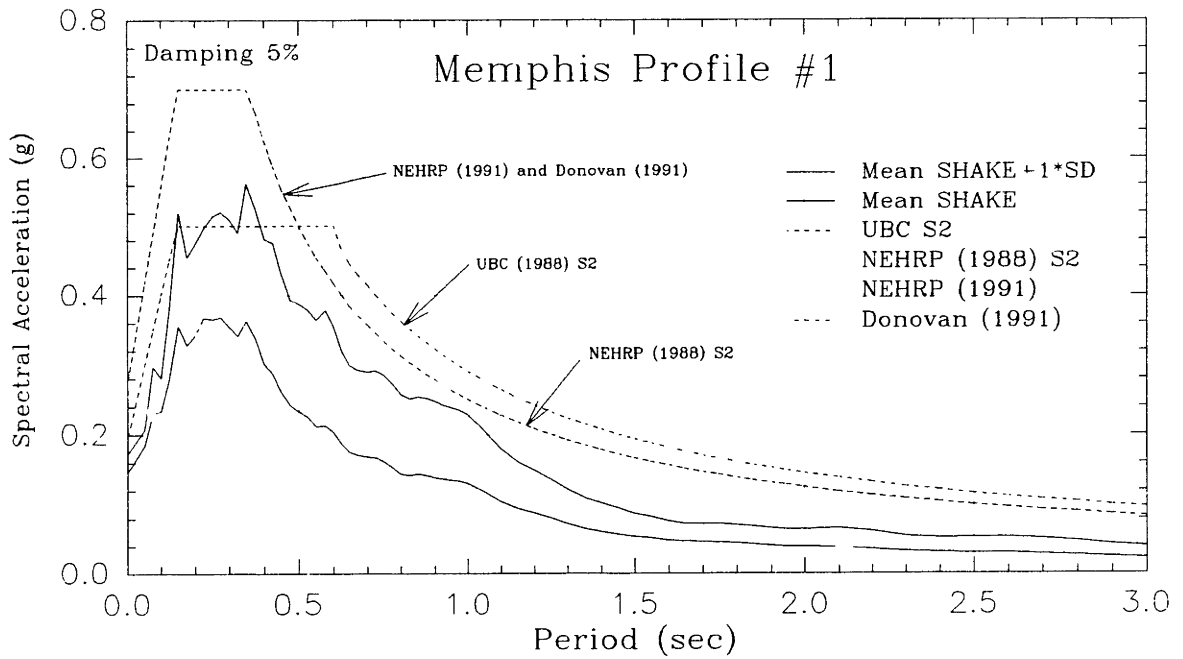


Figure 4-22 Comparison of Response Spectra and Ratio of Response Spectra for Memphis Profile #1.

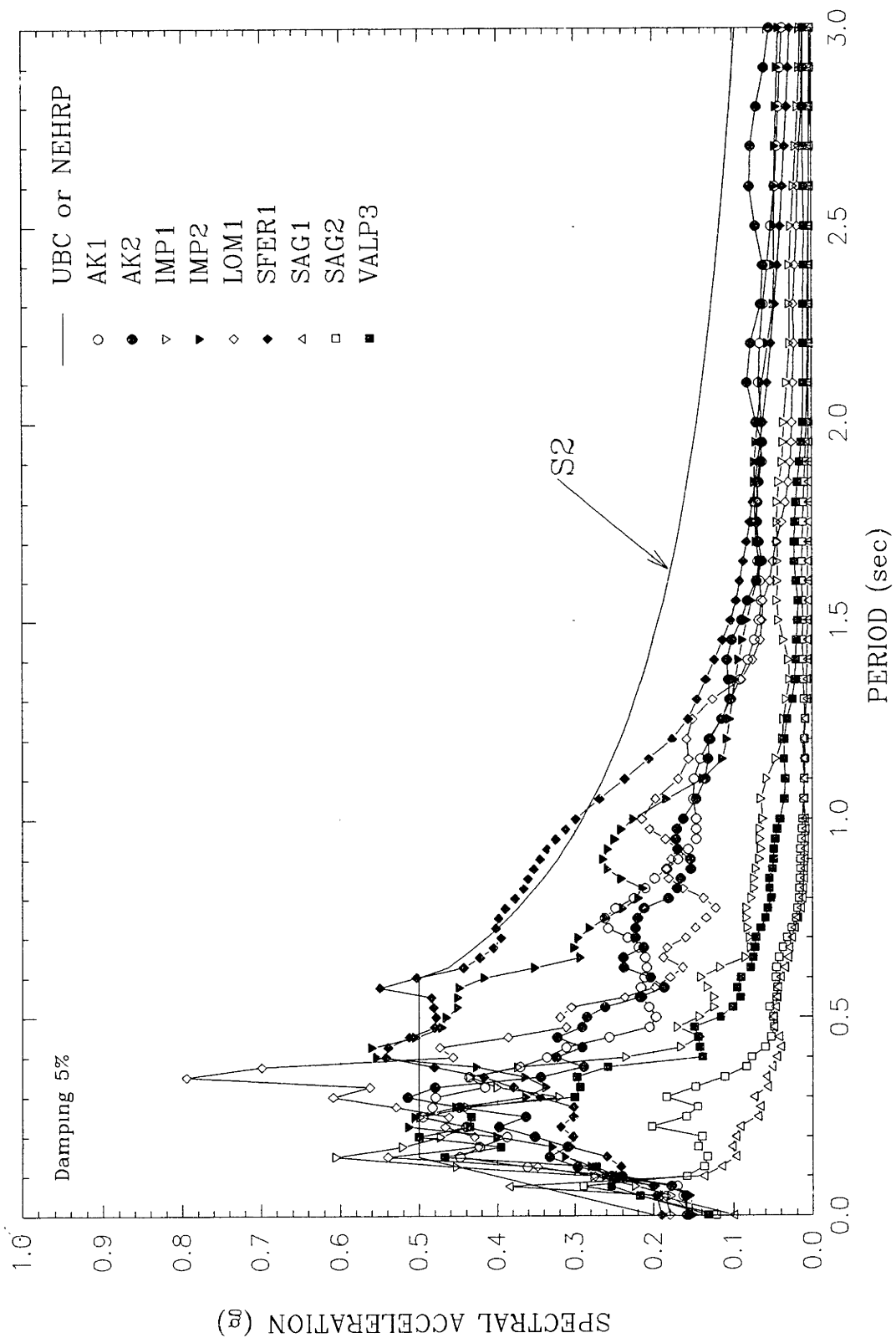


Figure 4-23 Computed Surface Response Spectra for Memphis Profile #1.

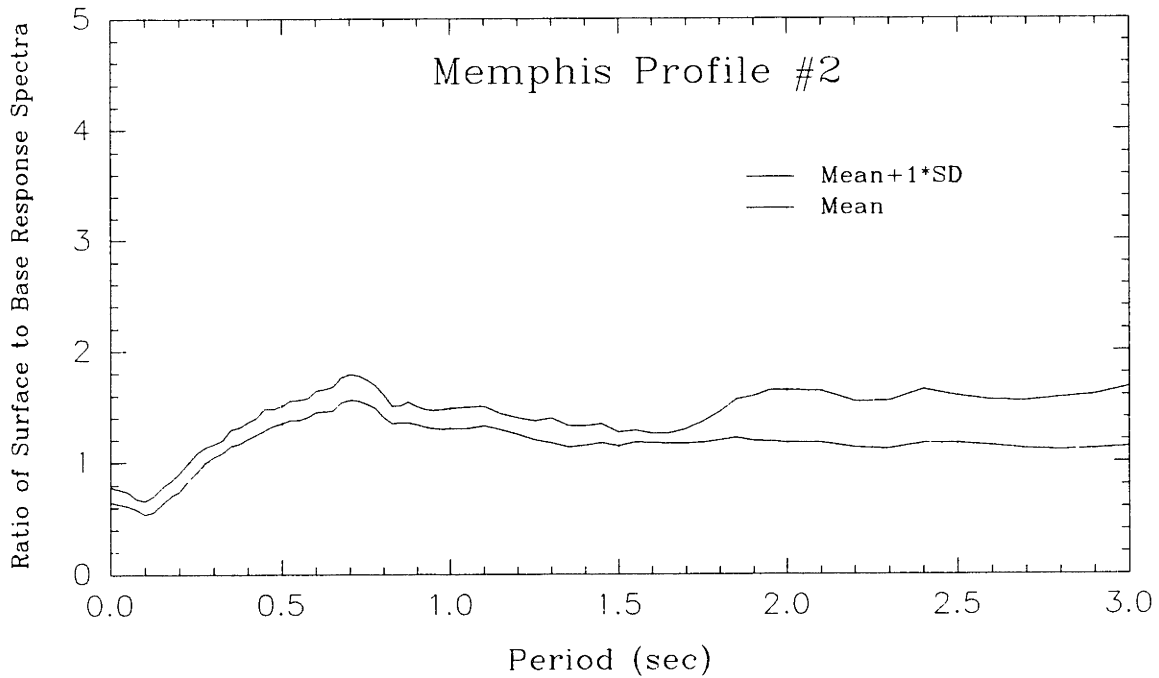
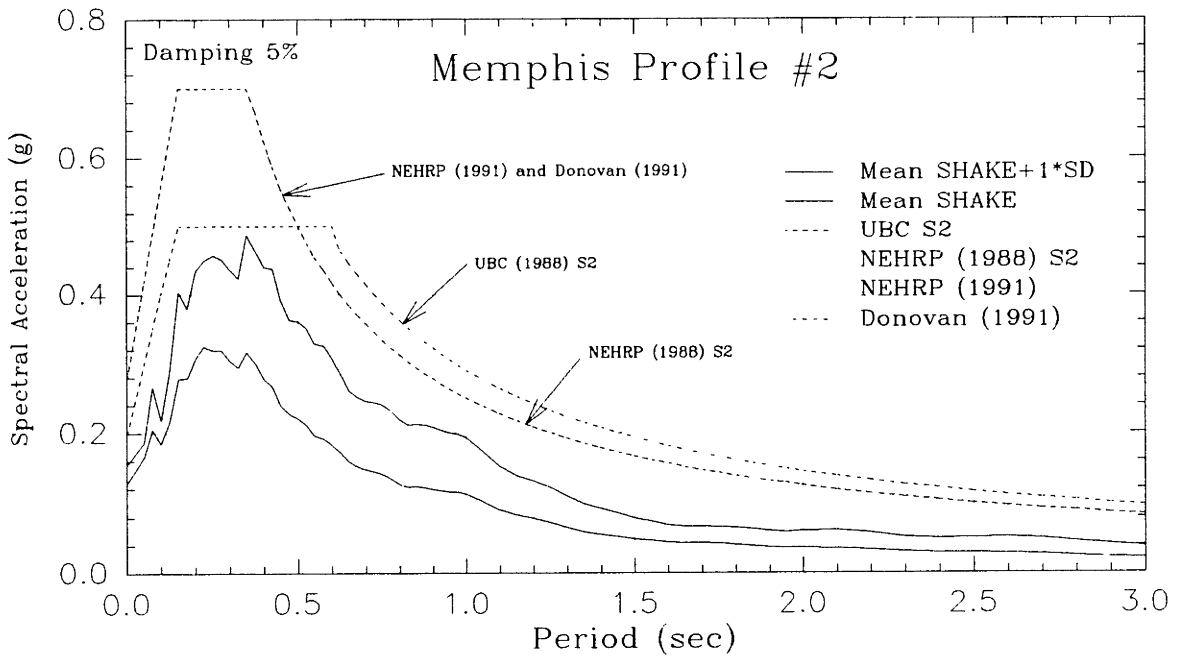


Figure 4-24 Comparison of Response Spectra and Ratio of Response Spectra for Memphis Profile #2.

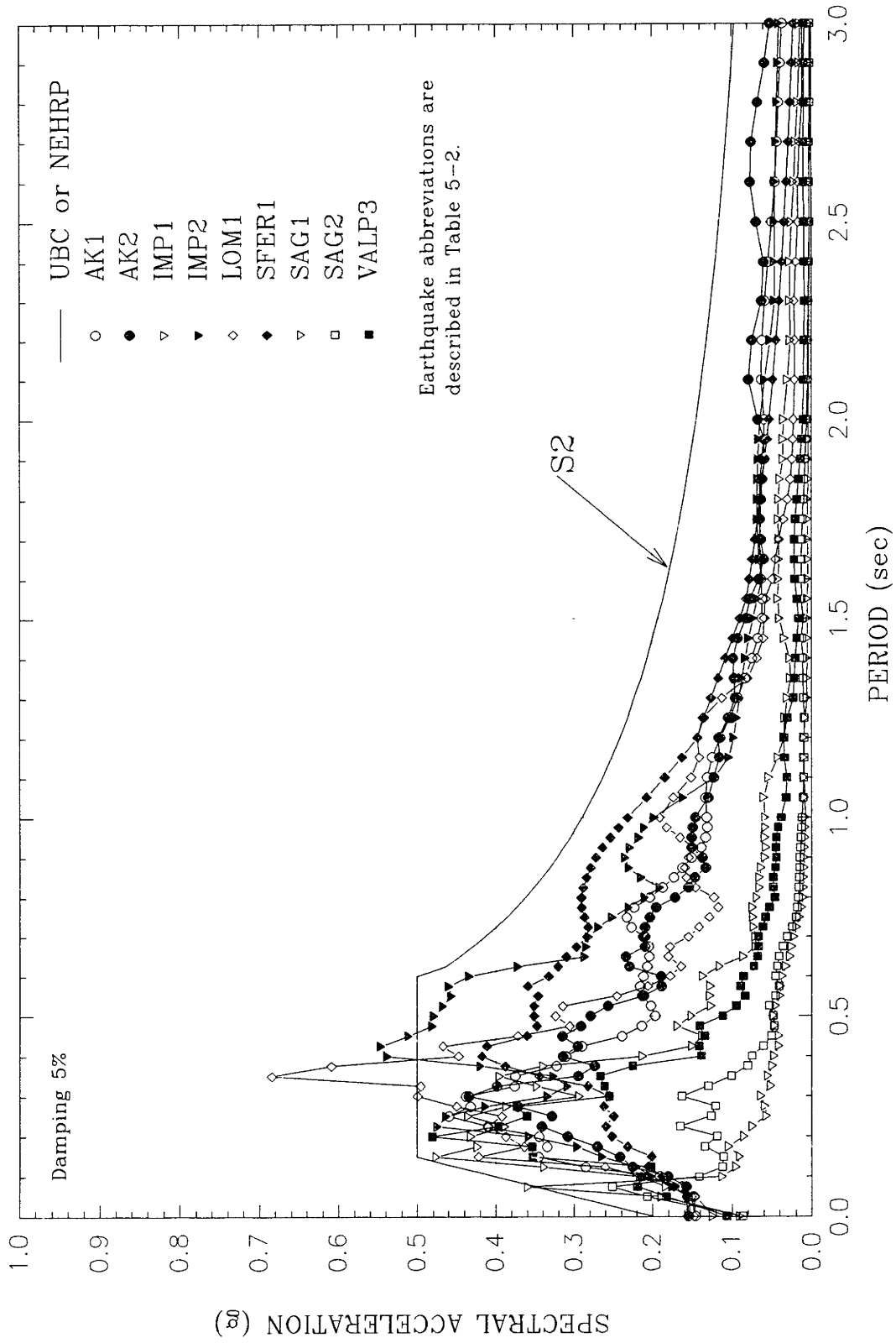


Figure 4-25 Computed Surface Response Spectra for Memphis Profile #2.

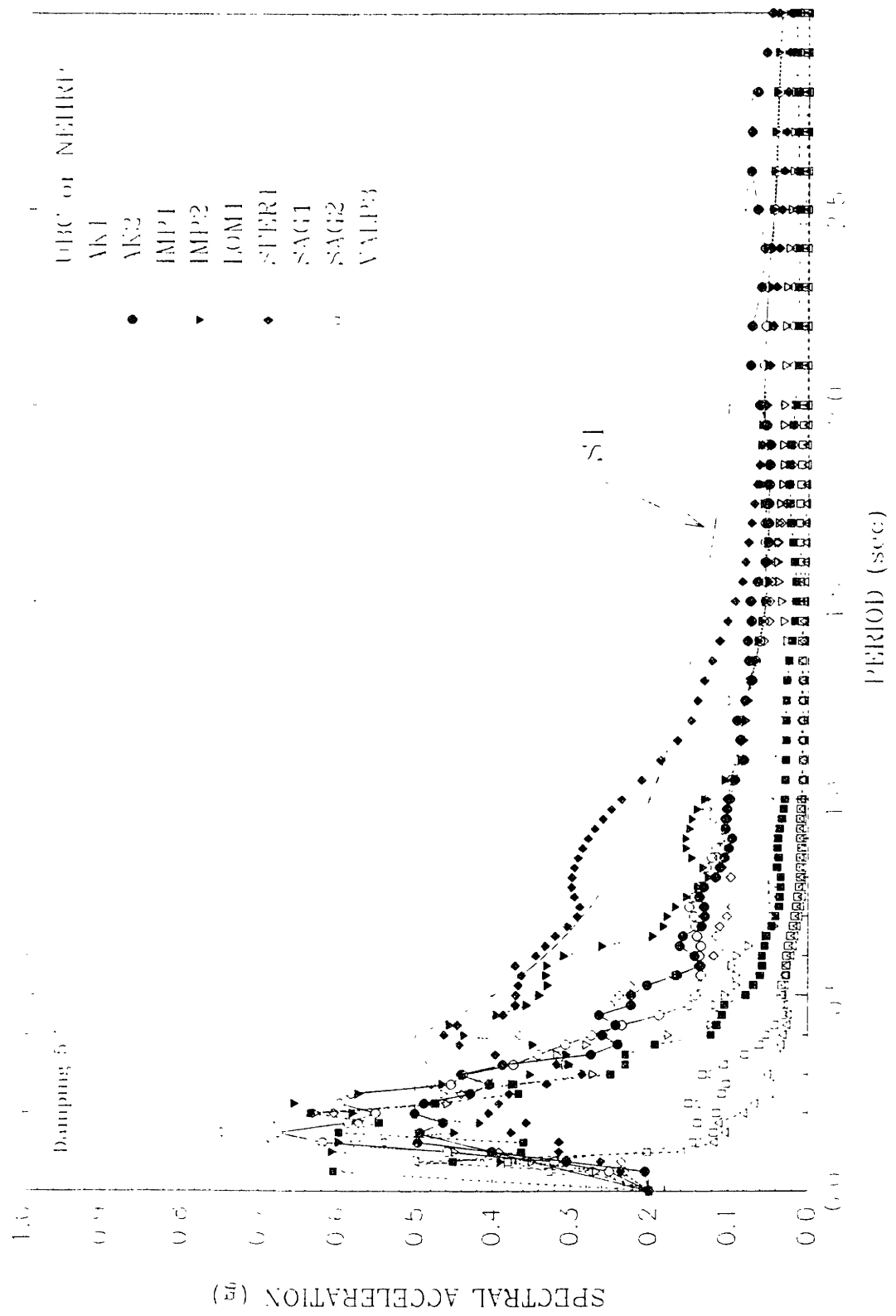


Figure 4-26 Input Earthquake Base Response Spectra for Memphis

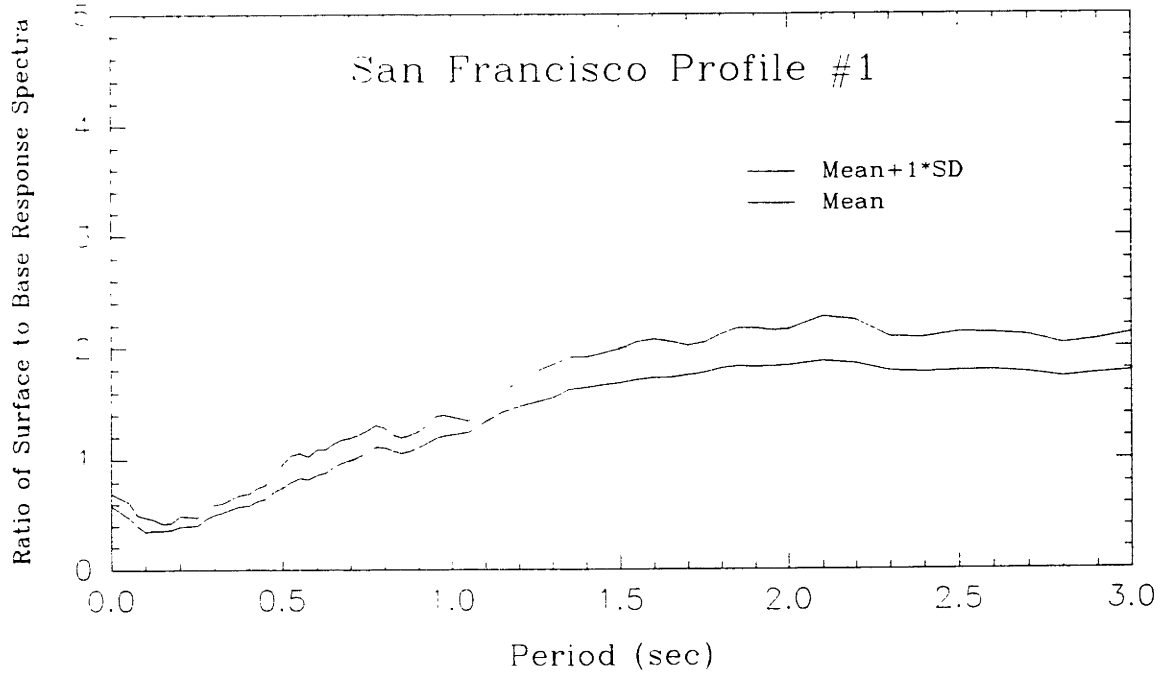
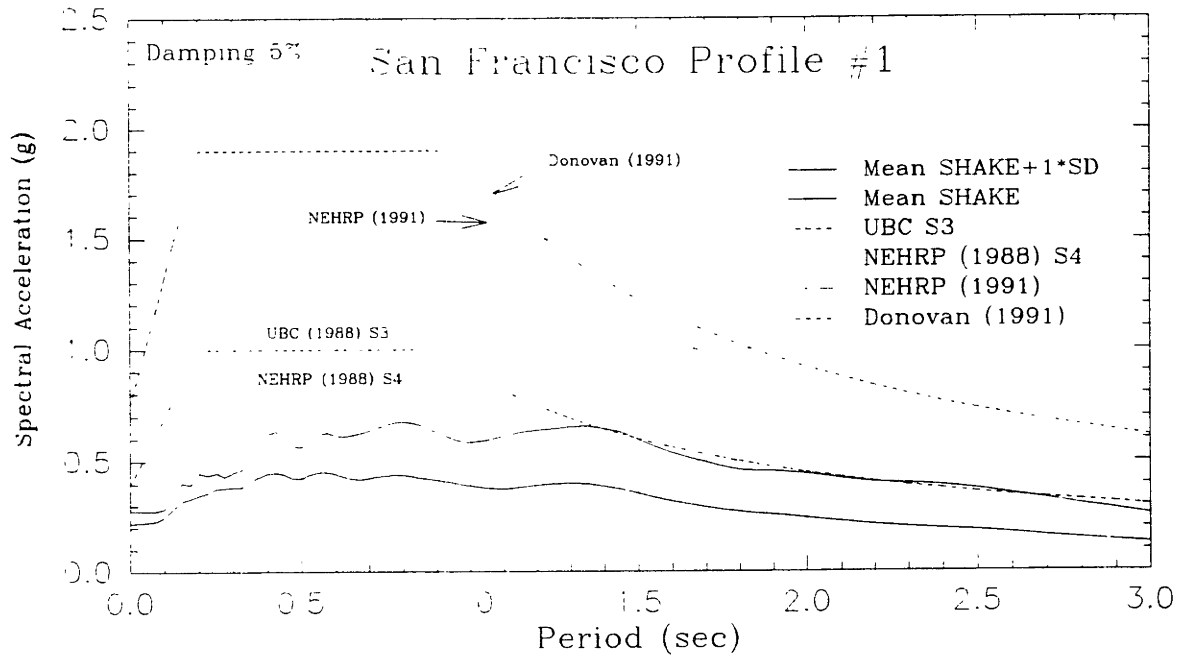


Figure 4-27 Comparison of Response Spectra and Ratio of Response Spectra for San Francisco Profile #1.

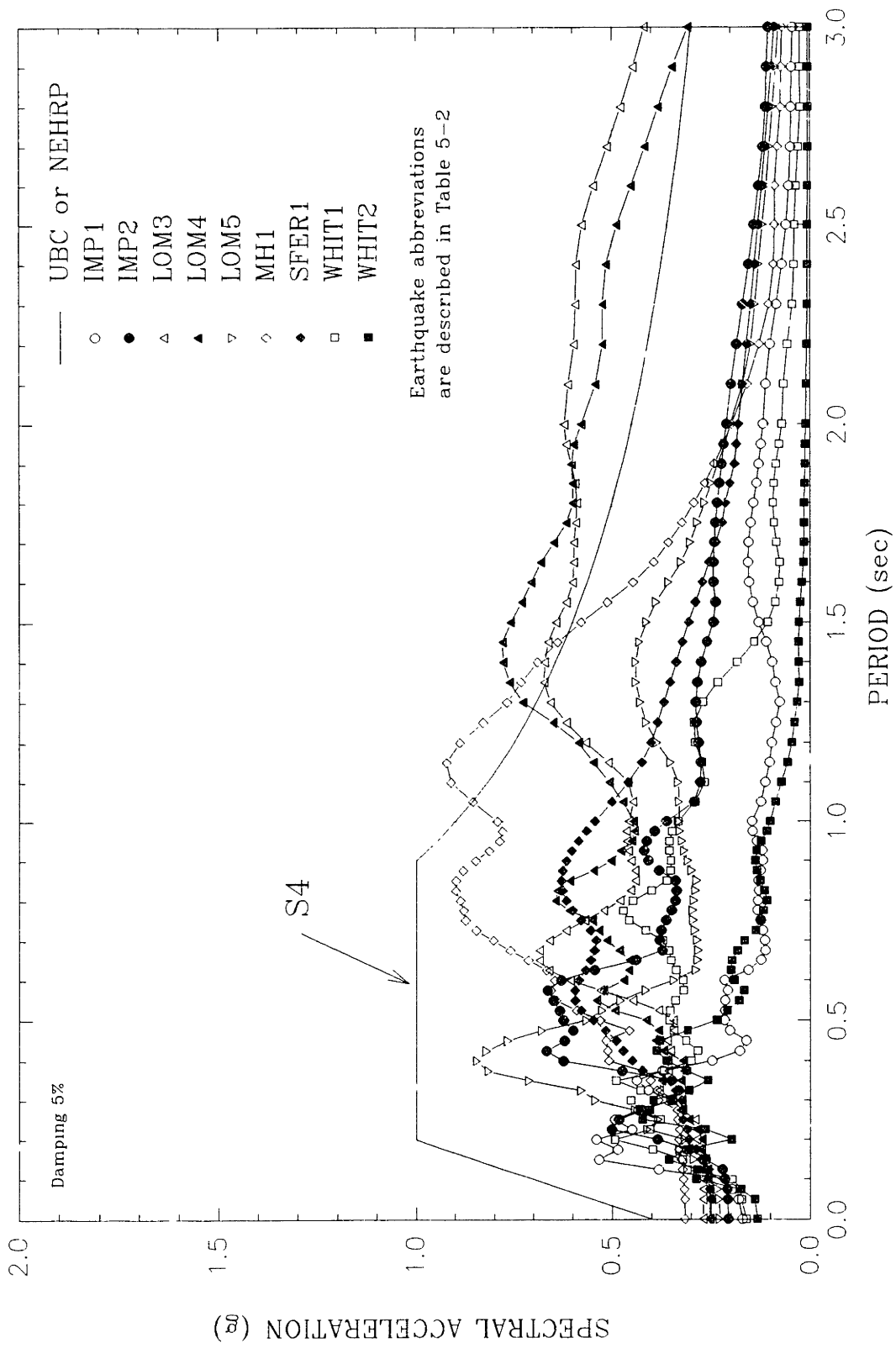


Figure 4-28 Computed Surface Response Spectra for San Francisco Profile #1.

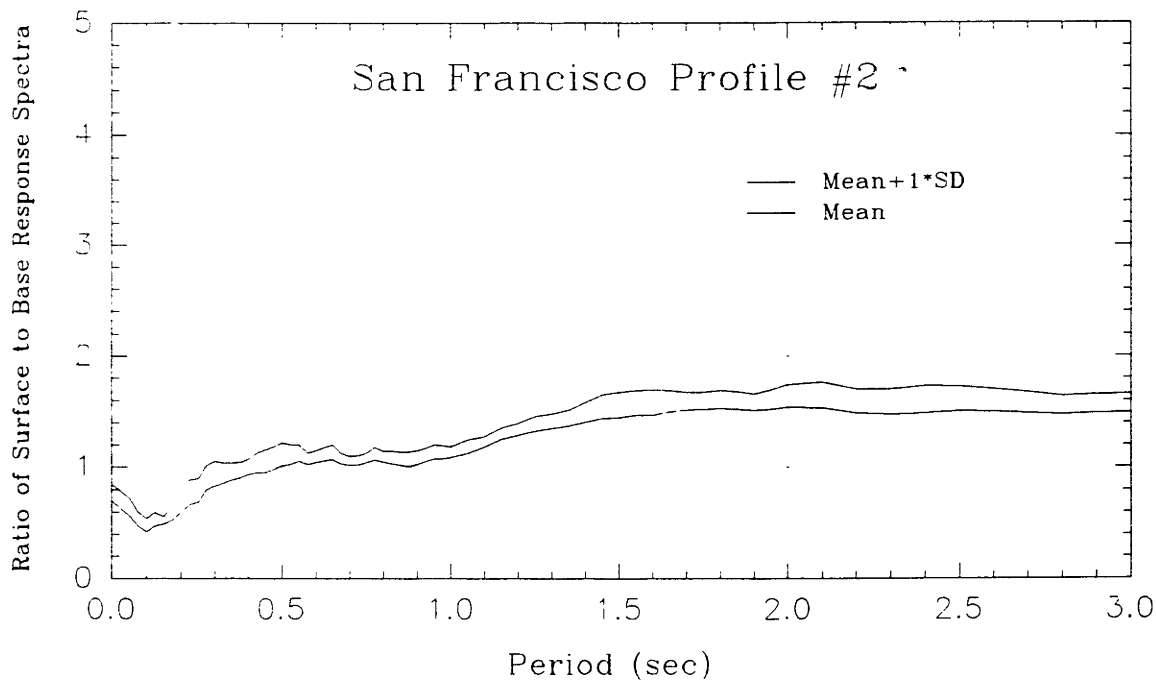
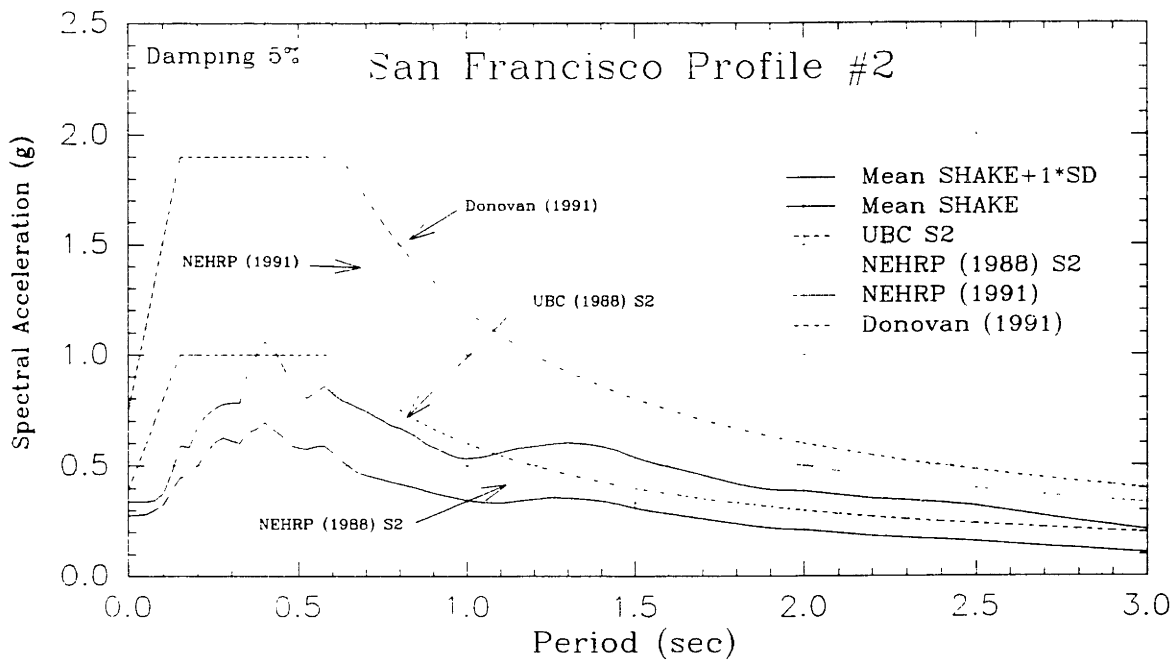


Figure 4-29 Comparison of Response Spectra and Ratio of Response Spectra for San Francisco Profile #2.

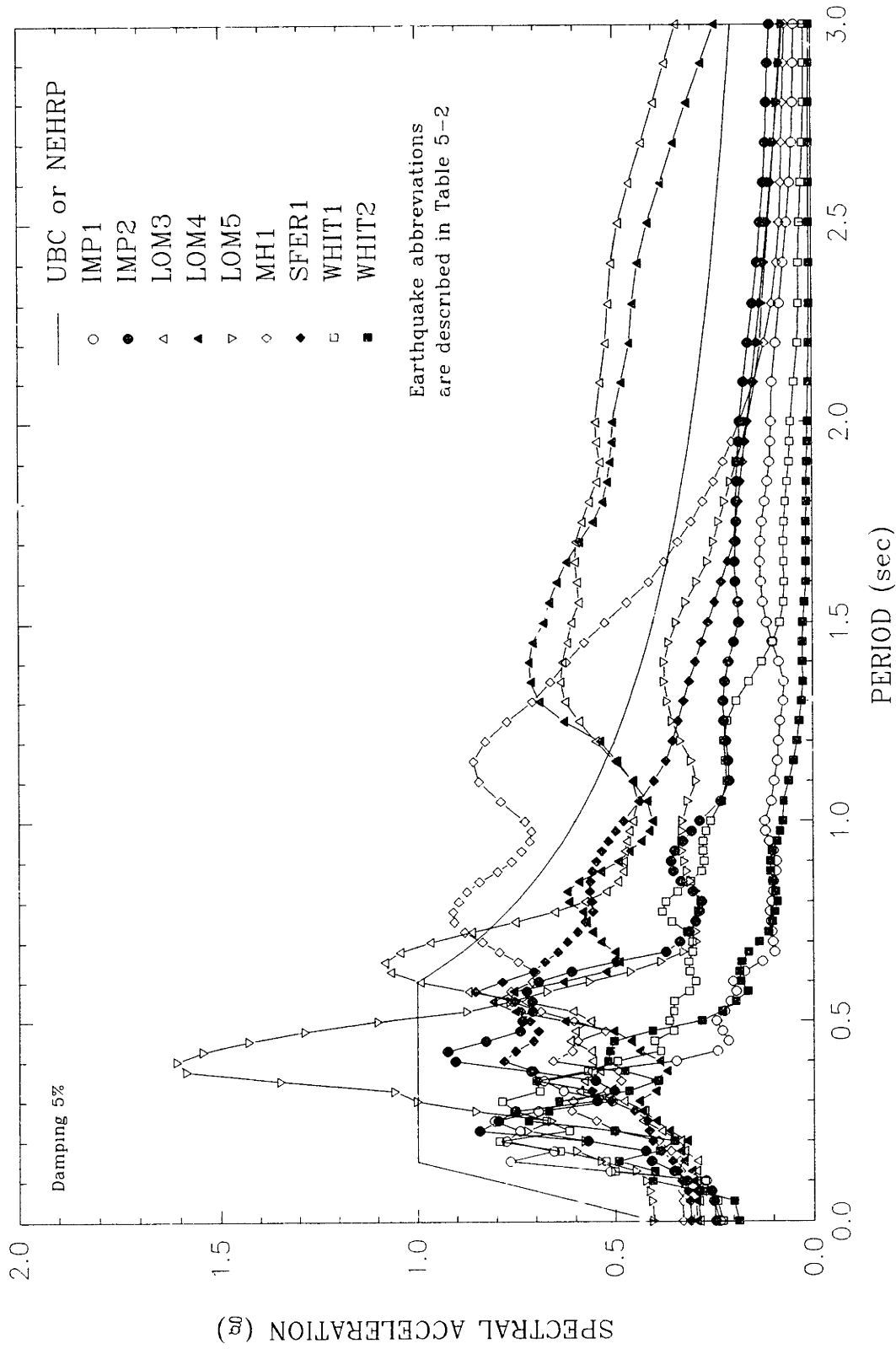


Figure 4-30 Computed Surface Response Spectra for San Francisco Profile #2.

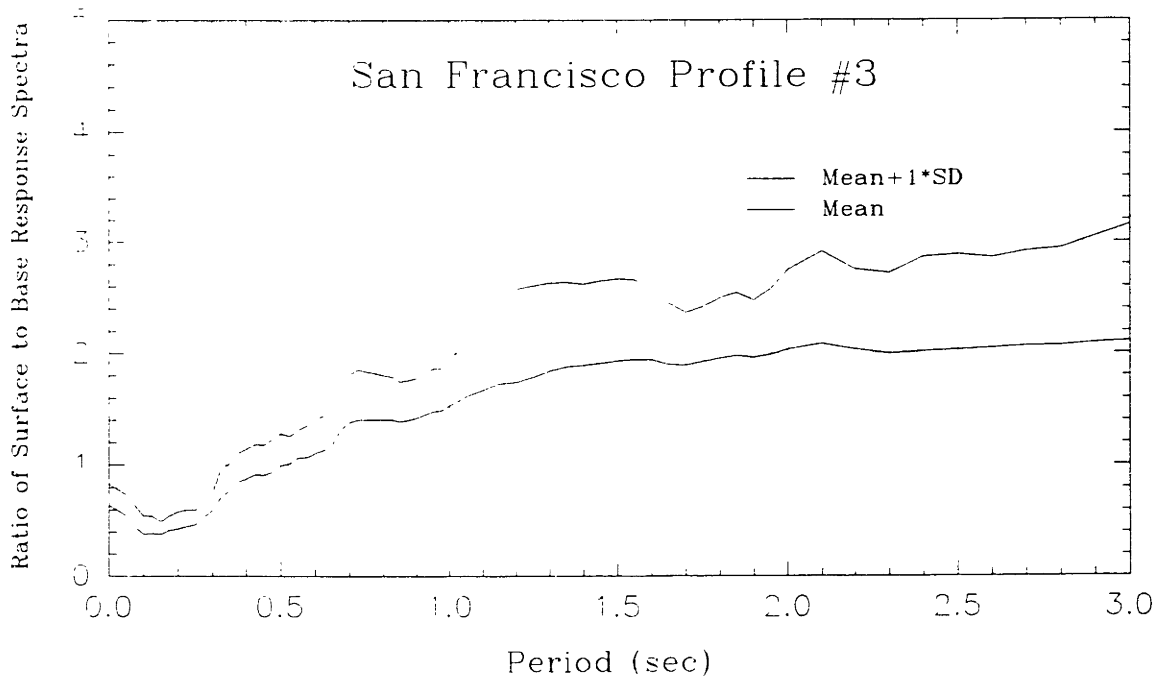
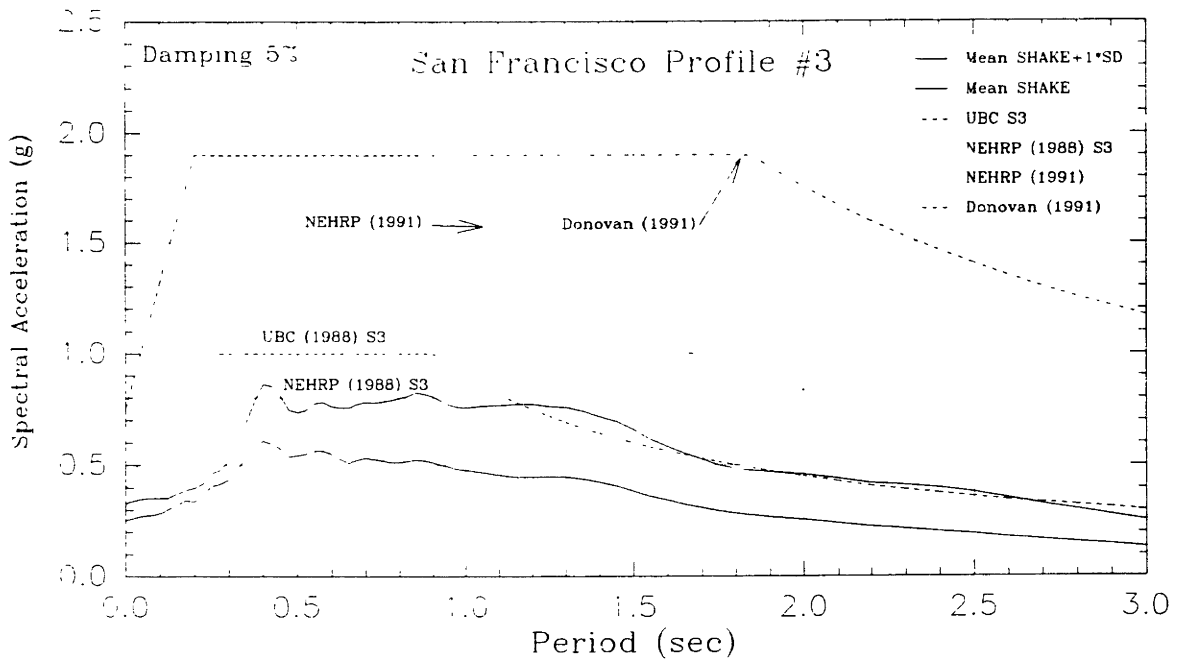


Figure 4-31 Comparison of Response Spectra and Ratio of Response Spectra for San Francisco Profile #3.

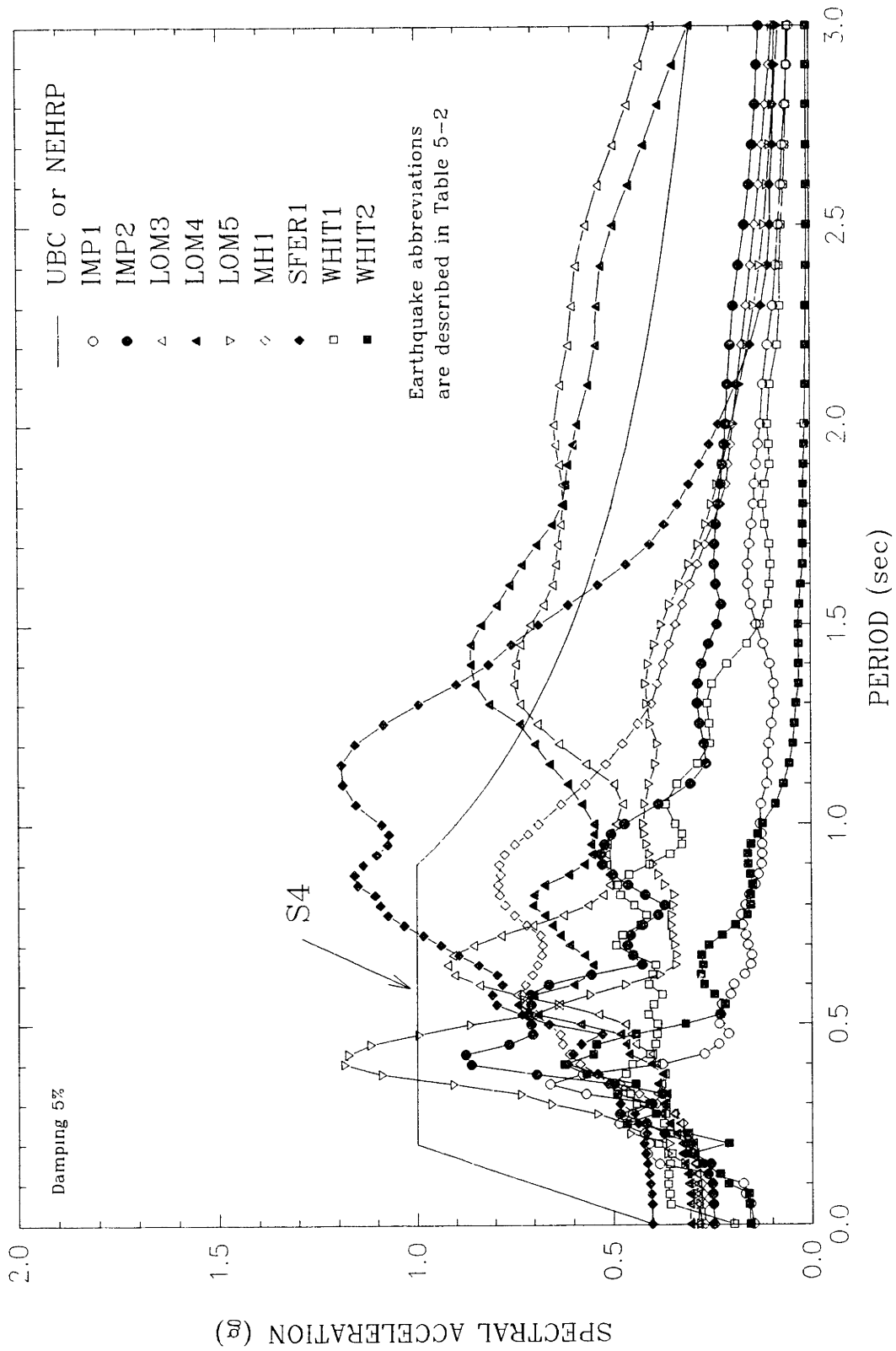


Figure 4-32 Computed Surface Response Spectra for San Francisco Profile #3.

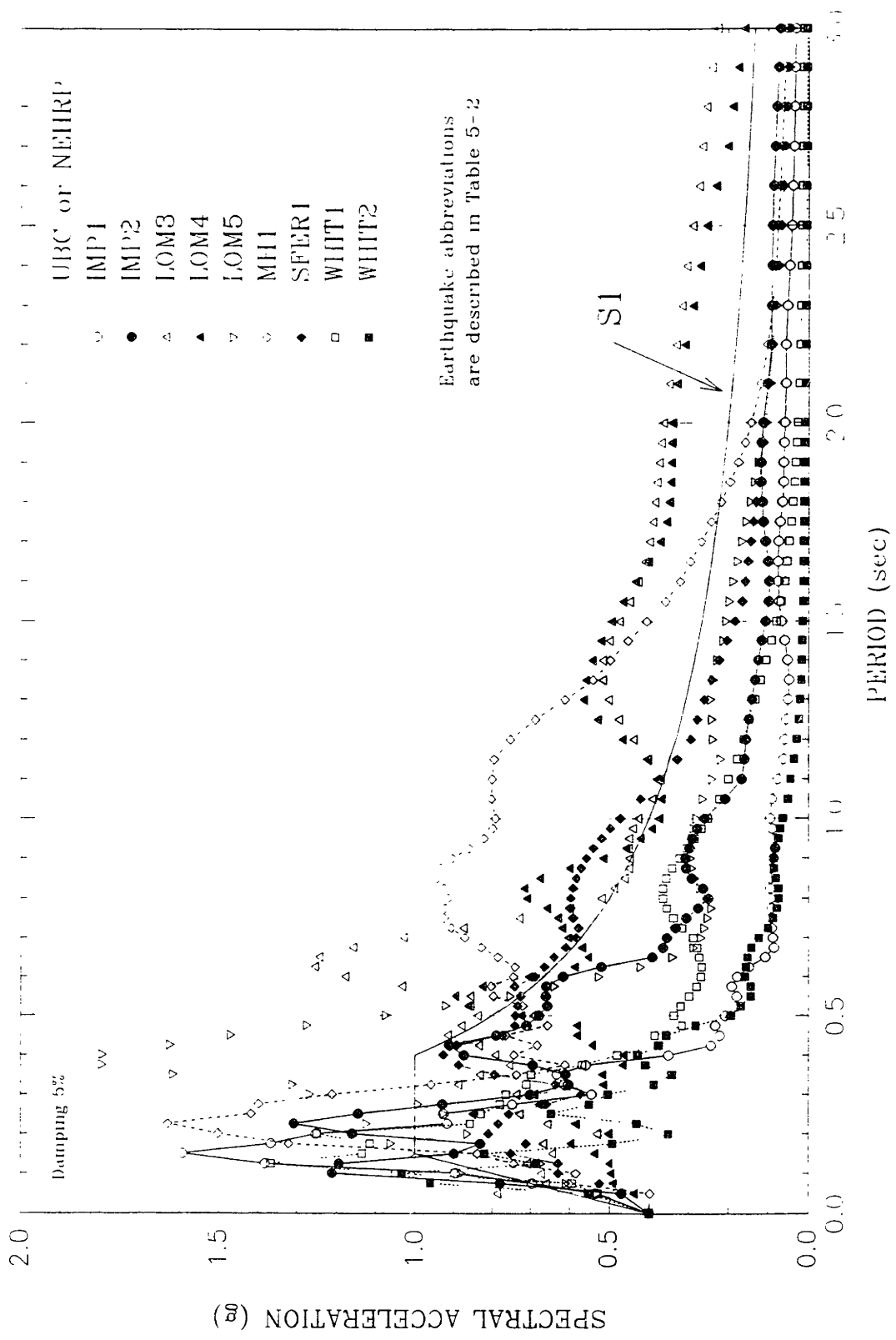


Figure 4-33 Input Earthquake Base Response Spectra for San Francisco.

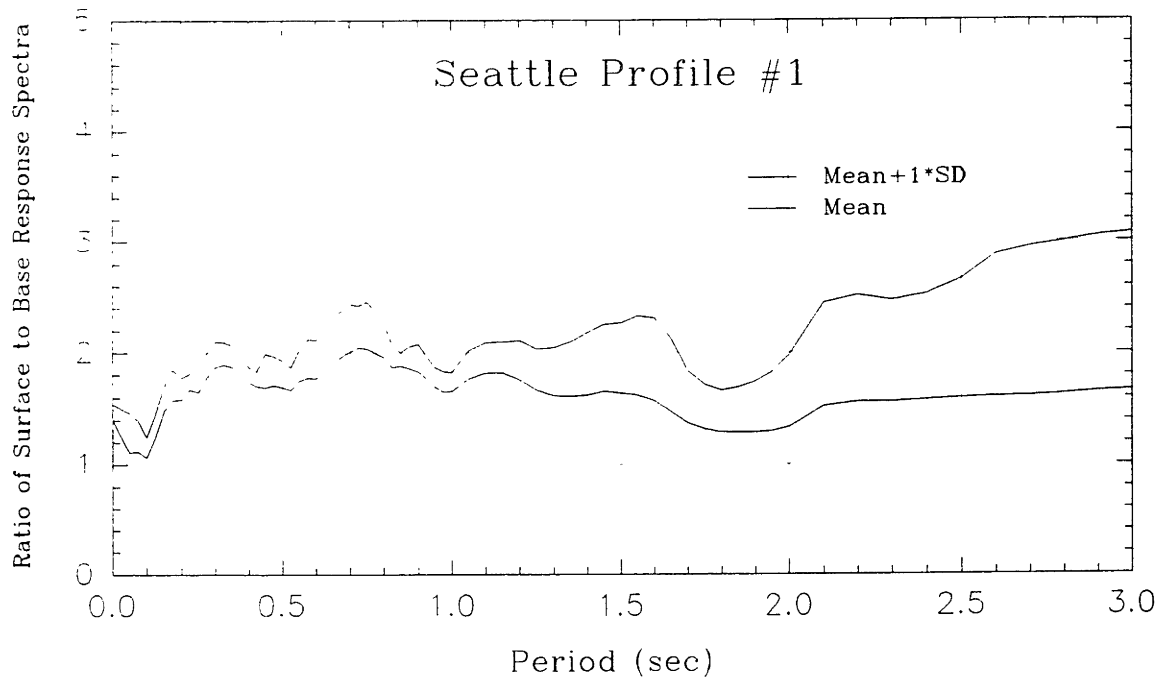
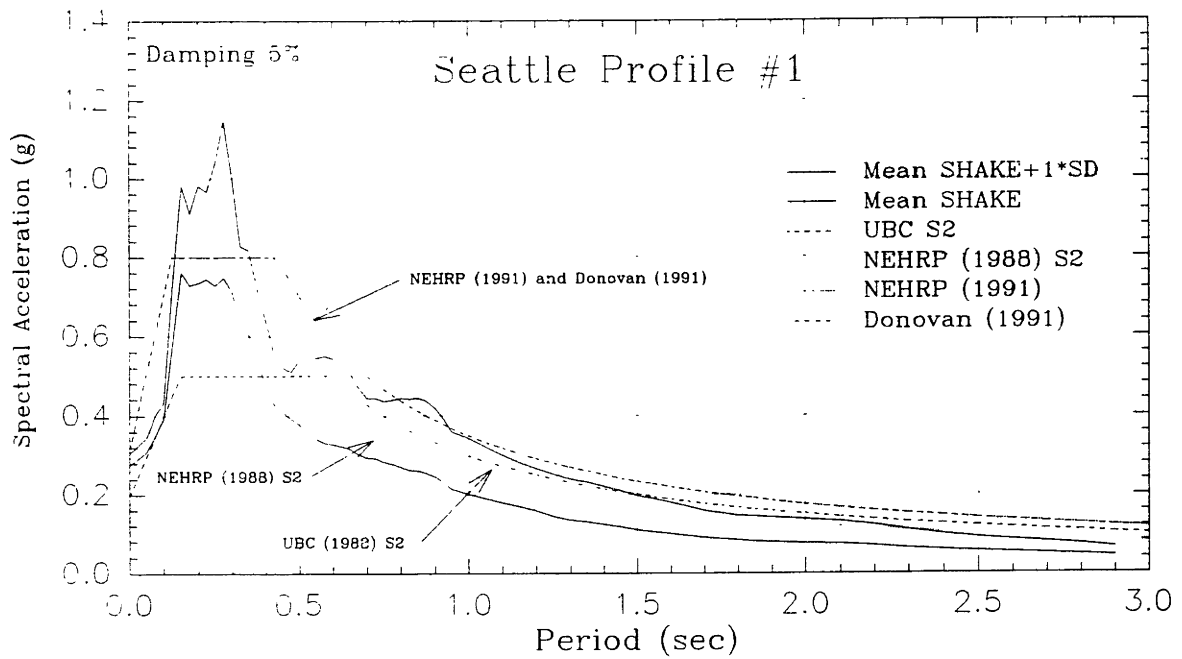


Figure 4-34 Comparison of Response Spectra and Ratio of Response Spectra for Seattle Profile #1.

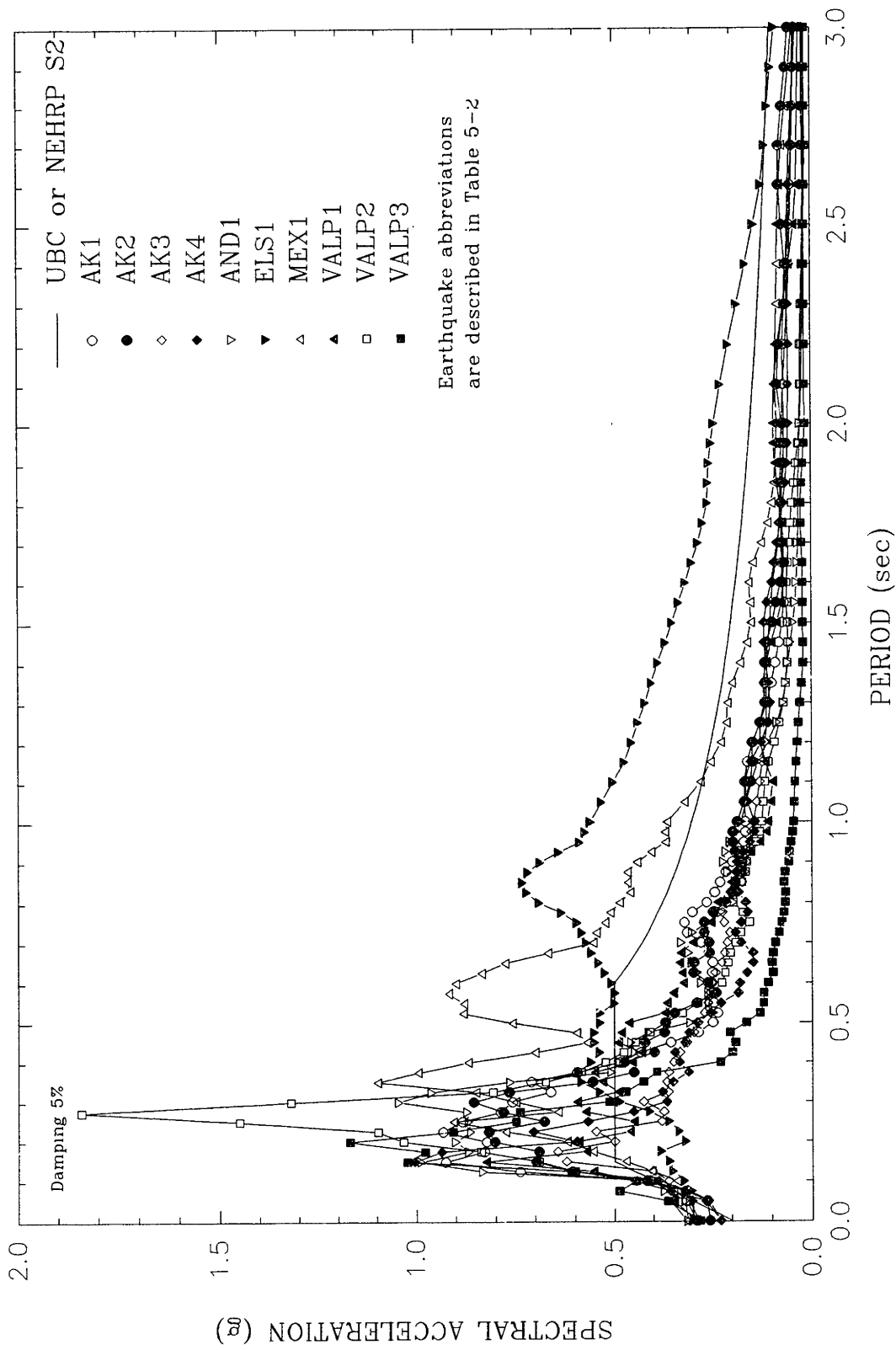


Figure 4-35 Computed Surface Response Spectra for Seattle Profile #1.

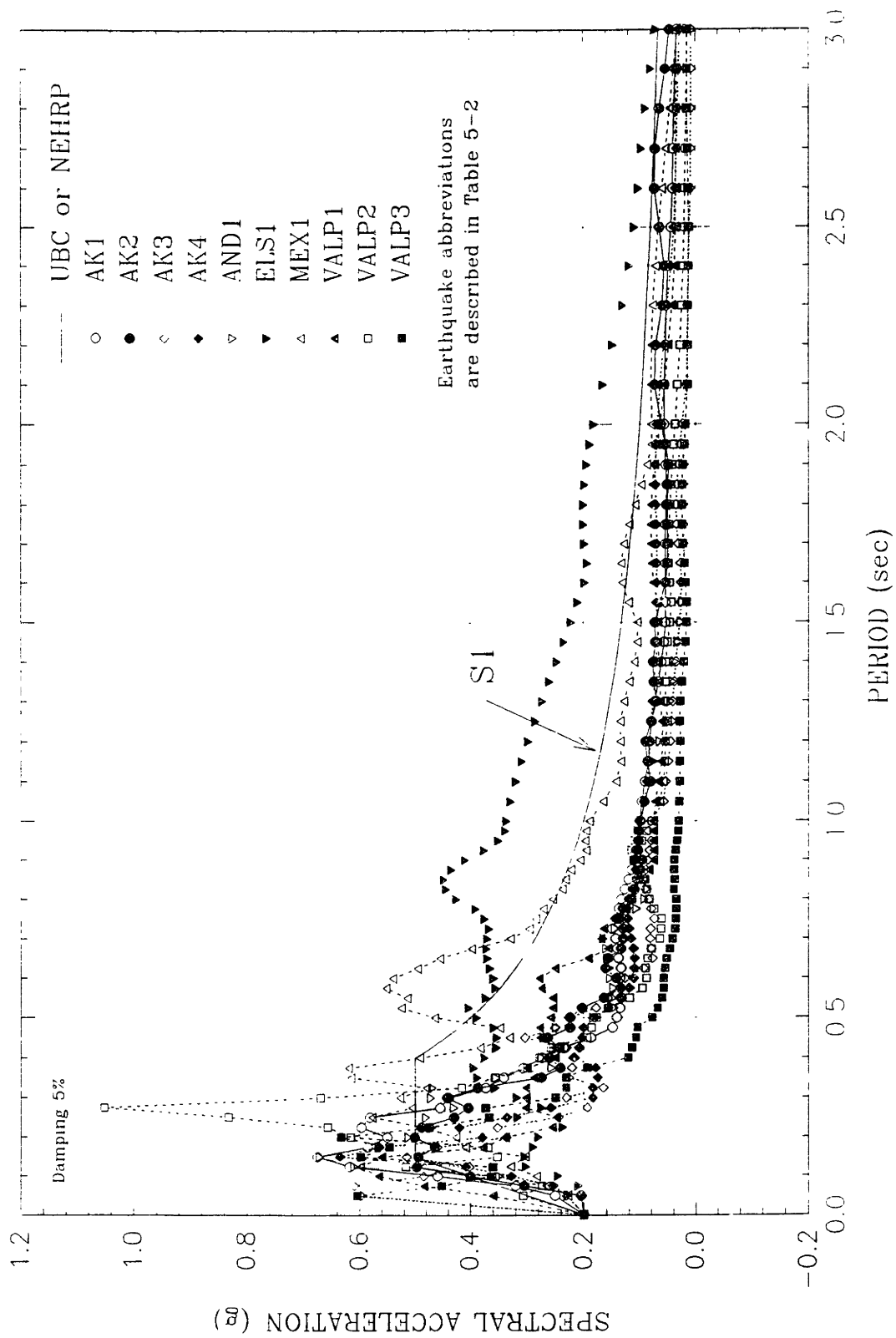
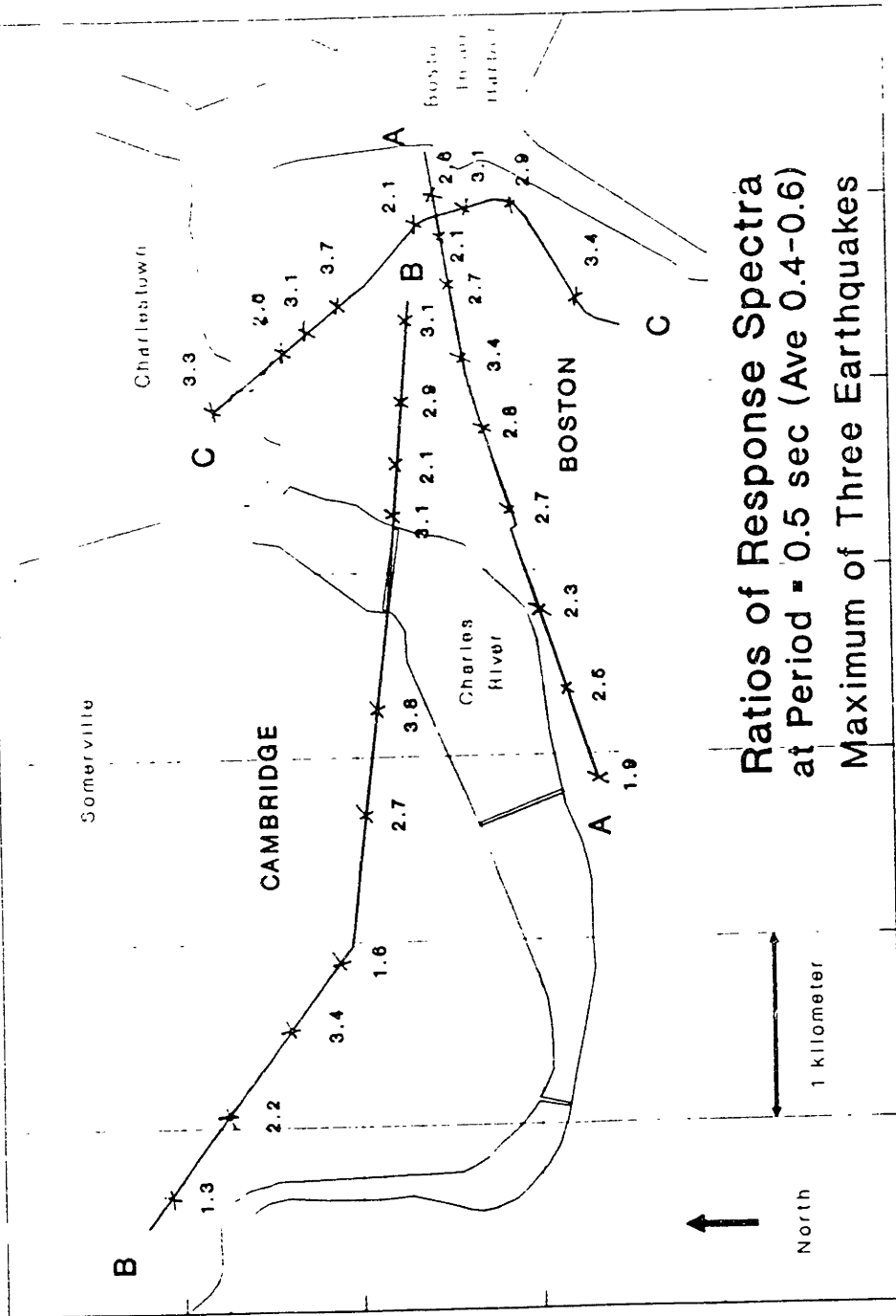


Figure 4-36 Input Earthquake Base Response Spectra for Seattle.



**Ratios of Response Spectra
at Period = 0.5 sec (Ave 0.4-0.6)
Maximum of Three Earthquakes**

Figure 4-37 Map of Boston showing Spectral Ratios Computed for $T = 0.5$ seconds. (After Wysocky, 1990)

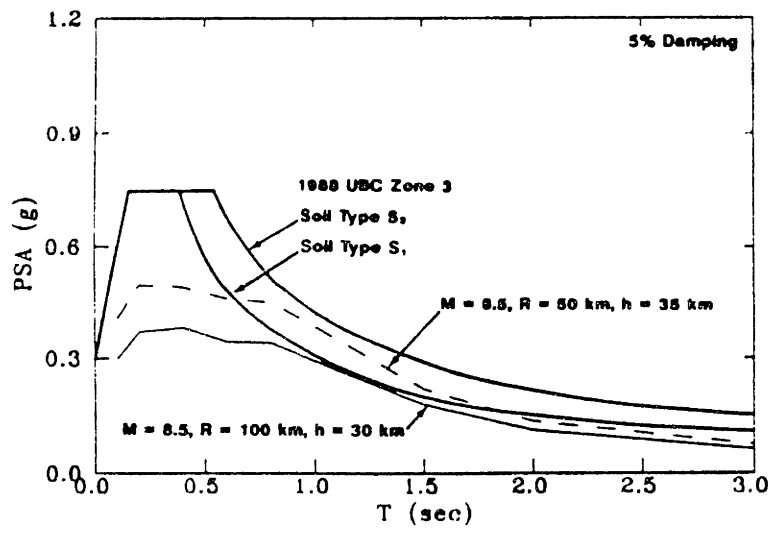


Figure 4-38 Estimated Spectra for the Seattle Area Computed Using Attenuation Relationships. (After Crouse, 1991)

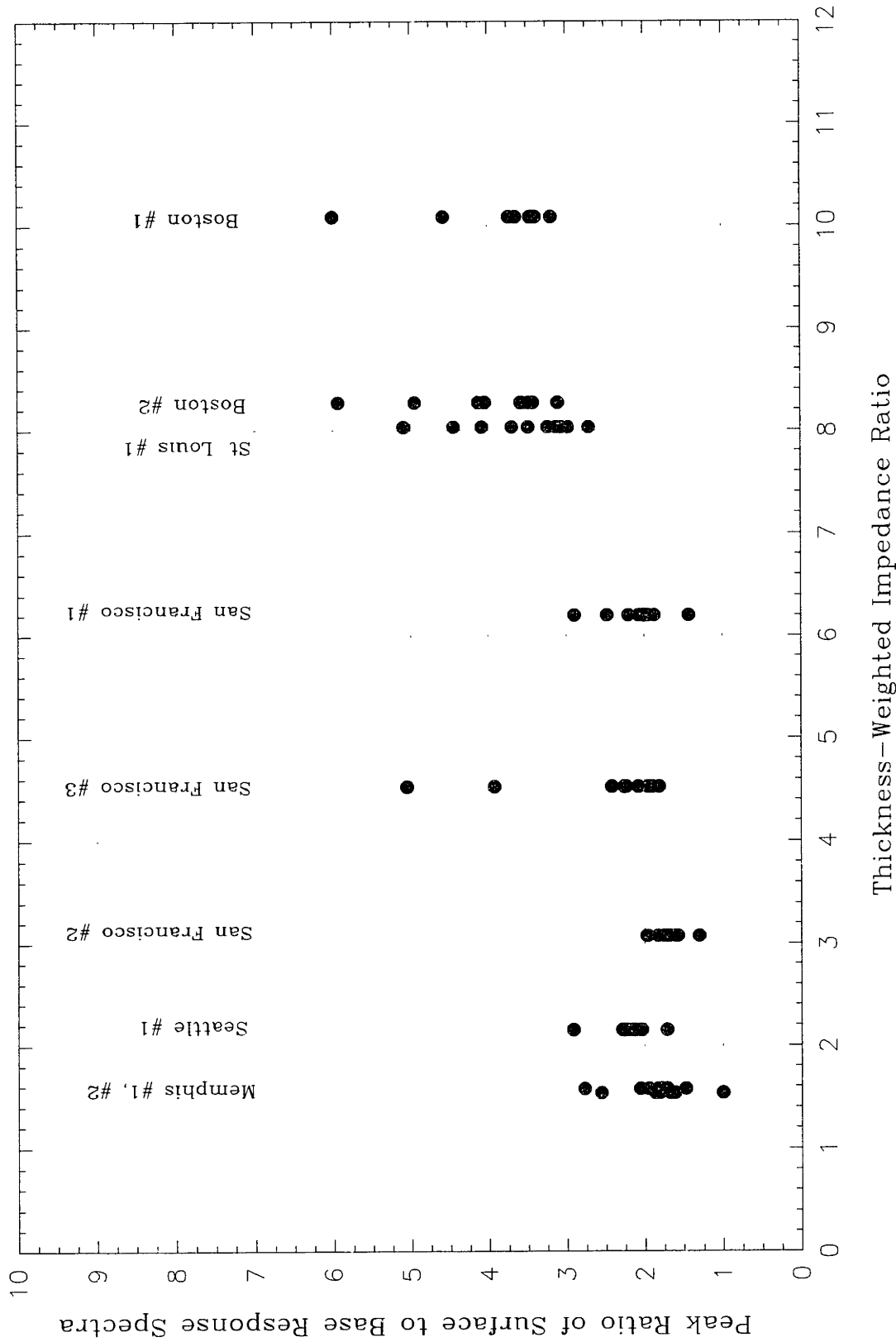


Figure 4-39 Variation of Peak Ratio of Response with Thickness-Weighted Impedance Ratio for City Profiles Analyzed.

CHAPTER 5

INVESTIGATION OF THE EFFECTS OF IMPEDANCE RATIO ON LOCAL SITE RESPONSE

The relevant theory concerning amplification of earthquake motions was presented in Chapter 2. The theory was first formulated in the late 1960's (e.g. Roesset and Whitman, 1969), and has indirectly influenced the formulation of building code provisions. Several researchers have called for more explicit inclusion of results of the theory (e.g. Jacob 1990).

In order to investigate the effects of the impedance ratio on local site response, a simple study was undertaken using the SHAKE program. The objective of the study was to demonstrate the relative influence of impedance ratio, level of shaking, and soil column properties on the site response. The results of the study will be compared with the theory presented in Chapter 2, and applied to the analyses of the city profiles presented in Chapter 4.

5.1 Description of SHAKE Analyses

Figure 5-1 illustrates the soil profiles and input parameters employed for the analyses. The soil profile was kept at a constant total thickness of 150 feet, but the thickness weighted impedance ratio was changed by placing a soft clay layer of varying thickness in the center of a medium dense sand. The thickness of the clay layer varied between 0, 20, 50, 100, and 150 feet, and so changed from the NEHRP and UBC classification of S1 with 0 feet, S3 with 20 feet, and S3 or S4 with 50, 100 and 150 feet. (The profile with 50 feet of soft clay would be classified as S3 in NEHRP and S4 in UBC.) Each soil profile was analyzed resting on three different elastic half-spaces, with shear wave velocities of 2500, 5000, and 7500 fps.

The shear wave velocity of the soft clay was 500 fps and had a plasticity index of 30. The dynamic soil properties were the same as used for the analyses of the city

profiles and were described in Section 4.3. The water table was located at the surface of the profile.

Three levels of shaking, 0.1g, 0.3g, and 0.5g, were used as input peak rock accelerations in the analyses.

Two different earthquakes were input into each profile: the Pasadena record for the 1952 Kern County earthquake; and the N135 component of the Superstition Mountain record of the Imperial Valley 1979 earthquake. Acceleration time histories for the two earthquakes are shown in Figure 5-2, and response spectra for each of the three input accelerations are shown in Figure 5-3. Although recorded on soil and consequently including some site modification effects, the Kern County earthquake was chosen for its broad range of frequency content typical of many WUS earthquakes. The Imperial Valley record was selected for its predominantly higher frequency content which would be more typical of EUS earthquakes.

5.2 Presentation of Results

The response spectra and corresponding ratios of response spectra (RRS) for each soil profile are shown for a different earthquake and a different level of shaking in Figures 5-4 through 5-15. The current NEHRP response spectra are shown for comparison. It should be noted that, in each of these plots, for each soil profile there are three response spectra with the same legend; they represent different elastic half-space shear wave velocities, with in each case the lower, middle, and upper spectrum being for base shear wave velocities of 2500, 5000, and 7500 fps respectively.

Although the plots are somewhat confusing at first due to the representation of fifteen different response spectra or RRS, it is considered that study of the spectra on the same graph can assist in understanding the influence of the different parameters involved, and indeed may be clearer than many equations describing local site response. The relative influences are discussed in the next section.

The peak RRS are tabulated in Table 5-1 and are plotted against thickness weighted impedance ratio in Figures 5-16 and 5-17.

5.3 Discussion of Results

From Figures 5-4 through 5-15 it is evident that amplification of the longer period components in the "softer" profiles and shorter period components in the "denser" profiles occurred; this is well understood from a consideration of the fundamental period of the soil profile, and is the basis for the current site factors in building codes, as discussed in Chapter 2. It can also be seen that the amplification decreases with increasing levels of shaking due to modulus degradation and increased damping. Again this is well understood and these effects are included for in the NEHRP Recommended Provisions (BSSC, 1988) by a reduction factor for S3 and S4 profiles if the peak acceleration is greater than 0.3g.

From Figures 5-4, 5-6 and 5-8, it can be seen that the input base response spectrum for the Kern County earthquake exceeds the NEHRP code spectra at most periods. This may be due to site modification effects included in the acceleration time history. Any comparison of the surface response spectra with the code design spectra would therefore be meaningless, although the RRS and the relative changes in the surface response spectra can be used in analysis of the different factors influencing site response.

In Figures 5-10, 5-12 and 5-14, it can be seen that for the Imperial Valley earthquake, the computed surface response spectra at short periods exceeded the code design spectra for most soil profiles, although the input earthquake response spectrum also did this over a short range of period. At longer periods, even the computed surface response spectra for the S4 sites did not exceed the S1 code spectrum.

There is also a quite noticeable difference between the results from the Kern County and Imperial Valley earthquakes for the RRS. In general, the results from the Kern County earthquake are in agreement with the code provisions and are as expected; referring to Figures 5-5, 5-7 and 5-9, at periods less than about 1.0 second the RRS was typically around one, and at longer periods the spectral ratios were higher,

especially for profiles with thicker clay layers.

The results from the Imperial Valley analyses are quite different; the spectral amplifications for the "denser" sites at shorter periods are larger in most cases than those for "softer" sites at long periods - which is the opposite of what would be expected. This is however in agreement with the observations from the analyses for the city profiles described in Chapter 4. The difference between the Kern County and Imperial Valley results is thought to occur as a result of the higher dynamic strains induced by the Kern County earthquake when both earthquakes are normalized to the same peak acceleration. The peak ratio of response spectra for both earthquakes occurs at the fundamental period of the soil profile after shaking, and this is at higher periods for the Kern County earthquake due to the higher strain levels. Consequently, the profiles with longer periods are amplified more by the Kern County earthquake, and those with shorter periods are amplified more by the Imperial Valley earthquake.

It should be noted that it can be misleading to simply look at the ratio of response spectra as a measure of the response; it can be seen by comparing, for example, Figures 5-10 and 5-11 that at the peak spectral amplification, the response is relatively small because the base spectral accelerations are small at the fundamental period of the profile after shaking. Of more practical interest with respect to the magnitude of the spectral ordinates in Figure 5-10, are the spectral ratios approaching 2.5 at periods between 0.1 and 0.3 seconds, where base response is higher.

The peak RRS were plotted against the thickness weighted impedance ratios for the various soil profiles, and the results are shown in Figures 5-16 through 5-18. It can be seen from Figure 5-16 that there is a trend of increasing peak RRS with increasing impedance ratio. This trend is less pronounced at higher levels of acceleration. There is also considerably more scatter at lower levels of shaking. It can be seen that for a given earthquake and a given soil profile, the peak response will increase as the impedance ratio increases. It can also be seen that this trend levels off somewhat with increasing impedance ratio. It should be noted, however, that the peak RRS depicted in Figures 5-16 through 5-18 include the effects of the soil column, and are not simply a function of the impedance ratio.

From the RRS plots in Figures 5-4 through 5-15, the relative effects of level of shaking, soil profile, and impedance ratio can be seen. For each input acceleration and each earthquake, the effect of impedance ratio can be observed by comparing the spectra with the same legend, with the increasing RRS being due to the increase in the shear wave velocity of the elastic half-space. This is most noticeable from the Imperial Valley results for 0.1g shown in Figure 5-11. In addition, the effect of the soil column on the spectral amplification for each impedance ratio can be observed by comparing the curves with the different legends.

Thus, the effects of the impedance ratio and the soil column can be separated approximately. It is therefore possible from these plots to extrapolate a soil and an impedance factor for each earthquake and input acceleration. These two factors combine to form the overall site factor and can be defined algebraically as follows:

$$S = S_i S_s \quad (\text{Eq. 5.1})$$

where S = overall site factor, S_i = impedance factor, and S_s = soil factor. The three factors can be defined as follows:

$$S = \frac{S_{A \text{ surface}}}{S_{A \text{ rock}}} ; S_s = \frac{S_{A \text{ surface (2500)}}}{S_{A \text{ rock}}} ; S_i = \frac{S_{A \text{ surface}}}{S_{A \text{ surface (2500)}}} \quad (\text{Eq. 5.2})$$

where $S_{A \text{ surface}}$ is the spectral acceleration at the surface of a profile with any base shear wave velocity, $S_{A \text{ surface (2500)}}$ is the spectral acceleration at the surface of a profile with a base shear wave velocity 2500 fps, and $S_{A \text{ rock}}$ is the earthquake spectral acceleration.

By taking as a baseline the RRS for the S1 site and dividing it into the RRS for the other profiles, the soil factor was calculated, and is shown in Figure 5-17. The soil factor thus defined is similar for each impedance ratio. In a similar manner, an impedance factor was calculated using the RRS for an elastic half space shear wave velocity of 2500 fps as baseline and is shown for each earthquake and elastic half-space in Figures 5-20 and 5-21. The soil factor defined above (since it is based on the surface response for a soil profile over an elastic half-space shear wave velocity

of 2500 fps), can be considered similar to the soil factors included in the current codes, which are based on empirical data from Californian sites with bedrock shear wave velocities around 3000 fps. The impedance factor defined above can therefore be considered as applying to sites where bedrock is harder than Californian "soft" rock sites.

From Figure 5-19, it is apparent that the soil factors are similar for both earthquakes at low levels of shaking, and that the Kern County earthquake soil factor decreased as the level of shaking increased, but did not vary significantly for the Imperial Valley earthquake.

It can also be observed from Figure 5-19 that the soil factor is in broad agreement with the soil factors currently used in building codes. The shape and magnitude is typical of that expected, being around one at periods up to 1.0 second (with some de-amplification in the softer deposits) and there is an increasing response at longer periods for softer sites, with the factor for the S4 site in the 1.8 to 2.0 range.

The impedance factors varied noticeably between the two earthquakes, and also varied markedly with respect to frequency and soil type. In general, the impedance factors are higher for "denser" soil profiles, and decrease with increasing levels of shaking.

The separation of a site factor into an impedance and a soil factor is in general agreement with the equation presented in Chapter 2 from Roesset and Whitman (1969):

$$1/A_2(\omega) = 1/IR + 1/A_1(\omega) \quad (\text{Eq. 5.3})$$

where $A_2(\omega)$ is an overall site amplification function, IR is the impedance ratio and $A_1(\omega)$ is a rigid rock or soil profile amplification function. It should be noted that the above equation is formulated in terms of peak displacement (or acceleration) and not in terms of ratio of response spectra, and only the concept of linking an impedance and soil factor is considered.

5.4 Application to Analysis of City Profiles

The information on the relative effects of level of shaking and soil profile on the impedance amplification were applied to the results presented in Chapter 4 for the city profiles. The peak RRS calculated and originally presented in Figure 4-39 were divided by a soil factor and a level of shaking factor in order to try and isolate impedance effects. The factors were based on engineering judgement and on the results presented in this chapter and are shown in Table 5-2. The impedance factors plotted against impedance ratio are shown in Figure 5-22. It can be seen that for the sites with a high impedance ratio, Boston and St. Louis, impedance factors between 1.5 and 2.5 are common, depending on the input earthquake. This is in broad agreement with the results presented earlier in this chapter, although there is some circular logic to this conclusion, since the previous results were used to derive the city profile impedance factors.

The calculation of a thickness weighted impedance factor requires detailed information about the soil profile and is not really suitable for specification in building codes; it would be much simpler to specify the factor in terms of the base shear wave velocity. The impedance factors previously calculated, plotted against base shear wave velocity are shown in Figure 5-24.

5.5 Conclusions

It has been demonstrated that the amplification of response can, with satisfactory approximation, be considered the product of an impedance and a soil factor. This conclusion is supported by the theory presented in Chapter 2 and by the results from the analyses of city profiles undertaken in Chapter 4.

The computed soil factors are in good agreement with the site factors in current code provisions.

For profiles with a base shear wave velocity greater than 3500 fps and where peak design accelerations are less than around 0.2g, an impedance factor of 1.5 would

appear to be reasonable estimate of the effects of impedance ratio. For profiles with base shear wave velocities less than 3500 fps, or subjected to levels of shaking higher than 0.2g, an additional impedance factor is not warranted.

Peak Input Acceleration	Vr (fps)	H clay (ft)	I*	Vr/V*	V* (fps)	T* (sec)	Kern County	Imperial Valley
							Peak RRS	Peak RRS
0.1g	2500	0	3.6	3.0	844	0.71	2.19	2.86
		20	4.1	3.3	761	0.79	2.35	2.71
		50	4.8	3.8	666	0.90	2.82	3.00
		100	5.9	4.5	558	1.08	3.20	2.75
		150	6.8	5.0	500	1.20	3.40	2.44
	5000	0	7.1	5.9	844	0.71	2.54	3.91
		20	8.1	6.6	761	0.79	2.69	3.30
		50	9.6	7.5	666	0.90	3.38	3.71
		100	11.8	9.0	558	1.08	3.38	3.12
	7500	150	13.6	10.0	500	1.20	3.70	2.75
		0	10.7	8.9	844	0.71	3.92	4.42
		20	12.2	9.9	761	0.79	2.67	3.62
		50	14.3	11.3	666	0.90	3.62	3.99
		100	17.8	13.4	558	1.08	3.90	3.29
	0.3g	2500	150	20.5	15.0	500	1.20	4.12
0			3.6	3.0	844	0.71	2.30	2.48
20			4.1	3.3	761	0.79	2.46	2.59
50			4.8	3.8	666	0.90	2.52	2.45
100			5.9	4.5	558	1.08	2.85	2.43
5000		150	6.8	5.0	500	1.20	2.83	2.63
		0	7.1	5.9	844	0.71	2.45	3.11
		20	8.1	6.6	761	0.79	2.64	3.08
		50	9.6	7.5	666	0.90	2.81	2.77
7500		100	11.8	9.0	558	1.08	3.15	2.74
		150	13.6	10.0	500	1.20	3.10	3.00
		0	10.7	8.9	844	0.71	2.49	3.40
		20	12.2	9.9	761	0.79	2.68	3.28
		50	14.3	11.3	666	0.90	2.92	2.87
0.5g		2500	100	17.8	13.4	558	1.08	3.27
	150		20.5	15.0	500	1.20	3.19	3.15
	0		3.6	3.0	844	0.71	2.13	2.37
	20		4.1	3.3	761	0.79	2.27	2.25
	50		4.8	3.8	666	0.90	2.39	2.15
	5000	100	5.9	4.5	558	1.08	2.51	2.49
		150	6.8	5.0	500	1.20	2.43	2.77
		0	7.1	5.9	844	0.71	2.30	2.84
		20	8.1	6.6	761	0.79	2.44	2.53
	7500	50	9.6	7.5	666	0.90	2.55	2.36
		100	11.8	9.0	558	1.08	2.71	2.74
		150	13.6	10.0	500	1.20	2.58	3.12
		0	10.7	8.9	844	0.71	2.36	2.99
		20	12.2	9.9	761	0.79	2.50	2.63
	7500	50	14.3	11.3	666	0.90	2.60	2.43
100		17.8	13.4	558	1.08	2.77	2.84	
150		20.5	15.0	500	1.20	2.63	3.25	

I*, V*, T* are Thickness – Weighted Average Impedance Ratio, Soil Shear Wave Velocity and Fundamental Period as defined in Jacob (1990). Peak RRS is the peak ratio of the surface to base acceleration response spectra.

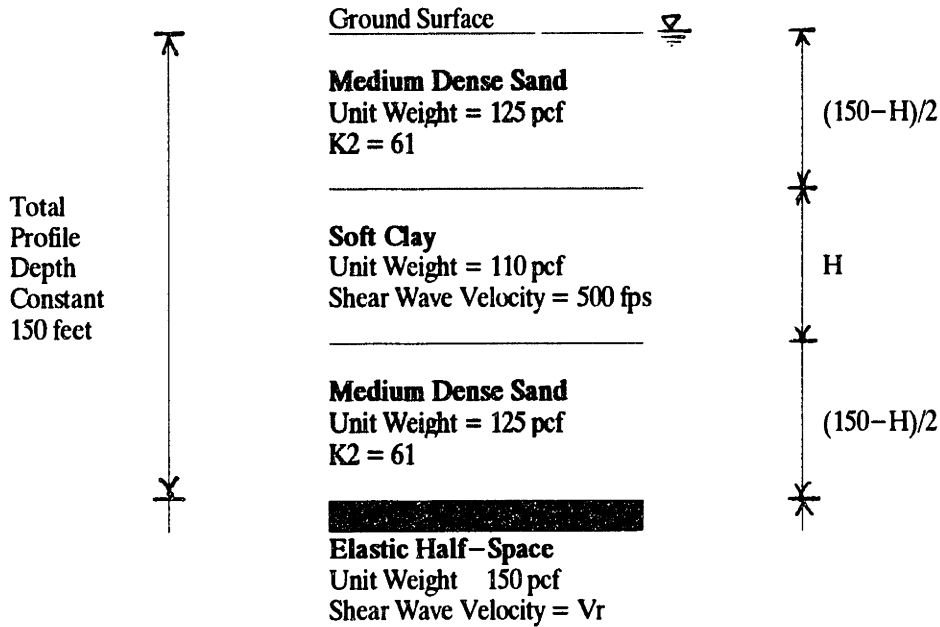
Table 5–1 Results of Analyses with Varying Impedance Ratio

Profile	Level of Shaking Factor	Soil Factor
Boston #1	1.15	1.7
Boston #2	1.15	1.6
Memphis #1	1.1	1.2
Memphis #2	1.1	1.2
St Louis #1	1.15	1
San Francisco #1	1	2
San Francisco #2	1	1.2
San Francisco #3	1	1.9
Seattle #1	1.1	1.2

Note

The peak ratios of response spectra computed for each input earthquake were divided by the above tabulated factors in order to try and isolate the effects of impedance ratio on the peak RRS.

Table 5–2 Factors Used to Compute Impedance Ratios from Peak Ratio of Response Spectra for City Profiles



Vr (fps)	H clay (ft)	Impedance Ratio I*	Vr/V*	V* (fps)	T* (sec)
2500	0	3.6	3.0	844	0.71
	20	4.1	3.3	761	0.79
	50	4.8	3.8	666	0.90
	100	5.9	4.5	558	1.08
	150	6.8	5.0	500	1.20
5000	0	7.1	5.9	844	0.71
	20	8.1	6.6	761	0.79
	50	9.6	7.5	666	0.90
	100	11.8	9.0	558	1.08
	150	13.6	10.0	500	1.20
7500	0	10.7	8.9	844	0.71
	20	12.2	9.9	761	0.79
	50	14.3	11.3	666	0.90
	100	17.8	13.4	558	1.08
	150	20.5	15.0	500	1.20

I*, Vr*, and T* are Thickness-Weighted Averages

Three levels of Shaking were Analyzed for each Profile:

0.1g, 0.3g, and 0.5g

Two Input Earthquakes were analyzed for each Profile:

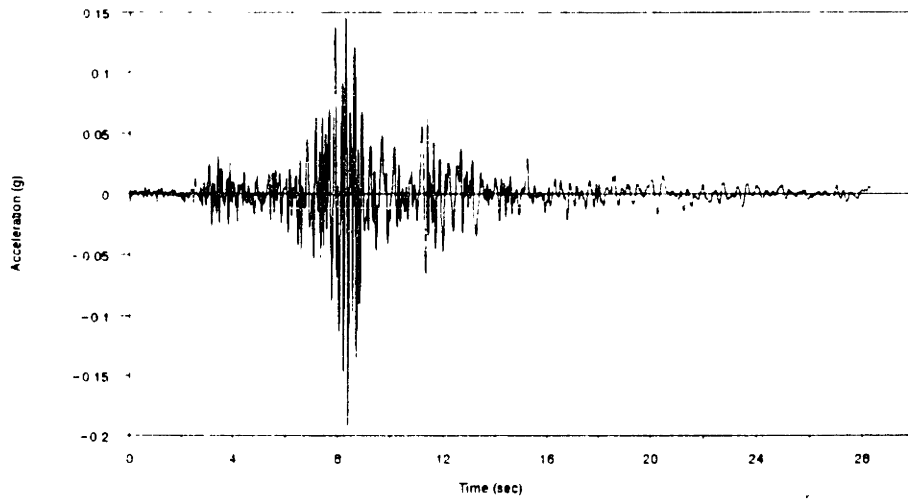
Kern County (1952)

Imperial Valley (1979)

Figure 5-1 Description of Profiles Analyzed with Varying Impedance Ratio

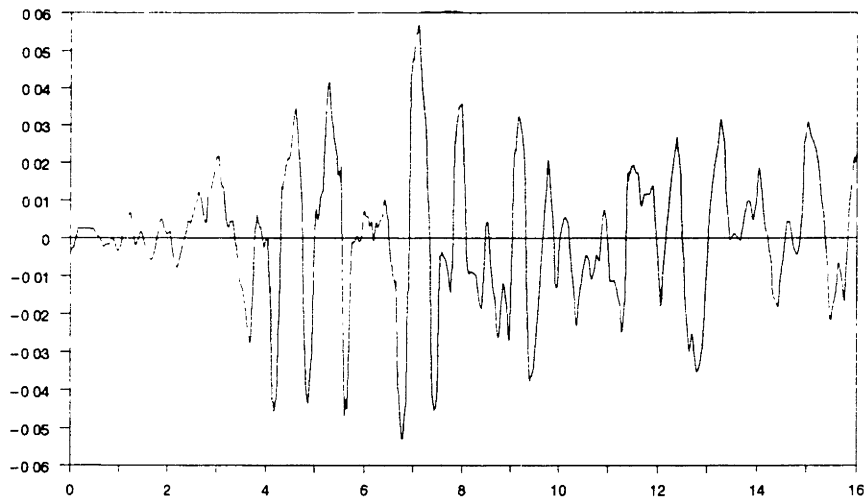
Imperial Valley (1979)

Superstition Mountain N135 Component



Kern County (1952)

Pasadena



The above earthquakes were scaled to peak accelerations of 0.1g, 0.3g, and 0.5g.

Figure 5-2 Acceleration Time Histories of Input Earthquakes for Analysis of Impedance Effects

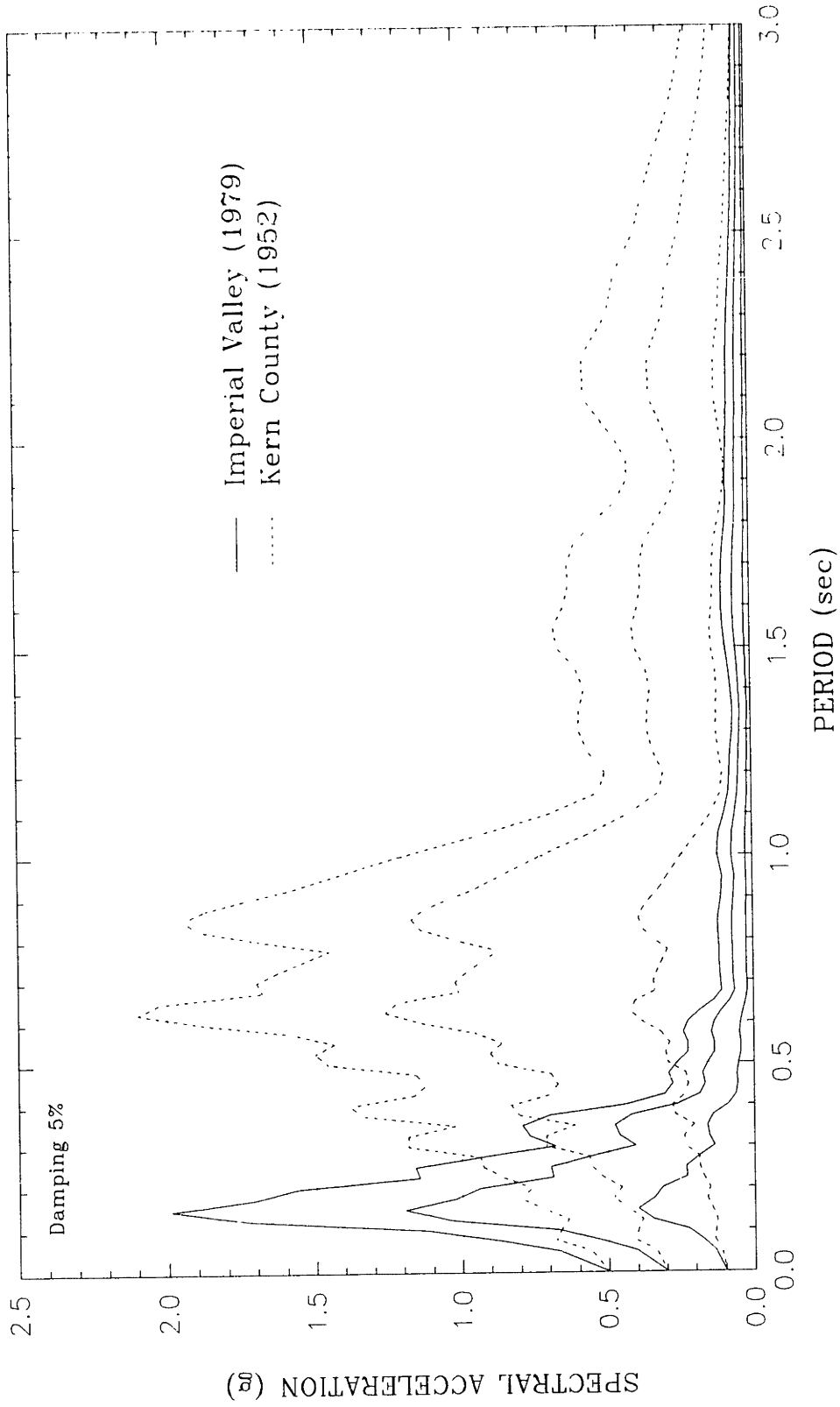


Figure 5-3 Input Earthquake Base Response Spectra for Analysis of 150 ft Thick Soil Column with a Varying Thickness of Soft Clay Between Medium Sand.

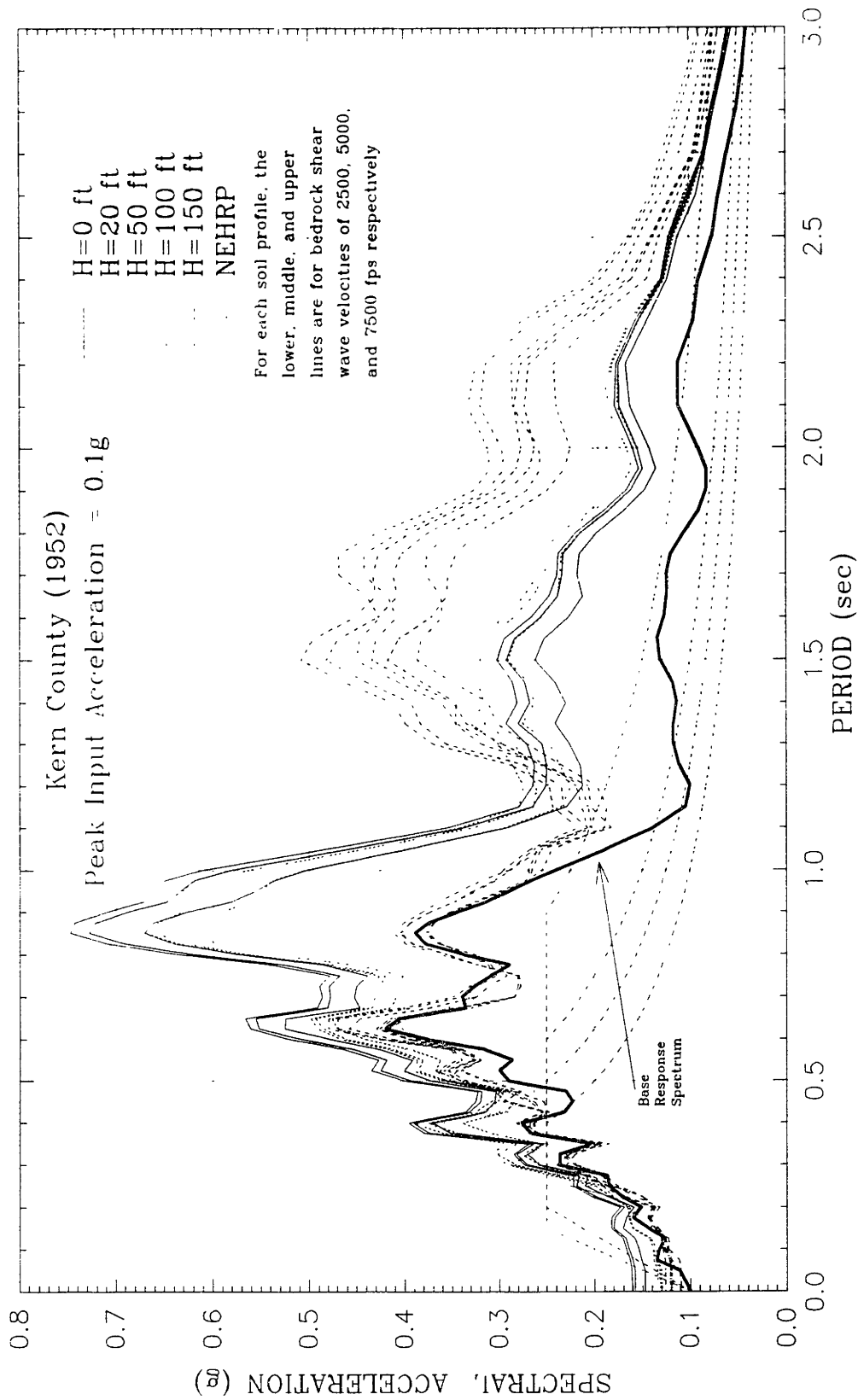


Figure 5-4 Response Spectra for a 150 ft Thick Soil Column with a Soft Clay Layer Between Medium Dense Sand from the Kern County (1952) Pasadena Record with a Peak Input Acceleration of 0.1g.

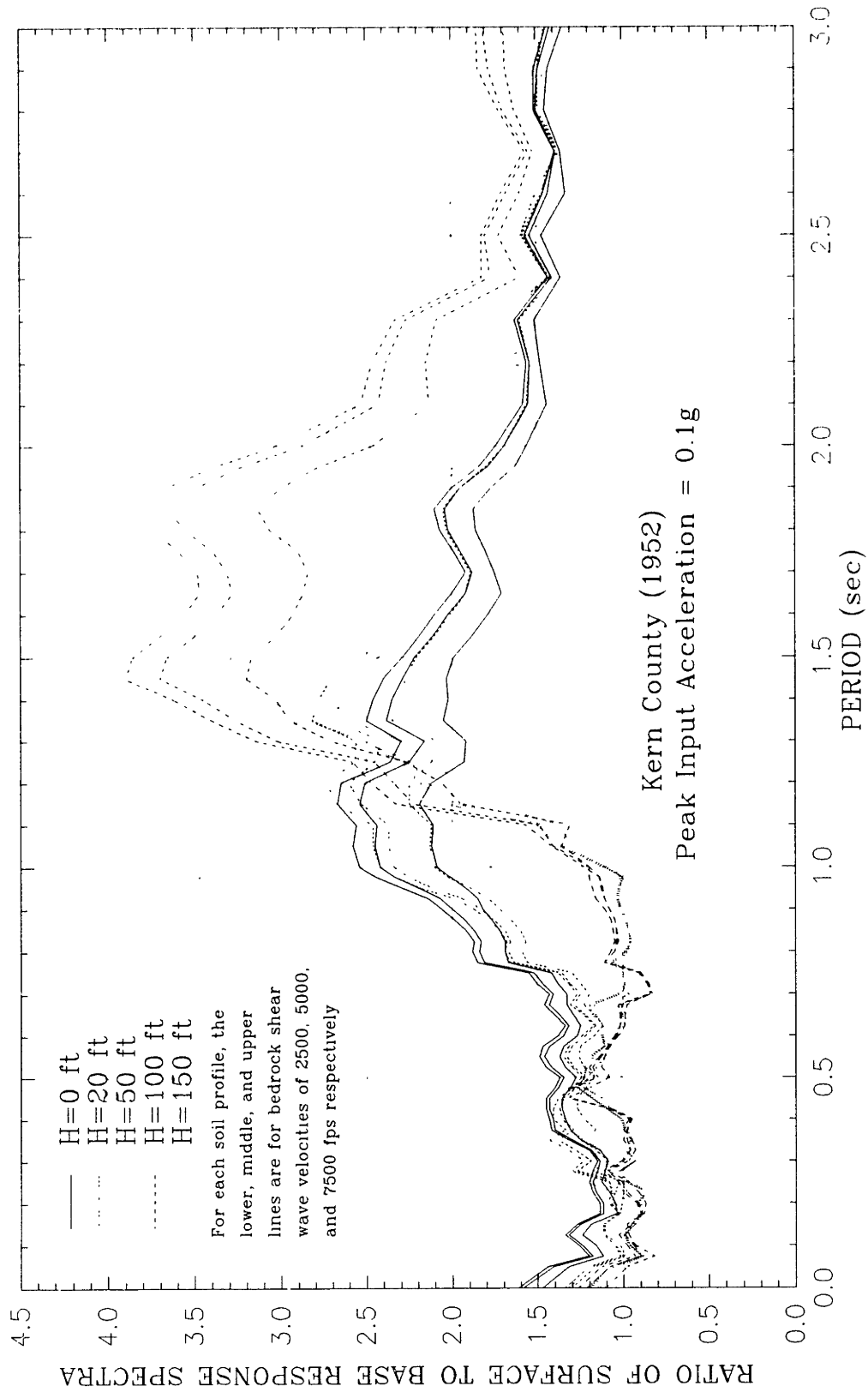


Figure 5-5 Ratio of Response Spectra for a 150 ft Thick Soil Column with a Soft Clay Layer Between Medium Dense Sand from the Kern County (1952) Pasadena Record with a Peak Input Acceleration of 0.1g.

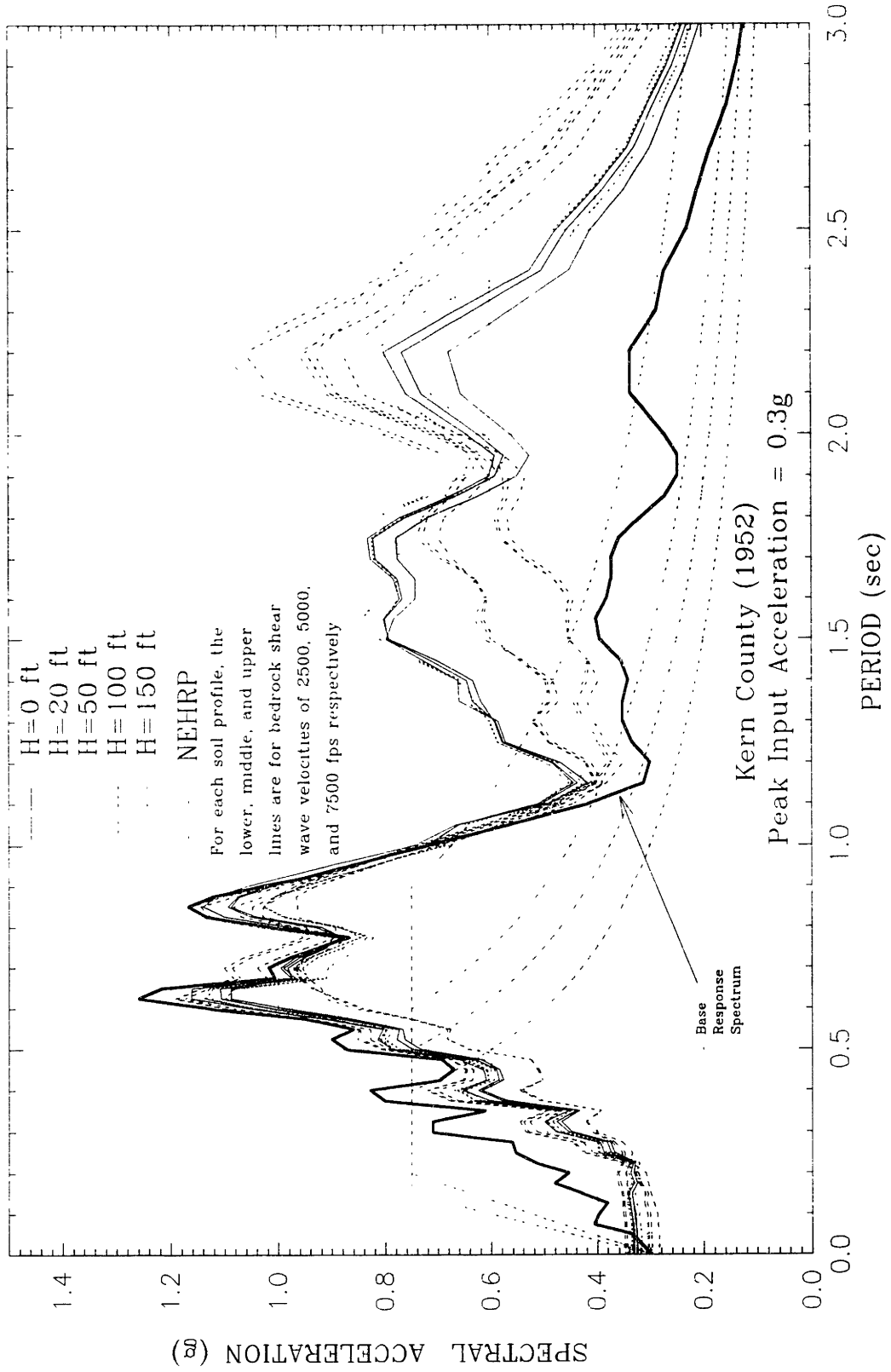


Figure 5-6 Response Spectra for a 150 ft Thick Soil Column with a Soft Clay Layer Between Medium Dense Sand from the Kern County (1952) Pasadena Record with a Peak Input Acceleration of 0.3g.

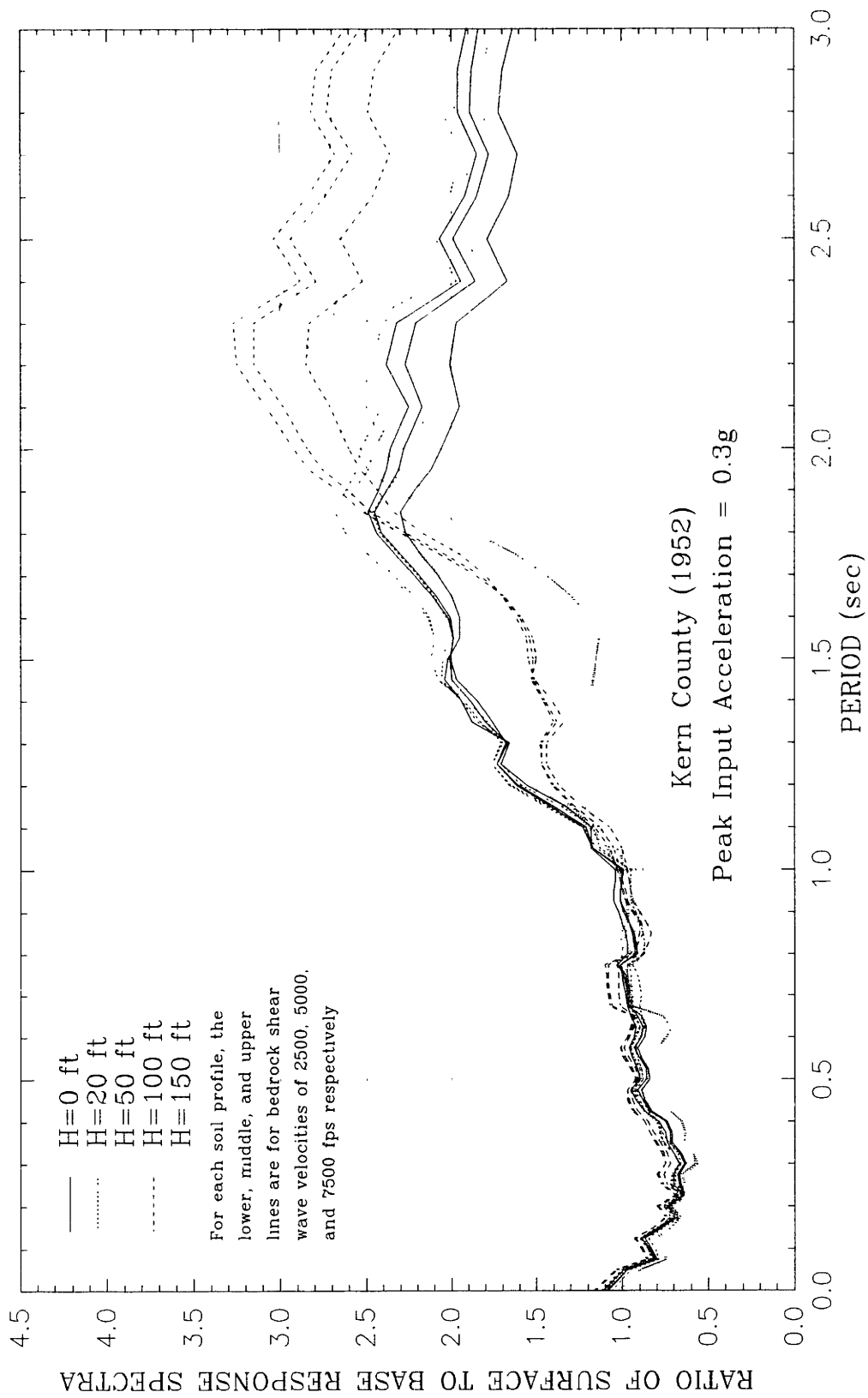


Figure 5-7 Ratio of Response Spectra for a 150 ft Thick Soil Column with a Soft Clay Layer Between Medium Dense Sand from the Kern County (1952) Pasadena Record with a Peak Input Acceleration of 0.3g.

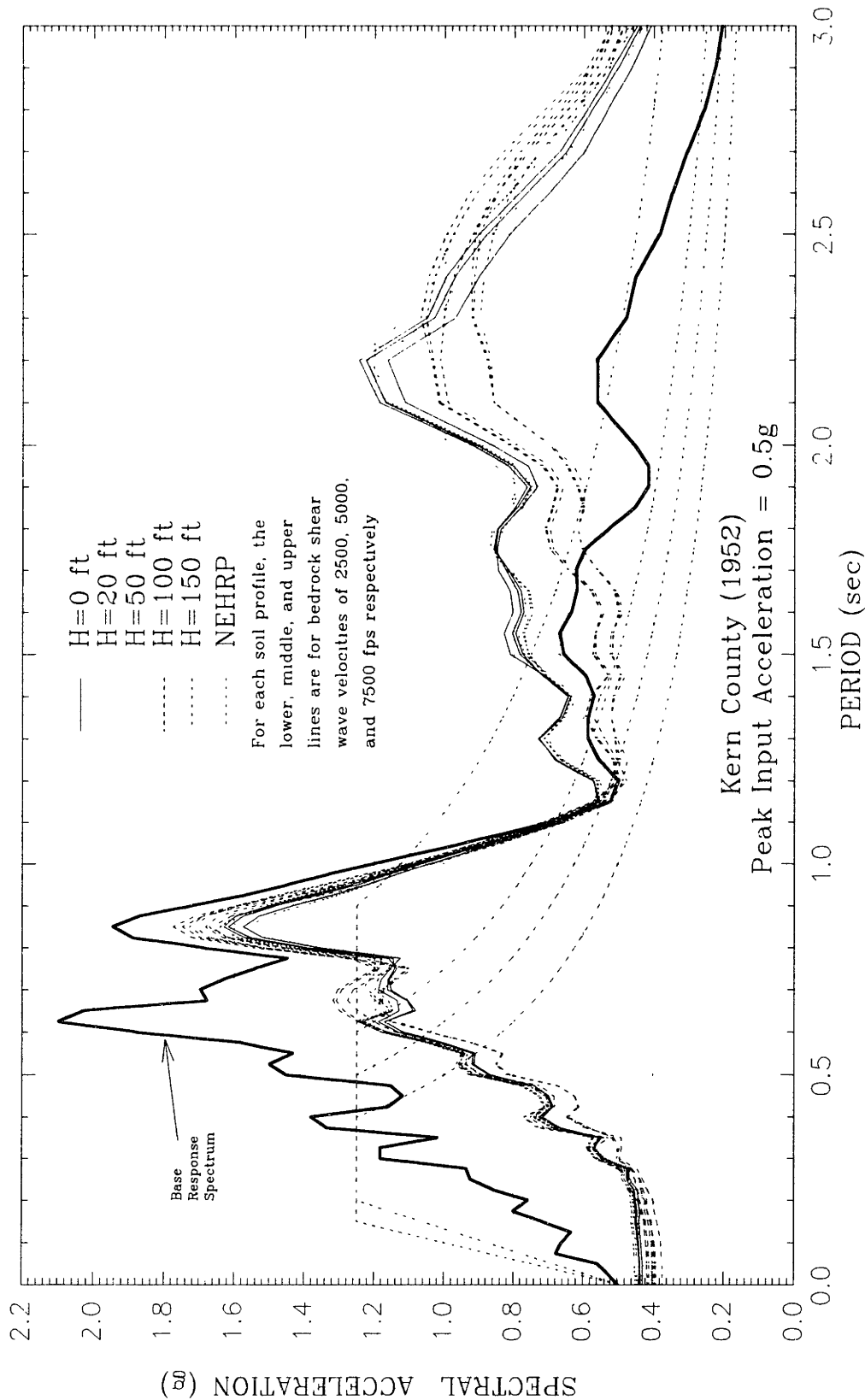


Figure 5-8 Response Spectra for a 150 ft Thick Soil Column with a Soft Clay Layer Between Medium Dense Sand from the Kern County (1952) Pasadena Record with a Peak Input Acceleration of 0.5g.

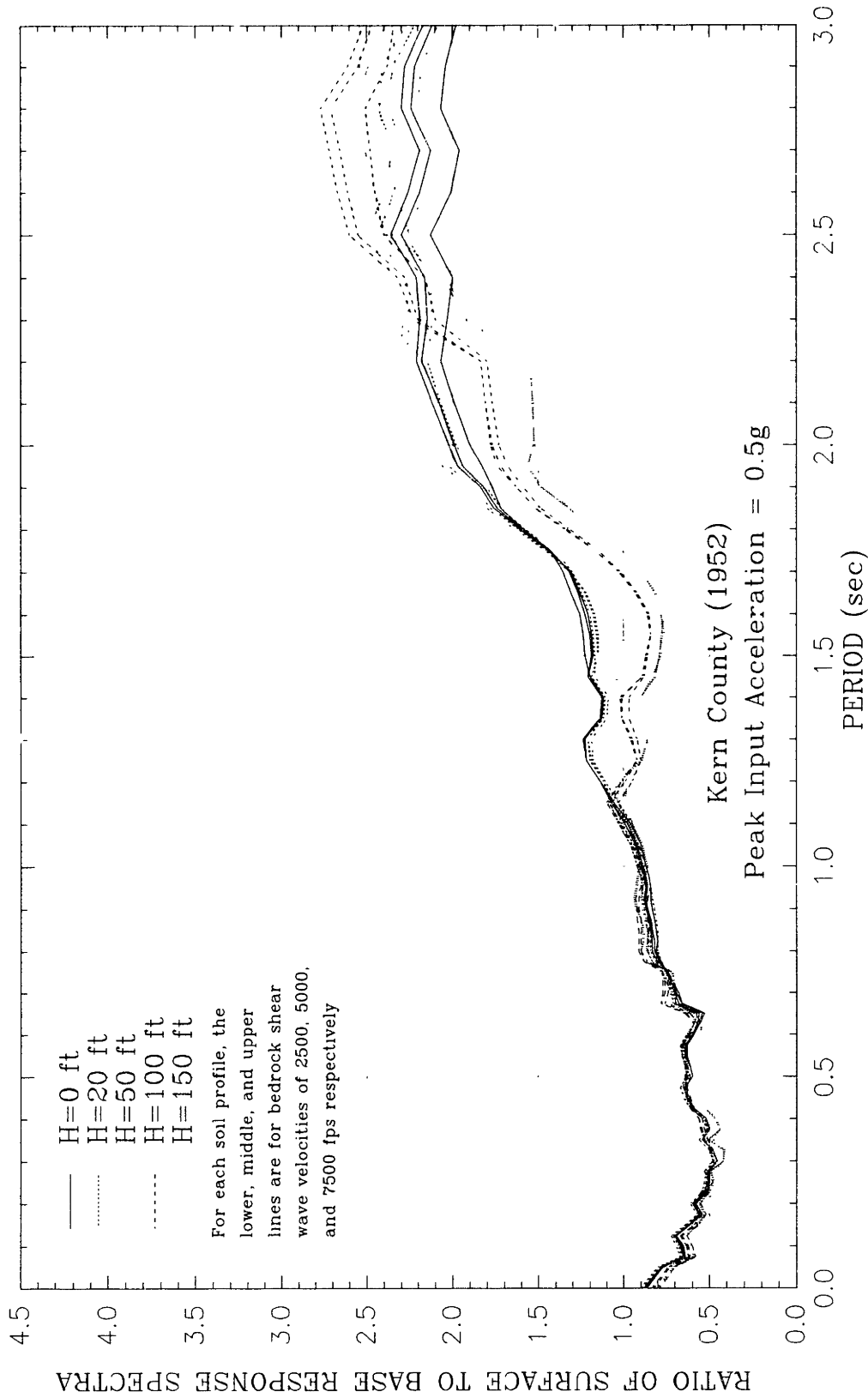


Figure 5-9 Ratio of Response Spectra for a 150 ft Thick Soil Column with a Soft Clay Layer Between Medium Dense Sand from the Kern County (1952) Pasadena Record with a Peak Input Acceleration of 0.5g.

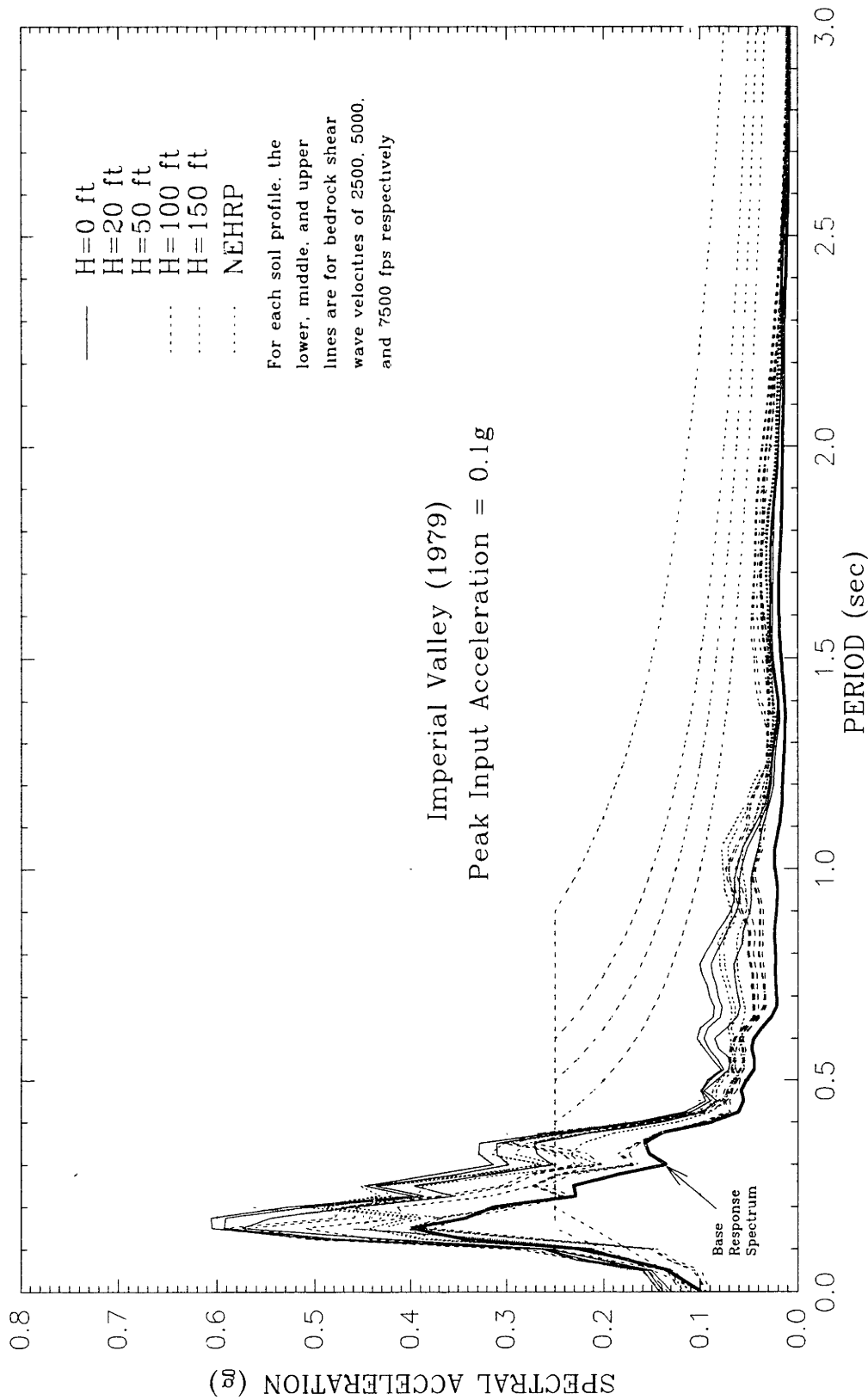


Figure 5-10 Response Spectra for a 150 ft Thick Soil Column with a Soft Clay Layer Between Medium Dense Sand from the Imperial Valley (1979) Superstition Mountain N135 Record with a Peak Input Acceleration of 0.1g.

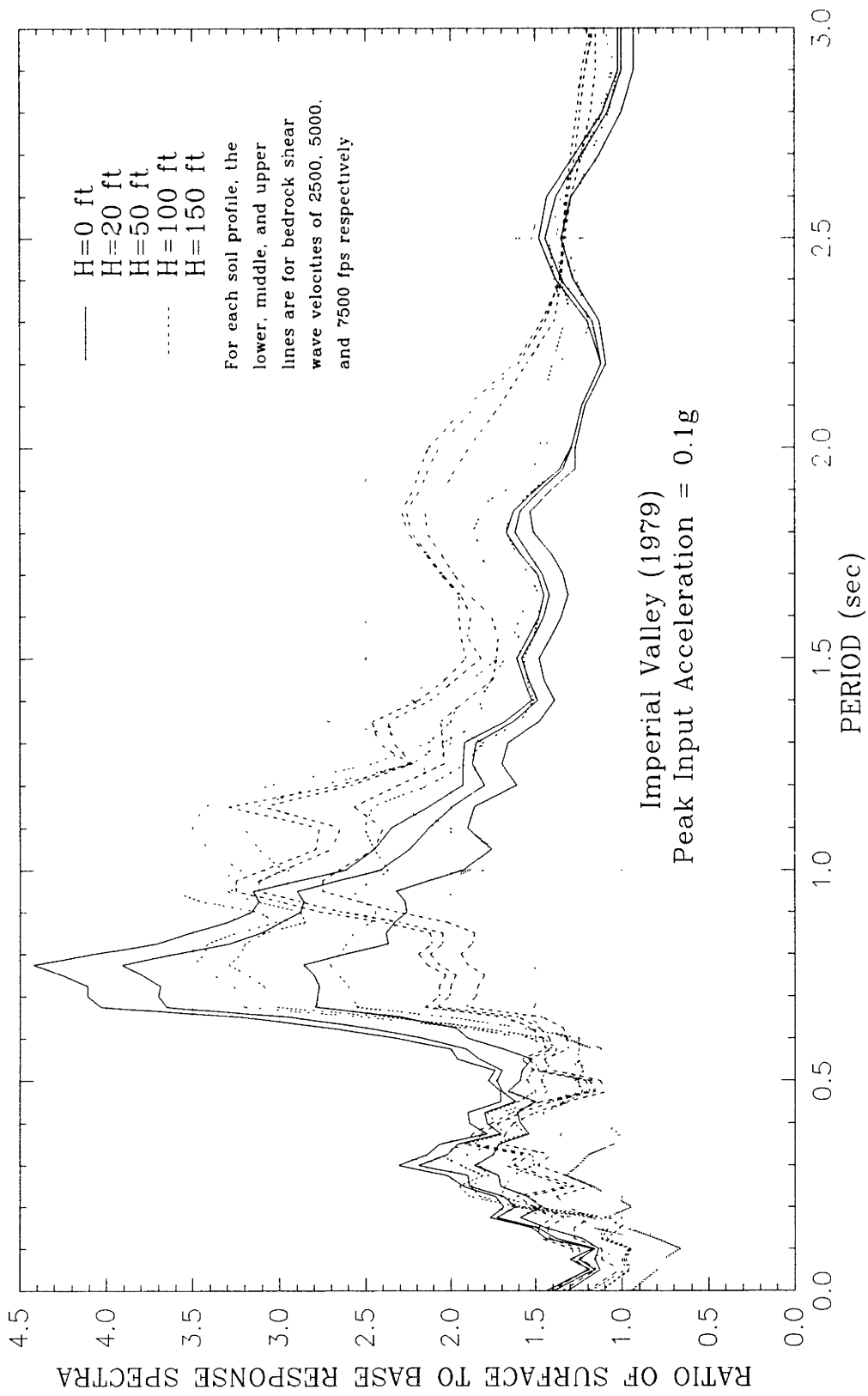


Figure 5-11 Ratio of Response Spectra for a 150 ft Thick Soil Column with a Soft Clay Layer Between Medium Dense Sand from the Imperial Valley (1979) Superstition Mountain N135 Record with a Peak Input Acceleration of 0.1g.

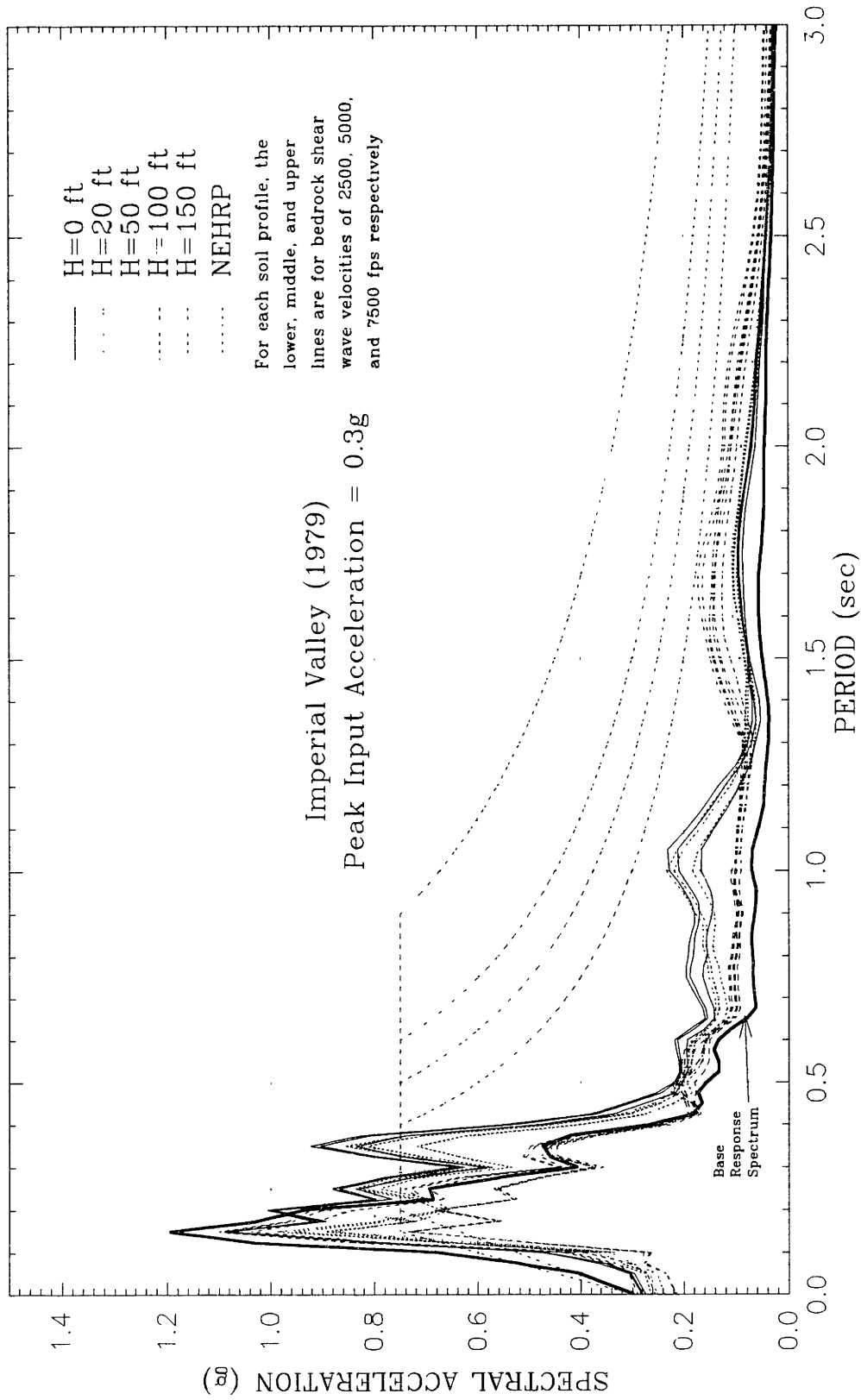


Figure 5-12 Response Spectra for a 150 ft Thick Soil Column with a Soft Clay Layer Between Medium Dense Sand from the Imperial Valley (1979) Superstition Mountain N135 Record with a Peak Input Acceleration of 0.3g.

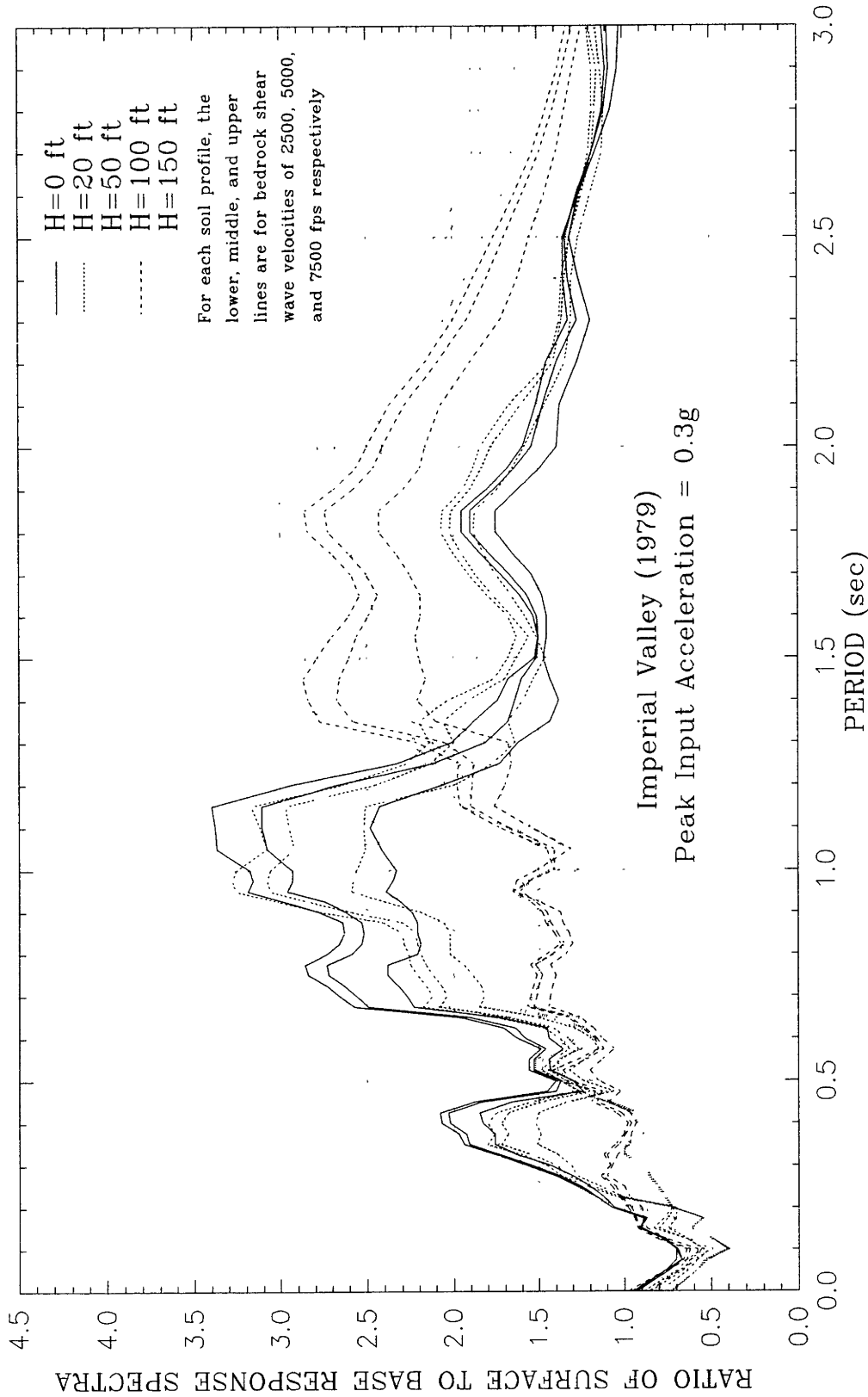


Figure 5-13 Ratio of Response Spectra for a 150 ft Thick Soil Column with a Soft Clay Layer Between Medium Dense Sand from the Imperial Valley (1979) Superstition Mountain N135 Record with a Peak Input Acceleration of 0.3g.

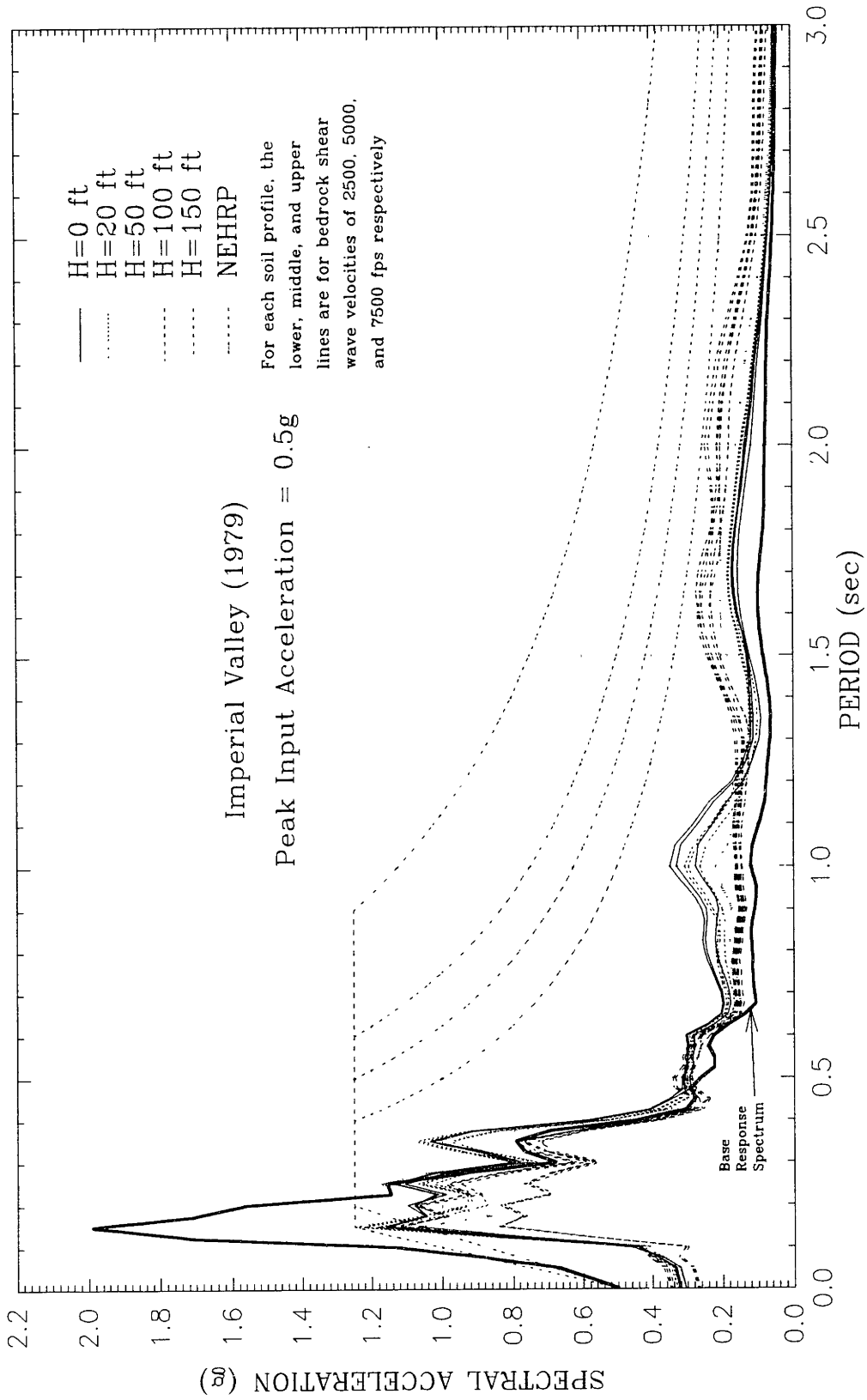


Figure 5-14 Response Spectra for a 150 ft Thick Soil Column with a Soft Clay Layer Between Medium Dense Sand from the Imperial Valley (1979) Superstition Mountain N135 Record with a Peak Input Acceleration of 0.5g.

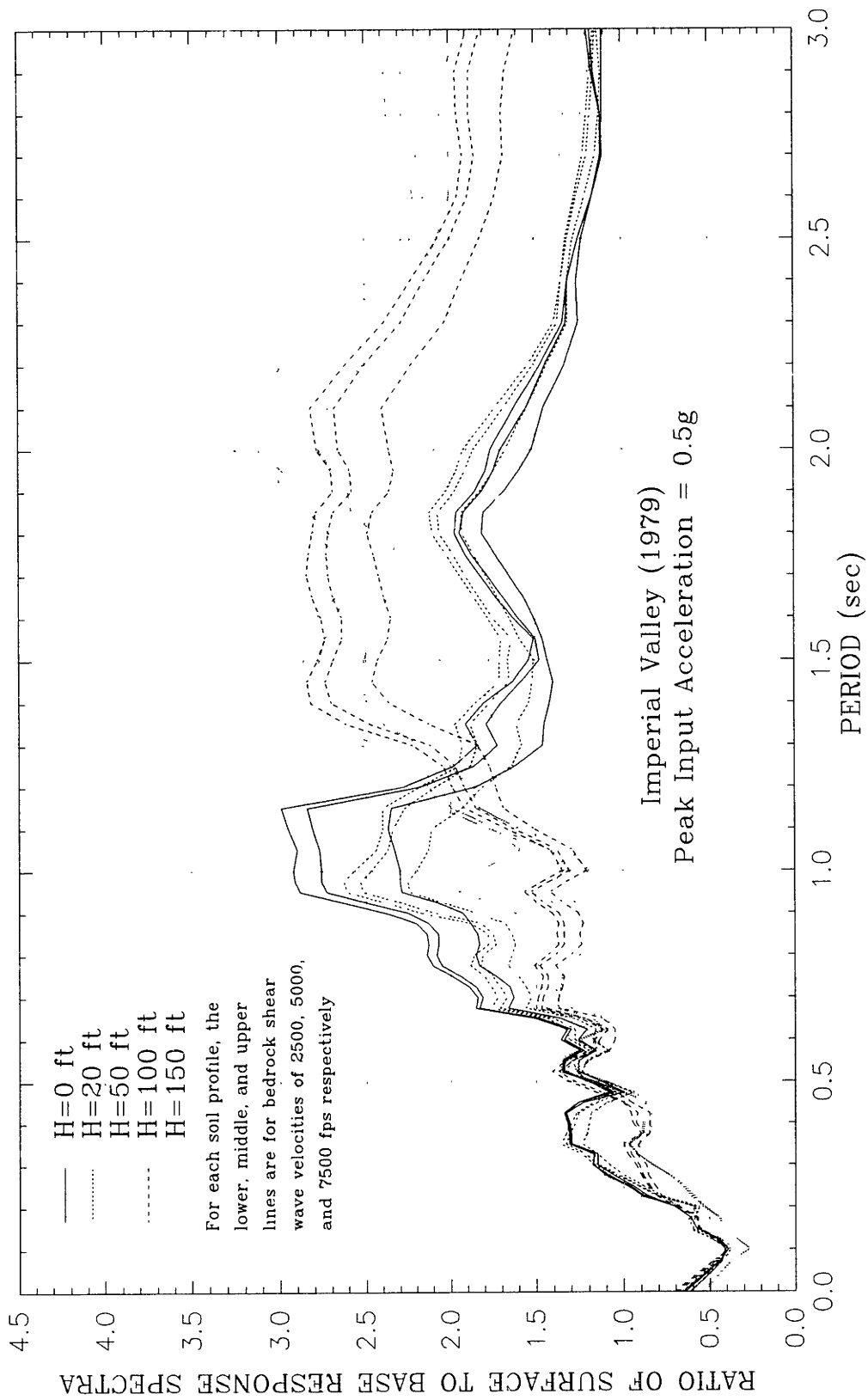


Figure 5-15 Ratio of Response Spectra for a 150 ft Thick Soil Column with a Soft Clay Layer Between Medium Dense Sand from the Imperial Valley (1979) Superstition Mountain N135 Record with a Peak Input Acceleration of 0.5g.

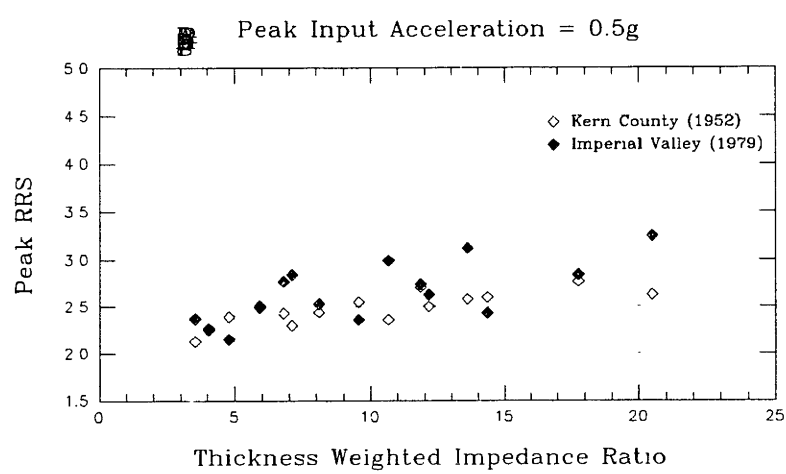
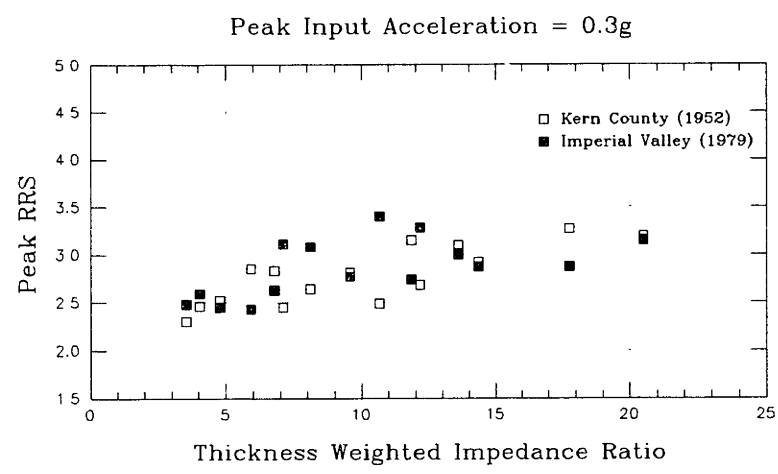
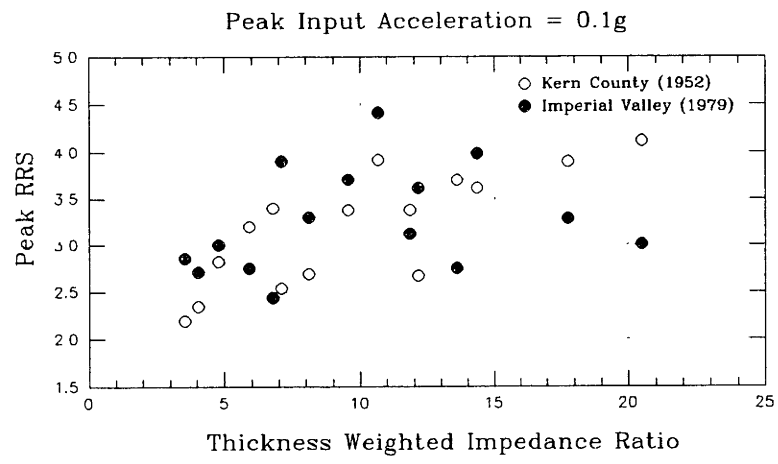


Figure 5-16 Peak Ratio of Response Spectra for a 150 ft Thick Soil Profile with a Layer of Clay in the Center of a Medium Sand.

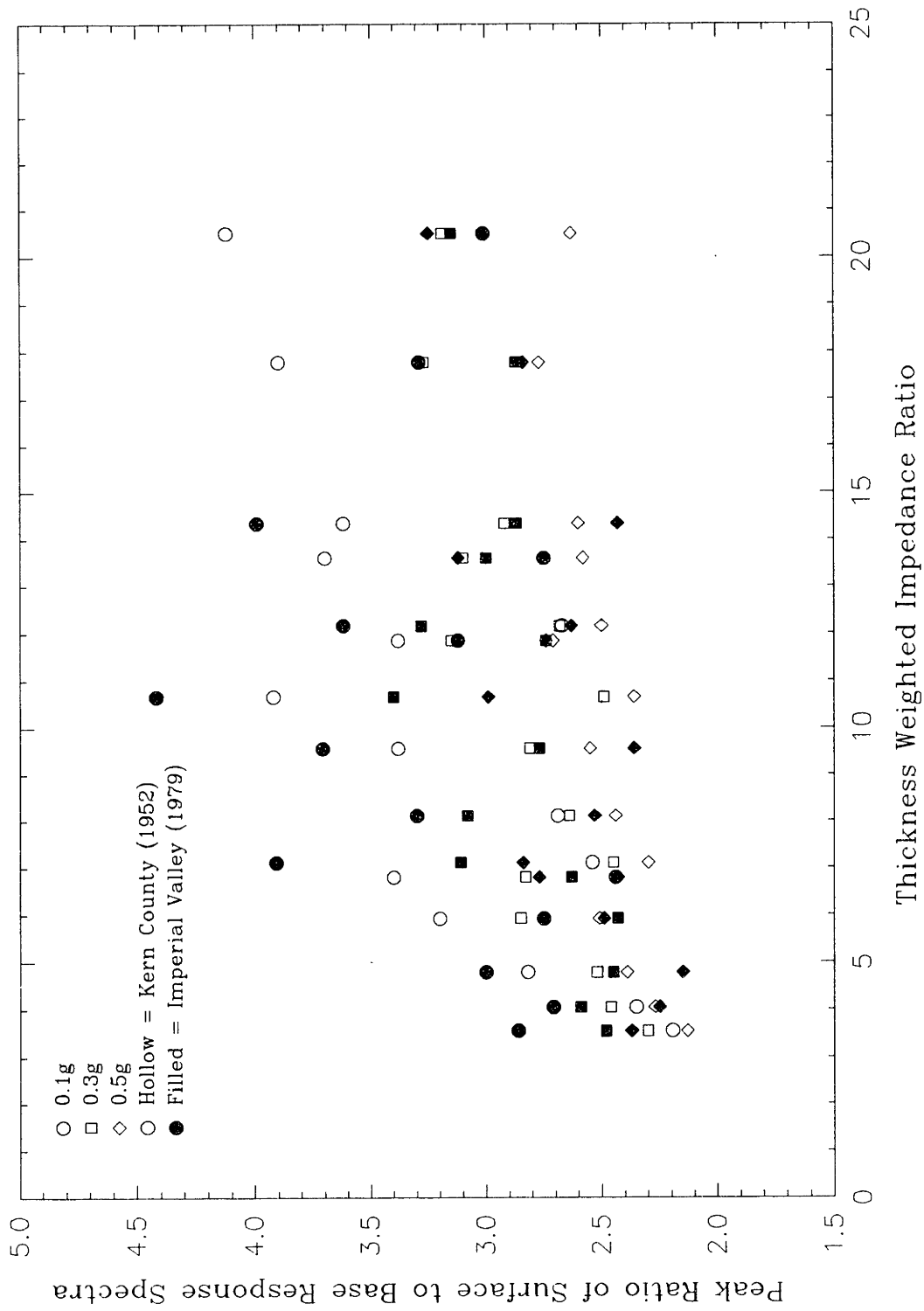


Figure 5-17 Amplification of Spectral Acceleration in a 150 ft thick Soil Profile with a Layer of Clay of Varying Thickness in the Center of a Medium Sand.

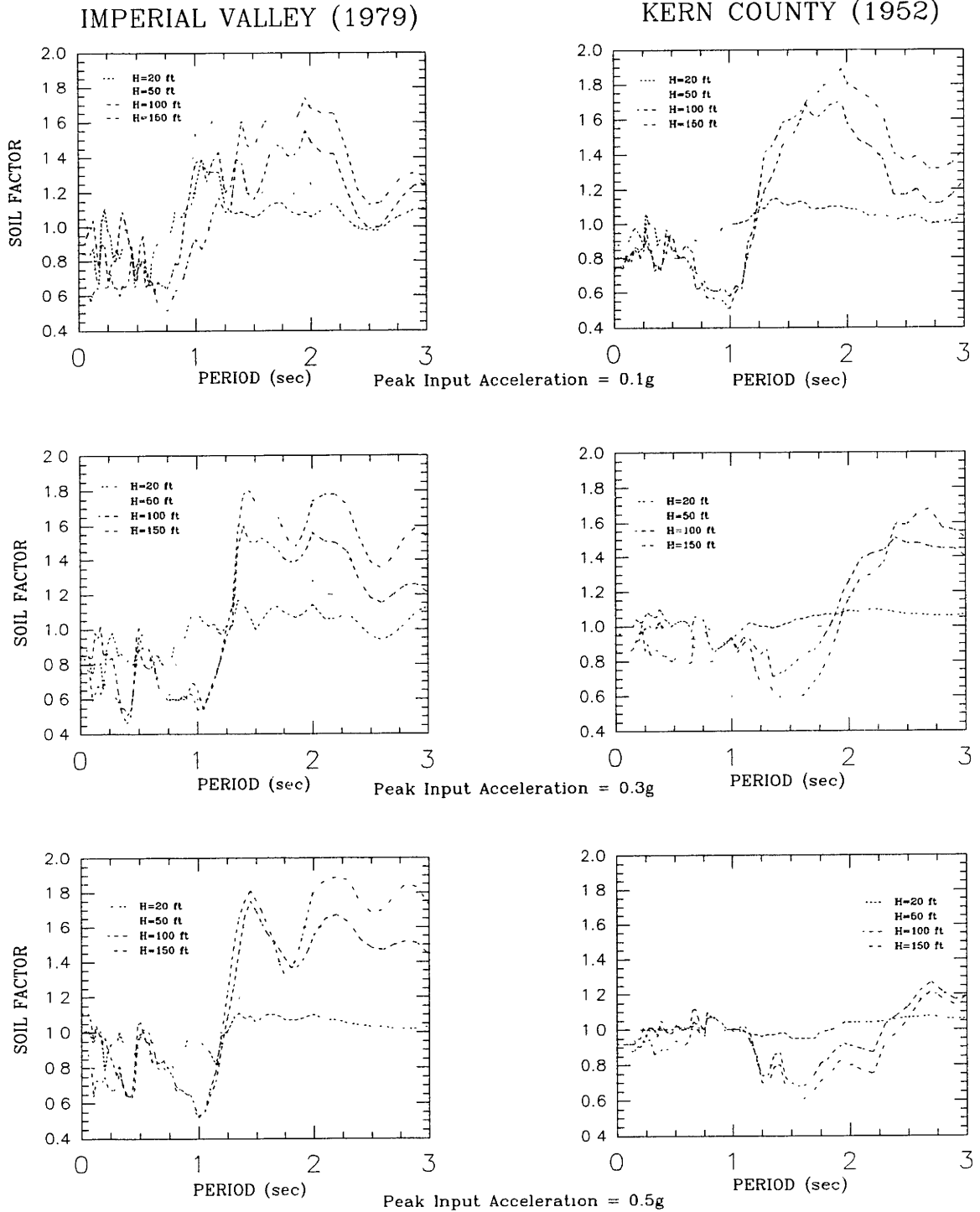


Figure 5-18 Soil Factors Computed Using Response Spectra for the S1 Medium Dense Sand Profiles (H=0) as Baseline, for Imperial Valley (1979) and Kern County (1952).

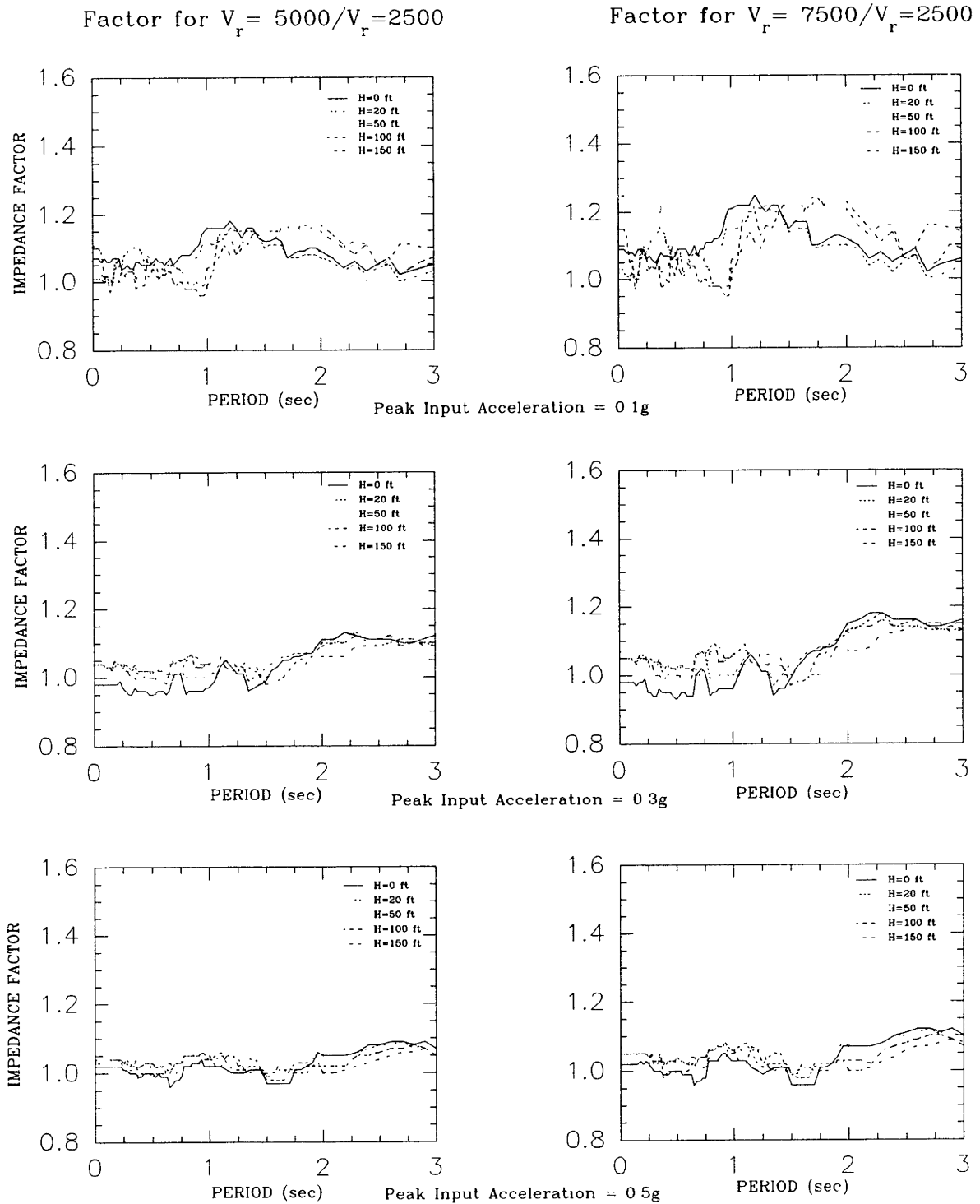


Figure 5-19 Impedance Factors Computed Using Response Spectra For Soil Profiles on Bedrock with a Shear Wave Velocity of 2500 fps as Baseline, for Kern County (1952).

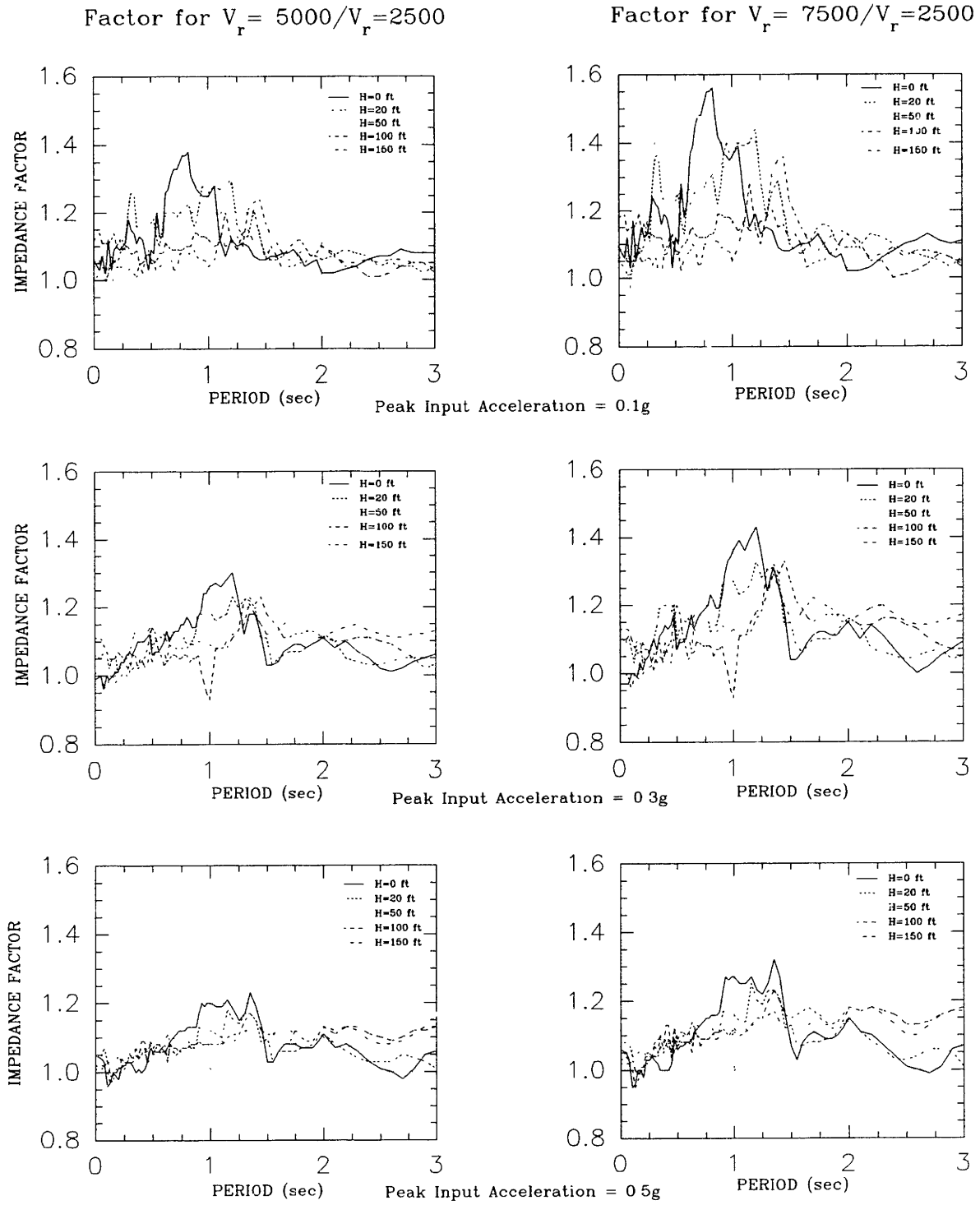


Figure 5-20 Impedance Factors Computed Using Response Spectra For Soil Profiles on Bedrock with a Shear Wave Velocity of 2500 fps as Baseline, for Imperial Valley (1979).

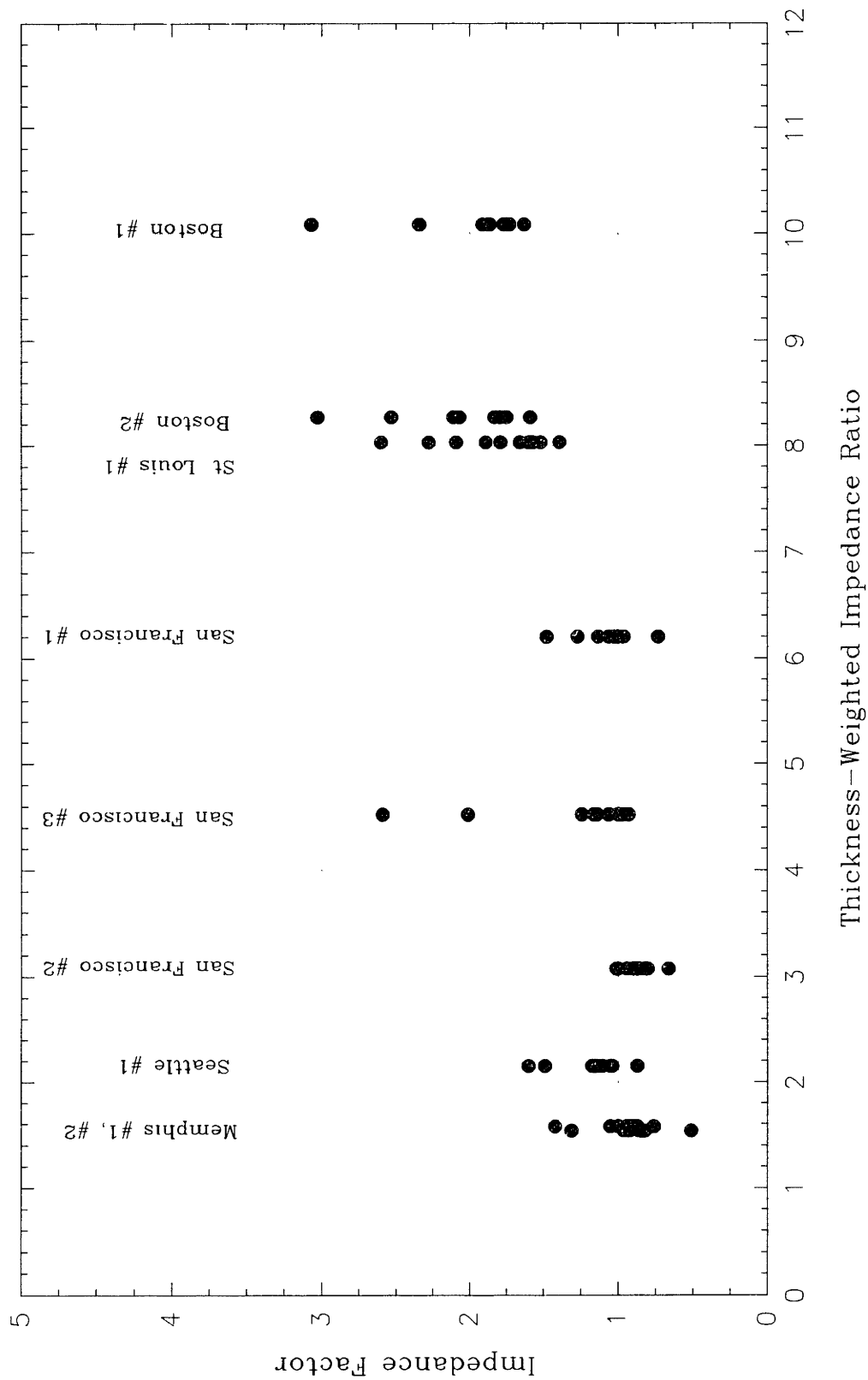


Figure 5-21 Impedance Factor for City Profiles Analyzed Computed by Factoring out the Effects of the Soil Column and the level of Shaking from the Peak Ratio of Response Spectra.

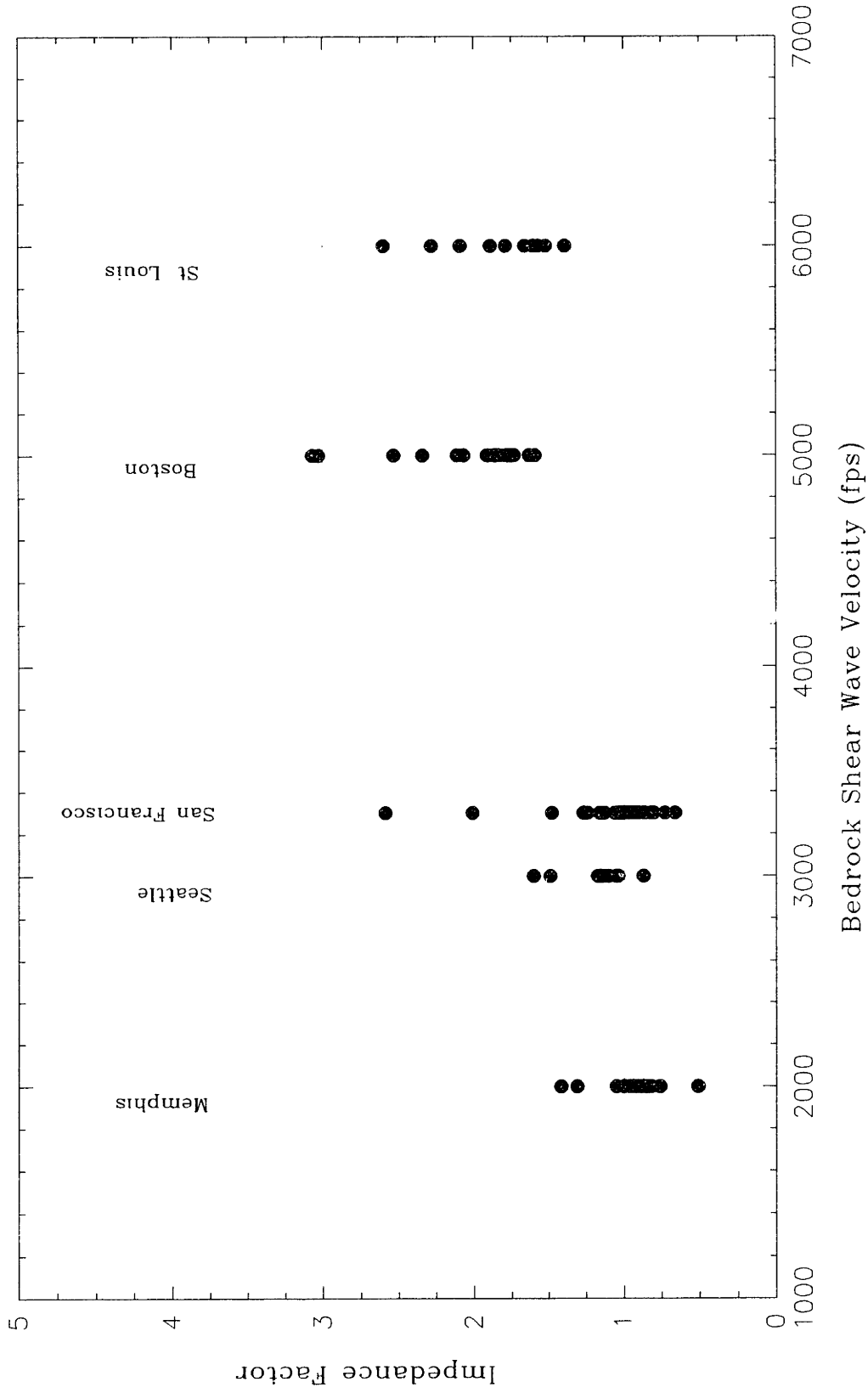


Figure 5-22 Variation of Computed Impedance Factor with Bedrock Shear Wave Velocity for City Profiles Analyzed.

CHAPTER 6

DISCUSSION OF RESULTS

In this chapter, the conclusions and observations from the review of current code criteria and the results of the analyses performed will be discussed. The implications of this research with respect to existing code provisions will be highlighted.

Since the development of current code criteria in the 1970's, considerable progress has been made in understanding local site response. It is apparent from the previous chapters that this is a very complex subject, and code drafters have had to balance the problem of characterizing those complexities, while maintaining the codes sufficiently simple that they can be easily understood and applied by practicing engineers.

The conclusions and observations will be discussed separately for the site category definitions, site factors, and response spectra.

6.1 Site Category Definitions

The current site categories are deliberately vague and broad in scope. The main advantage of this approach is that qualified professionals can exercise judgement in application of the code. An example of a case where this would be appropriate is the set of Boston profiles described in Chapter 4. Boston blue clay, with a shear wave velocity around 575 fps, is a soft clay, and will amplify longer period components of motion, but would be classified as S1 if specific parameters such as a shear wave velocity less than 500 fps, or a plasticity index of greater than 50 were included in the definitions of S3 and S4.

The main disadvantage of the vague definitions is the possibility of mis-interpretation by inexperienced users, although this can be overcome somewhat by including detailed commentaries or appendices, clearly referenced in the code. The example from the proposed New York City code shown in Table 2-5 would provide suitable

guidance.

A problem with having four (or even five or six) site categories is that discrete steps in response are implied. Since the fundamental site period is a controlling factor in the local site response, several researchers have suggested its use as way to provide a continuous range in the soil factor. However, problems with calculations of the site period, particularly where there is no significant impedance contrast to considerable depths, has caused experienced professionals to reject site period as a yardstick (Whitman, 1992).

It has been suggested for New York that an additional category be included for "hard" rock (Jacob, 1990). In the current codes, shallow stiff deposits are combined with all types of rock, even though the response for a rock site will be considerably less than that for one of an S1 site. This has been clearly demonstrated in Chapters 4 and 5. The proposal for New York City therefore has merit for national codes.

From the site category questionnaire responses described in Chapter 3, there is clearly considerable confusion and uncertainty about the definitions for soft clay in categories S3 and S4. The study in Chapter 5 provides a good illustration of the effect of increasing thickness of soft clay although it should be noted that the strength of clay used was to the higher end of soft clay strengths. By examining the increased response for the profile with 50 ft of soft clay in Figures 5-4 through 5-15, and in Figure 5-19, it can be concluded that use of the UBC definition of 40 feet as the division between S3 and S4 is more appropriate than the 70 feet proposed by the NEHRP 1988 provisions.

6.2 Site Factors

The research presented in this study has in general supported the claims made by some researchers (e.g. Jacob, 1990, Dobry, 1990) that EUS sites with high impedance ratios are not adequately covered by the existing codes. Jacob (1990) suggested the use of an additional factor of 0.67 for rock and a factor of 2.5 for soft clay, which provides an amplification for soft clay of nearly four times that for rock.

This is a simple and relatively uncontroversial measure which would not create too much opposition in the code drafting process, and which to some extent allows for the effects of the impedance; it should be noted that this measure was included primarily to provide an increased response for S4 sites, whereas the results of this research indicate that all sites, particularly S1 sites in fact, will experience higher spectral accelerations through the effects of impedance ratios. The additional impedance factor of 1.5 developed in Chapter 5 would be applied to all site categories.

By limiting its application to sites with high impedance ratios experiencing design accelerations of less than 0.2g, the impedance factor would have little to no effect for sites in, for example, California, where current codes appear to be satisfactory. Clearly, before such a factor is introduced, further evidence of its applicability would be required. In particular, empirical evidence from recorded earthquakes is really necessary.

Although not checked in the course of this study, there may be information in the current database from "hard" rock sites in California, where the recurrence of smaller 0.1g earthquakes is relatively frequent.

The introduction of an additional impedance factor is likely to be politically very difficult, even if technically sound documentation is found to support the conclusions of this research. One problem with an impedance factor is that it has been shown to be variable with regard to period and input earthquake, and so will be overly conservative at some periods. Exactly the same arguments can be made concerning the current site factors however.

In order to better account for the complexities of the site factor it has been suggested that a large matrix of different factors be developed representing source characteristics, level of shaking, impedance ratio, and soil factor (Whitman, 1992). The development of these factors is an extensive task and the results would be politically difficult to implement; depending on the number of factors in each category, as many as 90 factors may have to be evaluated. Although this is likely to produce better representation of the site factor by a single number, the additional

complexities may not be warranted. There is considerable advantage to the approach of providing a single conservative number in building codes, while allowing engineers to reduce this factor if more detailed studies are undertaken. The use of a matrix of factors is discussed further in the following section on the response spectra.

It has been suggested that the S2 category should be the reference factor of 1.0, instead of the S1 category as currently (Whitman, in preparation). The reason for this is that S2 is a much more common site category than S1, which was supported by the survey results presented in Chapter 3.

6.3 Design Response Spectra

The current code response spectra contribute to the confusion surrounding the site categories because the spectral ratios are not the same as the site factors, and the difference is not well explained. In addition, there is no S4 spectrum in UBC 1988. It would seem reasonable that consistent spectra for each category should be provided in the codes.

The NEHRP 1988 S4 spectrum provided satisfactory results in this study, although additional research is required on spectra for soft clays, because several researchers have found the longer period response to be higher than current design spectra. It should be noted that the addition of the S4 NEHRP spectrum to UBC would require a reduction in the current S3 spectrum, because they are quite similar. (This can be seen in Figure 2-17.)

The use of the design spectra developed from probabilistic hazard maps of spectral ordinance seems a logical progression from the current empirical code spectra. The results of this study indicate that the maps can be successfully applied and provide similar spectra to existing codes. One considerable advantage of the use of spectral acceleration maps, is that the practice of scaling the design spectrum by a peak acceleration is removed. This procedure is deficient because velocity and displacement spectral ordinance are amplified at interim and long periods respectively, and was discussed in more detail in Section 4.4.

Another advantage of the hazard map spectra is that some relatively complex factors might be included in the contours, thus making the application of more rigorous solutions relatively simple. For example, with respect to the matrix of site factors discussed in the previous section, source and level of shaking effects could be included in the contours, thus greatly simplifying the matrix of site factors. In addition, by including a hazard map for spectral acceleration at 2.0 seconds, in addition to the current 0.3 and 1.0 seconds, factors could be applied which more closely allow for the varying periodic response of different soil profiles. For example, for S4 sites, factors less than 1 could be applied to the 0.3 second ordinate and factors greater than 2 could be applied to the 2 second ordinate. Appropriate factors for the other site categories would be applied.

Clearly, the above procedure again errs on the more complex representation of local site response in building codes. A factor which should be considered with the more complex formulations of code criteria is the increased time required for their development and implementation into codes; with the current rate of progress in inexpensive and powerful computers, improved understanding of local site response, and improvement of earthquake record databases, by the time the code provisions are prepared, it may be comparatively common to perform site specific response analyses. However, experienced engineers would be required to perform site specific response analyses, and there will still be a need for a simpler code method to account for local site response.

CHAPTER 7

CONCLUSIONS AND RECOMMENDATIONS

Based on the review of existing code provisions and suggested alternatives, and on the results of the site categories questionnaire and SHAKE analyses, conclusions and recommendations were made.

7.1 Conclusions

- The current code provisions date from studies undertaken in the early 1970's, and do not adequately represent the current state of knowledge of local site response.
- The existing code provisions are not well understood by the profession because of vague category definitions, and inconsistencies within individual codes and between different model and national codes.
- The site category definitions should remain essentially simple to allow interpretation by qualified professionals, but clearly referenced appendices or commentaries should provide detailed guidance.
- The current code provisions do not satisfactorily cover the response of many EUS sites where there are low levels of shaking and high impedance ratios. Most WUS sites do appear to be adequately covered.
- Sites with high impedance ratios experience an increased response, particularly at low levels of shaking. Further research into recorded response at "hard" rock sites to confirm the theoretical studies should be undertaken prior to including the effect directly in building codes.
- After subtraction of impedance ratio effects, current soil factors appear to be satisfactory, although analysis of soft clay sites should continue; EUS sites are not well covered by the codes because of impedance ratio effects at small levels of shaking, while WUS sites are covered by the code criteria because impedance

effects are typically less significant.

- The uniform hazard spectral acceleration maps provide an improved method of generating elastic response spectra, although further research into their use is required before incorporating them into building codes.

7.2 Recommendations

1. Alterations to Code Provisions

- A site category for "hard" rock should be added, and defined as having a shear wave velocity greater than 3500 fps.
- A response spectrum for each site category should be included, with spectral ratios consistent with the soil factors. The use of the current NEHRP S4 spectrum in UBC would be better than providing nothing, even although it may be inadequate for some soft clay sites.
- Different model and national codes should provide consistent definitions and factors.

2. Further Research

- A detailed study of the existing earthquake database to update the work carried out by Seed et al (1976) and Mohraz (1976) should be undertaken.
- An investigation into empirical data on the effects of impedance ratio at "hard" rock sites in California, particularly at low levels of shaking would complement the theoretical studies presented in this thesis.
- Further theoretical studies similar to that presented in Chapter 5, but analyzing profiles with softer clay layers would help prepare a satisfactory S4 spectrum.

- Collection of analyses for individual cities with more detailed study of seismicity and selection of input earthquakes would enable more conclusive recommendations to be made.

REFERENCES

Abbreviations

ASCE	American Society of Civil Engineers
BSSA	Bulletin of the Seismological Society of America
EERI	Earthquake Engineering Research Institute
NCEER	National Center for Earthquake Engineering Research
USGS	United States Geological Survey

Aki K., "Local Site effects on strong ground motion," Earthquake Engineering and Soil Dynamics II, Geotech. Spec. Pub. No. 20, June 1988 pp103-155.

Algermissen, S.T., Whitman, R.V., "Seismic Zonation in the Eastern United States," Proc. 4th Int'l Conf. on Seismic Zonation, EERI, at Stanford Univ., 1991.

Algermissen, S.T., Leyendecker, E.V., Bollinger, G.A., Donovan, N.C., Ebel, J.E., Joyner, W.B., Luft, R.W., Singh, J.P., "Probabilistic Ground-motion Hazard Maps of Response Spectral Ordinates for the United States," Proc. 4th Int'l Conf. on Seismic Zonation, EERI, at Stanford Univ., 1991.

American National Standards Institute, "Minimum Design Loads for Buildings and Other Structures," ANSI/ASCE 7-88, ASCE, Dec. 1988.

Applied Technology Council, Tentative Provisions for the Development of Seismic Regulations for Buildings, ATC3-06, National Bureau of Standards, Spec. Pub. 510, Washington D.C. June 1978.

Biot, M.A., "A mechanical Analyzer for the prediction of earthquake stresses," BSSA, Vol. 31, 1941, pp 151-171.

Building Seismic Safety Council, NEHRP Recommended Provisions for the Development of Seismic Regulations for New Buildings. Part 1, Provisions, prepared by BSSC for FEMA, Washington D.C. 1985.

Building Seismic Safety Council, NEHRP Recommended Provisions for the Development of Seismic Regulations for New Buildings. Part 2 Commentary, prepared by BSSC for FEMA, Washington D.C. 1985 .

Campbell, K.W., "Strong Motion Attenuation Relations: A ten year perspective," Earthquake Spectra, Vol.1, No4, EERI, Aug. 1985 pp759-804.

Christian J.T., "Developing Ground Motions in Practice," Earthquake Engineering and Soil Dynamics II, Geotech. Spec. Pub. No. 20, June 1988 pp405-429.

Coffman, J.L., and Hake, C.A., "Earthquake History of the United States," Publication 41-1 Reprinted with Supplement, USGS, Boulder CO, 1982.

Constantoupolous, I.V., Roesset, J.M., Christian, J.T., "A comparison of linear and exact nonlinear analysis of soil amplification," Proc. 5th World Conf. on Earthquake Engineering, Rome, Italy, paper 225, 1973.

Crouse, C.B., Vyas, Y.K., and Schell, B.A., "Ground Motions from Subduction Zone Earthquakes," BSSA, Vol. 78, 1988, pp1-25.

Crouse, C.B., "Ground-Motion Attenuation Equations for Earthquakes on the Cascadia Subduction Zone," Earthquake Spectra, Vol. 7, No. 2, EERI, 1991, pp201-236.

Dobry R., Vucetic M., "Dynamic properties and response of soft clay deposits," Int'l Symp. on Geotech. Eng. of Soft Soils, Mexico City, Aug. 1987.

Dobry R., Vucetic M., "Effect of Soil Plasticity on Cyclic Response," Jrnl. Geotech. Eng. Div., ASCE, Vol , No GT , January, 1991.

Donovan, N.C., Bornstein, A.E., "Uncertainties in Seismic Risk Procedures," Jrnl. Geotech. Eng. Div., ASCE, 104, 1978.

Donovan, N.C., "Engineering Applications of Seismic Studies," International Workshop, Santiago, Chile, June 4-7, 1991.

Earthquakes and Volcanoes, USGS, Vol. 21, No. 5, 1989.

- Finn, W.D.L., Martin, G.R., and Lee, M.R.W., "Comparison of Dynamic Analyses for Saturated Sands," presented at the Conference on Earthquake Engineering and Soil Dynamics, Pasadena, CA, 1978.
- Friberg, P.A., Susch, C.A.T., "A User's Guide to Strongmo: Version 1.0 of NCEER's Strong-Motion Data Access Tool for PC's and Terminals," NCEER Technical Report NCEER-90-0024, Nov. 1990.
- Gupta, K.G., "Response Spectrum Method in Seismic Analysis of Structures," Blackwell Scientific Publications, Cambridge MA., 1990.
- Hardin, B.O., and Drnevich, V.P., "Shear Modulus and Damping in Soils: Design Equations and Curves," *Jrnl. Soil Mech. and Found. Div.*, ASCE, Vol. 98, No. SM7, 1972, pp 667-692.
- Herrmann, R.B., and Nuttli, O.W., "Scaling and Attenuation Relations for Strong Ground Motions in Eastern North America," *Proc. Eighth World Conf, Earthquake Eng.*, Vol. 2, Prentice Hall Inc., Englewood Cliffs, New Jersey, 1984, pp 305-309.
- Ho, C.L., Kornher, H., Tsiatas, G., "Ground Motion Model for Puget Sound Cohesionless Soil Sites," *Earthquake Spectra*, Vol. 7, No. 2, EERI, 1991, pp237-266.
- Housner, G. W., "An investigation of the effects of earthquakes on buildings," Ph. D. Thesis, Cal Tech, Pasadena, 1941.
- Idriss, I.M., and Seed, H.B., "Seismic Response of Horizontal Soil Layers," *Jrnl. Soil Mech. and Found. Eng.*, ASCE, Vol 94, No SM4, July, 1968, pp1003-1031.
- Idriss, I.M., "Earthquake Ground Motions," Lecture Notes, Course on strong ground motion, EERI, Pasadena CA, 1987.
- Iwasaki, T., Tatsuoka, F., Tokida, K., and Yoshida, S., "Shear Moduli of Sand Under Cyclic Torsional Shear Loading," *Soils and Foundations*, Vol. 18, No. 1, March 1978, pp39-56.
- Jacob, K.H., Gariel, J.C., Armbruster, J., Hough, S., and Tuttle, M., "Site Specific Ground Motion Estimates for New York City," *Proc. 4th US Nat'l. Conf. on Earthquake Eng.*, Palm Springs, CA., May, 1990.

- Jacob, K.H., "Seismic Hazards and the Effects of Soils on Ground Motion for the Greater New York Metropolitan Region," submitted to Continuing Education Seminar of the NYC Metropolitan Section of ASCE, New York City, Nov. 1990.
- Joyner, W.B., Boore, D.M., "Prediction of Earthquake Response Spectra," USGS Open-File Report No. 82-977, 1982.
- Joyner, W.B., Boore, D.M., "Measurement Characterization and Prediction of Strong Ground Motion," Earthquake Engineering and Soil Dynamics II, Geotech. Spec. Pub. No. 20, June 1988, pp43-102.
- Kanai, K., "Relation between the nature of surface layer and the amplitudes of earthquake motions," Bull. Earthquake Res. Inst., Tokyo Univ., Vol. 30, 1952, pp31-37.
- Luft, R.W., "Comparison among earthquake codes," Earthquake Spectra, Vol. 5, No. 4, 1989.
- Martin, P.P., Seed, H.B., "MASH: A Computer Program for the Non-linear Analysis of Vertically Propagating Shear Waves in a Horizontally Layered Soil Deposit," Report No. EERC 78/23, UCB, Berkeley, CA., 1978.
- Martin, P.P., Seed, H.B., "One Dimensional Dynamic Ground Response Analysis," Jnl. Geotech. Eng. Div., ASCE, Vol 108, No GT7, July, 1982, 935-952.
- McGarr, A., "Scaling of Ground Motion Parameters, State of Stress, and Focal Depth," Jnl. Geophys. Res., Vol. 89, 1984, pp 6969-6979.
- Mohraz, B., Hall W.J., Newmark, N.M., "A study of vertical and horizontal earthquake spectra," Nathan M. Newmark, Consulting Engineering Services, Urbana, Illinois, AEC Report No 1254, 1972.
- Mohraz, B., "A study of earthquake response spectra for different geological conditions," BSSA, Vol. 66, No 3, June 1976, pp 915-935.
- Ng, K.W., Chang, T-S, and Hwang, H-H.M., "Subsurface Conditions of Memphis and Shelby County," NCEER Technical Report No. NCEER-89-0021, July 1989.

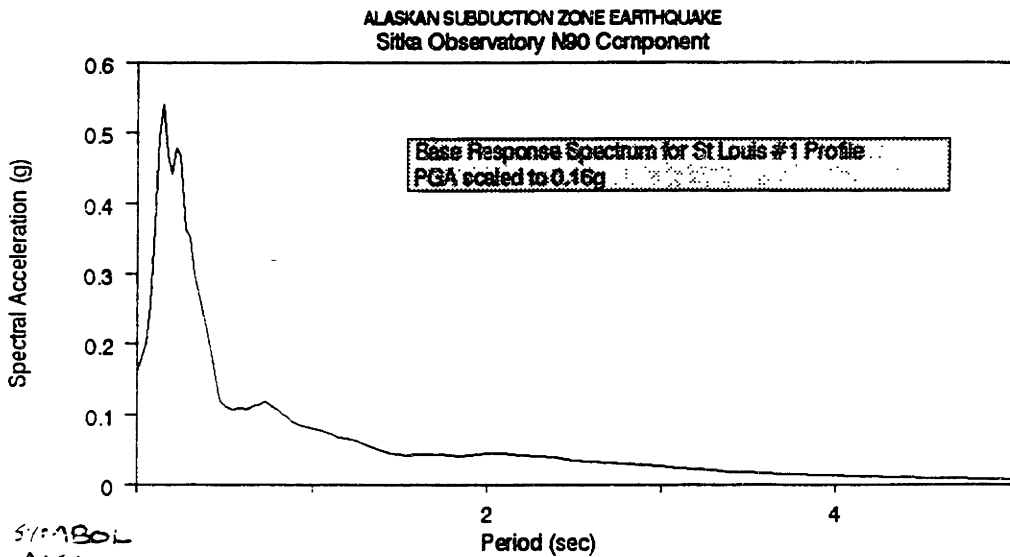
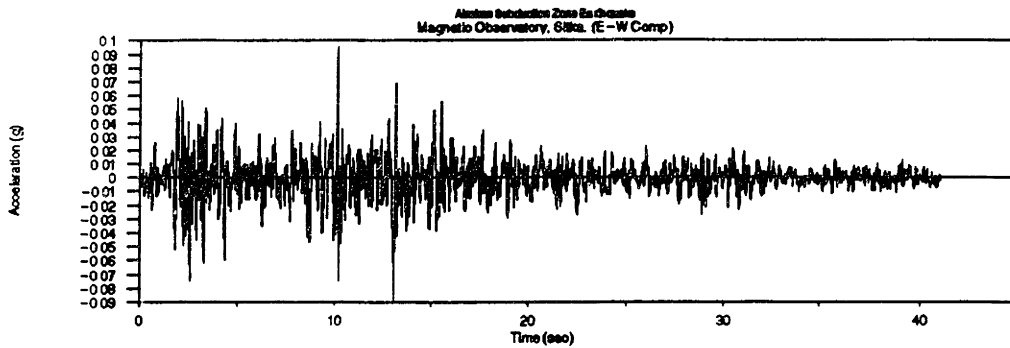
- Nuttli, O.W., "The Mississippi Valley Earthquakes of 1811 and 1812; Intensities, Ground Motion and Magnitudes," BSSA, Vol. 63, No. 1, Feb. 1973, pp227-248.
- Roesset, J. M., and Whitman, R.V., "Theoretical Background for Amplification Studies," Research Report R69-15, MIT, Cambridge MA, 1969.
- Schnabel P.B., Lysmer, J., and Seed, H.B., "SHAKE: A Computer Program for Earthquake Response Analysis of Horizontally Layered Sites," Report No. EERC 72/12, UCB, Berkeley, CA., 1972.
- Seed, H.B., Idriss, I.M., "Soil Moduli and Damping Factors for Dynamic Response Analysis," Report No. EERC 70-10, UCB, Berkeley, CA., 1970.
- Seed, H.B., Whitman, R.V., Dezfuleian, H., Dobry, R., Idriss, I.M., "Soil Conditions and Building Damage in 1967 Caracas Earthquake," Jnl. Soil Mech. and Found. Eng., ASCE, Vol 98, No 8, Aug. 1972, pp787-806.
- Seed, H.B., Idriss, I.M., "Ground Motions and Liquefaction During Earthquakes," EERI monograph, Berkeley, CA., Dec. 1982.
- Seed, H.B., Ugas, C., and Lysmer, J., "Site dependent spectra for earthquake resistant design," BSSA, Vol. 66, No. 1, February, 1976, pp221-243.
- Shannon and Wilson Inc., and Agbabian Assoc., "Site Dependent Effects at Strong-Motion Accelerograph Stations," NUREG/CR-1639, Nucl. Reg. Comm., 1980.
- Singh, J.P., "A simple method for generating synthetic time histories for design of base isolation systems," Proc. Applied Technology Council Seminar on Base Isolation and Passive Energy Dissipation Devices, San Francisco, March 1986.
- Singh, J.P., and Tabatabaie, M., "Strong Motion Data - Application to Multiple Support Structures," Geotechnical News, Canadian Geotechnical Society, March 1991 pp38-42.
- Structural Engineers Association of California, "Recommended Lateral Force Requirements and Commentary," 1988.

- Sun, J. I., Galeschi, R., and Seed, H.B., "Dynamic Moduli and Damping Ratios for Cohesive Soils," EERC-UCB 88/15, Berkeley, CA., Dec. 1988.
- Uniform Building Code 1985, International Conference of Building Officials, Whittier CA, 1985.
- Uniform Building Code 1988, International Conference of Building Officials, Whittier CA, 1988.
- Weston Geophysical Corporation, "Regional Geological, Geophysical and Seismological Studies Related to the New Brunswick Earthquakes," Report prepared for Yankee Atomic Electric Co., 1986.
- Whitman, R.V., "Soil Dynamics," (manuscript in preparation).
- Whitman, R.V., "Site Categories Workshop," held in 1991, and manuscript in preparation.
- Whitman, R.V., "Site Effects Workshop," held at NCEER, Buffalo NY, October 24-25, 1991, to be published by NCEER in 1992.
- Woodward Clyde Consultants, and Booker Assoc., "Seismic Condition Survey, Phase 1," Report to Illinois Department of Transportation, Feb. 1991.
- Wysockey, M.H., "Earthquake Ground Motion Zonation in the Boston Area," MIT, Civil Engineering Department, SM Thesis, 1990.

Appendix A

Input Earthquake Response Spectra and Time Histories

<u>Symbol</u>	<u>Input Earthquake</u>	<u>Figure #</u>
AK1	Alaskan Subduction Zone Earthquake	Figure A1
AK2	Sitka Earthquake	Figure A2
AK3	Alaskan Subduction Zone Earthquake	Figure A3
AK4	Alaskan Subduction Zone Earthquake	Figure A4
AND1	Andreanof Islands, Alaska Earthquake	Figure A5
ELS1	San Salvador Earthquake	Figure A6
IMP1	Imperial Valley Earthquake	Figure A7
IMP2	Imperial Valley Earthquake	Figure A8
LOM1	Santa Cruz Mtns (Loma Prieta) Earthquake	Figure A9
LOM2	Santa Cruz Mtns (Loma Prieta) Earthquake	Figure A10
LOM3	Santa Cruz Mtns (Loma Prieta) Earthquake	Figure A11
LOM4	Santa Cruz Mtns (Loma Prieta) Earthquake	Figure A12
LOM5	Santa Cruz Mtns (Loma Prieta) Earthquake	Figure A13
MEX1	Michoacan, Mexico City Earthquake	Figure A14
MH1	Morgan Hill Earthquake	Figure A15
SAG1	Saguenay Earthquake	Figure A16
SAG2	Saguenay Earthquake	Figure A17
SFER1	San Fernando Earthquake	Figure A18
VALP1	Valparaiso Central Chile Earthquake	Figure A19
VALP2	Valparaiso Central Chile Earthquake	Figure A20
VALP3	Valparaiso Central Chile Earthquake	Figure A21
WHIT1	Whittier Earthquake	Figure A22
WHIT2	Whittier Earthquake	Figure A23



SYMBOL
AK1

NCEER ASCII STRONG-MOTION DATA FORMAT
EVENT PARAMETERS:

DATE: year=1972 month= 7 day=30
 TIME: hour|minute (24hr)=2145 second=21.000 time code=UTC
 LOCATION: latitude= 56.77000 longitude= -135.91000 depth (km)= 29.0
 NAME: ALASKAN SUBDUCTION ZONE EARTHQUAKE
 EVENT.DEPTH : 29.000000
 EVENT.MAG_B : 7.600000
 EVENT.MAG_W : 6.500000

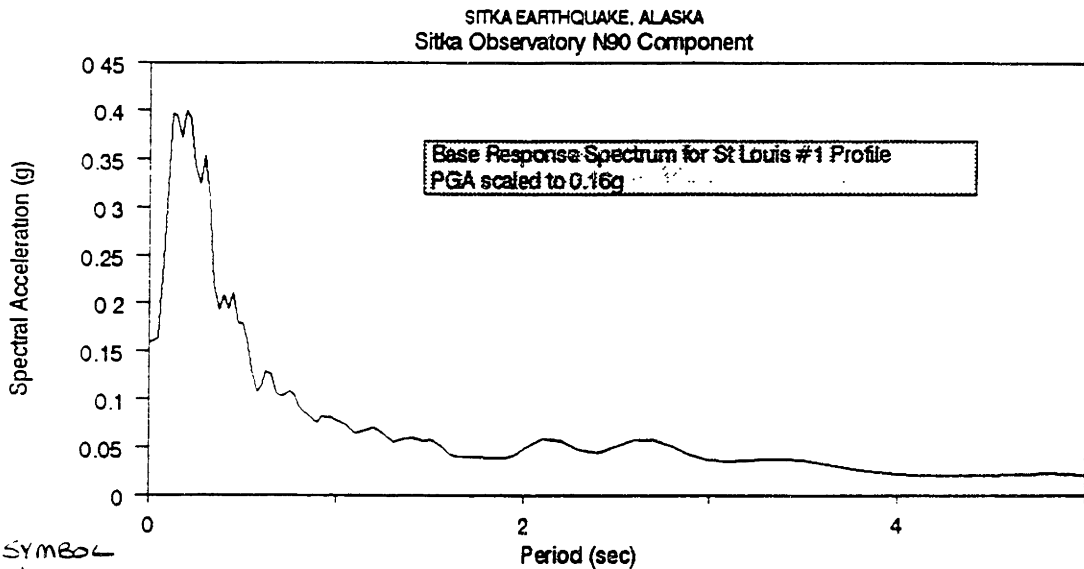
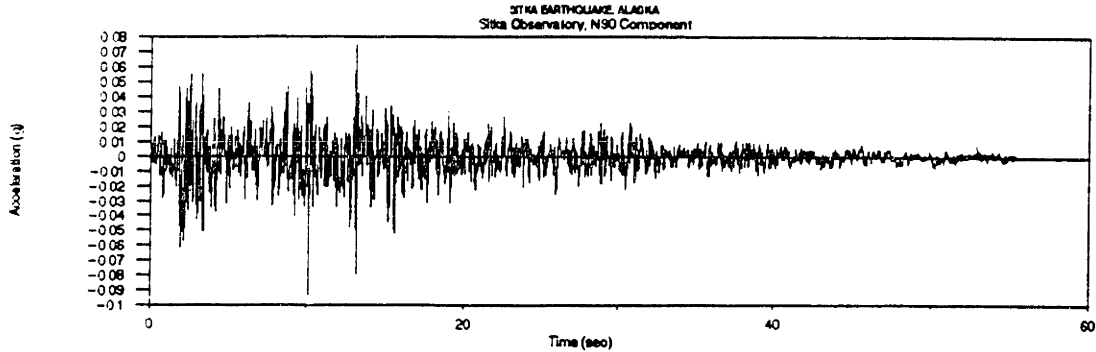
SITE PARAMETERS:

LOCATION: latitude= 57.06000 longitude= -135.32001 elevation (m)= 0.0
 SITE ID: 2714 SMO - SITKA, ALASKA OBSERVATORY
 CODE: 2714S
 SITE STRUCTURE : FREE-FIELD, CONCRETE VAULT
 SITE GEOLOGY : BEDROCK, GREYWACKE

RECORD/TRACE PARAMETERS:

EPICENTRAL DISTANCE: distance (km)= 48.4 azi
 SPECS: sampling rate (sec)=0.005
 TRACE.PEAK_VALUE : 93.630000
 TRACE.HIGH_PASS : 0.150000
 TRACE.LOW_PASS : 50.000000
 TRACE.SENSITIVITY : 7.010000
 TRACE.FREQUENCY : 20.408000
 TRACE.DAMPING : 0.570000

Figure A-1



SYMBOL
AK2

NCEER ASCII STRONG-MOTION DATA FORMAT

EVENT PARAMETERS:

DATE: year=1972 month= 7 day=30
 TIME: hour/minute (24hr)=2145 second=21.000 time code=UTC
 LOCATION: latitude= 55.82000 longitude= -135.67999 depth (km)= 25.0
 NAME: SITKA EARTHQUAKE
 EVENT.DEPTH : 29.000000
 EVENT.MAG_B : 7.600000
 EVENT.MAG_W : 6.500000

SITE PARAMETERS:

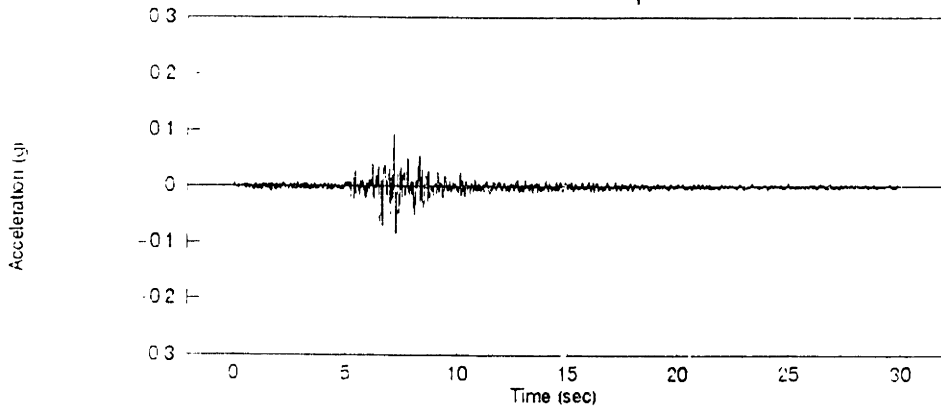
LOCATION: latitude= 57.06000 longitude= -135.32001 elevation (m)= 0.0
 SITE ID: 2714 SMO - SITKA, ALASKA OBSERVATORY
 CODE: 2714S
 SITE.STRUCTURE : FREE-FIELD, CONCRETE VAULT
 SITE.GEOLOGY : BEDROCK, GREYWACKE

RECORD/TRACE PARAMETERS

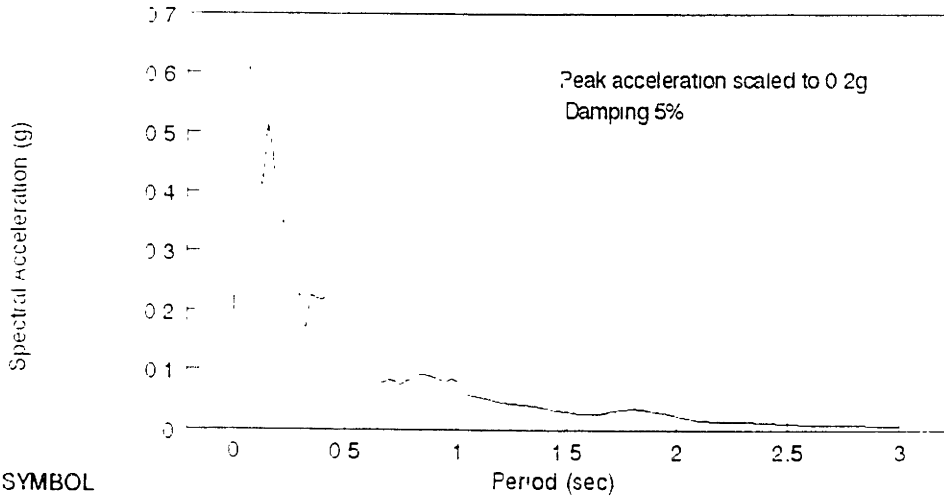
EPICENTRAL DISTANCE: distance (km)= 34.6
 SPECS: sampling rate (sec)=0.020
 TRACE.PEAK_VALUE : 91.340000
 TRACE.HIGH_PASS : 0.080000
 TRACE.LOW_PASS : 27.000000
 TRACE.SENSITIVITY : 0.000000
 TRACE.FREQUENCY : 20.408000
 TRACE.DAMPING : 0.570000

Figure A-2

ALASKAN SUBDUCTION ZONE EARTHQUAKE
SANAK. AK N188 Component



Acceleration Response Spectrum



SYMBOL

AK3

EVENT PARAMETERS:

DATE year=1987 month=6 day=21
 TIME hour=minute (24hr)=0548 second=0.000 time code=UTC
 LOCATION latitude= 54.12000 longitude= -162.38699 depth (km)= 2.0
 NAME ALASKAN SUBDUCTION ZONE EARTHQUAKE
 MAGNITUDE Mb=7.6 Ms=6.5

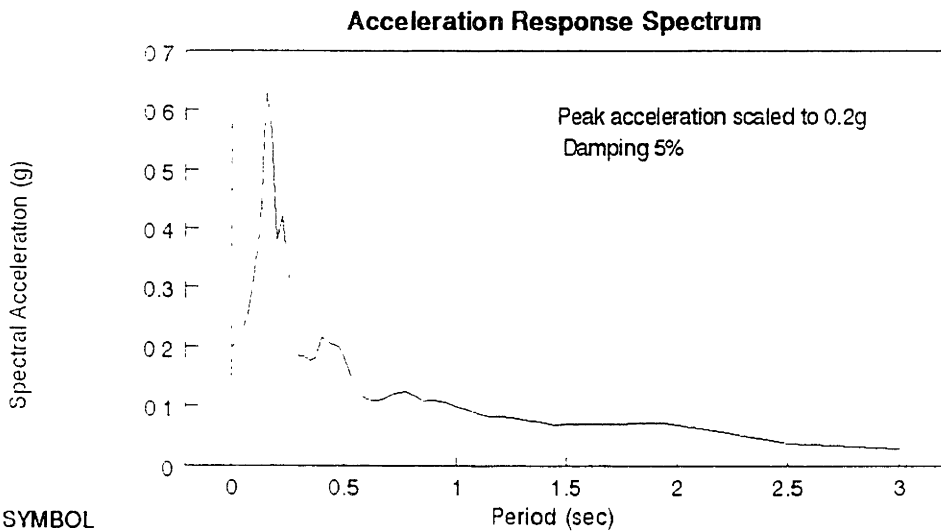
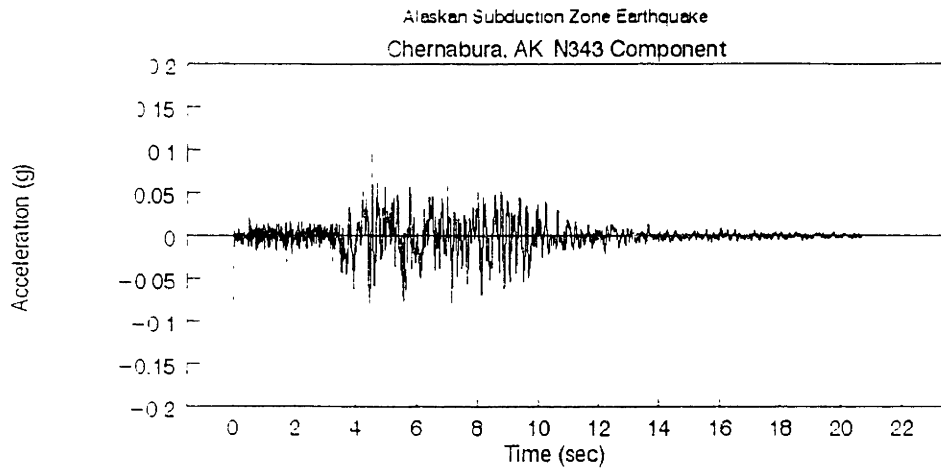
SITE PARAMETERS:

LOCATION latitude= 54.47400 longitude= -162.77530 elevation (m)= 0.0
 SITE ID SNK 2777 - SANAK ALASKA
 CODE SNK27
 SITE STRUCTURE
 SITE GEOLOGY

RECORD/TRACE PARAMETERS:

EPICENTRAL DISTANCE distance (km)= 46.9 azimuth (deg)=N147.2
 SPECS sampling rate (sec)=0.005

Figure A-3



SYMBOL

AK4

EVENT PARAMETERS:

DATE year=1985 month=10 day=9

TIME hour (minute (24hr))=0934 second= 0.000 time code=UTC

LOCATION latitude= 54.73600 longitude= -159.46899 depth (km)= 15.0

NAME ALASKAN SUBDUCTION ZONE EARTHQUAKE

MAGNITUDE Mb=7.6 Ms=6.5

SITE PARAMETERS:

LOCATION latitude= 54.82030 longitude= -159.58830 elevation (m)= 0.0

SITE ID. CNB 2776 - CHERNABURA ALASKA

CODE CNB27

SITE STRUCTURE

SITE GEOLOGY

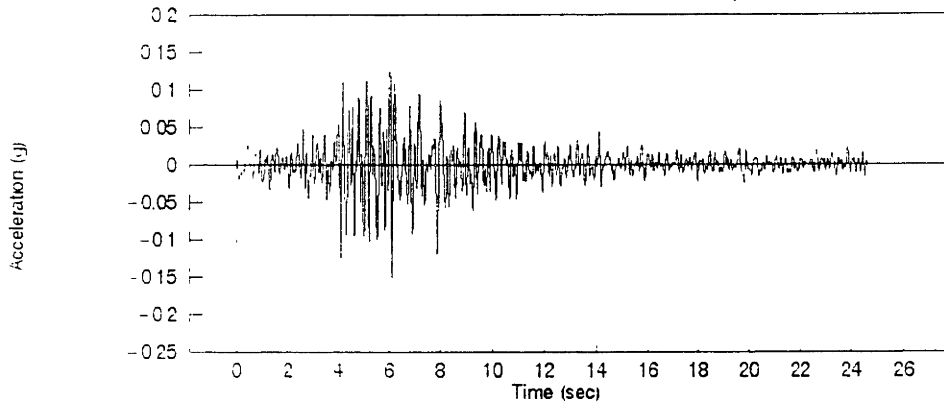
Figure A-4

RECORD/TRACE PARAMETERS:

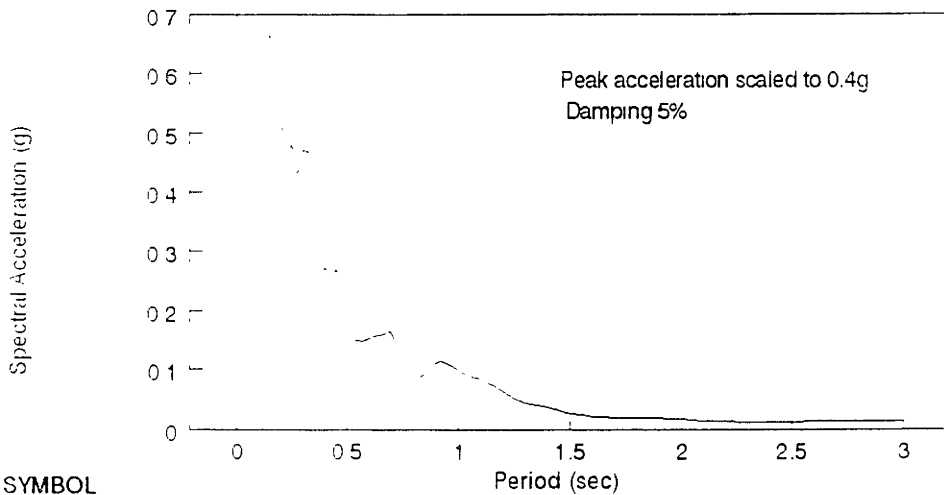
EPICENTRAL DISTANCE distance (km)= 12.1 azimuth (deg)=N140.7

SPECS. sampling rate (sec)=0.005

ANDREANOF ISLANDS, ALASKA EARTHQUAKE OF MAY 2, 1971
ADAK, AK U.S. NAVAL BASE N270 Component



Acceleration Response Spectrum



SYMBOL
AND1

EVENT PARAMETERS:

DATE year=1971 month=5 day=2
 TIME hour (minute (24hr))=0608 second=27.300 time code=UTC
 LOCATION latitude= 51.40000 longitude= -177.20000 depth (km)= 43.0
 NAME ANDREANOF ISLANDS ALASKA EARTHQUAKE OF MAY 2,1971
 MAGNITUDE (Ms) 7.1

SITE PARAMETERS:

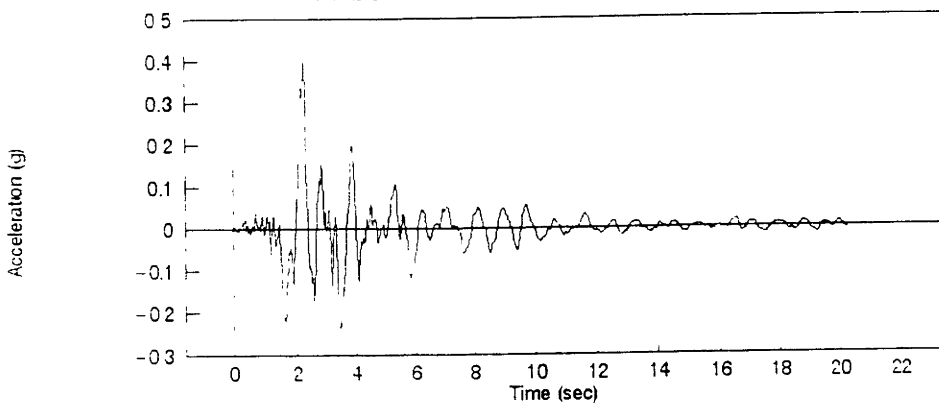
LOCATION latitude= 51.88000 longitude= -176.58000 elevation (m)= 0.0
 SITE ID 2701 ADN - ADAK, ALASKA U.S. NAVAL BASE
 CODE 2701A
 SITE STRUCTURE Hanger Building
 SITE GEOLOGY Basalt

RECORD/TRACE PARAMETERS:

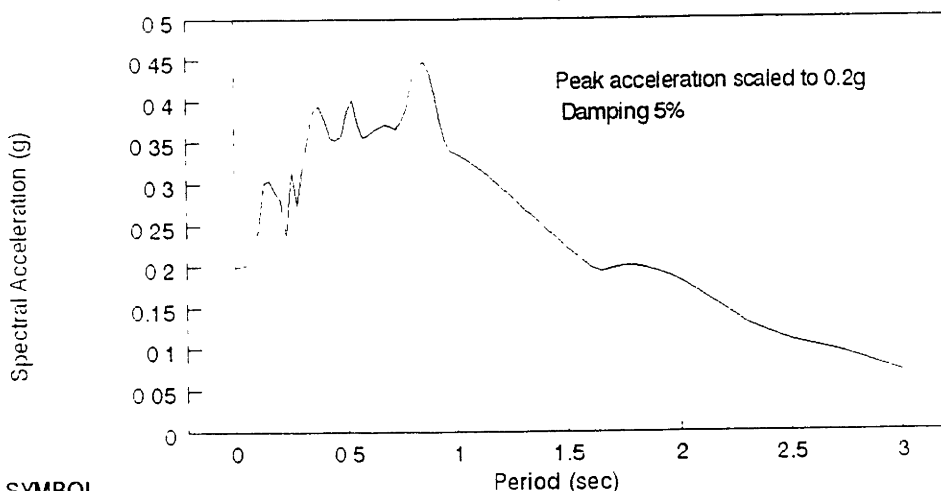
EPICENTRAL DISTANCE distance (km)= 68.6
 SPECS sampling rate (sec)=0.020

- Figure A-5

SAN SALVADOR EARTHQUAKE
NATL GEOGRAPHICAL INST N180 Component



Acceleration Response Spectrum



SYMBOL

ELS1

EVENT PARAMETERS:

DATE year=1986 month=10 day=10
 TIME hour:minute (24hr)=17:49 second=23.700 time code=UTC
 LOCATION latitude= 13.82900 longitude= -89.12600 depth (km)= 8.0
 NAME: SAN SALVADOR EARTHQUAKE

MAGNITUDE Ms=5.4 Mb=5.0

SITE PARAMETERS:

LOCATION latitude= 13.71400 longitude= -89.17100 elevation (m)= 0.0
 SITE ID: 90005 - NATL GEOGRAFICAL INST - (NIVEL/FLOOR: 1)
 CODE: 90005

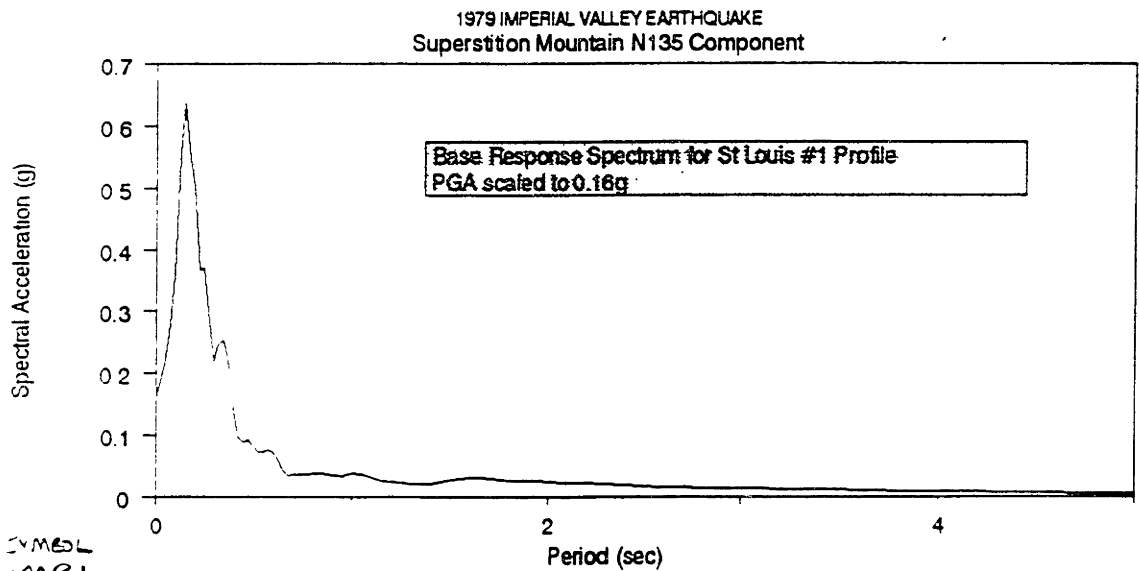
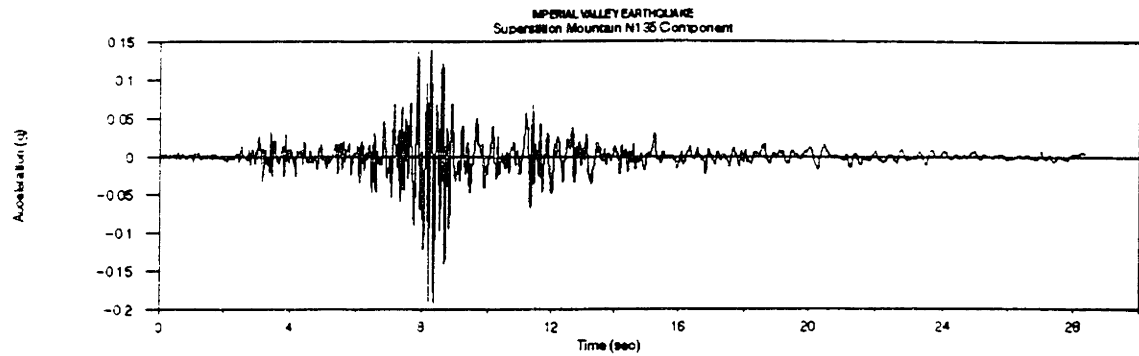
SITE STRUCTURE 1 Story Building

SITE GEOLOGY Fluviatile Fumice

RECORD/TRACE PARAMETERS:

EPICENTRAL DISTANCE distance (km)= 13.6 azimuth (deg)= N 20° E
 SPECS. sampling rate (sec)=0.020

Figure A-6



SYMBOL
IMPI

NCEER ASCII STRONG-MOTION DATA FORMAT

EVENT PARAMETERS:

DATE: year=1979 month=10 day=15
 TIME: hour|minute (24hr)=2316 second=54.500 time code=UTC
 LOCATION: latitude= 32.63300 longitude= -115.33300 depth (km)= 12.0
 NAME: IMPERIAL VALLEY EARTHQUAKE
 event.depth : 12.000000
 event.mag_l : 7.000000
 event.mag_s : 6.900000
 event.mag_b : 5.700000

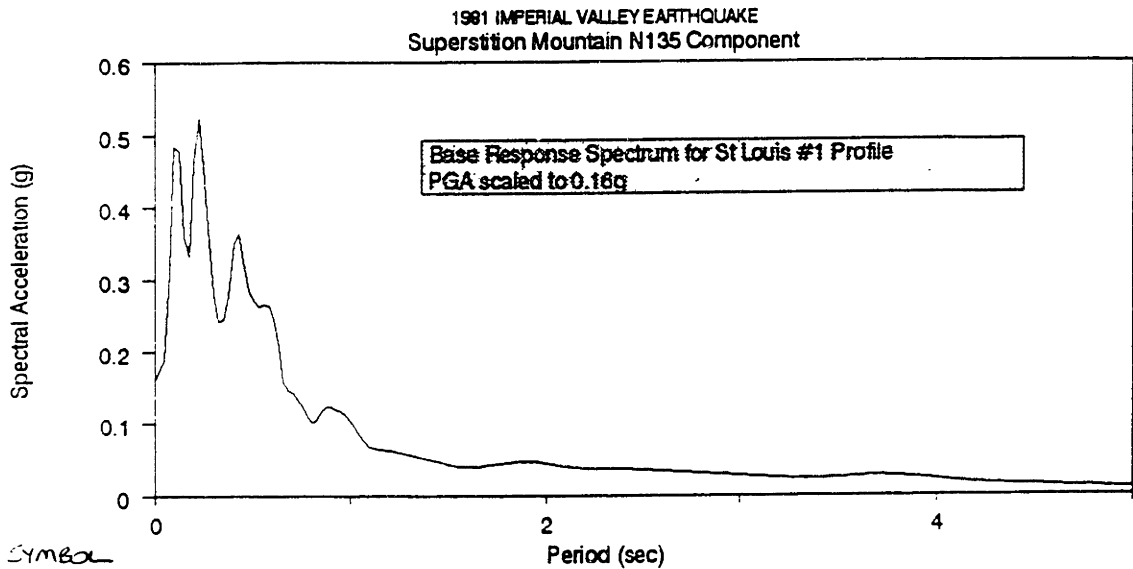
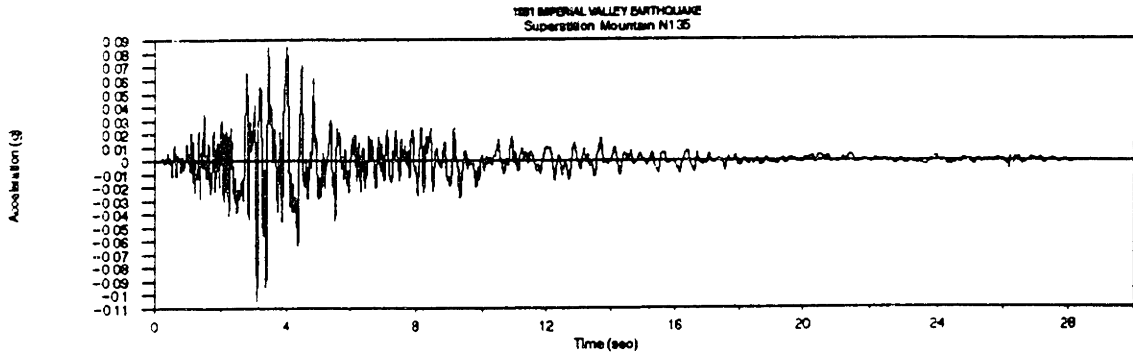
RECORD/TRACE PARAMETERS

EPICENTRAL DISTANCE: distance (km)= 57.6
 SPECS: sampling rate (sec)=0.010
 trace.peak_value : 189.210010
 trace.high_pass : 0.170000
 trace.low_pass : 23.000000
 trace.sensitivity : 0.000000
 trace.frequency : 25.000000
 trace.damping : 0.570000

SITE PARAMETERS:

LOCATION: latitude= 32.95000 longitude= -115.82000 elevation (m)= 0.0
 SITE ID: 206 - SUPERSTITION MOUNTAIN
 CODE: 206
 site.structure : 1-STORY BLDG
 site.geology : BEDROCK, GRANITE

Figure A-7



SYMBOL
IMP2

NCEER ASCII STRONG-MOTION DATA FORMAT

EVENT PARAMETERS:

DATE: year=1991 month= 4 day=26
 TIME: hour|minute (24hr)=1209 second=28 400 time code=UTC
 LOCATION: latitude= 33.13300 longitude= -115.63000 depth (km)= 6.0
 NAME: IMPERIAL VALLEY EARTHQUAKE
 event.depth : 6 000000
 event.mag_l : 0.000000
 event.mag_s : 6.000000
 event.mag_b : 5.500000

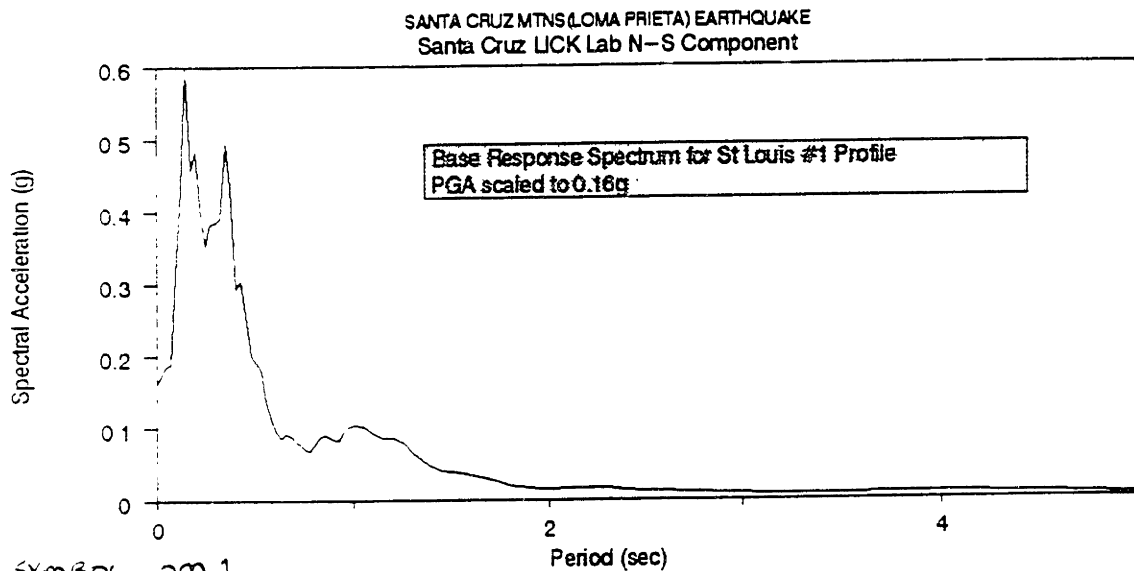
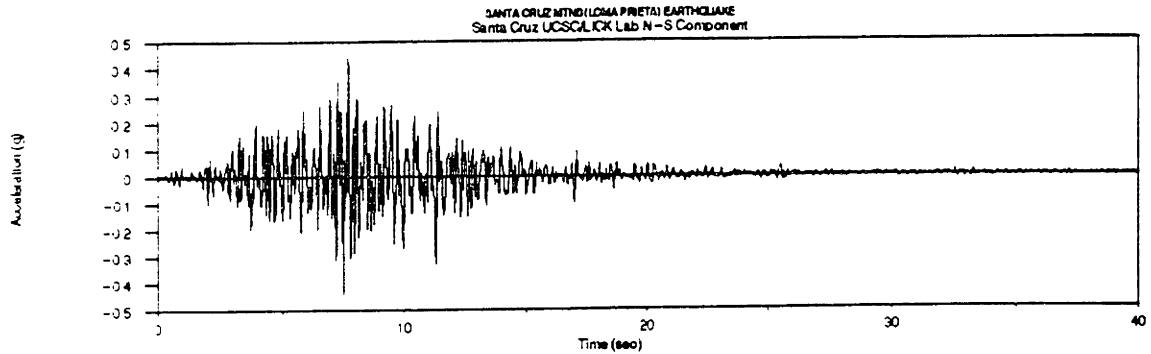
SITE PARAMETERS:

LOCATION: latitude= 32.93500 longitude= -115.82300 elevation (m)= 0.0
 SITE ID: 286 - SUPERSTITIION MOUNTAIN,CALIFORNIA
 CODE: 286
 site.structure : 1-STORY BLDG
 site.geology : BEDROCK, GRANITE

RECORD/TRACE PARAMETERS

EPICENTRAL DISTANCE: distance (km)= 25.5
 SPECS. sampling rate (sec)=0.010
 trace.peak_value : 102.470000
 trace.high_pass : 0.100000
 trace.low_pass : 23.000000
 trace.sensitivity : 0.000000
 trace.frequency : 25.641000
 trace.damping : 0.600000

Figure A-8



SYMBOL LOM 1

NCEER ASCII STRONG-MOTION DATA FORMAT

EVENT PARAMETERS:

DATE: year=1989 month=10 day=18
 TIME: hour:minute (24hr)=0004 second= 2.200 time code=UTC
 LOCATION: latitude= 37.03700 longitude= -121.80300 depth (km)= 18.0
 NAME: SANTA CRUZ MTNS (LOMA PRIETA) EARTHQUAKE
 event.depth : 18.000000
 event.mag_l : 7.000000
 event.mag_s : 7.100000
 event.mag_b : 0.000000

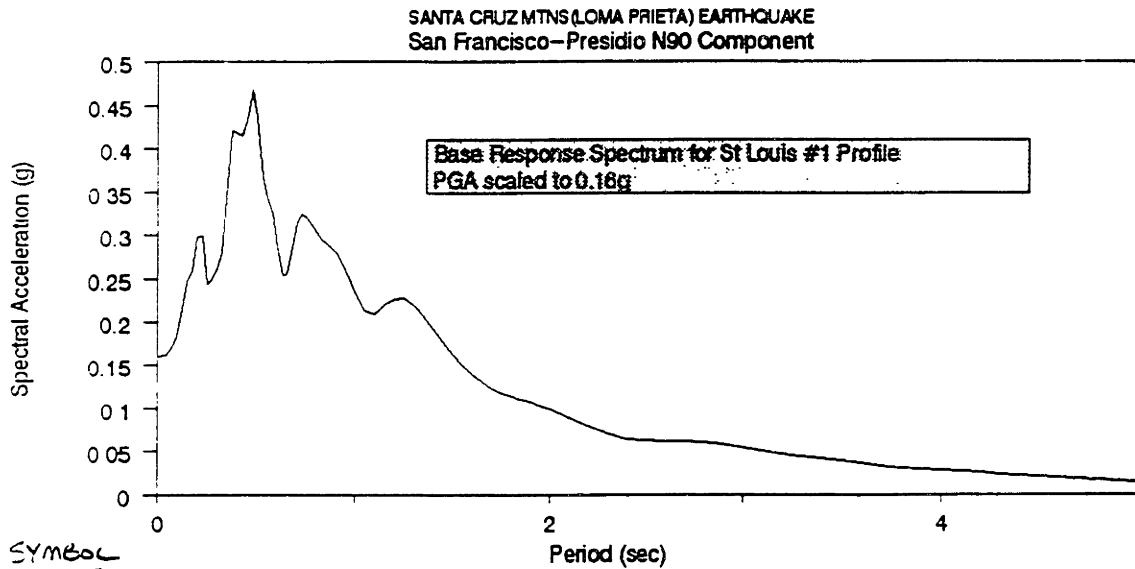
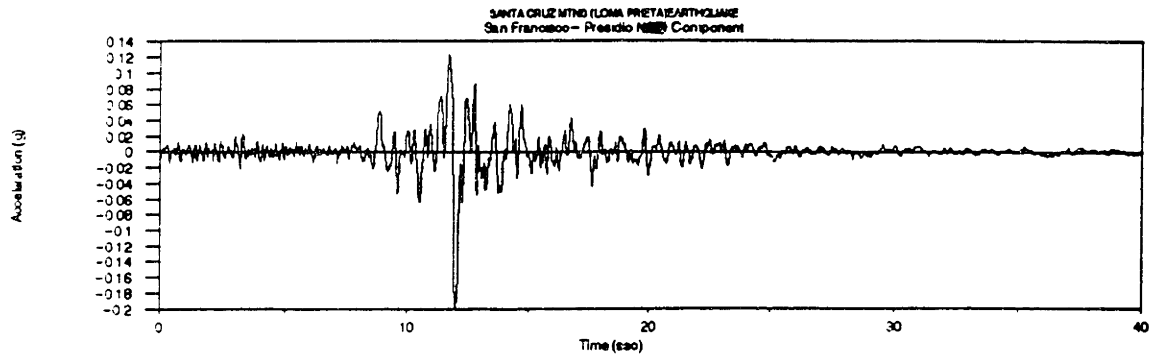
SITE PARAMETERS:

LOCATION: latitude= 37.00100 longitude= -122.06000 elevation (m)= 0.0
 SITE ID: 58135 - SANTA CRUZ - UCSC/LICK LAB.
 CODE: 58135
 site.structure : 1 STORY BLDG
 site.geology : BEDROCK, LIMESTONE

RECORD/TRACE PARAMETERS

EPICENTRAL DISTANCE: distance (km)= 23.2
 SPECS: sampling rate (sec)=0.020
 trace.peak_value : 433.117000
 trace.high_pass : 0.050000
 trace.low_pass : 23.000000
 trace.sensitivity : 1.880000
 trace.frequency : 25.575000
 trace.damping : 0.620000

Figure A-9



SYMBOL
L0M2

NCEER ASCII STRONG-MOTION DATA FORMAT

EVENT PARAMETERS:

DATE: year=1989 month=10 day=18
 TIME: hour|minute (24hr)=0004 second= 2.200 time code=UTC
 LOCATION: latitude= 37.03700 longitude= -121.80300 depth (km)= 18.0
 NAME: SANTA CRUZ MTNS (LOMA PRIETA) EARTHQUAKE
 event.depth : 18.000000
 event.mag_m : 7.000000
 event.mag_s : 7.100000
 event.mag_b : 0.000000

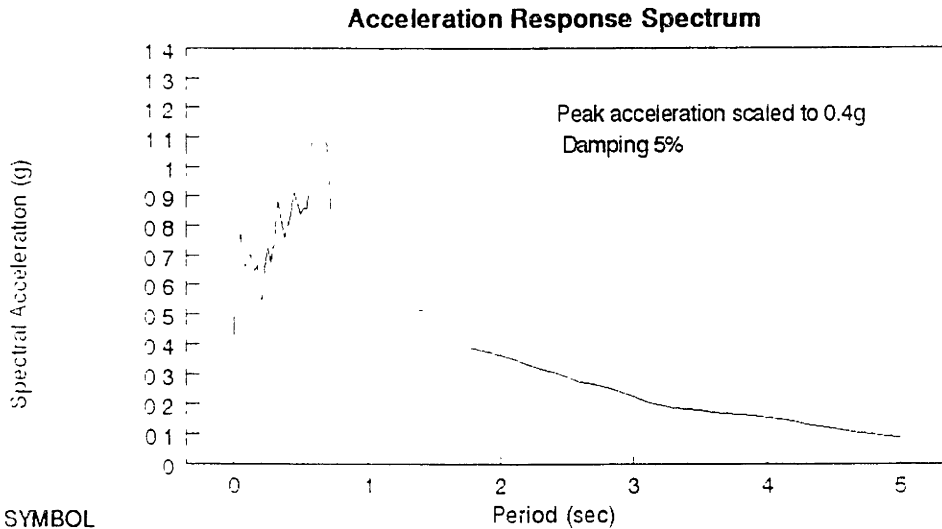
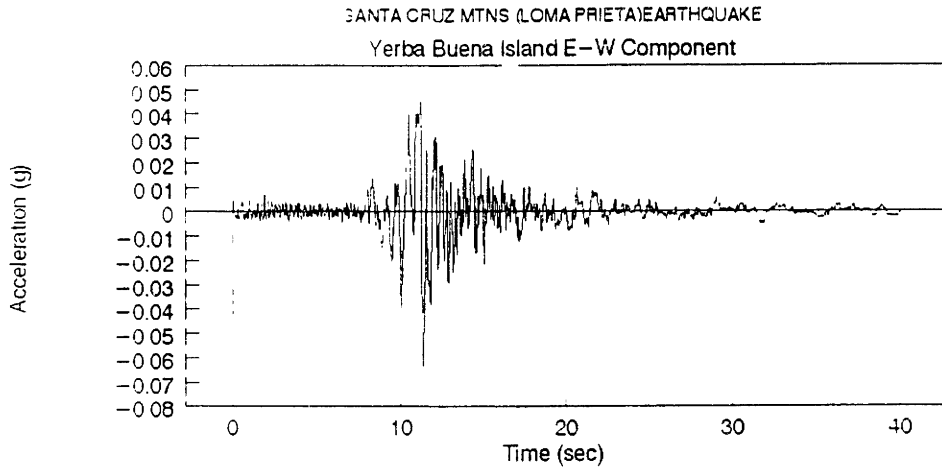
RECORD/TRACE PARAMETERS

EPICENTRAL DISTANCE: distance (km)= 101.8
 SPECS: sampling rate (sec)=0.020
 trace.peak_value : 194.873000
 trace.high_pass : 0.080000
 trace.low_pass : 23.000000
 trace.sensitivity : 1.630000
 trace.frequency : 25.773000
 trace.damping : 0.600000

SITE PARAMETERS:

LOCATION: latitude= 37.79200 longitude= -122.45700 elevation (m)= 0.0
 SITE ID: 58222 - SAN FRANCISCO - PRESIDIO
 CODE: 58222
 site.structure : FREE FIELD
 site.geology : BEDROCK, SERPENTINE

Figure A-10



SYMBOL

LOM3

EVENT PARAMETERS:

DATE year=1989 month=10 day=18
 TIME hour:minute (24hr)=00:04 second= 2.200 time code=UTC
 LOCATION latitude= 37.03700 longitude= -121.80300 depth (km)= 18.0
 NAME SANTA CRUZ MTNS (LOMA PRIETA) EARTHQUAKE
 MAGNITUDE Ms=7.1 MI=7.0

SITE PARAMETERS:

LOCATION latitude= 37.81000 longitude= -122.36000 elevation (m)= 0.0
 SITE ID 58163 - YERBA BUENA ISLAND
 CODE 58163

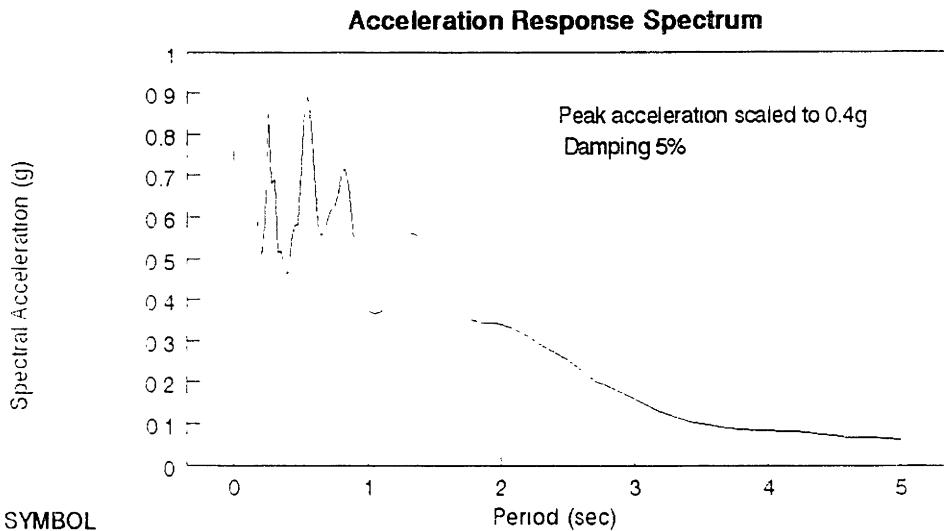
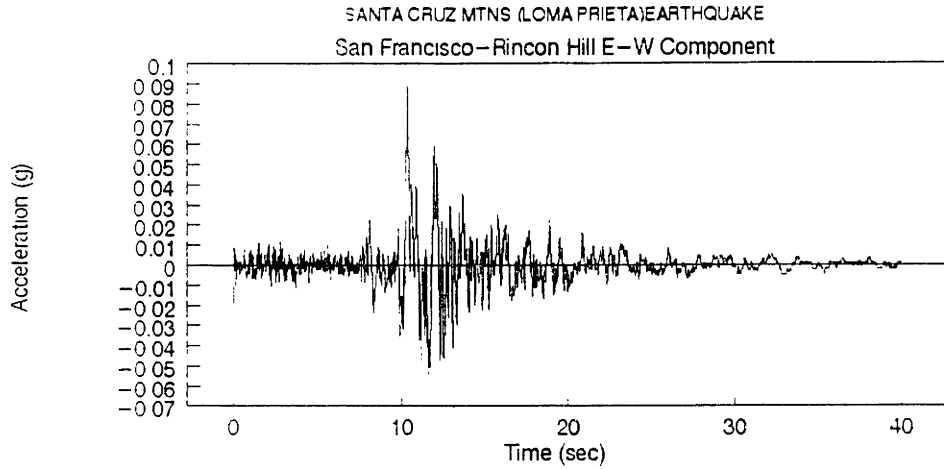
SITE STRUCTURE 1 Story Building

SITE GEOLOGY Franciscan Melange

RECORD/TRACE PARAMETERS:

EPICENTRAL DISTANCE distance (km)= 99.0 azimuth= 199
 SF ECS sampling rate (sec)= 0.020

Figure A-11



SYMBOL

LOM4

EVENT PARAMETERS:

DATE year=1989 month=10 day=18

TIME hour(minute (24hr))=0004 second= 2 200 time code=UTC

LOCATION latitude= 37.03700 longitude= -121.80300 depth (km)= 18.0

NAME SANTA CRUZ MTNS (LOMA PRIETA) EARTHQUAKE

MAGNITUDE Ms=7.1 Ml=7.0

SITE PARAMETERS:

LOCATION latitude= 37.79000 longitude= -122.39000 elevation (m)= 0.0

SITE ID 58151 - SAN FRANCISCO - RINCON HILL

CODE 58151

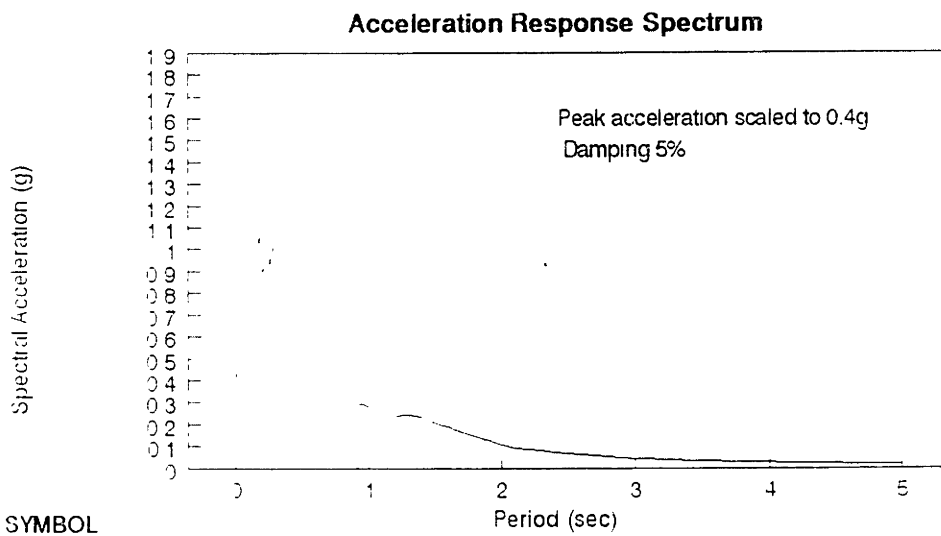
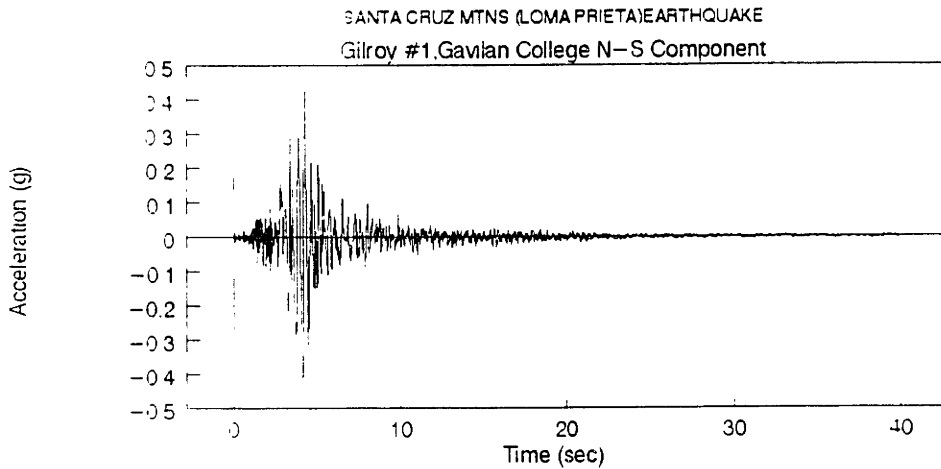
SITE STRUCTURE Free-Field

SITE GEOLOGY Franciscan Melange

RECORD/TRACE PARAMETERS:

EPICENTRAL DISTANCE distance (km)= 98.4 **Figure A.12**

SPECS sampling rate (sec)=0.020



SYMBOL

LOM5

EVENT PARAMETERS:

DATE year=1989 month=10 day= 8
 TIME hour:minute :second= 22:04 second= 2 200 time code=UTC
 LOCATION latitude= 37 03700 longitude= -121 80300 depth (km)= 18 0
 NAME SANTA CRUZ MTNS (LOMA PRIETA) EARTHQUAKE
 MAGNITUDE Ms=7.1 Mw=7.0

SITE PARAMETERS:

LOCATION latitude= 36 97300 longitude= -121 57200 elevation (m)= 0 0
 SITE ID 47379 - GILROY #1 - GAVILAN COLLEGE, WATER TANK
 CODE 47379

SITE STRUCTURE Instrument Shelter

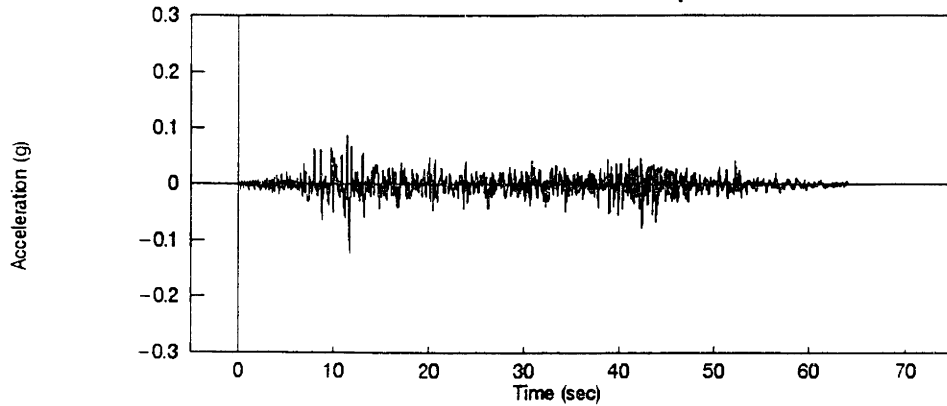
SITE GEOLOGY Sandstone, Shale and Chert

RECORD/TRACE PARAMETERS:

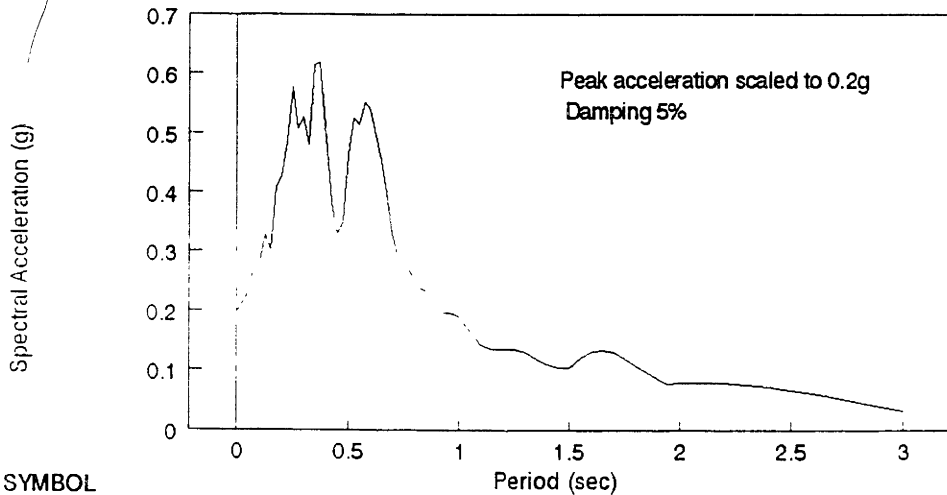
EPICENTRAL DISTANCE distance (km)= 21.8 azimuth (deg)= N289.1
 SPECS sampling rate (sec)= 0.020

Figure A-13

MICHOACAN, MEXICO CITY EARTHQUAKE
VILE - LA VILLITA N90 Component



Acceleration Response Spectrum



SYMBOL

MEX1

EVENT PARAMETERS:

DATE year=1985 month=9 day=19

TIME hour|minute (24hr)=13|17 second=47.300 time code=UTC

LOCATION latitude= 18.19000 longitude= -102.53300 depth (km)= 28.0

NAME: MICHOACAN, MEXICO CITY EARTHQUAKE

MAGNITUDE, Mb=6.3 Ms=7.6

SITE PARAMETERS:

LOCATION: latitude= 18.04700 longitude= -102.18400 elevation (m)= 0.0

SITE ID: VILE - LA VILLITA

CODE: VILE

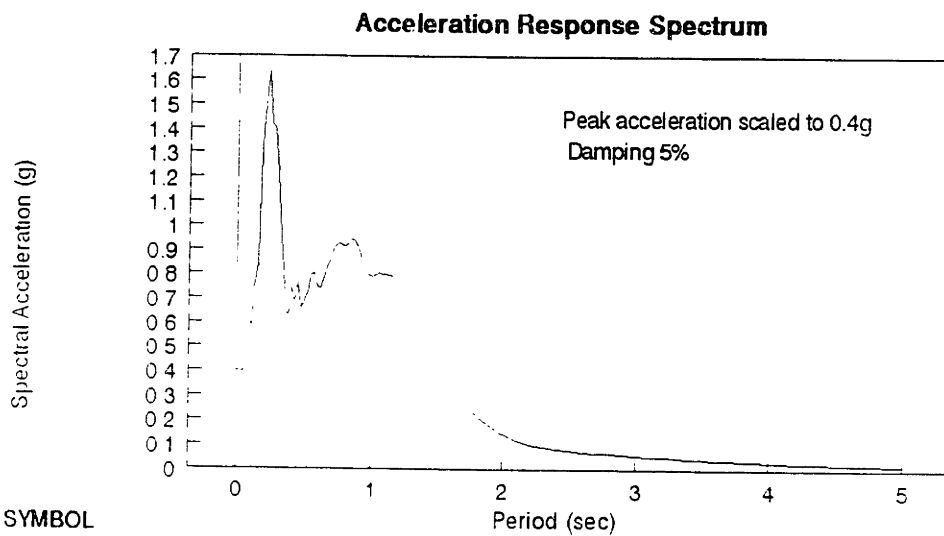
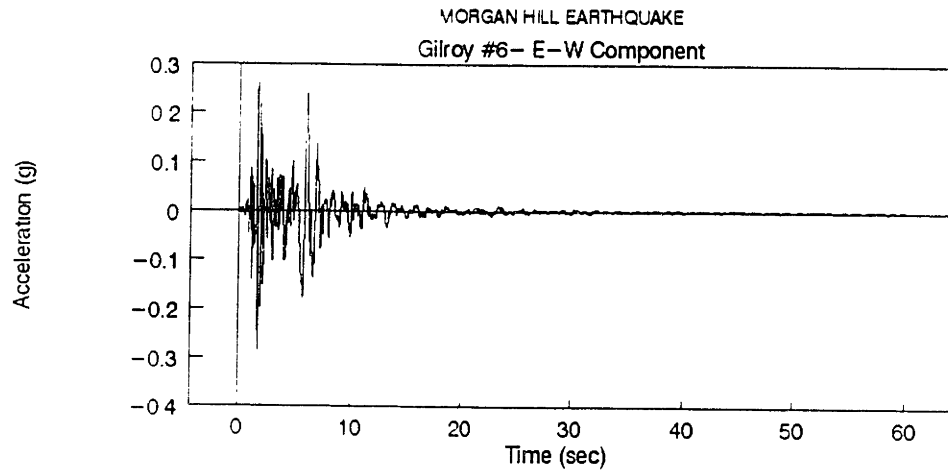
SITE STRUCTURE Free-field

SITE GEOLOGY: Tonelite

RECORD/TRACE PARAMETERS:

EPICENTRAL DISTANCE: distance (km)= 40.2 **Figure A-14**

SPECS. sampling rate (sec)=0.010



SYMBOL

MH1

EVENT PARAMETERS:

DATE year=1984 month= 4 day=24

TIME hour:minute (24hr)=21:15 second=19.000 time code=UTC

LOCATION latitude= 37.31700 longitude= -121.68700 depth (km)= 9.0

NAME: MORGAN HILL EARTHQUAKE

MAGNITUDE $M_L=6.2$

SITE PARAMETERS:

LOCATION latitude= 37.02600 longitude= -121.48400 elevation (m)= 0.0

SITE ID: 57383 - GILROY #6

CODE 57383

SITE STRUCTURE 1 Story Building

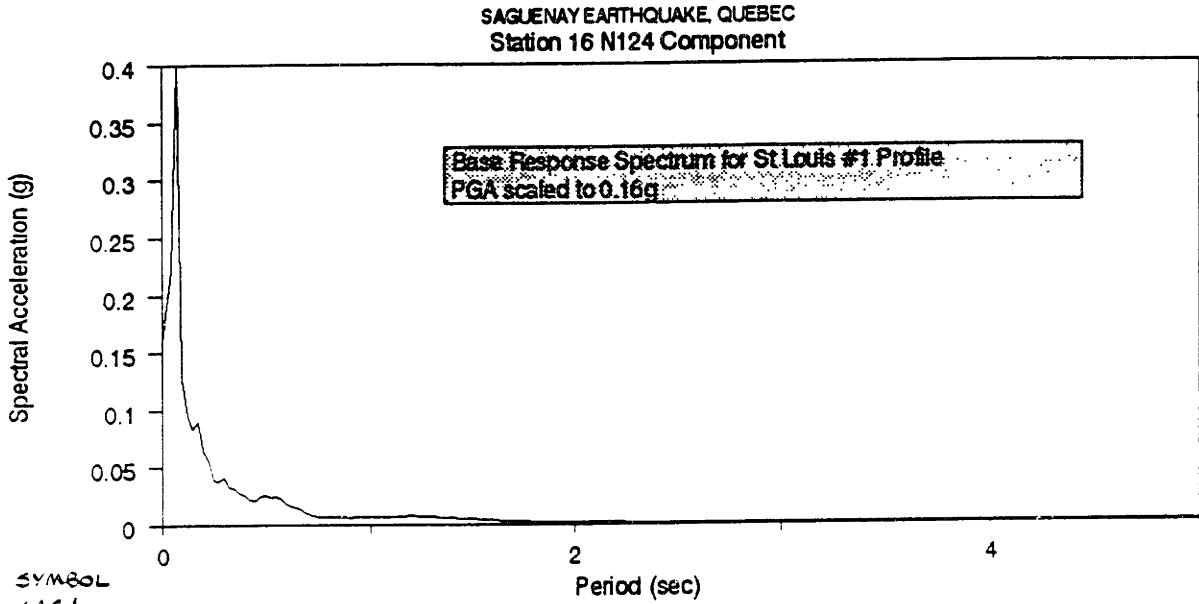
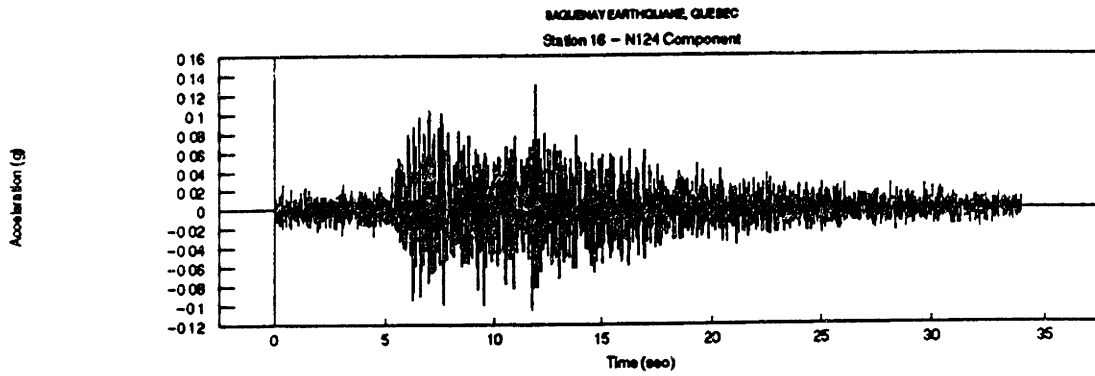
SITE GEOLOGY Bedrock

RECORD/TRACE PARAMETERS:

EPICENTRAL DISTANCE distance (km)= 36.7 azimuth (deg)=N331.7

SPECS. sampling rate (sec)=0.020

Figure A-15



SYMBOL
SAGEL

NCEER ASCII STRONG-MOTION DATA FORMAT

EVENT PARAMETERS:

DATE: year=1988 month=11 day=25
 TIME: hour|minute (24hr)=2346 second= 4.500 time code=UTC
 LOCATION: latitude= 48.12100 longitude= -71.18600 depth (km)= 28.0
 NAME: Saguenay earthquake
 event.depth : 28.000000
 event.mag_l : 0.000000
 event.mag_s : 6.000000
 event.mag_b : 0.000000

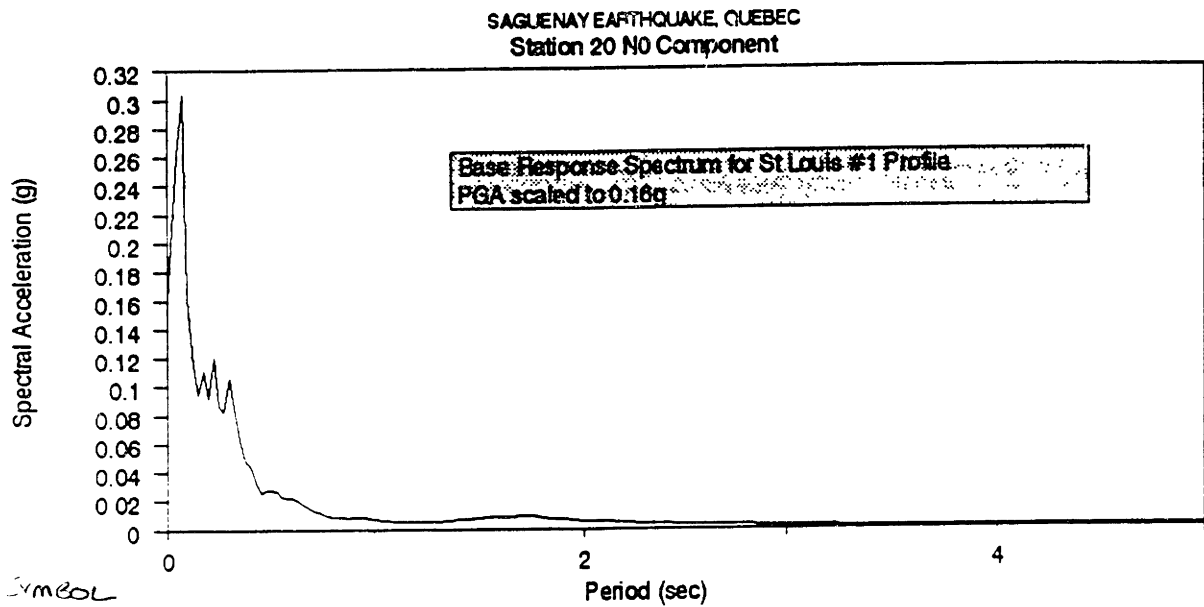
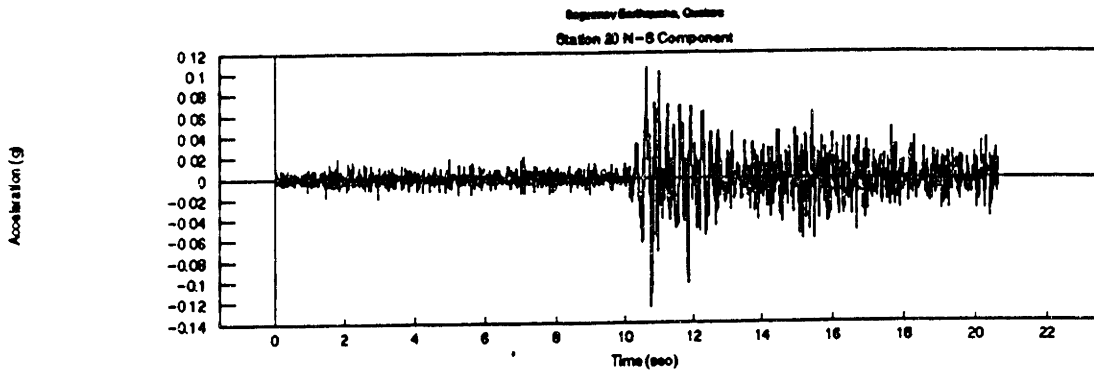
RECORD/TRACE PARAMETERS

EPICENTRAL DISTANCE: distance (km)= 43.1
 SPECS: sampling rate (sec)=0.005
 trace.peak_value : 128.660000

SITE PARAMETERS:

LOCATION: latitude= 48.49020 longitude= -71.01230 elevation (m)= 0.0
 SITE ID: Site - 16 - , Chicoutimi-Nord, PQ
 CODE: 16
 site structure : 2 STORY WOOD FRAME BLDG
 site.geology : BEDROCK

Figure A-16



SYMBOL
SAGZ

NCEER ASCII STRONG-MOTION DATA FORMAT

EVENT PARAMETERS:

DATE: year=1988 month=11 day=25
 TIME: hour|minute (24hr)=2346 second= 4.500 time code=UTC
 LOCATION: latitude= 48.12100 longitude= -71.18600 depth (km)= 28.0
 NAME: Saguenay earthquake
 event.depth : 28.000000
 event.mag_l : 0.000000
 event.mag_s : 6.000000
 event.mag_b : 0.000000

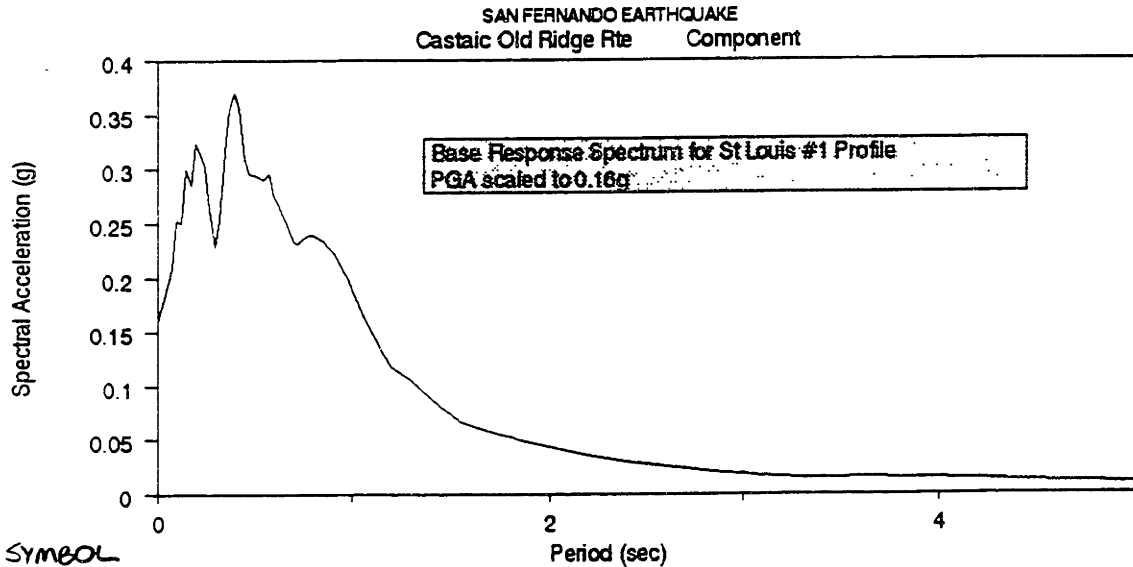
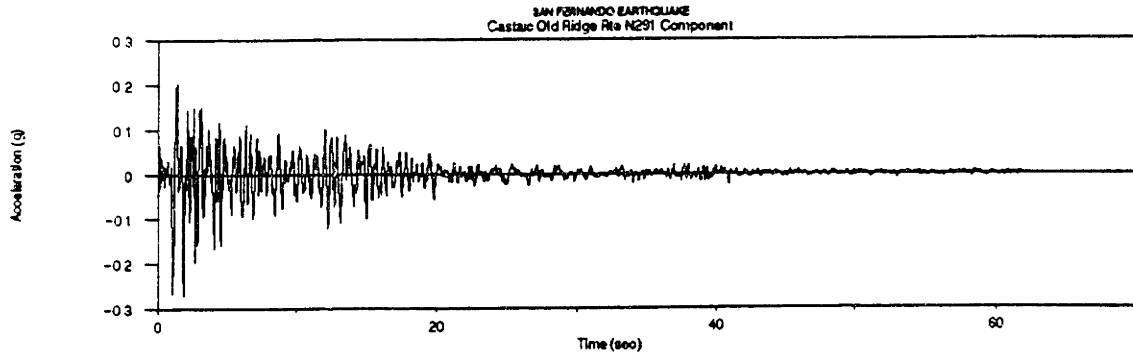
RECORD/TRACE PARAMETERS

EPICENTRAL DISTANCE: distance (km)= 90.4
 SPECS: sampling rate (sec)=0.005
 trace.peak_value : 123.070000

SITE PARAMETERS:

LOCATION: latitude= 47.54960 longitude= -70.32730 elevation (m)= 0.0
 SITE ID: Site - 20 -, Les Eboulements, PQ
 CODE: 20
 site.structure : ABOVE GROUND SEISMIC VAULT
 site.geology : BEDROCK

Figure A-17



SYMBOL
SFER 1

NCEER ASCII STRONG-MOTION DATA FORMAT

EVENT PARAMETERS:

DATE: year=1971 month= 2 day= 9
 TIME: hour|minute (24hr)=1400 second=40.600 time code=UTC
 LOCATION: latitude= 34.40000 longitude= -118.43000 depth (km)= 9.0
 NAME: SAN FERNANDO EARTHQUAKE
 event.depth : 9.000000
 event.mag_l : 0.000000
 event.mag_s : 0.000000
 event.mag_b : 6.200000

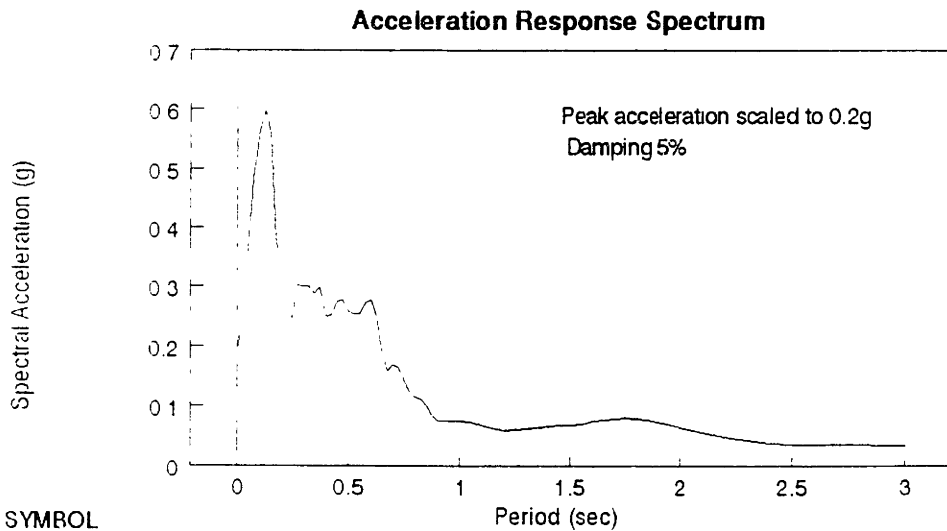
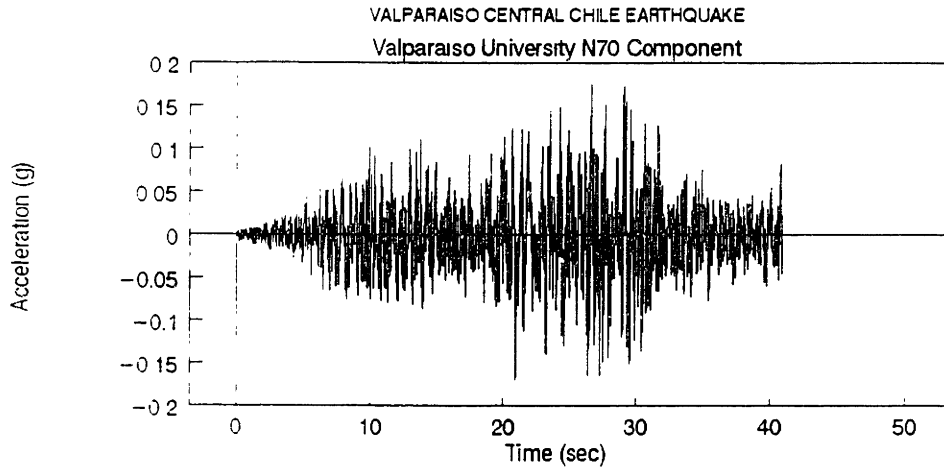
RECORD/TRACE PARAMETERS

EPICENTRAL DISTANCE: distance (km)= 27.0264
 SPECS: sampling rate (sec)=0.020
 trace.peak_value : 265.400000
 trace.high_pass : 0.070000
 trace.low_pass : 25.000000
 trace.sensitivity : 0.000000
 trace.frequency : 19.608000
 trace.damping : 0.636000

SITE PARAMETERS:

LOCATION: latitude= 34.55500 longitude= -118.65667 elevation (m)= 0.0
 SITE ID: STATION NO. - 110 - CASTAIC OLD RIDGE ROUTE, CAL
 CODE: 110
 site.structure : INSTRUMENT SHELTER
 site.geology : BEDROCK, SANDSTONE

Figure A-18



SYMBOL

VALP1

EVENT PARAMETERS:

DATE year=1985 month= 3 day= 3

TIME hour:minute (24hr)=22:46 second=56.000 time code=UTC

LOCATION latitude= -33.13500 longitude= -71.87100 depth (km)= 33.0

NAME VALPARAISO CENTRAL CHILE EARTHQUAKE

MAGNITUDE Mb=6.7 Ms=7.8

SITE PARAMETERS:

LOCATION latitude= -33.03000 longitude= -71.62000 elevation (m)= 0.0

SITE ID VALPARAISO UNIVERSITY OF SANTA MARIA

CODE VALPA

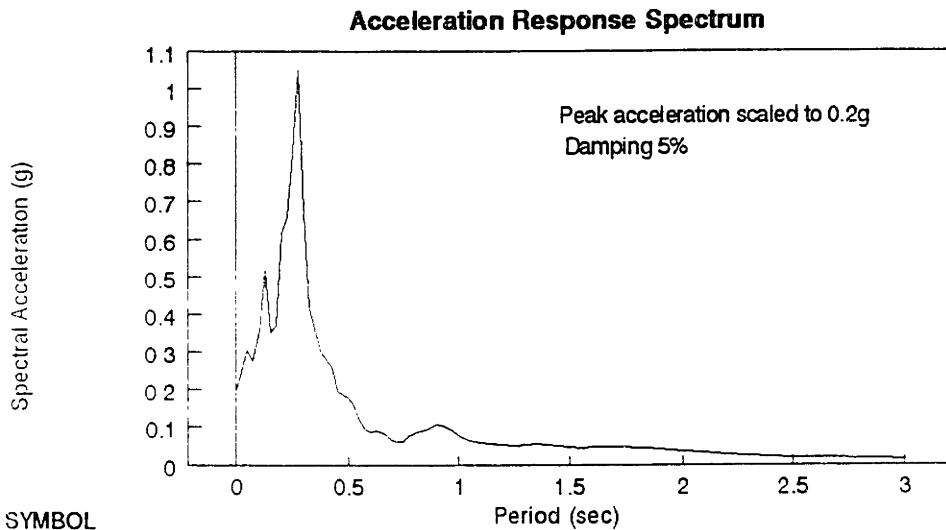
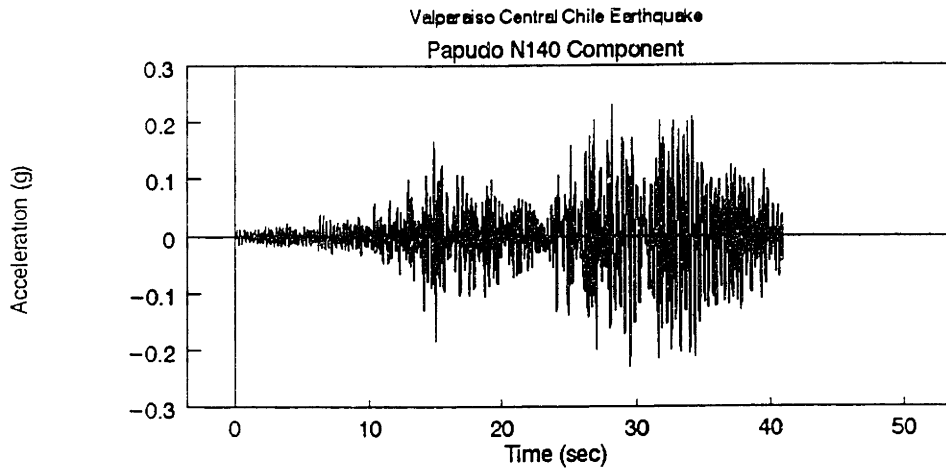
SITE STRUCTURE: 1 Story Building

SITE GEOLOGY Volcanic

RECORD/TRACE PARAMETERS: Figure A-19

EPICENTRAL DISTANCE distance (km)= 26.2 azimuth (deg)=N243.5

SPECS. sampling rate (sec)=0.005



SYMBOL

VALP2

EVENT PARAMETERS:

DATE: year=1985 month= 3 day= 3

TIME: hour (minute (24hr))=2246 second=56 000 time code=UTC

LOCATION: latitude= -33.13500 longitude= -71 87100 depth (km)= 33.0

NAME VALPARAISO CENTRAL CHILE EARTHQUAKE

MAGNITUDE: Mb=6.7 Ms=7.8

SITE PARAMETERS:

LOCATION: latitude= -32.51000 longitude= -71.45000 elevation (m)= 0.0

SITE ID: PAPUDO 1-STORY BLDG

CODE: PAPUD

SITE STRUCTURE: 1 Story Building

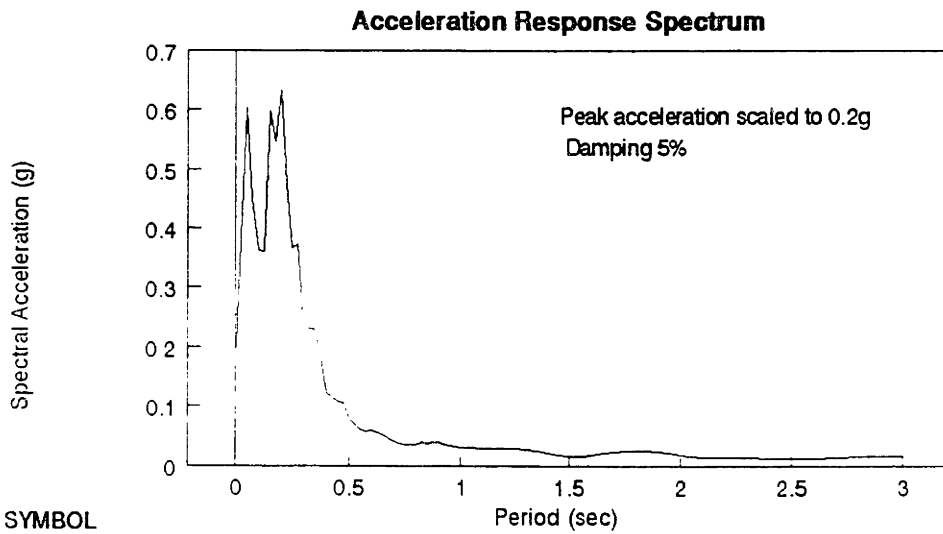
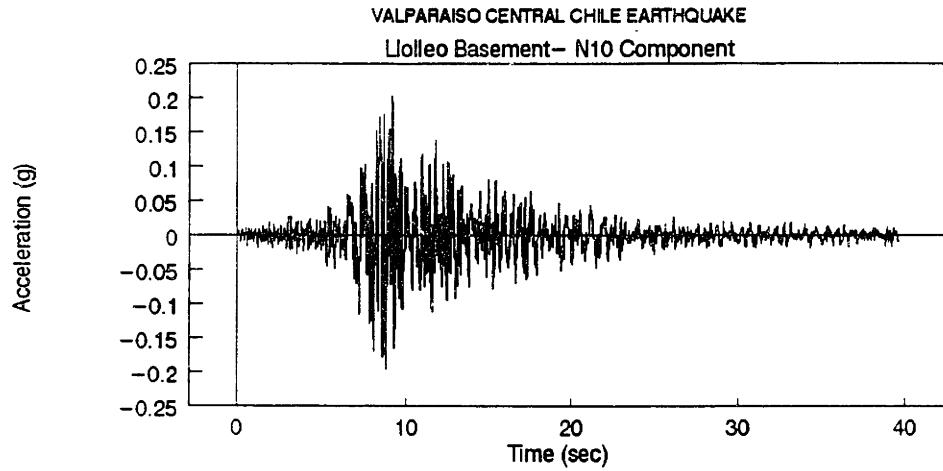
SITE GEOLOGY: Sandstone and Volcanic

RECORD/TRACE PARAMETERS:

EPICENTRAL DISTANCE: distance (km)= 79.7 azimuth (deg)= 120.3

SPECS: sampling rate (sec)=0.005

Figure A-20



SYMBOL

VALP3

EVENT PARAMETERS:

DATE. year=1985 month= 4 day= 9

TIME: hour|minute (24hr)=0156 second=59.400 time code=UTC

LOCATION. latitude= -34.13100 longitude= -71.61800 depth (km)= 38.0

NAME: VALPARAISO CENTRAL CHILE EARTHQUAKE

MAGNITUDE: Mb=6.3 Ms=7.2

SITE PARAMETERS:

LOCATION: latitude= -32.63000 longitude= -71.63000 elevation (m)= 0.0

SITE ID: LLOLLEO BASMENT 1 - STORY BLDG

CODE: LLOLL

SITE STRUCTURE: 1 Story Building

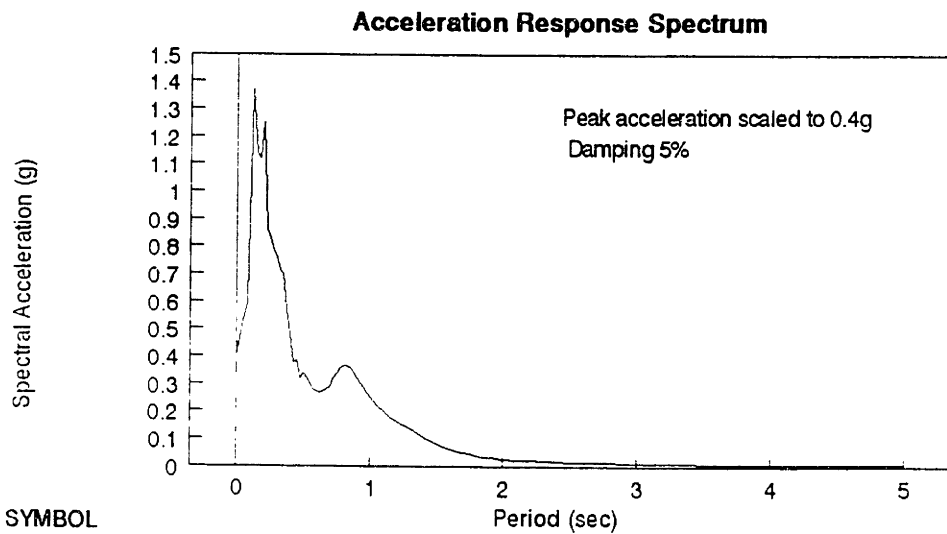
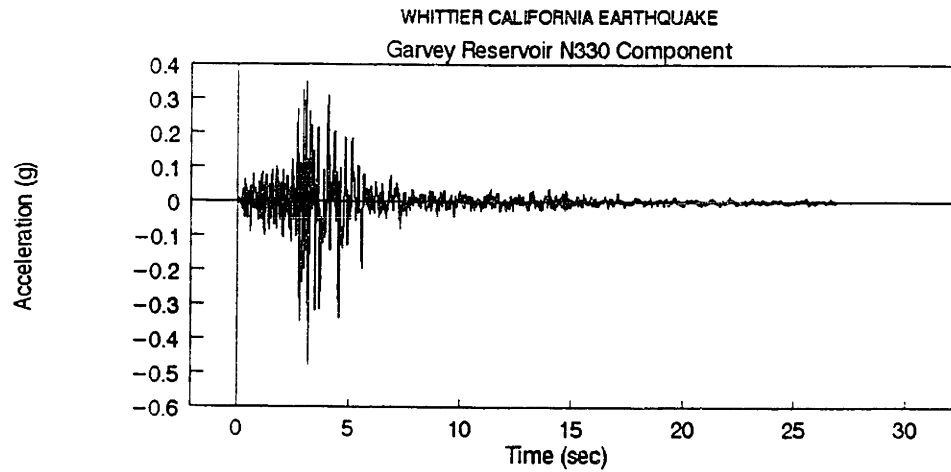
SITE GEOLOGY: Sandstone and Volcanic

RECORD/TRACE PARAMETERS:

EPICENTRAL DISTANCE. distance (km)= 166.5 azimuth (deg)= 1179.6

SPECS. sampling rate (sec)=0.005

Figure A-21



SYMBOL

WHIT1

EVENT PARAMETERS:

DATE: year=1987 month=10 day= 1
 TIME: hour/minute (24hr)=1442 second= 0 000 time code=UTC
 LOCATION: latitude= 34 06000 longitude= -118 08000 depth (km)= 10 0
 NAME: Whittier, Calif Earthquake of October 1, 1987
 MAGNITUDE: MI=6.1

SITE PARAMETERS:

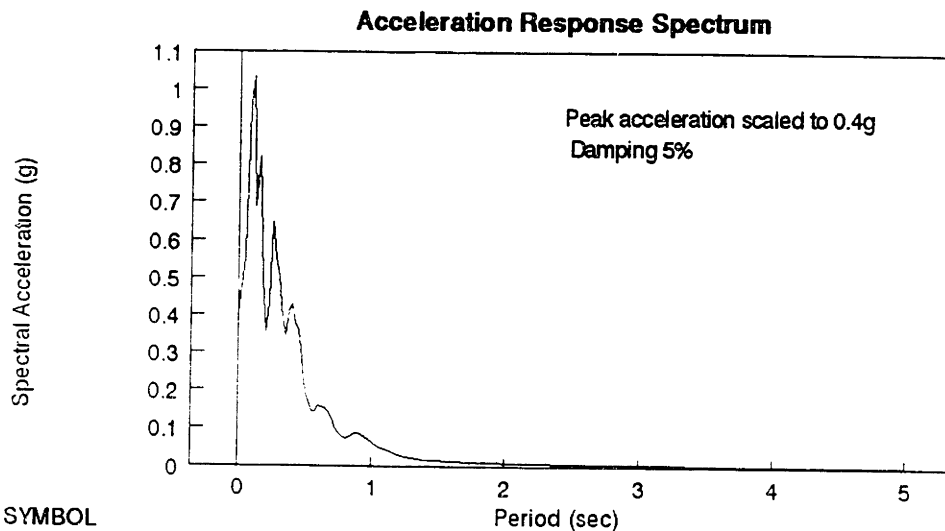
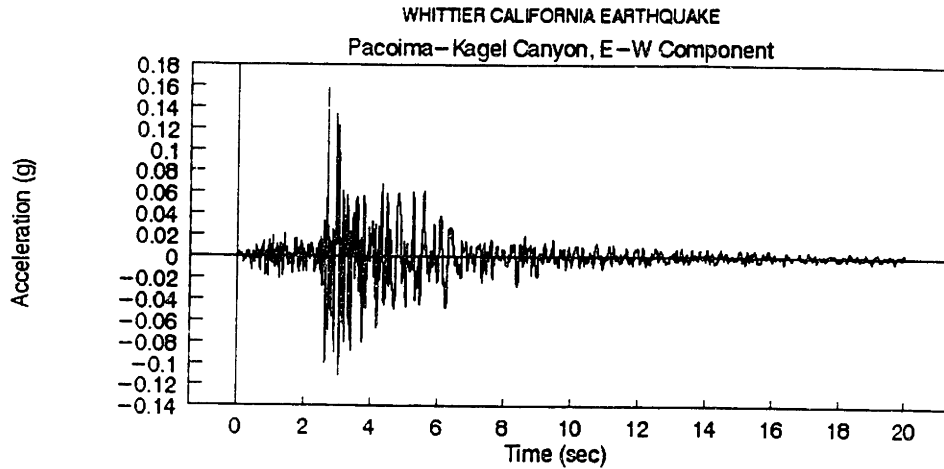
LOCATION: latitude= 0.00000 longitude= 0.00000 elevation (m)= 0.0
 SITE ID: GARVEY RE - SERVOIR - CONTROL BUILDING
 CODE: GARVE
 SITE STRUCTURE: Earth Dam

SITE GEOLOGY: Bedrock

RECORD/TRACE PARAMETERS:

EPICENTRAL DISTANCE: distance (km)=2.98 azimuth (deg)=N307.3
 SPECS: sampling rate (sec)=0.005

Figure A-22



SYMBOL

WHIT2

EVENT PARAMETERS:

DATE: year=1987 month=10 day= 1

TIME: hour/minute (24hr)=1442 second= 0.000 time code=UTC

LOCATION: latitude= 34 06000 longitude= -118 08000 depth (km)= 10.0

NAME: WHITTIER,CALIF. EARTHQUAKE OF OCTOBER 1, 1987

MAGNITUDE: MI=6.1

SITE PARAMETERS:

LOCATION: latitude= 34.28800 longitude= -118.37500 elevation (m)= 0.0

SITE ID: 24088 - PACOIMA - KAGEL CANYON

CODE: 24088

SITE STRUCTURE: 1 Story Building

SITE GEOLOGY: Tertiary Sandstone

RECORD/TRACE PARAMETERS:

EPICENTRAL DISTANCE: distance (km)= 37.1 azimuth (deg)=N132.8

SPECS: sampling rate (sec)=0.010

Figure A-23